A Step Forward:

Lentiviral Gene Therapy as a Cure for Pompe Disease

Qiushi Liang

Een stap vooruit:
Lentivirale gentherapie als behandeling voor de ziekte van Pompe

Qiushi Liang

The research described in this thesis was financially supported by the Netherlands Organization for Health Research ZonMw (project number: 40-40300-98-07010) and the Erasmus University Medical Center. The author was supported by the China Scholarship Council (File No. 201206240040)

The studies presented in this thesis was performed in the Department of Hematology and the Department of Clinical Genetics, Erasmus University Medical Center, Rotterdam, The Netherlands.

ISBN:	978-94-6332-220-1
Author:	Qiushi Liang
Cover Design:	Mike Broeders
Layout:	Optima Grafische Communicatie B.V.
Printed by:	GVO drukkers & vormgevers B.V.

A Step Forward:

Lentiviral Gene Therapy as a Cure for Pompe Disease

Een stap vooruit:
Lentivirale gentherapie als behandeling voor de ziekte van Pompe

Proefschrift

ter verkrijging van de graad van doctor aan de Erasmus Universiteit Rotterdam
op gezag van de rector magnificus Prof.dr. H.A.P. Pols
en volgens besluit van het College voor Promoties.

De openbare verdediging zal plaatsvinden op
dinsdag 26 september 2017 om 13:30 uur

door

Qiushi Liang
geboren te Chengdu, China

Erasmus University Rotterdam

PROMOTIECOMMISSIE

Promotoren:	Prof.dr. A.T. van der Ploeg
	Prof.dr. A.G. Vulto
Overige leden:	Prof.dr. P.A.E. Sillevis Smitt
	Prof.dr. R.C. Hoeben
	Prof.dr. B. Bigger
Copromotoren:	Dr. W.W.M. Pijnappel
	Dr. N.P. van Til

CONTENTS

Chapter 1

Introduction - Part 1

1. BACKGROUND OF POMPE DISEASE

Pompe disease (OMIM number 232300), also called glycogen storage disease type II, acid maltase deficiency, is an autosomal recessive lysosomal storage disorder caused by the deficiency of lysosomal acid α-glucosidase (GAA).[1,2] Although most of the glycogen degradation takes place in the cytoplasm, approximately 10% of glycogen is deposited in the lysosomes[3] via autophagic vacuoles which is further hydrolyzed by the lysosomal GAA at both α-1,4 and α-1,6 linkages into glucose (Figure 1A).[4-7] The deficiency of GAA causes excessive glycogen accumulation within the lysosomes, which triggers cascades of pathological changes and eventually leads to structural damage of cells and tissues, and functional impairment (Figure 1B).[8] The *GAA* gene is located on the long arm of chromosome 17 (q25.2-q25.3). Approximately 500 distinct pathogenic mutations (www.pompecenter.nl) in the acid α-glucosidase gene (*GAA*) have been described to date, and the overall incidence in the population is about 1 in 40,000 newborns.[9]

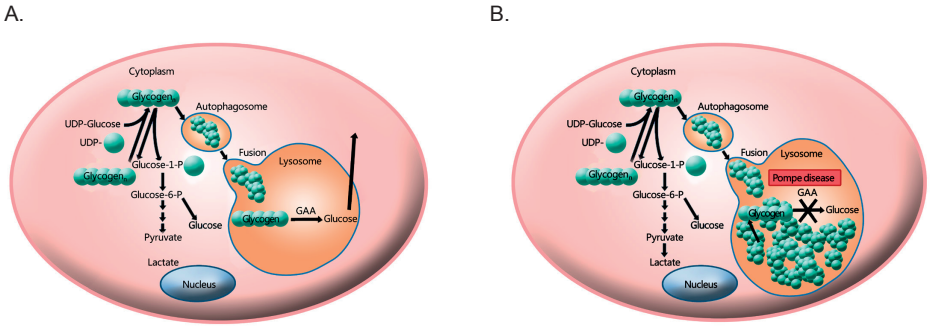

Figure 1. Lysosomal glycogen accumulation in Pompe disease. (A) Glycogen degradation in healthy cells. (B) Glycogen accumulation in Pompe disease.

2. CLINICAL PRESENTATION

The clinical picture of Pompe disease is predominantly featured by myopathy. The disease presents as a continuous clinical spectrum. Below the presentations during infancy, childhood and adulthood are described. The clinical severity correlates with the amount of residual GAA enzyme activity. In the most severe form, classic infantile patients usually have less than 1% residual activity whereas in the milder presentations, the children and adult patients may possess up to 20% of the normal GAA activity.

Classic infantile Pompe disease

The clinical manifestations of classic infantile Pompe disease, the most severe type, usually start within the first months of age. The presenting symptoms are feeding problems, failure to thrive, muscle weakness and respiratory problems including airway infections and respiratory dysfunction.[10-12] Heart is also involved in classic infantile patients characterized by progressive cardiac hypertrophy with a thickening of the left ventricular posterior wall and/or intra-ventricular septum. This can cause outflow tract obstruction and heart failure,[13] which will further add to pulmonary dysfunction. In addition, the large heart size can obstruct lung function by steric hindrance and development of atelectasis. Motor development is severely delayed and major developmental milestones including rolling over, sitting, crawling or standing are generally not reached. Upon clinical examination, patients usually present with prominent hypotonia with head lag, enlarged tongue, absent/decreased deep tendon reflexes and hepatomegaly in some cases. This population of patients usually dies of cardiorespiratory failure within 1 year of age.

Additionally, new symptoms have been described in long survivors of classic infantile Pompe disease[14] treated with enzyme replacement therapy (ERT), which has significantly improved prospects of patients who previously died before the age of one year. Hearing deficits;[15-19] ptosis and myopia;[20,21] speech disorders, dysphagia and facial muscle weakness; [14,18,22-27] osteopenia and osteoporosis[14,28,29] are commonly observed.

Importantly, apart from glycogen deposits in muscles, autopsy results of infantile patients showed glycogen accumulation in cortical neurons, brainstem nuclei, glial cells and oligodendrocytes.[8,30-36] The clinical significance of these findings is still not fully evident, but cognitive decline has been observed in long survivors of classic infantile patients,[19,37-39] which is accompanied by structural abnormalities in the brain including delayed myelination[40] and periventricular white matter abnormalities.[37-39] In a severe case, the patient showed intellectual disability and behavioral problems at school age with white matter abnormalities extending to the subcortical area.[39]

Childhood Pompe disease

Pompe disease may also present in infants and children without expression of the characteristic "classic infantile" features. Essentially, compared to classic infantile patients, childhood Pompe patients have more slowly progressive mobility and respiratory problems. In some cardiomegaly may occur but this is not as prominent as in the classic infantile patients.[41] First complaints include delayed motor development, limb-girdle weakness and fatigue. Scoliosis[42] and rigid spine[43,44] may be prominent.

Respiratory function is progressively impaired and patients usually die due to respiratory failure before the end of third decade.[1]

Adult Pompe disease

The clinical picture of adult Pompe disease is featured by slowly progressive proximal myopathy and/or respiratory distress with the heart usually spared. However, the age of onset, the rate of disease progression and the degree of skeletal and respiratory muscle involvement varies between patients. The most prominent presenting symptoms are related to limb-girdle weakness, including difficulties in performing sports, climbing stairs, rising from an armchair, walking and rising from a lying position.[45] Fatigue, muscle cramps and back pain may also be observed.[46,47] Weakness in the respiratory muscles especially the diaphragm[48] lead to symptoms including hypoventilation and obstructive sleep apnea syndrome.[49,50] Both motor and respiratory function diminish gradually over varied periods of time that eventually cause the use of wheelchair and ventilation support.[51-53] Eventually, patients die most likely from pulmonary complications.

Other unusual signs include scoliosis,[54] rigid spine syndrome,[55] tongue weakness,[56] bulbar muscle weakness,[57,58] speech disorder[59] and ptosis.[60] The hearing deficits still remain debatable as the presenting symptom in LOPD because the prevalence was similar compared to the general population in two studies[61,62] whereas in another two reports with a smaller sample size, the percentage was higher in patient cohorts.[63,64] Glycogen accumulation in smooth muscles could lead to 1) vascular pathology including aortic stiffness, dilated arteriopathy and aneurisms of the ascending aorta and the basilar artery in brain;[65-68] 2) Gastric and urinary tract problems.[69-71]

Glycogen accumulation in adult patients was relatively spared in neurons and glia in brain.[67,72,73] While primary glycogen infiltration was rather insignificant, secondary lesions featured by proliferating glia/gliosis was rather prominent in the white matter of the brain especially in the subependymal zone.[67] In line with rather mild glycogen load in the brain, so far cognitive function of adult patients was thought to be normal. Only in one study using resting-state functional MRI, functional connective abnormalities related to executive functioning, planning and abstract reasoning was described, which was confirmed by significantly impaired executive functions in neuropsychological evaluations.[74] Collectively, to determine if brain function is also affected in adult Pompe patients, more in depth studies are needed. So far adult Pompe patients seem to perform intellectually on a normal level. Peripheral nervous impairment, featured by small-fiber neuropathy (SFN) has also been described as a relevant neurological symptom in adult Pompe patients.[75] It has been suggested to af-

fect both myelinated and unmyelinated nerves responsible for pain and temperature sensation, which might cause patients to feel painful paresthesia in the extremities.[76] SFN in the form of axonal degeneration and loss of epidermal nerve fibers was shown in skin biopsies of two symptomatic adult patients experiencing burning sensations of fingers and toes and 50% (22 out of 44) of the patients were found positive on a SFN screening list.[77] This was likely to be caused by glycogen accumulation in the Schwann cells of the peripheral nerves described by a few biopsies done in childhood and adult patients.[78,79] Whether these findings lead to clinical symptoms in adults with Pompe disease such as peripheral neuropathy remains a matter of debate and also needs further investigation.

3. PATHOPHYSIOLOGY

The pathogenic cascade in Pompe disease starts with accumulated lysosomal glycogen provoking lysosomal compartment expansion, and affecting its integrity, leading to disturbed lysosomal dysfunction. Given the central role of the lysosome in maintaining cellular homeostasis,[80] secondary cellular dysfunction has been confirmed in Pompe disease and other LSDs.[81,82] These pathogenic cascades are discussed below.

Defective autophagy

Autophagy is a major intracellular degradative pathway that regulates processes of degradation and recycling of cellular constituents, organelle turnover (such as impaired lysosome)[83,84] and management of environmental induced stress including nutrient starvation and oxidative stress. During autophagy, especially macroautophagy, a portion of the cytoplasm is sequestered into a double-membrane autophagosome, which further fuses with an endosome and/or lysosome, forming an autolysosome. Subsequently, the cargo is delivered to the lysosome for degradation and recycling.[85-88] Autophagic flux, referring to the rate of lysosomal processing of autophagosomes, is malfunctioning in LSDs leading to massive cellular autophagic buildup.[89-91] In Pompe disease, this impaired autophagic flux is detrimental to muscle function[92,93] and is caused by insufficient autophagosome-lysosome fusion, characterized by combined elevation of autophagic substrates and autophagosome-associated LC3-II accumulation. As a result, massive autophagic buildup including dysfunctional mitochondria and toxic polyubiquitinated proteins aggregate that eventually promote cell death.[94-96]

Aberrant mitochondria

Mitochondria are complex organelles that play a central role in cellular energy metabolism, oxidative homeostasis, calcium signaling and apoptosis.[97,98] Mitochondrial

quality is maintained by autophagy (macroautophagy in particular) through selective elimination of dysfunctional mitochondria, known as mitophagy.[99-101] Mitophagy failure can lead to a destructive cellular cascade. Due to apparent autophagic block in Pompe disease, it is not surprising to detect deformed and potential dysfunctional mitochondria or autophagosomes with partly degraded mitochondria in muscle cells from both mice with Pompe disease and Pompe patients.[102,103]

Mitochondria are the major energy producing organelles. Via oxidative phosphorylation, they are the producers of ATP.[104] If mitophagy is impaired, they are also key generators of reactive oxygen species (ROS).[105] High levels of ROS induce oxidative stress, which is harmful for cells.[106,107] Furthermore, mitochondria serve as a cytosolic buffer for calcium by transiently storing calcium and work closely with endoplasmic reticulum (ER) to maintain Ca^{2+} homeostasis.[108,109] Processes as the aforementioned, including depleted ATP supply, excessive ROS production and mitochondria Ca^{2+} overload, stimulate the opening of mitochondrial outer membrane. This results in release of pro-apoptotic factors normally contained in mitochondria.[110] For instance, the release of cytochrome c or apoptosis-inducing factor can trigger caspase-dependent or caspase- independent forms of apoptosis.[111-114]

Accumulated lipofuscin

Lipofuscin is an autofluorescent inclusion composed of highly cross-linked materials that are indigestible by the lysosome. In Pompe disease, it has been reported to accumulate in neurons and astrocytes of the spinal cord of a LOPD patient and also in muscle fibers.[67,115,116] Lipofuscin formation is usually associated with oxidative damage to cytosolic proteins or mitochondrial oxidative stress.[117] Gradual intralysosomal accumulation of lipofuscin reduces the lysosomal degradation capacity and enhances impairment of autophagy flux, which leads to the accumulation of aberrant mitochondria. Malfunctioned mitochondria will in turn upregulate ROS generation and eventually accelerate the production of lipofuscin. This vicious circle is postulated in the "mitochondrial-lysosomal axis theory of ageing".[118,119] Therefore, either when it occurs as result of ageing or disease, lipofuscin is a sign of mitochondrial dysfunction and oxidative stress,[120,121] and the accumulation indicates that the cross-talk between lysosomes and mitochondria is impaired.

In conclusion, accumulation of metabolic products and the secondary cellular dysfunction featured by flawed autophagy and worn-out mitochondria seem to be the common cellular pathology shared by the majority of LSDs, a process which has also been observed in skeletal muscle cells of Pompe patients. Furthermore, the build-up of non-contractile inclusions, interferes with the contractility of muscle fibers.[122,123]

Autophagic build-up will eventually also impair the intracellular trafficking of lysosomal enzymes to the lysosomes in which the cation-independent mannose 6-phosphate receptor (CI-MPR) plays a crucial role. This may further aggravate build-up of non-degradable products. CI-MPR are present in the trans Golgi network and on the cellular membrane and guide both newly synthesized endogenous lysosomal enzymes and exogenously administered enzymes to the lysosomal compartment. Thus, disturbance of intracellular trafficking will also negatively affect uptake of intravenously administered GAA, which is aimed to serve as enzyme replacement therapy.[124]

4. ENZYME REPLACEMENT THERAPY

Rationale

Under physiological circumstances, acid α-glucosidase (GAA) is synthesized as a protein precursor of 110 kDa that undergoes N-linked glycosylation of all seven potential glycosylation sites in the endoplasmic reticulum by attachment of carbohydrate side chains to asparagine residues in the precursor protein.[125,126] At least two of these carbohydrate side chains are subsequently phosphorylated in the Golgi system to create mannose-6-phosphate (M6P) residues critical for the targeting of the GAA precursor to the lysosome through the cation-independent mannose 6-phosphate receptor (CI-MPR).[125,127,128] Further maturation of GAA is required for acquisition of catalytic activity. This takes place in the lysosome and involves the proteolytic processing of precursor GAA into an intermediate form of 95 kDa, and finally generating the mature forms of 76 and 70 kDa.[129,130] Along this pathway, a small portion of the newly synthesized GAA precursor escapes and enters the Golgi secretory pathway.[131] These secreted precursors have molecular size of 110 kDa and are usually partially phosphorylated. Therefore, in principle, they can be taken up by surrounding cells through CI-MPR-mediated endocytosis.[132] This natural uptake pathway from the extracellular medium into cells is the major principle underlying the feasibility of enzyme replacement therapy.[133,134]

Therapeutic outcome

Enzyme replacement therapy (ERT) with recombinant human acid α-glucosidase (rhGAA) produced from Chinese ovary cells has gained market approval in 2006 for Pompe disease. Different dosing regimens have been used to treat classic infantile Pompe patients, varying from 20 mg/kg every other week to maximally 40 mg/kg every week. Long-term follow-up has shown that ERT significantly diminishes cardiac hypertrophy, and improves pulmonary and motor function. Children also reach new motor milestones, such as sitting and walking, which were not achieved prior to the

availability of ERT. Overall, it has shown to prolong the ventilation-free survival and life expectancy of classic infantile patients substantially compared to the natural disease course.[135,136,137] For children and adults with non-classic Pompe disease, treated with the standard dosage of 20 mg/kg every other week, ERT has shown to increase walking distance and muscle strength, and improve or stabilize pulmonary function.[138-143] ERT has also shown to improve the quality of life and to increase survival rate in these patients.[144,145]

Limitations

Besides the positive effects, ERT also has limitations. Apart from the requirement of life-long bi-weekly/weekly administrations, and very high costs, ERT is not curative. Not only does the magnitude of response vary among individuals, but there are also still residual symptoms even in the best responders, indicating the need for better alternative treatment options.[18,146] This insufficiency could be attributed first to the poor phosphorylation of rhGAA with resultant insufficient M6P residues that limit the uptake of ERT in the target tissues.[147,148] Furthermore, immune responses against infused rhGAA may severely counteract the uptake of the enzyme and therapeutic outcome. In particular in classic infantile patients there is a growing body of evidence that high sustained antibody titers against rhGAA interfere with the efficacy of ERT.[149,150] Although several immune tolerance induction regimens have been applied in the clinic, the sample size is rather small and the effects of long term immune suppression awaits further investigation.[151,152] Moreover, it has been speculated that muscle dysfunction may in part be attributed to neurological components. For instance, deficient efferent phrenic nerve output to the diaphragm was suggested to lead to respiratory insufficiency in a Pompe mouse model.[153] Extensive glycogen accumulation in phrenic motor neurons in the ventral cervical spinal cord (C4),[36,153,154] and motor neuron XII (hypoglossal nucleus) in the brainstem[31,32,34,155] has been suggested to be the underlying cause. As ERT cannot pass the blood-brain barrier, the underlying neurological abnormalities will persist and may impede the overall clinical outcome. Importantly, cognitive decline has been described as a new emerging symptom in long survivors of classic infantile patients.[19,37-39] This renders current ERT insufficient for the treatment of CNS symptoms.[156,157]

Strategies to improve the efficacy of ERT

To increase the abundance of M6P moieties, attempts are being made to artificially add more M6P residues to rhGAA,[158-160] or to use a combination of genetically modified yeast and bacteria to produce M6P-modified GAA.[161] The former is currently tested in a Phase III clinical trial (NCT02782741).

Another approach is to circumvent the necessity for posttranslational modification of the GAA protein by exploiting the insulin-like growth factor II (IGFII) binding region of the CI-MPR to mediate intracellular uptake and subsequent trafficking to the lysosome.[162] The CI-MPR is a bi-functional receptor that binds M6P, but with an even higher affinity also IGFII.[162-164] The fusion of a fragment of insulin-like growth factor II (IGFII) to the GAA enzyme resulted in a 26-fold more efficient *in vitro* uptake in the rat L6 myoblasts compared to normal rhGAA. *In vivo*, ERT with the IGFII fusion protein was 5-fold more effective in clearing glycogen in skeletal muscles of Pompe mice compared to rhGAA, and resulted in more pronounced respiratory improvement.[162,165] This product was subsequently tested in a Phase III clinical trial (NCT01924845). We have incorporated this technique in our lentiviral gene therapy studies detailed in Chapter 3.

Another option which is explored to improve efficacy of ERT is oral co-administration of chaperones (duvoglustat HCl, i.e. AT2220 or miglustat, i.e. AT2221). The chaperone stabilizes intravenously delivered rhGAA, which leads to a longer half-life of GAA in the plasma and skeletal muscles.[166,167] With this approach, a greater glycogen reduction was achieved in heart and skeletal muscle in a Pompe mouse model compared to rhGAA supplied without a chaperone.[168,169] However, to what extent it can help to improve clinical manifestations in patients, and whether these chaperones have side effects (for example by inhibiting alpha-glucosidase since it transiently binds to the active side) needs further analysis.

Other attempts including substrate reduction therapy[170-172] and upregulation of the CI-MPR by a selective β2-agonist (clenbuterol)[173] are also currently explored in preclinical models. While the long term effects in animal models still needs further investigation, these adjunctive therapies are likely to demand the co-administration of ERT. This would mean that they still cannot circumvent the limitations of current ERT, including restricted distribution to the nervous system and occurrence of immune reactions. In addition, long-term use of β2-agonist, like clenbuterol, is not advisable due to several side effects, in particular it is cardiotoxic.[174]

5. GENE THERAPY

Gene therapy is an attractive potentially curative treatment for Pompe disease. Introduction of functional copies of the GAA gene can lead to a continuous internal source of enzyme production. Self-generated enzyme excreted by a depot of cells or organs can be delivered systemically via the circulation to affected cells and tissues, and

the enzyme can be taken up via the CI-MPR as in ERT. Compared to conventional ERT, this approach could provide long-term correction of GAA deficiency. Two major gene therapy approaches have been investigated for Pompe disease. These include *in vivo* delivery of adeno-associated virus (AAV) vectors and *ex vivo* delivery of genetically modified hematopoietic stem progenitor cells (HSPCs) by lentiviral vectors (LV). As the treatment for central nervous system has been extensively discussed in Chapter 2, here, we will focus on the effects of gene therapy addressing the muscular problems in Pompe disease.

In vivo adeno-associated virus (AAV) mediated gene therapy

Adeno-associated virus (AAV) is a single-stranded DNA parvovirus that has been developed into a promising gene delivery vector due to its tissue specificity which is dependent on its serotype, and its long term expression primarily as nonintegrated episomes, which highly reduces the risk of oncogene activation.[175-178] Transduction of AAV is initiated via binding to a variety of cell surface receptors that are serotype-specific.[179-183] Several hybrid AAV vectors containing a GAA transgene have been engineered using the genome of AAV2 and capsid protein of other AAV serotypes including AAV 2/1,[184-188] AAV 2,[184] AAV 2/5,[189,190] AAV 2/6,[191] AAV 2/7[191,192] and AAV 2/8.[192-195] Among these, AAV2/8 is widely used as one of the most potent serotypes to systemically deliver the deficient GAA due to its high tropism for liver, which could serve a major source to generate recombinant human GAA for cross-correction of cardiac and skeletal muscles throughout the body.[196,197]

Systemic delivery of GAA containing AAV2/8 using either a ubiquitous or a muscle-specific promoter was most efficient in clearing glycogen storage in the heart and the diaphragm of Pompe mice. Other skeletal muscles including quadriceps femoris, tibialis anterior and gastrocnemius were more refractory to AAV, and only partial glycogen reduction was achieved. Nevertheless, motor function improved compared to results obtained in *Gaa* knockout mice.[192-194] A liver-specific promoter has been used to induce immune tolerance to GAA.[198-201] Consequently, co-packaging of liver-specific and muscle-specific AAV particles has been proposed aiming to combine immune tolerance induction and therapeutic efficacy in mice.[202] Another option might be localized administration of AAV to the diaphragm[203] or to tibialis anterior (NCT02240407), which can be relevant for children and adult patients with specific abnormalities in restricted areas. First attempts of AAV gene therapy targeting the diaphragm have been performed in children with classic infantile Pompe disease with subtle improvement in unassisted tidal volume.[203]

So far, AAV gene therapy induces partial but not complete phenotypic correction in a Pompe mouse model. Clinically, AAV gene therapy was pioneered to treat patients with hemophilia B in which a small increase of the deficient factor IX to above 1% of the physiologic levels substantially ameliorated the severe bleeding phenotype.[204] However, the AAV vector dose required to mitigate the symptoms in Pompe disease amounted to 10- to 50- fold more than that used to treat hemophilia B mice, implying a much higher therapeutic threshold in this disease background.[202,205,206] While the overall efficacy of this therapy requires further improvement, pre-existing immunity against the AAV capsid due to the natural exposure in early life is a major concern in clinical application.[207] In children, the average prevalence of neutralizing antibody was already 21.5%.[208] This not only prevents the use of certain serotypes of AAV in subset of patients, but also prohibits its readministration. In addition, AAV episomes can be diluted out by cell division. Therefore, the long term efficacy of this therapy is uncertain especially in patients treated at young age.

Ex vivo lentiviral gene therapy

Human immunodeficiency virus (HIV) derived lentiviral vectors (LVs) are able to stably integrate into the host genome of non-dividing cells, and can achieve high levels of transduction and gene expression to provide a permanent source of a transgene product.[209,210] Compared to the early generation of γ-retroviral vectors, LVs induce more robust transgene expression in hematopoietic stem cells (HSCs) and their progeny.[211] Importantly, LVs exhibit lower genotoxicity compared to γ-retroviral vectors, in part by their different integration pattern, which favors actively transcribed genes[212,213] but without a preference for integration at sites where they may activate certain oncogenes.[214] Deletion of the U3 region in the 3' long terminal repeats (LTRs) to generate a self-inactivation (SIN) configuration further improved the vector design by 1) reducing the risk of generation of replication-competent virus upon integration;[215,216] and 2) reducing the risk of insertional upregulation of adjacent genes by incorporating internal promoters, i.e. possibly weaker physiological promoters or cell type-specific promoters.[217-219]

Hematopoietic stem cell transplantation was applied in several LSDs under the assumption that following reconstitution, healthy donor-derived hematopoietic stem cells (HSCs) and their progeny are capable of releasing functional enzyme into the circulation for cross-correction of target tissues.[220-222] Therefore, the insufficient supply of wildtype level of therapeutic enzyme has rendered this treatment inefficient in most LSDs including Pompe disease.[223] However, HSCs and their progeny stand out as a promising internal "enzyme factory", as they are capable of providing life-long continuous supply of the missing enzyme when transduced with LVs (Figure 2) and

because the cells can reach many tissues including the brain (Chapter 2). Importantly, central immune tolerance by HSCP transplantation holds major advantages over ERT and AAV gene therapy.[224,225] This has been explored further in Chapter 6.

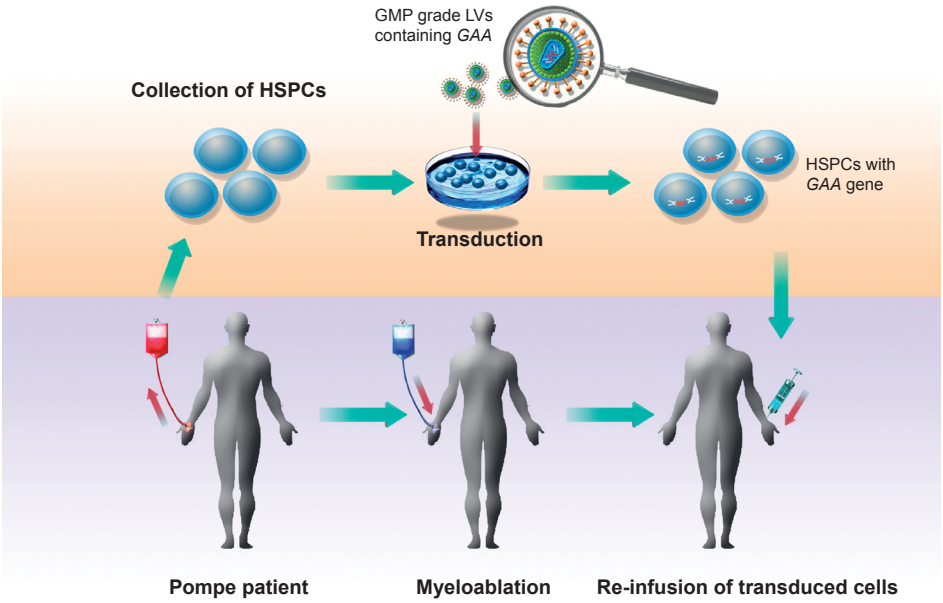

Figure 2. Hematopoietic stem cell mediated lentiviral gene therapy. Hematopoietic stem cell mediated lentiviral gene therapy starts with the collection of hematopoietic stem progenitor cells (HSPCs) from bone marrow or mobilized peripheral blood of the Pompe patient. The HSPCs are then transduced with good manufacturing practice (GMP) grade lentiviral vectors (LVs) harboring the *GAA* transgene. In the meantime, patient will be pre-conditioned with myeloablative chemotherapy. Finally, those genetically modified HSPCs will be transferred back to the conditioned patient for engraftment and hematopoietic reconstitution.

Ex vivo lentiviral gene therapy has first been successfully implemented in clinical trials to treat primary immune deficiencies severe combined immunodeficiency (SCID-X1) and Wiskott-Aldrich syndrome.[226-228] In lysosomal storage diseases, lentiviral gene therapy was pioneered in metachromatic leukodystrophy (MLD). Clinical data obtained from a phase I/II trial demonstrated stable engraftment of transduced HSPCs. This led to restoration of supraphysiological levels of the missing enzyme arylsulfatase A, and as a result, motor performance was normalized in most patients, which was accompanied by reduced demyelination.[229,230] No vector-associated oncogenesis has been reported in these ongoing clinical trials yet after a follow-up of 7 years. This highlights the safety of current LV vectors, and stimulates exploration of this approach for the clinical development of LV gene therapy for other disorders including Pompe disease.

In Pompe disease, the first attempt was performed in *Gaa* knockout mice using LVs carrying a native GAA transgene driven by a myeloproliferative sarcoma virus enhancer, negative control region deleted, dl587rev primer-binding site substituted (MND) promoter.[231] The efficacy of this approach was limited, achieving partial glycogen reduction only in the gastrocnemius, but not in the heart, which is surprising as the heart is the most responsive organ towards treatment with ERT. With an improved transduction regimen, it was demonstrated that reconstitution of the hematopoietic system with genetically modified hematopoietic stem cell progenitors using LVs driven by a spleen focus-forming viral (SF) promoter led to increased GAA activity in target tissues of Pompe mice. Subsequently, glycogen depositions were reduced and cardiac and motor function improved.[232] A codon-optimized version of GAA led to almost complete glycogen clearance in heart and skeletal muscles (Stok *et al*, submitted).

6. SCOPE AND OUTLINE OF THIS THESIS

Current *ex vivo* lentiviral gene therapy in Pompe mice has shown promising results in correcting anomalies in heart and skeletal muscles. However, this was achieved using a strong viral promoter (SF promoter) with a relatively high vector copy number, which may raise concerns of potential genotoxicity in a clinical setting. Most importantly, the brain was still poorly targeted. In the light of recently described neurological involvement in patients, we first reviewed therapeutic strategies that are currently available to address the central nervous system in **Chapter 2**. As the major goal of this thesis, as described in **Chapter 3**, we modified the vector design to improve the efficacy of hematopoietic stem cell mediated lentiviral gene therapy in a Pompe knockout mouse model. We demonstrated that with enhanced targeting of GAA protein using an IGFII tag and the SF promoter, full correction of glycogen accumulation and pathology was achieved in target tissues including the brain. Importantly, in this chapter, we also characterized pathology in the CNS, and found, for the first time, prominent neuroinflammation in a Pompe murine model. In **Chapter 4**, we performed a global proteomic analysis of skeletal muscle obtained from both gene therapy-treated and untreated Pompe mice. Using protein abundance as read out, we revealed several pathways that are impaired in skeletal muscle in the Pompe disease mouse model. The almost complete rescue of differentially expressed proteins to a wildtype level in gene therapy-treated mice provides solid evidence of its efficacy in reversing pathophysiology in addition to reducing glycogen accumulation. To further improve the biosafety of our therapy, in **Chapter 5**, we explored several clinically acceptable promoters, of which the MND promoter excelled as a valid replacement for the SF promoter. Finally, immune tolerance induced by *ex vivo* lentiviral stem cell gene therapy was investigated

in **Chapter 6**. We found that immune tolerance induced by lentiviral gene therapy was established both against the transgene product and against exogenous rhGAA in naïve Pompe mice, and that it was robust even at subtherapeutic dosing of LVs. This paves the way to safely use complementary ERT in combination with lentiviral gene therapy, which might be required if lentiviral gene therapy would have been achieved with insufficient efficacy. **Chapter 7** discusses the findings of this thesis, with a focus on the potential etiology of neuroinflammation and perspectives for future developments.

REFERENCES

1. Hirschhorn R, Reuser AJJ. Glycogen storage disease type II: acid α-glucosidase (acid maltase) deficiency. In: Scriver C, Beaudet, AL, Sly, WS and Valle, D ed. The Metabolic and Molecular Basis for Inherited Disease. New York: McGraw-Hill; 2001:3389–3420.
2. van der Ploeg AT, Reuser AJ. Pompe's disease. *Lancet*. 2008;372(9646):1342-1353.
3. Geddes R, Stratton GC. The influence of lysosomes on glycogen metabolism. *Biochem J*. 1977;163(2):193-200.
4. Hers HG. alpha-Glucosidase deficiency in generalized glycogenstorage disease (Pompe's disease). *Biochem J*. 1963;86:11-16.
5. Brown BI, Brown DH, Jeffrey PL. Simultaneous absence of alpha-1,4-glucosidase and alpha-1,6-glucosidase activities (pH 4) in tissues of children with type II glycogen storage disease. *Biochemistry*. 1970;9(6):1423-1428.
6. Jeffrey PL, Brown DH, Brown BI. Studies of lysosomal alpha-glucosidase. I. Purification and properties of the rat liver enzyme. *Biochemistry*. 1970;9(6):1403-1415.
7. Jeffrey PL, Brown DH, Brown BI. Studies of lysosomal alpha-glucosidase. II. Kinetics of action of the rat liver enzyme. *Biochemistry*. 1970;9(6):1416-1422.
8. Thurberg BL, Lynch Maloney C, Vaccaro C, et al. Characterization of pre- and post-treatment pathology after enzyme replacement therapy for Pompe disease. *Lab Invest*. 2006;86(12):1208-1220.
9. Kuo WL, Hirschhorn R, Huie ML, Hirschhorn K. Localization and ordering of acid alpha-glucosidase (GAA) and thymidine kinase (TK1) by fluorescence in situ hybridization. *Hum Genet*. 1996;97(3):404-406.
10. van den Hout HM, Hop W, van Diggelen OP, et al. The natural course of infantile Pompe's disease: 20 original cases compared with 133 cases from the literature. *Pediatrics*. 2003;112(2):332-340.
11. Howell RR, Byrne B, Darras BT, Kishnani P, Nicolino M, van der Ploeg A. Diagnostic challenges for Pompe disease: an under-recognized cause of floppy baby syndrome. *Genet Med*. 2006;8(5):289-296.
12. Kishnani PS, Hwu WL, Mandel H, Nicolino M, Yong F, Corzo D. A retrospective, multinational, multicenter study on the natural history of infantile-onset Pompe disease. *J Pediatr*. 2006;148(5):671-676.
13. Seifert BL, Snyder MS, Klein AA, O'Loughlin JE, Magid MS, Engle MA. Development of obstruction to ventricular outflow and impairment of inflow in glycogen storage disease of the heart: serial echocardiographic studies from birth to death at 6 months. *Am Heart J*. 1992;123(1):239-242.
14. Prater SN, Banugaria SG, DeArmey SM, et al. The emerging phenotype of long-term survivors with infantile Pompe disease. *Genet Med*. 2012;14(9):800-810.
15. Kamphoven JH, de Ruiter MM, Winkel LP, et al. Hearing loss in infantile Pompe's disease and determination of underlying pathology in the knockout mouse. *Neurobiol Dis*. 2004;16(1):14-20.

16. Kishnani PS, Nicolino M, Voit T, et al. Chinese hamster ovary cell-derived recombinant human acid alpha-glucosidase in infantile-onset Pompe disease. *J Pediatr.* 2006;149(1):89-97.
17. van Capelle CI, Goedegebure A, Homans NC, Hoeve HL, Reuser AJ, van der Ploeg AT. Hearing loss in Pompe disease revisited: results from a study of 24 children. *J Inherit Metab Dis.* 2010;33(5):597-602.
18. Hahn A, Praetorius S, Karabul N, et al. Outcome of patients with classical infantile pompe disease receiving enzyme replacement therapy in Germany. *JIMD Rep.* 2015;20:65-75.
19. Matsuoka T, Miwa Y, Tajika M, et al. Divergent clinical outcomes of alpha-glucosidase enzyme replacement therapy in two siblings with infantile-onset Pompe disease treated in the symptomatic or pre-symptomatic state. *Mol Genet Metab Rep.* 2016;9:98-105.
20. Slingerland NW, Polling JR, van Gelder CM, van der Ploeg AT, Bleyen I. Ptosis, extraocular motility disorder, and myopia as features of pompe disease. *Orbit.* 2011;30(2):111-113.
21. Prakalapakorn SG, Proia AD, Yanovitch TL, et al. Ocular and histologic findings in a series of children with infantile pompe disease treated with enzyme replacement therapy. *J Pediatr Ophthalmol Strabismus.* 2014;51(6):355-362.
22. Muller CW, Jones HN, O'Grady G, Suárez AH, Heller JH, Kishnani PS. Language and speech function in children with infantile Pompe disease. *Journal of Pediatric Neurology.* 2009;7(2):147-156.
23. van Gelder CM, van Capelle CI, Ebbink BJ, et al. Facial-muscle weakness, speech disorders and dysphagia are common in patients with classic infantile Pompe disease treated with enzyme therapy. *J Inherit Metab Dis.* 2012;35(3):505-511.
24. Chien YH, Lee NC, Chen CA, et al. Long-term prognosis of patients with infantile-onset Pompe disease diagnosed by newborn screening and treated since birth. *J Pediatr.* 2015;166(4):985-991 e981-982.
25. Zeng YT, Hwu WL, Torng PC, et al. Longitudinal follow-up to evaluate speech disorders in early-treated patients with infantile-onset Pompe disease. *Eur J Paediatr Neurol.* 2016.
26. Jones HN, Muller CW, Lin M, et al. Oropharyngeal dysphagia in infants and children with infantile Pompe disease. *Dysphagia.* 2010;25(4):277-283.
27. Swift G, Cleary M, Grunewald S, Lozano S, Ryan M, Davison J. Swallow Prognosis and Follow-Up Protocol in Infantile Onset Pompe Disease. *JIMD Rep.* 2016.
28. Case LE, Hanna R, Frush DP, et al. Fractures in children with Pompe disease: a potential long-term complication. *Pediatr Radiol.* 2007;37(5):437-445.
29. van den Berg LE, Zandbergen AA, van Capelle CI, et al. Low bone mass in Pompe disease: muscular strength as a predictor of bone mineral density. *Bone.* 2010;47(3):643-649.
30. Caddell JL, Whittemore R. Observations on generalized glycogenosis with emphasis on electrocardiographic changes. *Pediatrics.* 1962;29:743-763.
31. Crome L, Cumings JN, Duckett S. Neuropathological and Neurochemical Aspects of Generalized Glycogen Storage Disease. *J Neurol Neurosurg Psychiatry.* 1963;26:422-430.
32. Mancall EL, Aponte GE, Berry RG. Pompe's Disease (Diffuse Glycogenosis) with Neuronal Storage. *J Neuropathol Exp Neurol.* 1965;24:85-96.

33. Gambetti P, DiMauro S, Baker L. Nervous system in Pompe's disease. Ultrastructure and biochemistry. *J Neuropathol Exp Neurol*. 1971;30(3):412-430.
34. Martin JJ, de Barsy T, van Hoof F, Palladini G. Pompe's disease: an inborn lysosomal disorder with storage of glycogen. A study of brain and striated muscle. *Acta Neuropathol*. 1973;23(3):229-244.
35. Martini C, Ciana G, Benettoni A, et al. Intractable fever and cortical neuronal glycogen storage in glycogenosis type 2. *Neurology*. 2001;57(5):906-908.
36. Teng YT, Su WJ, Hou JW, Huang SF. Infantile-onset glycogen storage disease type II (Pompe disease): report of a case with genetic diagnosis and pathological findings. *Chang Gung Med J*. 2004;27(5):379-384.
37. Rohrbach M, Klein A, Kohli-Wiesner A, et al. CRIM-negative infantile Pompe disease: 42-month treatment outcome. *J Inherit Metab Dis*. 2010;33(6):751-757.
38. Ebbink BJ, Aarsen FK, van Gelder CM, et al. Cognitive outcome of patients with classic infantile Pompe disease receiving enzyme therapy. *Neurology*. 2012;78(19):1512-1518.
39. Ebbink BJ, Poelman E, Plug I, et al. Cognitive decline in classic infantile Pompe disease: An underacknowledged challenge. *Neurology*. 2016;86(13):1260-1261.
40. Chien YH, Lee NC, Peng SF, Hwu WL. Brain development in infantile-onset Pompe disease treated by enzyme replacement therapy. *Pediatr Res*. 2006;60(3):349-352.
41. van Capelle CI, van der Meijden JC, van den Hout JM, et al. Childhood Pompe disease: clinical spectrum and genotype in 31 patients. *Orphanet J Rare Dis*. 2016;11(1):65.
42. Roberts M, Kishnani PS, van der Ploeg AT, et al. The prevalence and impact of scoliosis in Pompe disease: lessons learned from the Pompe Registry. *Mol Genet Metab*. 2011;104(4):574-582.
43. Fadic R, Waclawik AJ, Brooks BR, Lotz BP. The rigid spine syndrome due to acid maltase deficiency. *Muscle Nerve*. 1997;20(3):364-366.
44. Kostera-Pruszczyk A, Opuchlik A, Lugowska A, et al. Juvenile onset acid maltase deficiency presenting as a rigid spine syndrome. *Neuromuscul Disord*. 2006;16(4):282-285.
45. Hagemans ML, Winkel LP, Van Doorn PA, et al. Clinical manifestation and natural course of late-onset Pompe's disease in 54 Dutch patients. *Brain*. 2005;128(Pt 3):671-677.
46. Hagemans ML, van Schie SP, Janssens AC, van Doorn PA, Reuser AJ, van der Ploeg AT. Fatigue: an important feature of late-onset Pompe disease. *J Neurol*. 2007;254(7):941-945.
47. Gungor D, Schober AK, Kruijshaar ME, et al. Pain in adult patients with Pompe disease: a cross-sectional survey. *Mol Genet Metab*. 2013;109(4):371-376.
48. Wens SC, Ciet P, Perez-Rovira A, et al. Lung MRI and impairment of diaphragmatic function in Pompe disease. *BMC Pulm Med*. 2015;15:54.
49. Margolis ML, Howlett P, Goldberg R, Eftychiadis A, Levine S. Obstructive sleep apnea syndrome in acid maltase deficiency. *Chest*. 1994;105(3):947-949.
50. Kansagra S, Austin S, DeArmey S, Kazi Z, Kravitz RM, Kishnani PS. Longitudinal polysomnographic findings in infantile Pompe disease. *Am J Med Genet A*. 2015;167A(4):858-861.

51. Hagemans ML, Hop WJ, Van Doorn PA, Reuser AJ, Van der Ploeg AT. Course of disability and respiratory function in untreated late-onset Pompe disease. *Neurology*. 2006;66(4):581-583.
52. Van der Beek NA, Hagemans ML, Reuser AJ, et al. Rate of disease progression during long-term follow-up of patients with late-onset Pompe disease. *Neuromuscul Disord*. 2009;19(2):113-117.
53. van der Beek NA, van Capelle CI, van der Velden-van Etten KI, et al. Rate of progression and predictive factors for pulmonary outcome in children and adults with Pompe disease. *Mol Genet Metab*. 2011;104(1-2):129-136.
54. van der Beek NA, de Vries JM, Hagemans ML, et al. Clinical features and predictors for disease natural progression in adults with Pompe disease: a nationwide prospective observational study. *Orphanet J Rare Dis*. 2012;7:88.
55. Laforet P, Doppler V, Caillaud C, et al. Rigid spine syndrome revealing late-onset Pompe disease. *Neuromuscul Disord*. 2010;20(2):128-130.
56. Dubrovsky A, Corderi J, Lin M, Kishnani PS, Jones HN. Expanding the phenotype of late-onset Pompe disease: tongue weakness: a new clinical observation. *Muscle Nerve*. 2011;44(6):897-901.
57. Hobson-Webb LD, Jones HN, Kishnani PS. Oropharyngeal dysphagia may occur in late-onset Pompe disease, implicating bulbar muscle involvement. *Neuromuscul Disord*. 2013;23(4):319-323.
58. Jones HN, Crisp KD, Asrani P, Sloane R, Kishnani PS. Quantitative assessment of lingual strength in late-onset Pompe disease. *Muscle Nerve*. 2015;51(5):731-735.
59. Szklanny K, Gubrynowicz R, Iwanicka-Pronicka K, Tylki-Szymanska A. Analysis of voice quality in patients with late-onset Pompe disease. *Orphanet J Rare Dis*. 2016;11(1):99.
60. Groen WB, Leen WG, Vos AM, Cruysberg JR, van Doorn PA, van Engelen BG. Ptosis as a feature of late-onset glycogenosis type II. *Neurology*. 2006;67(12):2261-2262.
61. van der Beek NA, Verschuure H, Reuser AJ, van der Ploeg AT, van Doorn PA, Poublon RM. Hearing in adults with Pompe disease. *J Inherit Metab Dis*. 2012;35(2):335-341.
62. Montagnese F, Barca E, Musumeci O, et al. Clinical and molecular aspects of 30 patients with late-onset Pompe disease (LOPD): unusual features and response to treatment. *J Neurol*. 2015;262(4):968-978.
63. Musumeci O, Catalano N, Barca E, et al. Auditory system involvement in late onset Pompe disease: a study of 20 Italian patients. *Mol Genet Metab*. 2012;107(3):480-484.
64. Hanisch F, Rahne T, Plontke SK. Prevalence of hearing loss in patients with late-onset Pompe disease: Audiological and otological consequences. *Int J Audiol*. 2013;52(12):816-823.
65. Wens SC, Kuperus E, Mattace-Raso FU, et al. Increased aortic stiffness and blood pressure in non-classic Pompe disease. *J Inherit Metab Dis*. 2014;37(3):391-397.
66. El-Gharbawy AH, Bhat G, Murillo JE, et al. Expanding the clinical spectrum of late-onset Pompe disease: dilated arteriopathy involving the thoracic aorta, a novel vascular phenotype uncovered. *Mol Genet Metab*. 2011;103(4):362-366.

67. Kretzschmar HA, Wagner H, Hubner G, Danek A, Witt TN, Mehraein P. Aneurysms and vacuolar degeneration of cerebral arteries in late-onset acid maltase deficiency. *J Neurol Sci.* 1990;98(2-3):169-183.

68. Laforet P, Petiot P, Nicolino M, et al. Dilative arteriopathy and basilar artery dolichoectasia complicating late-onset Pompe disease. *Neurology.* 2008;70(22):2063-2066.

69. Remiche G, Herbaut AG, Ronchi D, et al. Incontinence in late-onset Pompe disease: an underdiagnosed treatable condition. *Eur Neurol.* 2012;68(2):75-78.

70. Karabul N, Skudlarek A, Berndt J, et al. Urge incontinence and gastrointestinal symptoms in adult patients with pompe disease: a cross-sectional survey. *JIMD Rep.* 2014;17:53-61.

71. McNamara ER, Austin S, Case L, Wiener JS, Peterson AC, Kishnani PS. Expanding our understanding of lower urinary tract symptoms and incontinence in adults with pompe disease. *JIMD Rep.* 2015;20:5-10.

72. Martin JJ, de Barsy T, den Tandt WR. Acid maltase deficiency in non-identical adult twins. A morphological and biochemical study. *J Neurol.* 1976;213(2):105-118.

73. Hobson-Webb LD, Proia AD, Thurberg BL, Banugaria S, Prater SN, Kishnani PS. Autopsy findings in late-onset Pompe disease: a case report and systematic review of the literature. *Mol Genet Metab.* 2012;106(4):462-469.

74. Borroni B, Cotelli MS, Premi E, et al. The brain in late-onset glycogenosis II: a structural and functional MRI study. *J Inherit Metab Dis.* 2013;36(6):989-995.

75. Chan J, Desai AK, Kazi ZB, et al. The emerging phenotype of late-onset Pompe disease: A systematic literature review. *Mol Genet Metab.* 2016.

76. Lacomis D. Small-fiber neuropathy. *Muscle Nerve.* 2002;26(2):173-188.

77. Hobson-Webb LD, Austin SL, Jain S, Case LE, Greene K, Kishnani PS. Small-fiber neuropathy in pompe disease: first reported cases and prospective screening of a clinic cohort. *Am J Case Rep.* 2015;16:196-201.

78. Origuchi Y, Itai Y, Matsumoto S, Matsuishi T. Quantitative histological study of the sural nerve in a child with acid maltase deficiency (glycogenosis type II). *Pediatr Neurol.* 1986;2(6):346-349.

79. Fidzianska A, Lugowska A, Tylki-Szymanska A. Late form of Pompe disease with glycogen storage in peripheral nerves axons. *J Neurol Sci.* 2011;301(1-2):59-62.

80. Xu H, Ren D. Lysosomal physiology. *Annu Rev Physiol.* 2015;77:57-80.

81. Lim JA, Kakhlon O, Li L, Myerowitz R, Raben N. Pompe disease: Shared and unshared features of lysosomal storage disorders. *Rare Dis.* 2015;3(1):e1068978.

82. Bellettato CM, Scarpa M. Pathophysiology of neuropathic lysosomal storage disorders. *J Inherit Metab Dis.* 2010;33(4):347-362.

83. Hung YH, Chen LM, Yang JY, Yang WY. Spatiotemporally controlled induction of autophagy-mediated lysosome turnover. *Nat Commun.* 2013;4:2111.

84. Maejima I, Takahashi A, Omori H, et al. Autophagy sequesters damaged lysosomes to control lysosomal biogenesis and kidney injury. *Embo J.* 2013;32(17):2336-2347.

85. Yang Z, Klionsky DJ. Mammalian autophagy: core molecular machinery and signaling regulation. *Curr Opin Cell Biol.* 2010;22(2):124-131.

86. Klionsky DJ. The molecular machinery of autophagy: unanswered questions. *J Cell Sci*. 2005;118(Pt 1):7-18.

87. Kuma A, Mizushima N. Physiological role of autophagy as an intracellular recycling system: with an emphasis on nutrient metabolism. *Semin Cell Dev Biol*. 2010;21(7):683-690.

88. Singh R, Cuervo AM. Autophagy in the cellular energetic balance. *Cell Metab*. 2011;13(5):495-504.

89. Settembre C, Fraldi A, Jahreiss L, et al. A block of autophagy in lysosomal storage disorders. *Hum Mol Genet*. 2008;17(1):119-129.

90. Ballabio A. Disease pathogenesis explained by basic science: lysosomal storage diseases as autophagocytic disorders. *Int J Clin Pharmacol Ther*. 2009;47 Suppl 1:S34-38.

91. Ballabio A, Gieselmann V. Lysosomal disorders: from storage to cellular damage. *Biochim Biophys Acta*. 2009;1793(4):684-696.

92. Nascimbeni AC, Fanin M, Masiero E, Angelini C, Sandri M. The role of autophagy in the pathogenesis of glycogen storage disease type II (GSDII). *Cell Death Differ*. 2012;19(10):1698-1708.

93. Nascimbeni AC, Fanin M, Masiero E, Angelini C, Sandri M. Impaired autophagy contributes to muscle atrophy in glycogen storage disease type II patients. *Autophagy*. 2012;8(11):1697-1700.

94. Lieberman AP, Puertollano R, Raben N, Slaugenhaupt S, Walkley SU, Ballabio A. Autophagy in lysosomal storage disorders. *Autophagy*. 2012;8(5):719-730.

95. Boya P, Gonzalez-Polo RA, Casares N, et al. Inhibition of macroautophagy triggers apoptosis. *Mol Cell Biol*. 2005;25(3):1025-1040.

96. Raben N, Hill V, Shea L, et al. Suppression of autophagy in skeletal muscle uncovers the accumulation of ubiquitinated proteins and their potential role in muscle damage in Pompe disease. *Hum Mol Genet*. 2008;17(24):3897-3908.

97. Nunnari J, Suomalainen A. Mitochondria: in sickness and in health. *Cell*. 2012;148(6):1145-1159.

98. Vakifahmetoglu-Norberg H, Ouchida AT, Norberg E. The role of mitochondria in metabolism and cell death. *Biochem Biophys Res Commun*. 2017;482(3):426-431.

99. Kim I, Rodriguez-Enriquez S, Lemasters JJ. Selective degradation of mitochondria by mitophagy. *Arch Biochem Biophys*. 2007;462(2):245-253.

100. Wang K, Klionsky DJ. Mitochondria removal by autophagy. *Autophagy*. 2011;7(3):297-300.

101. Youle RJ, Narendra DP. Mechanisms of mitophagy. *Nat Rev Mol Cell Biol*. 2011;12(1):9-14.

102. Lim JA, Li L, Kakhlon O, Myerowitz R, Raben N. Defects in calcium homeostasis and mitochondria can be reversed in Pompe disease. *Autophagy*. 2015;11(2):385-402.

103. Sato Y, Kobayashi H, Higuchi T, Shimada Y, Ida H, Ohashi T. Metabolomic Profiling of Pompe Disease-Induced Pluripotent Stem Cell-Derived Cardiomyocytes Reveals That Oxidative Stress Is Associated with Cardiac and Skeletal Muscle Pathology. *Stem Cells Transl Med*. 2017;6(1):31-39.

104. Huttemann M, Lee I, Samavati L, Yu H, Doan JW. Regulation of mitochondrial oxidative phosphorylation through cell signaling. *Biochim Biophys Acta.* 2007;1773(12):1701-1720.

105. Liu Y, Fiskum G, Schubert D. Generation of reactive oxygen species by the mitochondrial electron transport chain. *J Neurochem.* 2002;80(5):780-787.

106. Li J, O W, Li W, Jiang ZG, Ghanbari HA. Oxidative stress and neurodegenerative disorders. *Int J Mol Sci.* 2013;14(12):24438-24475.

107. Schieber M, Chandel NS. ROS function in redox signaling and oxidative stress. *Curr Biol.* 2014;24(10):R453-462.

108. Carafoli E. Calcium signaling: a tale for all seasons. *Proc Natl Acad Sci U S A.* 2002;99(3):1115-1122.

109. Pizzo P, Pozzan T. Mitochondria-endoplasmic reticulum choreography: structure and signaling dynamics. *Trends Cell Biol.* 2007;17(10):511-517.

110. Green DR, Kroemer G. The pathophysiology of mitochondrial cell death. *Science.* 2004;305(5684):626-629.

111. Liu X, Kim CN, Yang J, Jemmerson R, Wang X. Induction of apoptotic program in cell-free extracts: requirement for dATP and cytochrome c. *Cell.* 1996;86(1):147-157.

112. Ott M, Robertson JD, Gogvadze V, Zhivotovsky B, Orrenius S. Cytochrome c release from mitochondria proceeds by a two-step process. *Proc Natl Acad Sci U S A.* 2002;99(3):1259-1263.

113. Susin SA, Lorenzo HK, Zamzami N, et al. Molecular characterization of mitochondrial apoptosis-inducing factor. *Nature.* 1999;397(6718):441-446.

114. Green D, Kroemer G. The central executioners of apoptosis: caspases or mitochondria? *Trends Cell Biol.* 1998;8(7):267-271.

115. Feeney EJ, Austin S, Chien YH, et al. The value of muscle biopsies in Pompe disease: identifying lipofuscin inclusions in juvenile- and adult-onset patients. *Acta Neuropathol Commun.* 2014;2:2.

116. Lim JA, Li L, Raben N. Pompe disease: from pathophysiology to therapy and back again. *Front Aging Neurosci.* 2014;6:177.

117. Jung T, Bader N, Grune T. Lipofuscin: formation, distribution, and metabolic consequences. *Ann N Y Acad Sci.* 2007;1119:97-111.

118. Terman A, Gustafsson B, Brunk UT. The lysosomal-mitochondrial axis theory of postmitotic aging and cell death. *Chem Biol Interact.* 2006;163(1-2):29-37.

119. Terman A, Kurz T, Navratil M, Arriaga EA, Brunk UT. Mitochondrial turnover and aging of long-lived postmitotic cells: the mitochondrial-lysosomal axis theory of aging. *Antioxid Redox Signal.* 2010;12(4):503-535.

120. Gray DA, Woulfe J. Lipofuscin and aging: a matter of toxic waste. *Sci Aging Knowledge Environ.* 2005;2005(5):re1.

121. Terman A, Brunk UT. Oxidative stress, accumulation of biological 'garbage', and aging. *Antioxid Redox Signal.* 2006;8(1-2):197-204.

122. Drost MR, Hesselink RP, Oomens CW, van der Vusse GJ. Effects of non-contractile inclusions on mechanical performance of skeletal muscle. *J Biomech*. 2005;38(5):1035-1043.

123. Hesselink RP, Wagenmakers AJ, Drost MR, Van der Vusse GJ. Lysosomal dysfunction in muscle with special reference to glycogen storage disease type II. *Biochim Biophys Acta*. 2003;1637(2):164-170.

124. Cardone M, Porto C, Tarallo A, et al. Abnormal mannose-6-phosphate receptor trafficking impairs recombinant alpha-glucosidase uptake in Pompe disease fibroblasts. *Pathogenetics*. 2008;1(1):6.

125. Hermans MM, Wisselaar HA, Kroos MA, Oostra BA, Reuser AJ. Human lysosomal alpha-glucosidase: functional characterization of the glycosylation sites. *Biochem J*. 1993;289 (Pt 3):681-686.

126. Jongen SP, Gerwig GJ, Leeflang BR, et al. N-glycans of recombinant human acid alpha-glucosidase expressed in the milk of transgenic rabbits. *Glycobiology*. 2007;17(6):600-619.

127. Hasilik A, Neufeld EF. Biosynthesis of lysosomal enzymes in fibroblasts. Phosphorylation of mannose residues. *J Biol Chem*. 1980;255(10):4946-4950.

128. Reuser AJ, Kroos M, Oude Elferink RP, Tager JM. Defects in synthesis, phosphorylation, and maturation of acid alpha-glucosidase in glycogenosis type II. *J Biol Chem*. 1985;260(14):8336-8341.

129. Wisselaar HA, Kroos MA, Hermans MM, van Beeumen J, Reuser AJ. Structural and functional changes of lysosomal acid alpha-glucosidase during intracellular transport and maturation. *J Biol Chem*. 1993;268(3):2223-2231.

130. Moreland RJ, Jin X, Zhang XK, et al. Lysosomal acid alpha-glucosidase consists of four different peptides processed from a single chain precursor. *J Biol Chem*. 2005;280(8):6780-6791.

131. Hoefsloot LH, Willemsen R, Kroos MA, et al. Expression and routeing of human lysosomal alpha-glucosidase in transiently transfected mammalian cells. *Biochem J*. 1990;272(2):485-492.

132. Reuser AJ, Kroos MA, Ponne NJ, et al. Uptake and stability of human and bovine acid alpha-glucosidase in cultured fibroblasts and skeletal muscle cells from glycogenosis type II patients. *Exp Cell Res*. 1984;155(1):178-189.

133. Van Hove JL, Yang HW, Wu JY, Brady RO, Chen YT. High-level production of recombinant human lysosomal acid alpha-glucosidase in Chinese hamster ovary cells which targets to heart muscle and corrects glycogen accumulation in fibroblasts from patients with Pompe disease. *Proc Natl Acad Sci U S A*. 1996;93(1):65-70.

134. Bijvoet AG, Kroos MA, Pieper FR, et al. Recombinant human acid alpha-glucosidase: high level production in mouse milk, biochemical characteristics, correction of enzyme deficiency in GSDII KO mice. *Hum Mol Genet*. 1998;7(11):1815-1824.

135. Kishnani PS, Corzo D, Leslie ND, et al. Early treatment with alglucosidase alpha prolongs long-term survival of infants with Pompe disease. *Pediatr Res*. 2009;66(3):329-335.

136. Nicolino M, Byrne B, Wraith JE, et al. Clinical outcomes after long-term treatment with alglucosidase alfa in infants and children with advanced Pompe disease. *Genet Med*. 2009;11(3):210-219.

137. van Gelder CM, Poelman E, Plug I, et al. Effects of a higher dose of alglucosidase alfa on ventilator-free survival and motor outcome in classic infantile Pompe disease: an open-label single-center study. *J Inherit Metab Dis*. 2016;39(3):383-390.

138. van Capelle CI, Winkel LP, Hagemans ML, et al. Eight years experience with enzyme replacement therapy in two children and one adult with Pompe disease. *Neuromuscul Disord*. 2008;18(6):447-452.

139. van der Ploeg AT, Barohn R, Carlson L, et al. Open-label extension study following the Late-Onset Treatment Study (LOTS) of alglucosidase alfa. *Mol Genet Metab*. 2012;107(3):456-461.

140. de Vries JM, van der Beek NA, Hop WC, et al. Effect of enzyme therapy and prognostic factors in 69 adults with Pompe disease: an open-label single-center study. *Orphanet J Rare Dis*. 2012;7:73.

141. Regnery C, Kornblum C, Hanisch F, et al. 36 months observational clinical study of 38 adult Pompe disease patients under alglucosidase alfa enzyme replacement therapy. *J Inherit Metab Dis*. 2012;35(5):837-845.

142. Bembi B, Pisa FE, Confalonieri M, et al. Long-term observational, non-randomized study of enzyme replacement therapy in late-onset glycogenosis type II. *J Inherit Metab Dis*. 2010;33(6):727-735.

143. Angelini C, Semplicini C, Ravaglia S, et al. Observational clinical study in juvenile-adult glycogenosis type 2 patients undergoing enzyme replacement therapy for up to 4 years. *J Neurol*. 2012;259(5):952-958.

144. Gungor D, Kruijshaar ME, Plug I, et al. Quality of life and participation in daily life of adults with Pompe disease receiving enzyme replacement therapy: 10 years of international follow-up. *J Inherit Metab Dis*. 2016;39(2):253-260.

145. Gungor D, Kruijshaar ME, Plug I, et al. Impact of enzyme replacement therapy on survival in adults with Pompe disease: results from a prospective international observational study. *Orphanet J Rare Dis*. 2013;8:49.

146. Chakrapani A, Vellodi A, Robinson P, Jones S, Wraith JE. Treatment of infantile Pompe disease with alglucosidase alpha: the UK experience. *J Inherit Metab Dis*. 2010;33(6):747-750.

147. Zhao KW, Neufeld EF. Purification and characterization of recombinant human alpha-N-acetylglucosaminidase secreted by Chinese hamster ovary cells. *Protein Expr Purif*. 2000;19(1):202-211.

148. Togawa T, Takada M, Aizawa Y, Tsukimura T, Chiba Y, Sakuraba H. Comparative study on mannose 6-phosphate residue contents of recombinant lysosomal enzymes. *Mol Genet Metab*. 2014;111(3):369-373.

149. Banugaria SG, Prater SN, Ng YK, et al. The impact of antibodies on clinical outcomes in diseases treated with therapeutic protein: lessons learned from infantile Pompe disease. *Genet Med*. 2011;13(8):729-736.

150. van Gelder CM, Hoogeveen-Westerveld M, Kroos MA, Plug I, van der Ploeg AT, Reuser AJ. Enzyme therapy and immune response in relation to CRIM status: the Dutch experience in classic infantile Pompe disease. *J Inherit Metab Dis*. 2015;38(2):305-314.

151. Mendelsohn NJ, Messinger YH, Rosenberg AS, Kishnani PS. Elimination of antibodies to recombinant enzyme in Pompe's disease. *N Engl J Med*. 2009;360(2):194-195.

152. Kazi ZB, Prater SN, Kobori JA, et al. Durable and sustained immune tolerance to ERT in Pompe disease with entrenched immune responses. *JCI Insight*. 2016;1(11).

153. DeRuisseau LR, Fuller DD, Qiu K, et al. Neural deficits contribute to respiratory insufficiency in Pompe disease. *Proc Natl Acad Sci U S A*. 2009;106(23):9419-9424.

154. Sidman RL, Taksir T, Fidler J, et al. Temporal neuropathologic and behavioral phenotype of 6neo/6neo Pompe disease mice. *J Neuropathol Exp Neurol*. 2008;67(8):803-818.

155. Lee KZ, Qiu K, Sandhu MS, et al. Hypoglossal neuropathology and respiratory activity in pompe mice. *Front Physiol*. 2011;2:31.

156. Van der Ploeg AT, Kroos MA, Willemsen R, Brons NH, Reuser AJ. Intravenous administration of phosphorylated acid alpha-glucosidase leads to uptake of enzyme in heart and skeletal muscle of mice. *J Clin Invest*. 1991;87(2):513-518.

157. Desnick RJ, Schuchman EH. Enzyme replacement therapy for lysosomal diseases: lessons from 20 years of experience and remaining challenges. *Annu Rev Genomics Hum Genet*. 2012;13:307-335.

158. Zhu Y, Li X, Kyazike J, et al. Conjugation of mannose 6-phosphate-containing oligosaccharides to acid alpha-glucosidase improves the clearance of glycogen in pompe mice. *J Biol Chem*. 2004;279(48):50336-50341.

159. Zhu Y, Li X, McVie-Wylie A, et al. Carbohydrate-remodelled acid alpha-glucosidase with higher affinity for the cation-independent mannose 6-phosphate receptor demonstrates improved delivery to muscles of Pompe mice. *Biochem J*. 2005;389(Pt 3):619-628.

160. Zhu Y, Jiang JL, Gumlaw NK, et al. Glycoengineered acid alpha-glucosidase with improved efficacy at correcting the metabolic aberrations and motor function deficits in a mouse model of Pompe disease. *Mol Ther*. 2009;17(6):954-963.

161. Tiels P, Baranova E, Piens K, et al. A bacterial glycosidase enables mannose-6-phosphate modification and improved cellular uptake of yeast-produced recombinant human lysosomal enzymes. *Nat Biotechnol*. 2012;30(12):1225-1231.

162. Maga JA, Zhou J, Kambampati R, et al. Glycosylation-independent lysosomal targeting of acid alpha-glucosidase enhances muscle glycogen clearance in pompe mice. *J Biol Chem*. 2013;288(3):1428-1438.

163. Kornfeld S. Structure and function of the mannose 6-phosphate/insulinlike growth factor II receptors. *Annu Rev Biochem*. 1992;61:307-330.

164. Devi GR, Byrd JC, Slentz DH, MacDonald RG. An insulin-like growth factor II (IGF-II) affinity-enhancing domain localized within extracytoplasmic repeat 13 of the IGF-II/mannose 6-phosphate receptor. *Mol Endocrinol*. 1998;12(11):1661-1672.

165. Peng J, Dalton J, Butt M, et al. Reveglucosidase alfa (BMN 701), an IGF2-Tagged rhAcid alpha-Glucosidase, Improves Respiratory Functional Parameters in a Murine Model of Pompe Disease. *J Pharmacol Exp Ther*. 2017;360(2):313-323.

166. Kishnani P, Tarnopolsky M, Roberts M, et al. Duvoglustat HCl Increases Systemic and Tissue Exposure of Active Acid alpha-Glucosidase in Pompe Patients Co-administered with Alglucosidase alpha. *Mol Ther*. 2017.

167. Parenti G, Fecarotta S, la Marca G, et al. A chaperone enhances blood alpha-glucosidase activity in Pompe disease patients treated with enzyme replacement therapy. *Mol Ther*. 2014;22(11):2004-2012.

168. Khanna R, Flanagan JJ, Feng J, et al. The pharmacological chaperone AT2220 increases recombinant human acid alpha-glucosidase uptake and glycogen reduction in a mouse model of Pompe disease. *PLoS One*. 2012;7(7):e40776.

169. Khanna R, Powe AC, Jr., Lun Y, et al. The pharmacological chaperone AT2220 increases the specific activity and lysosomal delivery of mutant acid alpha-glucosidase, and promotes glycogen reduction in a transgenic mouse model of Pompe disease. *PLoS One*. 2014;9(7):e102092.

170. Douillard-Guilloux G, Raben N, Takikita S, Batista L, Caillaud C, Richard E. Modulation of glycogen synthesis by RNA interference: towards a new therapeutic approach for glycogenosis type II. *Hum Mol Genet*. 2008;17(24):3876-3886.

171. Douillard-Guilloux G, Raben N, Takikita S, et al. Restoration of muscle functionality by genetic suppression of glycogen synthesis in a murine model of Pompe disease. *Hum Mol Genet*. 2010;19(4):684-696.

172. Clayton NP, Nelson CA, Weeden T, et al. Antisense Oligonucleotide-mediated Suppression of Muscle Glycogen Synthase 1 Synthesis as an Approach for Substrate Reduction Therapy of Pompe Disease. *Mol Ther Nucleic Acids*. 2014;3:e206.

173. Han SO, Li S, Koeberl DD. Salmeterol enhances the cardiac response to gene therapy in Pompe disease. *Mol Genet Metab*. 2016;118(1):35-40.

174. Bilkoo P, Thomas J, Riddle CD, Kagaoan G. Clenbuterol toxicity: an emerging epidemic. A case report and review. *Conn Med*. 2007;71(2):89-91.

175. Grimm D, Kay MA. From virus evolution to vector revolution: use of naturally occurring serotypes of adeno-associated virus (AAV) as novel vectors for human gene therapy. *Curr Gene Ther*. 2003;3(4):281-304.

176. Balakrishnan B, Jayandharan GR. Basic biology of adeno-associated virus (AAV) vectors used in gene therapy. *Curr Gene Ther*. 2014;14(2):86-100.

177. Kotterman MA, Schaffer DV. Engineering adeno-associated viruses for clinical gene therapy. *Nat Rev Genet*. 2014;15(7):445-451.

178. Buchlis G, Podsakoff GM, Radu A, et al. Factor IX expression in skeletal muscle of a severe hemophilia B patient 10 years after AAV-mediated gene transfer. *Blood*. 2012;119(13):3038-3041.

179. Summerford C, Samulski RJ. Membrane-associated heparan sulfate proteoglycan is a receptor for adeno-associated virus type 2 virions. *J Virol*. 1998;72(2):1438-1445.

180. Kaludov N, Brown KE, Walters RW, Zabner J, Chiorini JA. Adeno-associated virus serotype 4 (AAV4) and AAV5 both require sialic acid binding for hemagglutination and efficient transduction but differ in sialic acid linkage specificity. *J Virol*. 2001;75(15):6884-6893.

181. Walters RW, Yi SM, Keshavjee S, et al. Binding of adeno-associated virus type 5 to 2,3-linked sialic acid is required for gene transfer. *J Biol Chem*. 2001;276(23):20610-20616.

182. Wu Z, Miller E, Agbandje-McKenna M, Samulski RJ. Alpha2,3 and alpha2,6 N-linked sialic acids facilitate efficient binding and transduction by adeno-associated virus types 1 and 6. *J Virol*. 2006;80(18):9093-9103.

183. Shen S, Bryant KD, Brown SM, Randell SH, Asokan A. Terminal N-linked galactose is the primary receptor for adeno-associated virus 9. *J Biol Chem*. 2011;286(15):13532-13540.

184. Fraites TJ, Jr., Schleissing MR, Shanely RA, et al. Correction of the enzymatic and functional deficits in a model of Pompe disease using adeno-associated virus vectors. *Mol Ther*. 2002;5(5 Pt 1):571-578.

185. Mah C, Fraites TJ, Jr., Cresawn KO, Zolotukhin I, Lewis MA, Byrne BJ. A new method for recombinant adeno-associated virus vector delivery to murine diaphragm. *Mol Ther*. 2004;9(3):458-463.

186. Mah CS, Falk DJ, Germain SA, et al. Gel-mediated delivery of AAV1 vectors corrects ventilatory function in Pompe mice with established disease. *Mol Ther*. 2010;18(3):502-510.

187. Mah C, Cresawn KO, Fraites TJ, Jr., et al. Sustained correction of glycogen storage disease type II using adeno-associated virus serotype 1 vectors. *Gene Ther*. 2005;12(18):1405-1409.

188. Mah C, Pacak CA, Cresawn KO, et al. Physiological correction of Pompe disease by systemic delivery of adeno-associated virus serotype 1 vectors. *Mol Ther*. 2007;15(3):501-507.

189. Cresawn KO, Fraites TJ, Wasserfall C, et al. Impact of humoral immune response on distribution and efficacy of recombinant adeno-associated virus-derived acid alpha-glucosidase in a model of glycogen storage disease type II. *Hum Gene Ther*. 2005;16(1):68-80.

190. Qiu K, Falk DJ, Reier PJ, Byrne BJ, Fuller DD. Spinal delivery of AAV vector restores enzyme activity and increases ventilation in Pompe mice. *Mol Ther*. 2012;20(1):21-27.

191. Sun B, Zhang H, Franco LM, et al. Correction of glycogen storage disease type II by an adeno-associated virus vector containing a muscle-specific promoter. *Mol Ther*. 2005;11(6):889-898.

192. Sun B, Young SP, Li P, et al. Correction of multiple striated muscles in murine Pompe disease through adeno-associated virus-mediated gene therapy. *Mol Ther*. 2008;16(8):1366-1371.

193. Sun B, Zhang H, Franco LM, et al. Efficacy of an adeno-associated virus 8-pseudotyped vector in glycogen storage disease type II. *Mol Ther*. 2005;11(1):57-65.

194. Ziegler RJ, Bercury SD, Fidler J, et al. Ability of adeno-associated virus serotype 8-mediated hepatic expression of acid alpha-glucosidase to correct the biochemical and motor function deficits of presymptomatic and symptomatic Pompe mice. *Hum Gene Ther*. 2008;19(6):609-621.

195. Sun B, Zhang H, Bird A, Li S, Young SP, Koeberl DD. Impaired clearance of accumulated lysosomal glycogen in advanced Pompe disease despite high-level vector-mediated transgene expression. *J Gene Med*. 2009;11(10):913-920.

196. Nakai H, Fuess S, Storm TA, Muramatsu S, Nara Y, Kay MA. Unrestricted hepatocyte transduction with adeno-associated virus serotype 8 vectors in mice. *J Virol.* 2005;79(1):214-224.

197. Wang Z, Zhu T, Qiao C, et al. Adeno-associated virus serotype 8 efficiently delivers genes to muscle and heart. *Nat Biotechnol.* 2005;23(3):321-328.

198. Franco LM, Sun B, Yang X, et al. Evasion of immune responses to introduced human acid alpha-glucosidase by liver-restricted expression in glycogen storage disease type II. *Mol Ther.* 2005;12(5):876-884.

199. Sun B, Kulis MD, Young SP, et al. Immunomodulatory gene therapy prevents antibody formation and lethal hypersensitivity reactions in murine pompe disease. *Mol Ther.* 2010;18(2):353-360.

200. Zhang P, Sun B, Osada T, et al. Immunodominant liver-specific expression suppresses transgene-directed immune responses in murine pompe disease. *Hum Gene Ther.* 2012;23(5):460-472.

201. Han SO, Ronzitti G, Arnson B, et al. Low-Dose Liver-Targeted Gene Therapy for Pompe Disease Enhances Therapeutic Efficacy of ERT via Immune Tolerance Induction. *Mol Ther Methods Clin Dev.* 2017;4:126-136.

202. Doerfler PA, Todd AG, Clement N, et al. Copackaged AAV9 Vectors Promote Simultaneous Immune Tolerance and Phenotypic Correction of Pompe Disease. *Hum Gene Ther.* 2016;27(1):43-59.

203. Smith BK, Collins SW, Conlon TJ, et al. Phase I/II trial of adeno-associated virus-mediated alpha-glucosidase gene therapy to the diaphragm for chronic respiratory failure in Pompe disease: initial safety and ventilatory outcomes. *Hum Gene Ther.* 2013;24(6):630-640.

204. Nathwani AC, Reiss UM, Tuddenham EG, et al. Long-term safety and efficacy of factor IX gene therapy in hemophilia B. *N Engl J Med.* 2014;371(21):1994-2004.

205. Falk DJ, Soustek MS, Todd AG, et al. Comparative impact of AAV and enzyme replacement therapy on respiratory and cardiac function in adult Pompe mice. *Mol Ther Methods Clin Dev.* 2015;2:15007.

206. Nathwani AC, Gray JT, Ng CY, et al. Self-complementary adeno-associated virus vectors containing a novel liver-specific human factor IX expression cassette enable highly efficient transduction of murine and nonhuman primate liver. *Blood.* 2006;107(7):2653-2661.

207. Boutin S, Monteilhet V, Veron P, et al. Prevalence of serum IgG and neutralizing factors against adeno-associated virus (AAV) types 1, 2, 5, 6, 8, and 9 in the healthy population: implications for gene therapy using AAV vectors. *Hum Gene Ther.* 2010;21(6):704-712.

208. Calcedo R, Morizono H, Wang L, et al. Adeno-associated virus antibody profiles in newborns, children, and adolescents. *Clin Vaccine Immunol.* 2011;18(9):1586-1588.

209. Bai Y, Soda Y, Izawa K, et al. Effective transduction and stable transgene expression in human blood cells by a third-generation lentiviral vector. *Gene Ther.* 2003;10(17):1446-1457.

210. Logan AC, Haas DL, Kafri T, Kohn DB. Integrated self-inactivating lentiviral vectors produce full-length genomic transcripts competent for encapsidation and integration. *J Virol*. 2004;78(16):8421-8436.

211. Naldini L, Blomer U, Gallay P, et al. In vivo gene delivery and stable transduction of nondividing cells by a lentiviral vector. *Science*. 1996;272(5259):263-267.

212. De Palma M, Montini E, Santoni de Sio FR, et al. Promoter trapping reveals significant differences in integration site selection between MLV and HIV vectors in primary hematopoietic cells. *Blood*. 2005;105(6):2307-2315.

213. Montini E, Cesana D, Schmidt M, et al. Hematopoietic stem cell gene transfer in a tumor-prone mouse model uncovers low genotoxicity of lentiviral vector integration. *Nat Biotechnol*. 2006;24(6):687-696.

214. Biffi A, Bartolomae CC, Cesana D, et al. Lentiviral vector common integration sites in preclinical models and a clinical trial reflect a benign integration bias and not oncogenic selection. *Blood*. 2011;117(20):5332-5339.

215. Zufferey R, Dull T, Mandel RJ, et al. Self-inactivating lentivirus vector for safe and efficient in vivo gene delivery. *J Virol*. 1998;72(12):9873-9880.

216. Bukovsky AA, Song JP, Naldini L. Interaction of human immunodeficiency virus-derived vectors with wild-type virus in transduced cells. *J Virol*. 1999;73(8):7087-7092.

217. Modlich U, Bohne J, Schmidt M, et al. Cell-culture assays reveal the importance of retroviral vector design for insertional genotoxicity. *Blood*. 2006;108(8):2545-2553.

218. Maruggi G, Porcellini S, Facchini G, et al. Transcriptional enhancers induce insertional gene deregulation independently from the vector type and design. *Mol Ther*. 2009;17(5):851-856.

219. Montini E, Cesana D, Schmidt M, et al. The genotoxic potential of retroviral vectors is strongly modulated by vector design and integration site selection in a mouse model of HSC gene therapy. *J Clin Invest*. 2009;119(4):964-975.

220. Orchard PJ, Blazar BR, Wagner J, Charnas L, Krivit W, Tolar J. Hematopoietic cell therapy for metabolic disease. *J Pediatr*. 2007;151(4):340-346.

221. Sauer M, Grewal S, Peters C. Hematopoietic stem cell transplantation for mucopolysaccharidoses and leukodystrophies. *Klin Padiatr*. 2004;216(3):163-168.

222. Boelens JJ, van Hasselt PM. Neurodevelopmental Outcome after Hematopoietic Cell Transplantation in Inborn Errors of Metabolism: Current Considerations and Future Perspectives. *Neuropediatrics*. 2016;47(5):285-292.

223. Howell JM, Dorling PR, Shelton JN, Taylor EG, Palmer DG, Di Marco PN. Natural bone marrow transplantation in cattle with Pompe's disease. *Neuromuscul Disord*. 1991;1(6):449-454.

224. Kang ES, Iacomini J. Induction of central deletional T cell tolerance by gene therapy. *J Immunol*. 2002;169(4):1930-1935.

225. Bagley J, Tian C, Sachs DH, Iacomini J. Induction of T-cell tolerance to an MHC class I alloantigen by gene therapy. *Blood*. 2002;99(12):4394-4399.

226. Aiuti A, Biasco L, Scaramuzza S, et al. Lentiviral hematopoietic stem cell gene therapy in patients with Wiskott-Aldrich syndrome. *Science*. 2013;341(6148):1233151.

227. Hacein-Bey Abina S, Gaspar HB, Blondeau J, et al. Outcomes following gene therapy in patients with severe Wiskott-Aldrich syndrome. *Jama*. 2015;313(15):1550-1563.

228. De Ravin SS, Wu X, Moir S, et al. Lentiviral hematopoietic stem cell gene therapy for X-linked severe combined immunodeficiency. *Sci Transl Med*. 2016;8(335):335ra357.

229. Biffi A, Montini E, Lorioli L, et al. Lentiviral hematopoietic stem cell gene therapy benefits metachromatic leukodystrophy. *Science*. 2013;341(6148):1233158.

230. Sessa M, Lorioli L, Fumagalli F, et al. Lentiviral haemopoietic stem-cell gene therapy in early-onset metachromatic leukodystrophy: an ad-hoc analysis of a non-randomised, open-label, phase 1/2 trial. *Lancet*. 2016;388(10043):476-487.

231. Douillard-Guilloux G, Richard E, Batista L, Caillaud C. Partial phenotypic correction and immune tolerance induction to enzyme replacement therapy after hematopoietic stem cell gene transfer of alpha-glucosidase in Pompe disease. *J Gene Med*. 2009;11(4):279-287.

232. van Til NP, Stok M, Aerts Kaya FS, et al. Lentiviral gene therapy of murine hematopoietic stem cells ameliorates the Pompe disease phenotype. *Blood*. 2010;115(26):5329-5337.

Chapter 2

Introduction - Part 2

Unmasking central nervous symptoms in classic infantile Pompe disease: treatment underway

Qiushi Liang, M.D.[1,2,3]; Hidde H.H. Huidekoper, M.D., Ph.D.[2,3]; Arnold G. Vulto, Pharm.D., Ph.D.[4]; Ans T. van der Ploeg, M.D., Ph.D.[2,3]; Niek P. van Til, Ph.D.[5,6]; W.W.M. Pim Pijnappel, Ph.D.[1,2,3]*

[1] Molecular Stem Cell Biology, Department of Clinical Genetics, Erasmus University Medical Center, 3015GE Rotterdam, The Netherlands
[2] Department of Pediatrics, Erasmus University Medical Center, 3015GE Rotterdam, The Netherlands
[3] Center for Lysosomal and Metabolic Diseases, Erasmus University Medical Center, 3015GE Rotterdam, The Netherlands
[4] Hospital Pharmacy, Erasmus University Medical Center, 3015GE Rotterdam, The Netherlands
[5] Department of Hematology, Erasmus University Medical Center, 3015GE Rotterdam, The Netherlands
[6] Current address: Laboratory of Translational Immunology, University Medical Center Utrecht, 3584CX Utrecht, The Netherlands
* Correspondence: Dr. W.W.M. Pim Pijnappel, Erasmus University Medical Center, 3015GE Rotterdam, The Netherlands.
Email: w.pijnappel@erasmusmc.nl.

Manuscript submitted

ABSTRACT

Pompe disease has been considered primarily as a muscle disease, in which continuous lysosomal glycogen built-up within the muscle fibers causes myopathy and eventual loss of muscle function. Recent discoveries of possible impaired motoneuron function and neurocognitive symptoms in classic infantile patients have broadened the spectrum of this historically "non-neuropathic" disease and raises concerns on the efficacy of the current standard of care, i.e. enzyme replacement therapy, which does not pass the blood-brain barrier. In this review, we explore new developments on treatments that have the potential to address both the central nervous system and peripheral abnormalities via systematic delivery. Three treatment options are discussed including ERT with chimeric enzyme, *in vivo* adeno-associated virus and *ex vivo* lentiviral gene therapy.

ABBREVIATIONS

AAV, adeno-associated virus; ARSA, arylsulfatase A; BBB, blood-brain barrier; CNS, central nervous system; CSF, cerebrospinal fluid; ERT, enzyme replacement therapy; GAA, acid α-glucosidase; GLD, globoid-cell leukodystrophy; GT, gene therapy; GVHD, graft versus host disease; HSCs, hematopoietic stem cells; HSPCs, hematopoietic stem progenitor cells; HSCT, hematopoietic stem cell transplantation; IGFIR, insulin-like growth factor I receptor; IGFII, insulin like growth factor II; IR, insulin receptor; LSD(s), lysosomal storage disease(s); LV, lentiviral vectors; M6P, mannose-6-phosphate; M6P/IGFIIR, mannose-6-phosphate/insulin-like growth factor receptor; MLD, metachromatic leukodystrophy; MPS, mucopolysaccharidosis; PNS, peripheral nervous system; rhGAA, recombinant human GAA.

INTRODUCTION

Pompe disease, also termed glycogen storage disease type II (GSDII, OMIM 232300), is a lysosomal storage disease (LSD) caused by deficiency of acid α-glucosidase (GAA). GAA deficiency leads to generalized glycogen accumulation that eventually causes tissue damage and the loss of function. Muscles, including cardiac, skeletal and smooth muscles, are most severely affected. The disease has a broad clinical spectrum.[1,2] Classic infantile Pompe disease (CIPD), characterized by complete GAA enzyme deficiency, is the most severe form. Patients present shortly after birth with a hypertrophic cardiomyopathy and progressive general skeletal muscle weakness. Without treatment, these patients die within the first year of life due to cardiorespiratory failure.[3,4] Childhood and adult Pompe disease exhibit a milder and more slowly progressive phenotype, which is explained by a partial deficiency and thereby residual activity of GAA.[5,6] The age of onset of these non-classic forms can vary from early childhood to late adulthood, but progressive skeletal muscle weakness eventually results in requirements for ventilator support and a wheelchair, which are hallmarks of these forms.[7,8]

Recently, the conventional view of muscular glycogen built-up[9] as the sole contributor to the underlying the motor pathology and dysfunction has been debated and the involvement of the nervous system in disease progression has been suggested by some authors. For instance, respiratory insufficiency is attributed to diaphragmatic contractile dysfunction.[10,11] So far it has been understood that this dysfunction is due to primary muscle damage. However, in a transgenic mouse model with restricted GAA expression in the skeletal muscles, respiratory function was still compromised despite normal diaphragm contractility.[12] Neurophysiological studies indicated that deficient phrenic nerve output to the diaphragm caused the diaphragmatic weakness. It was speculated that extensive glycogen accumulation in phrenic motor neurons located in the ventral cervical spinal cord (C4),[12,13] as shown in autopsy reports of classic infantile patients caused the deficient phrenic nerve output.[12,14]

Importantly, autopsy of infantile patients showed glycogen accumulation in cortical neurons, brainstem nuclei, glial cells and oligodendrocytes.[9,14-20] However, the clinical significance of these findings remained elusive due to the early mortality in untreated classic infantile patients that prevented long-term cognitive analysis.[3] Following the advent of enzyme replacement therapy (ERT) in 2006 using recombinant human GAA (rhGAA), life expectancy has improved in infantile patients. With growing age cognitive decline has been recognized as a new emerging symptom in some long-term surviving classic infantile patients.[21-24] This was accompanied by periventricular white

matter abnormalities observed on MRI scans.[21,23,24] In one severely affected patient, prominent intellectual disability (IQ of 48) and behavior problems at school were observed. In this particular patient MRI scans revealed white matter abnormalities extending to the subcortical area.[24]

With these developments and recent observations, a better understanding of the involvement of the central nervous system (CNS) in Pompe disease has become relevant since it may not only contribute to intellectual disability but potentially also to motor dysfunction and consequently to the development of new clinical manifestations. Most importantly, it renders current therapy insufficient as the blood-brain barrier (BBB) and blood-spinal cord barrier prevent the distribution of rhGAA to the central nervous system.

To address this unmet medical need, we focus on exploring possible alternative therapies that are capable of targeting the CNS as well as peripheral nerves via systematic delivery. Given the limited number of studies on the CNS in Pompe disease, preclinical and clinical advances for other LSDs, which are likely relevant for Pompe disease, are briefly discussed.

THERAPEUTIC STRATEGIES FOR SYSTEMATIC DELIVERY

The occurrence of CNS symptoms in classic infantile Pompe patients despite treatment with ERT pointed to the inefficacy of this treatment when it comes to CNS involvement. Recombinant human acid α-glucosidase (rhGAA) is a 110 kDa precursor molecule and the molecular weight and size of the therapeutic molecules are too large to cross the blood-brain barrier (BBB) and thereby the BBB prevents enzyme distribution to the CNS.[25] For the same reason, systematically delivered ERT for other LSDs failed to prevent, stabilize, slow down or reverse the progression of CNS symptoms.[26,27] Although high doses of ERT with early intervention have shown some positive results in the treatment of the CNS in animal models, in humans, ERT was not able to prevent cognitive decline in any LSDs tested so far.[28-32]

An alternative approach is direct administration of rhGAA to the brain by intrathecal/intraventricular or intracerebral injections. This provides access of therapeutic molecules to the brain via the intra-cerebrospinal fluid (CSF) or parenchyma. This approach has shown to promote clearance of lysosomal storage in the brain in animal models of several LSDs.[33-38] In small clinical trials, intrathecal enzyme therapy has been conducted in mucopolysaccharidosis (MPS) I, II and III patients and it was gener-

ally well tolerated.[39-42] However, it is unclear whether it can be considered as an optimal technique for widespread clinical application due to the highly invasive nature of the neurosurgical procedures involved, the potential risk of CNS infections and the lifelong need for repeated administration. Furthermore, drugs have to diffuse into the brain parenchyma from the CSF and the injection sites, resulting in focal and limited distribution. Thus, reaching therapeutically sufficient levels of enzyme activity that are homogenously present throughout the entire brain is another challange.[43,44] Most importantly, as Pompe disease is a systematic disease, not only the CNS needs treatment, but also the peripheral tissues, stressing the importance of a therapy resulting in widespread systemic delivery.

Collectively, the limitations of ERT in reaching the CNS highlight that there is an unmet medical need and warrants a surge for alternative therapeutic approaches that, via optimized routes of delivery, can efficiently correct the neurological symptoms without compromising its efficacy in peripheral tissues and organs. In this section, we will discuss such potential therapies for Pompe disease (Figure 1).

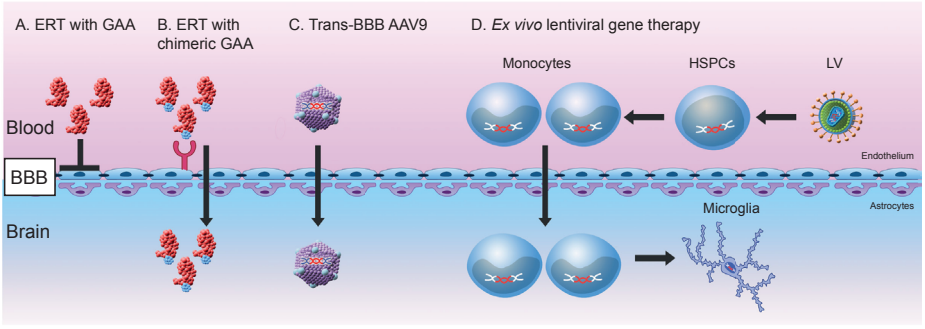

Figure 1. Therapeutic strategies of CNS neuropathies via systemic delivery. (A) The BBB blocks the GAA protein from circulation to enter the brain. (B) The GAA protein can be fused to a ligand or an antibody to have affinity for receptors on the BBB for transcytosis. (C) AAV9 carrying the therapeutic gene is able to bypass the BBB. (D) HSPCs can be transduced *ex vivo* with lentiviral vector expressing GAA. These modified stem cells can differentiate into monocytes which are capable of infiltrating the BBB and further settle down as microglia in the brain. Abbreviations: BBB, blood-brain barrier; ERT, enzyme replacement therapy; GAA, acid α-glucosidase; AAV, adeno-associated virus; LV, lentiviral vector; HSPCs, hematopoietic stem progenitor cells.

1. SYSTEMIC ERT WITH CHIMERIC rhGAA

Chimeric peptide technology

Despite its tight junctions, the BBB allows passage of large molecules, including proteins, via receptor-mediated transcytosis. These proteins are taken up via endocytosis

at the luminal side after receptor-ligand binding and then released via exocytosis at the abluminal side into the brain.[45] Via genetic engineering, specific BBB receptor ligands can be added to the large therapeutic proteins and serve as carriers to transport the newly synthesized chimeric protein complexes across the BBB.[46-49] The attached ligands can be either endogenous peptides, modified proteins or monoclonal antibodies that bind to specific BBB receptors. Via these methods, chimeric peptide technology has been used in several attempts to treat LSDs.[50,51]

Chimeric rhGAA tagged with insulin like growth factor II (IGFII)

As an initial attempt to improve targeting to skeletal muscle, a fragment of insulin like growth factor II (IGFII) that interacts with the IGFII binding site of the bifunctional mannose-6-phosphate/insulin-like growth factor II receptor (M6P/IGFIIR) was fused with rhGAA.[52] This diverted cellular uptake of the enzyme from the M6P binding domain to the IGFII-mediated binding domain of the M6P/IGFIIR. The rational was that cellular uptake would be independent of posttranslational modification of rhGAA with M6P, which is poor in high producing Chinese hamster ovary (CHO) cell lines.[53] IGFII tagged rhGAA showed 26-fold better cellular uptake *in vitro* compared to the untagged rhGAA, and 5-fold more efficient glycogen clearance in the heart and skeletal muscles in a knockout Pompe mouse model. Respiratory function also improved in a follow-up study in Pompe mice treated with the enzyme.[54] Importantly, pathology in brain was also evaluated in this study. Systematic delivery of IGFII-tagged rhGAA reduced the average severity score for both glycogen accumulation and vacuolization in neurons throughout the brain in Pompe mice, suggesting that IGFII-tagged rhGAA was able to pass the BBB.

Several pathways for transcytosis of this chimeric protein can be envisioned. First, IGFII-tagged rhGAA may pass the BBB by binding to the M6P/IGFIIR. This receptor is present on the BBB during embryonic development. However, it is developmentally downregulated at the BBB starting during late gestation and/or the early neonatal period and it is unclear to what extent it is exposed on the BBB in adults.[55-57] The IGFII tag might also facilitate binding of chimeric rhGAA to the insulin-like growth factor I receptor (IGFIR), which is also present on the BBB, and which has an even slightly higher affinity for IGFII compared to IGFI.[58] This cross reactivity also extends to the possible binding of IGFII to insulin receptor (IR). In fact, as one of the most abundant and active receptors expressed on the BBB, IR has been the target for the transcytosis of several lysosomal enzymes fused to an IR-specific monoclonal antibody. Evidence for the distribution of IR-antibody-tagged enzyme within the brain was confirmed in rhesus monkeys after intravenous administration of the various lysosomal enzymes deficient in mucopolysaccharidosis (MPS) I (Hurler syndrome),[59-61] MPS II (Hunter syn-

drome),[62] MPS IIIA,[63] MPS IIIB[64] and metachromatic leukodystrophy (MLD).[65] Therefore, theoretically, the M6P/IGFIIR, IGFIR and IR, either individually or combined, may play a role in facilitating the delivery of IGFII tagged GAA into the brain. To elucidate the exact mechanism, this subject needs further investigation.

Other highly expressed receptors on the brain capillary endothelium include the low density-lipoprotein receptor (LDLR) and transferrin receptor (TfR). These have also served as alternative targets for crossing the BBB. Chimeric proteins fused with either peptides or monoclonal antibodies directed to those receptors have been tested in several LSDs with promising outcomes.[66-68]

Limitations of chimeric peptide technology in ERT

The chimeric peptide technology enables delivery of lysosomal proteins targeting the peripheral tissues through a glycosylation-independent mechanism, while it also facilitates transport of the protein across the BBB. Because the microvasculature of the brain is so densely distributed, transcytosed proteins can, via this rich capillary network, assess the entire brain homogenously, and thereby might address the limitation of the rather restricted distribution obtained with intrathecal or intracerebral injections. The capacity to transport therapeutic enzymes by transcytosis remains largely unknown, and whether the reported partial glycogen reduction in the brain following systemic delivery of IGFII tagged GAA has any clinically relevant benefit requires more studies.[54] In addition, it has been reported that biweekly doses of 20 mg/kg GAA tagged with IGFII caused transient hypoglycemia in Pompe patients possibly by binding to the IR.[69,70] A similar phenomenon also occurred in primates that received chronically high doses of an iduronate 2-sulfatase (IDS)-IR monoclonal antibody fusion protein at 30 mg/kg.[71] Although the hypoglycemia could be managed by the addition of caloric intake or dextrose to the infusion in adults, the danger of permanent neurological damage caused by severe hypoglycemia especially in small children should not be neglected.[72,73] Finally, a common general drawback of ERT can be immune responses against the infused enzyme that may negatively interfere with therapeutic outcome.[74,75]

2. GENE THERAPY

Gene therapy is an attractive alternative treatment for Pompe disease and other LSDs.[76-80] Introduction of functional copies of the GAA gene can lead to the establishment of an endogenous source of enzyme production. Through cross-correction, self-generated enzyme excreted by a depot of cells or organs can be delivered systemi-

cally through the circulation, and the enzyme can be taken up via the M6P/IGFIIR (or other receptors) in the affected tissues. Compared to conventional ERT which requires life-long repetitive administrations, this therapy aims to provide direct or permanent correction of the genetic defect and long-term correction of GAA deficiency via a single administration. Two major gene therapy approaches have been investigated for Pompe disease. These include *in vivo* systemic delivery of adeno-associated virus (AAV) vectors and *ex vivo* delivery of genetically modified hematopoietic stem cell progenitors (HSCPs) via lentiviral vectors (LV), as will be discussed in the following sections.

2.1 *IN VIVO* SYSTEMIC AAV-MEDIATED GENE THERAPY

AAV tropism

Adeno-associated virus (AAV) is a single-stranded DNA parvovirus that has been developed into a promising gene delivery vector due to its tissue specificity which is dependent of its serotype, and long term expression primarily as nonintegrated episomes.[81-84] Transduction of AAV is initiated via serotype-specific binding to a variety of cell surface receptors,[85-89] thereby directing distinct tissue tropisms. For example, in rodents, AAV1 and AAV6 mediate high transduction efficiency in heart and skeletal muscles[90-93] whereas AAV8 generates robust transgene expression in liver when delivered systemically.[94,95] Regarding the CNS tropism, AAV4 and AAV7 predominantly transduce neurons while AAV1 and AAV5 transduce both neurons and glia cells following brain injection.[96-98] Yet, the impermeability of the BBB precludes the entry of most of the known serotypes into the CNS following systemic administration.

CNS transduction by AAV9

The discovery of the AAV9 serotype that has the unique property to effectively cross the BBB has broadened the potential of *in vivo* systemic AAV administration to address CNS related disease problems. In a mouse model, AAV9 demonstrated its ability to bypass the BBB in both neonatal and adult mice and to mediate widespread transduction of neural cells throughout the brain.[99] While the underlying mechanism remains elusive, it was speculated that crossing of the BBB was mediated by an active transport mechanism, as disruption of the BBB by mannitol did not increase the passage of AAV9.[100,101] The receptor(s) involved in this process remain(s) to be identified.

Interestingly, a differential transduction profile has been documented for AAV9. While neurons and astrocytes were equally transduced throughout the neonatal brain, transgene expression was primarily restricted to astrocytes with only focal/localized

neuronal expression in adult mice.[99] This age-dependent cellular tropism featured by widespread neuronal transduction in newborns versus exclusive glial preference in adult species was further confirmed in nonhuman primates.[100,102,103] However, the age related decline in neuronal transduction was contradicted by findings that preferential glia cell transduction was maintained in cynomolgus macaques at all time points from birth to 36 months of age.[104] For the application in Pompe disease, astrocyte-preferred transduction by AAV9 would be an advantage, as astrocytes have more prominent lysosomal glycogen deposits in comparison with the relatively spared cortical neurons, as judged from autopsy reports of classic infantile Pompe patients.[14,18,19,105] This finding is most likely due to the fact that in the brain, glycogen is predominantly present in astrocytes,[106,107] which serve as a source to deliver energy to neurons on demand.[108-110] Under physiological conditions, only a low but traceable amount of glycogen is present in neurons.[111] Therefore, it can be speculated that glycogen storage in astrocytes and consequences thereof may be an important driver behind CNS pathology in Pompe disease. Correction of aberrant astrocytic function has been proposed to prevent a cascade of downstream inflammatory reactions and thereby halt disease progression in similar diseases.[112] Theoretically, secreted enzyme from transduced astrocytes could provide therapeutics to surrounding neurons through cross-correction.

Systemic delivery of AAV9 has also been shown to have the potential to target the motor neurons in the spinal cord with high efficacy irrespective of age. This was observed both in murine[99,113] and primate models.[100,104,114] Therefore, an additional advantage of AAV9 gene therapy could be that it might be capable to address the spinal motor neuron pathology in Pompe disease.

Transduction of peripheral tissues by AAV9

Apart from tropism for the CNS, the peripheral tropism of AAV9, especially its distribution in heart and skeletal muscles, is important for the treatment of Pompe disease. Encouragingly, when compared to other serotypes, AAV9 showed the best distribution in murine heart, skeletal muscles and also liver, an important depot organ to generate and excrete therapeutics systemically.[90] In particular, the AAV9 vector appears to be the most natural cardiotropic serotype,[115] as it was able to transduce over 80% of the myocardium.[116,117] Widespread transduction in heart, skeletal muscles and liver was also demonstrated in primates,[100,104] further advocating AAV9 as a potential vehicle for targeting both the CNS and peripheral tissues in Pompe disease.

AAV9 in LSDs

Systemic delivery of AAV9 vector has been used to correct the enzyme deficiencies in several mouse models of LSDs including MPS IIIA,[118] MPS IIIB,[119,120] GM1 gangliosidosis,[121] Sandhoff disease [122] and MLD.[123] In general, AAV9 showed a long-term (more than 18 months)[119] global CNS (brain and spinal cord) and widespread somatic restoration of functional enzyme levels that led to systemic reduction of storage material, pathology and neuroinflammation. The treated mice also showed better behavioral performance and prolonged survival. Importantly, in contrast to a major phenotypic amelioration in treated neonates, the administration of AAV9 to adult Sandhoff mice of 6 weeks old did not effectively improve disease symptoms, highlighting the importance of early intervention in this disease.[122] The biodistribution of AAV9 and profiling of transgene expression was consistent between mice with MPS IIIB and primates.[124] Based on these promising data, a clinical trial using AAV9 via systemic administration was initiated in patients with MPS IIIA (NCT02716246). The outcome of this study will provide valuable insights in the safety and efficacy of using AAV9 vector in patients. A positive outcome is expected to further facilitate the development of this treatment for other LSDs.

AAV9 in Pompe disease

AAV gene therapy has been studied intensively in preclinical models of Pompe disease, focusing mainly on the treatment of muscle related symptoms including cardiomyopathy and skeletal muscle weakness. The systemic delivery of a hybrid AAV 2/8 vector, using the genome of AAV2 and capsid protein of AAV8, showed widespread GAA expression and subsequent glycogen clearance when initiated in young adult mice (up to 3-month old). This was most effective in the heart, followed by the diaphragm and other skeletal muscles.[125-127] Consequently, these treated mice showed long-term improvement of motor function.

When delivered systemically to Pompe mice, AAV 2/9 shared a similar pattern of biodistribution compared to AAV 2/8, but with at least 2-fold higher transduction efficiency.[126] It also sufficiently transduced distal hind limb muscles, which was a limitation of the AAV 2/8 pseudotype. Compared to standard biweekly ERT, a single systemic injection of AAV2/9 containing a muscle-specific desmin promoter (DES) resulted in improved respiratory function, as indicated by an increase in breathing frequency and a decrease in the expiratory breathing frequency and the total respiratory cycle time assessed by whole-body plethysmography.[128] The authors suspected that the partial correction of lower motoneurons had contributed to the improvement. Indeed, a significantly increased amount of AAV9 vector genome was detected in the spinal cord after treatment which was even higher than that found in the diaphragm.

This suggested either retrograde transport of the vector or through the blood-spinal barrier. However, analysis including enzymatic activity, glycogen content or morphology was lacking in this study, which would support the therapeutic relevance of the findings. A dual AAV9 system with both a tissue-restricted desmin (DES) promoter and a liver-specific promoter (LSP) subsequently confirmed restoration of GAA expression in the spinal cord and sciatic nerve, and glycogen clearance in the latter.[129] GAA expression in cardiac and skeletal muscles was not compromised, and this approach had the extra benefit of induced immune tolerance. Functional analyses showed improved muscle force and cardiac function.

So far, analysis of therapeutic outcome in brain has not been conducted in Pompe mouse models following systemic delivery of AAV9, possibly due to the rather recent clinical observation of CNS involvement in long term surviving infants. Building upon the success for other neuronopathic LSDs, it can be speculated that systemic delivery of AAV9 may be a valuable treatment option for Pompe disease for providing correction of neuronal tissues. This should be tested in future research.

Limitations of in vivo AAV gene therapy

For the translation to clinical application, several concerns of AAV gene therapy should be addressed. First, pre-existing immunity against AAV, due to natural exposure in the healthy population, is highly prevalent (47%) and this can mediate an immune response, thus restricting the use of AAV9 vectors to a subset of patients.[100,124,130] In particular, systemic exposure of AAV vectors can trigger both cell-mediated and humoral responses against either the AAV capsid or the transgene.[131-134] These induced immune responses have been observed in preclinical models and human trials that reduced the transduction of both somatic organs and the CNS, counteracted the therapeutic protein, and eliminated AAV-transduced hepatocytes with a concomitant loss of efficacy.[135-138] In a murine Pompe model, anti-GAA antibodies were formed following AAV delivery, and these impaired therapeutic outcome.[139,140] Although *in vivo* AAV gene therapy with a liver specific promoter induced peripheral tolerance to anti-GAA antibody formation via the generation of GAA-specific regulatory T-cells,[129,141-144] it remains questionable whether this strategy can be extrapolated to humans due to possible immunological differences. The durability of transgene expression over the lifespan of human has not been assessed yet. As the patients get older, an increasing amount of enzyme proportional to the growing body mass is needed. Repeated administrations of AAV vectors might therefore be required. However, the immune response triggered by the first administration precludes the readministration of the same vector. Moreover, due to the insufficiency to bypassing the BBB, only a small portion of peripheral delivered AAVs arrive in the CNS.[103] Consequently, a high vector

dose is required to treat global CNS pathology in an adult patient which increases the likelihood of stimulating AAV-capsid derived immune responses.[145] The majority of AAV genomes remain episomal, but in rare events AAV may also integrate and potentially cause insertional mutagenesis.[146-148] This risk is relatively low compared to integrating retroviral vectors. Lastly, transduction efficiency of human liver may be much less efficient by serotypes that worked well in animal models; for instance AAV2/8 tested in murine[94] and non-human primates[137] worked much better than in a clinical trial for hemophilia B.[149] This underlines the species specific differences in the translation of AAV-mediated gene therapy from animal models to human trials, due to differences in physiology, anatomy and size. It is also possible that species-dependent AAV tropisms exist and prevent translation of results in animal models to humans.

Taken together, the exciting finding of AAV9-mediated gene therapy paved the way for the development of transgene delivery to the CNS via non-invasive systemic injection.[101,150] While the therapeutic efficacy of AAV9 to correct brain pathology in Pompe disease awaits further evaluation, the development of an AAV-mediated immunomodulation regimen, and improved passage of the BBB[151] will further facilitate the clinical application of this treatment.[152]

2.2 *EX VIVO* LENTIVIRAL GENE THERAPY

2.2.1 Proof of principle: hematopoietic stem cell transplantation

Microglia: Effectors/vehicles for cross-correction in the CNS

The rationale of allogeneic hematopoietic stem cell progenitor (HSCP) transplantation for treating LSDs is based on the reconstitution of hematopoietic lineages by donor-derived, metabolically competent cells in vascular and extravascular compartments throughout the body. Following engraftment, hematopoietic stem cells (HSCs) and their progeny are capable of generating functional enzyme into the circulation to systemically delivery to the affected tissues. Among these hematopoietic cell types, monocytes can cross the BBB, enter the CNS and further differentiate and reside as active resting microglia, thus serving as a stable source of the enzyme *in situ*, available for cross-correction of neighboring host cells.[153,154]

Donor derived chimerism within the CNS microglia lineage following bone marrow transplantation has become evident in animal models. The bone marrow-derived microglia were traceable within the CNS as early as 3 days after transplantation, and contributed to a stabilized microglial donor chimerism of 30% at one year after

reconstitution.[155,156] Importantly, the distribution within the CNS was very broad covering cortex, hippocampus, thalamus, brainstem, cerebellum and spinal cord.[155,157] Consequently, the steady-state turnover of monocyte-derived microglial cells is able to provide a permanent source of therapeutics to a widespread area in the nervous system.[158]

The mechanism for such recruitment of peripheral monocytes remains elusive as it is an extremely rare event in healthy organisms.[159,160] First, the total body irradiation used for preconditioning exposes the brain to potential irradiation-induced changes[161] including 1) disrupted BBB permeability,[162] possibly caused by disrupted tight junction proteins[163] or induced endothelial cell apoptosis;[164] and 2) local induction of proinflammatory gene expression.[165,166] Both mechanisms may facilitate the recruitment of peripheral monocytes into the CNS. Indeed, in mice subjected to irradiation in which the CNS was protected, a dramatic reduction of donor-derived cells was observed,[154] suggesting that irradiation was a key factor for microglia reconstitution after transplantation. Furthermore, the disease state of the brain may promote microglial infiltration. This is supported by a prominent infiltration of peripheral monocytes into the CNS and preferential targeting of lipid storage sites in a MLD disease mouse model compared to wildtype mice.[167] Typically, neuroinflammation featured by microgliosis is a common response to damage to the CNS frequently seen in LSDs. Although the origin of this remains debatable, it has been postulated that, apart from local expansion,[160] monocytes from the blood stream can be recruited in a chemokine dependent manner.[168,169]

The conditioning drug busulfan is more commonly used in the clinic for HSCP transplantation, and has recently shown substantial priming potential in the brain by eliminating endogenous microglia to create space for engraftment and to promote early proliferation of donor cells.[170] Busulfan induced significantly more donor-derived microglial cells both in the short and the long term compared to irradiation.[171] In conclusion, donor derived microglia provides a way to deliver the missing enzyme across the BBB provided that sufficient brain conditioning is applied.

Clinical practice of hematopoietic stem cell transplantation

Allogeneic hematopoietic stem cell transplantation (HSCT) has been extensively performed in numerous LSDs and is the treatment option for a selected group of LSD patients.[172-174] These include MPS IH (Hurler syndrome), which shows impressive outcomes.[175,176] Long-term follow-up of Hurler patients after HSCT showed that cognitive functions improved or stabilized in most children and prevented progressive mental deterioration, decreased somatic pathology, and prolonged survival. It

was important that patients were treated pre-symptomatically or at an early course of the disease. This was in direct contrast to unfavorable neurological outcome in patients that were transplanted over two years of age, suggesting that irreversible cerebral damage occurred within the first two years of life.[177-183] Therefore, HSCT is only designated as a first line treatment option for MPS 1H patients who are before the age of 2.5 years, and show an early disease stage without severe neurological damage.[184,185] HSCT also showed therapeutic potential in MLD, depending on the disease variant (late-infantile, juvenile and adult form) and the stage of the disease at the time of transplant.[186] Overall, HSCT only benefited the pre- and early symptomatic late onset form (late-juvenile and adult form) by delaying the onset or halting progression of some of the CNS symptoms.[187-192] For early onset MLD (late infantile and early juvenile form), patients presenting symptoms invariably declined after HSCT, and it is still a matter of debate whether HSCT started in pre-symptomatic stage can be beneficial.[187,193] Similarly, globoid-cell leukodystrophy (GLD) patients of the late onset form, who are characterized by a more gradual rate of deterioration, are likely to benefit from HSCT with arrested disease progression, whereas symptomatic infants usually have a poor outcome.[194,195] Overall, the age and disease state at the time of transplant is paramount to the overall long-term prognosis due to the irreversibility of the neurological dysfunction.

Limitations of allogeneic hematopoietic stem cell transplantation

Taken together, HSCT often only arrests or slows down disease progression rather than to cure it completely. Responsive patients still suffer from considerable residual disease burden in the long run that hamper overall outcome, such as musculoskeletal symptoms in Hurler patients,[182] persistent peripheral neuropathy in MLD[186,187] and general loss of function in GLD.[195] These findings suggest that wildtype enzyme levels provided by healthy donor cells are often insufficient. The fact that HSCT does not ameliorate neuropsychological deterioration in a number of other LSDs including MPS II (Hunter syndrome) and MPS III (Sanfilipo syndrome) further support the notion that the natural lysosomal activity in hematopoietic cells is too low to be cross-corrective for most LSDs.[196-201] Other limitations of HSCT include the limited availability of human leukocyte antigen (HLA) matched healthy donors, high rates of engraftment failure, graft versus host disease (GVHD), and mortality and transplant-related morbidity.[202,203]

In the case of Pompe disease, the only classic infantile Pompe patient reported to have undergone HSCT died of complications from a haploidentical transplantation.[204] In addition, HSCT performed in Pompe cattle failed to reduce glycogen in muscles and spinal cord probably due to low levels of GAA produced by hematopoietic cells.[205]

These two experiments highlight the safety and efficacy concerns of HSCT in treating Pompe disease.

2.2.2 Enhancing the benefits: Hematopoietic stem cell-mediated lentiviral gene therapy

Rationale of ex vivo lentiviral gene therapy

By genetically modifying the patient's own HSCPs, *ex vivo* gene therapy takes advantage from an autologous transplantation source with the advantage of enzyme overexpression. Upon engraftment, corrected HSCs and their progenies can provide both systemic and local supranormal enzyme levels to aid in cross-correction.[206,207] Therefore, HSC-mediated gene therapy (GT) manages to circumvent the majority of the problems associated with allogeneic HSCT by providing a supranormal source of enzyme and by preventing GVHD and cell rejection, thereby reducing transplant-related morbidity and mortality. The availability of the patients' own stem cells for transplantation broadens the application of this therapy to literally all patients.

Lentiviral vectors (LVs) are most widely used for *ex vivo* gene delivery, as they stably and efficiently integrate into the host genome and can induce high gene expression, thus providing a permanent source of the overexpressed enzyme.[208,209]

HSC-mediated lentiviral gene therapy in LSDs

HSC-mediated lentiviral gene therapy has been intensively studied in LSDs and pioneered by application to metachromatic leukodystrophy (MLD), a lysosomal sphingolipid storage disorder caused by the deficiency of arylsulfatase A (ARSA).[202] MLD is characterized by extensive CNS and peripheral nervous system (PNS) involvement, in which motor decline and cognitive problems with demyelination are hallmarks.[210] Early work using GFP-transduced HSCPs revealed extensive migration of donor-derived GFP^+ progeny, namely macrophages/microglia, in both the CNS and PNS of a MLD mouse model, confirming that macrophages/microglia perform a carrier role from the periphery to the nervous system.[167] In subsequent work, transplantation of presymptomatic mice with transduced HSCPs that overexpressed the ARSA protein led to almost complete prevention of symptoms related to motor conduction, motor learning and coordination, and demyelination.[167] Failure to do so using wildtype HSCT emphasized again the crucial role for enzyme overexpression in order for this therapy to be efficacious. In a follow-up experiment, an increase of brain ARSA activity to the level of 10% of wildtype was determined to reverse the neuropathological abnormalities and neurological deficits in symptomatic MLD mice.[211] This study also provided clear evidence for local cross-correction and for the presence of ARSA en-

zyme in neurons and glia cells. Biosafety assessment showed a normal clonogenic capacity and multilineage differentiation of transduced human HSCPs.[212]

These promising data led to a phase I/II trial of HSCs-mediated lentiviral gene therapy in MLD patients. Preliminary data obtained from early onset MLD patients treated at the presymptomatic or very early symptomatic stage showed stable engraftment of transduced HSCPs, which resulted in supranormal levels of ARSA activity in hematopoietic lineages and in cerebrospinal fluid, indicative of sufficient enzyme delivery throughout the CNS in humans.[213,214] A near-normalization of motor performance was observed, while demyelination of the CNS and PNS was reduced compared to the natural history in treated children. In addition, the translation of the conditioning regimen from total body irradiation in the mouse model to busulfan in the human trial reassured that busulfan sufficiently conditioned the brain in human patients.

Favorable outcomes following HSC-mediated lentiviral gene therapy have been obtained in murine models of other LSDs associated with severe neurological symptoms, such as MPS I,[215] MPS II,[216] MPS III,[217,218] and GLD.[219] In general, the results showed establishment of supra-normal enzyme activities in the hematopoietic system and the affected tissues following stable reconstitution of genetically engineered HSCPs. Clearance of storage materials in both somatic and neuronal tissues supported the central role of cross-correction and supported the idea that macrophages/microglia are the vehicle for enzyme distribution in the nervous system. Biochemical improvements were accompanied by reversal of neurological phenotypes and, not surprisingly, the therapeutic efficacies markedly exceeded those exerted by transplantation of wildtype HSC.

HSC-mediated lentiviral gene therapy in Pompe disease

The first attempt to treat Pompe disease with genetically modified HSCPs was made in a GAA knockout mice model using myeloproliferative sarcoma virus enhancer, negative control region deleted, Dl587rev primer-binding site substituted (MND) as the internal promoter to drive expression of native GAA cDNA.[220] Although the rescue of GAA deficiency was limited to a below-wildtype level in bone marrow and peripheral blood cells, cross-correction occurred in skeletal muscle by reducing glycogen levels. Interestingly, correction of heart was refractory in this study, while heart is very susceptible to correction by ERT. Despite of unsatisfactory engraftment of GAA-corrected HSCPs and limited amount of organs analyzed, this study provided evidence for the possible realistic application of *ex vivo* gene therapy in Pompe disease.

The efficiency of this treatment was substantially improved by our group using a spleen focusing-forming virus (SFFV) promoter.[221] The overexpression of GAA in the hematopoietic lineage led to supranormal enzyme activity, and subsequent restoration of enzyme activity in target tissues, often above wildtype levels, including heart and diaphragm. These activity levels were associated with significant glycogen reduction and pathological reversal. Similar to wildtype levels of GAA activity in quadriceps femoris was not efficacious in clearing glycogen content, in line with earlier findings that skeletal muscles are difficult to treat.[222,223] Nevertheless, this treatment reversed cardiac hypertrophy and improved respiratory and motor function. Brain was also analyzed, but due to the limited restoration of GAA levels in this organ glycogen accumulation was not alleviated. In MLD, restoration of 10% of WT level of functional enzyme was adequate to reverse the pathology in the brain.[211] The threshold levels of enzymatic activity to correct CNS pathology in Pompe disease deserves further investigation.

In order to further improve the therapeutic efficacy, we recently improved the design of the lentiviral vector to 1) increase GAA expression by codon optimization of the cDNA[224] and/or 2) enhance the targeting to tissues by addition of a part of IGFII fused to the catalytic domains of GAA.[52] These modifications are currently under investigation and already showed promising results in correcting both CNS and peripheral phenotypes in a Pompe mouse model (manuscript in preparation).

Advantages of HSC-mediated lentiviral gene therapy

Compared to ERT and AAV, which require either regular infusion or potential re-administration, respectively, HSC-mediated lentiviral gene therapy serves as a cure for a lifetime by a single intervention that provides a permanent source of functional enzyme in HSCs and their progeny. Furthermore, by migration of macrophage/microglia into the CNS, systematic delivery is now possible for treating brain pathology while maintaining peripheral efficacy. Consequently, when enzyme activities in plasma were increased ~ 100-fold above WT levels, *ex vivo* lentiviral gene therapy resulted in an increase of ~200% enzyme WT levels in brain in comparison to only 6% WT restoration by *in vivo* liver-directed gene therapy in MPSI mice.[78] The higher enzyme levels achieved by *ex vivo* LV GT is probably due to the fact that the functional enzyme is produced from brain residing microglia derived from transduced HSCPs and is not limited to transcytosis at the BBB. In addition, HSC-mediated lentiviral gene therapy establishes robust immune tolerance both against the transgene product (GAA) and against ERT (rhGAA) (Liang *et al*, submitted).[220,221]

Safety concerns of HSC-mediated lentiviral gene therapy

While stable genomic integration is a pre-requisite for permanent transgene expression, it also raises concerns of insertional mutagenesis. Recent advances in lentiviral vector design using a third generation of self-inactivating vectors have substantially improved safety.[225-227] The recent reports of integration site analysis of hematopoietic cells from clinical trials showed a highly polyclonal engraftment of transduced donor cells without occurrence of aberrant clonal behavior or hematopoietic malignancies.[213,214,228] Nevertheless, the risk of insertional oncogenesis can never be completely avoided, and it is not possible to perform extensive quality controls on transduced HSCPs due to the inability to culture these cells for prolonged periods of time.[206] To reduce the risks, low vector copy number per cell and weak internal promoter are preferred.

CONCLUDING REMARKS

Skeletal muscles have long been the major target for treatment in Pompe disease. To develop strategies that solely target the skeletal muscles can now be challenged with recent insight in the involvement of the central nervous system. Most importantly, in light of this new phenotype, alternative therapies that can treat both muscle and CNS abnormalities should be further explored, because ERT cannot reach the brain. Hematopoietic stem cell mediated lentiviral gene therapy provides a promising choice of treatment for both the CNS and peripheral tissues.

ACKNOWLEDGEMENTS

This work was supported by The Netherlands Organization for Health Research ZonMw (project number: 40-40300-98-07010) and the Erasmus University Medical Center. Q.L was additionally supported by the China Scholarship Council (File No. 201206240040)

REFERENCES

1. Hirschhorn R, Reuser AJJ. Glycogen storage disease type II: acid α-glucosidase (acid maltase) deficiency. In: Scriver C, Beaudet, AL, Sly, WS and Valle, D ed. The Metabolic and Molecular Basis for Inherited Disease. New York: McGraw-Hill; 2001:3389–3420.
2. van der Ploeg AT, Reuser AJ. Pompe's disease. *Lancet*. 2008;372(9646):1342-1353.
3. van den Hout HM, Hop W, van Diggelen OP, et al. The natural course of infantile Pompe's disease: 20 original cases compared with 133 cases from the literature. *Pediatrics*. 2003;112(2):332-340.
4. Kishnani PS, Hwu WL, Mandel H, Nicolino M, Yong F, Corzo D. A retrospective, multinational, multicenter study on the natural history of infantile-onset Pompe disease. *J Pediatr*. 2006;148(5):671-676.
5. Wokke JH, Ausems MG, van den Boogaard MJ, et al. Genotype-phenotype correlation in adult-onset acid maltase deficiency. *Ann Neurol*. 1995;38(3):450-454.
6. Kroos M, Hoogeveen-Westerveld M, van der Ploeg A, Reuser AJ. The genotype-phenotype correlation in Pompe disease. *Am J Med Genet C Semin Med Genet*. 2012;160C(1):59-68.
7. Hagemans ML, Winkel LP, Van Doorn PA, et al. Clinical manifestation and natural course of late-onset Pompe's disease in 54 Dutch patients. *Brain*. 2005;128(Pt 3):671-677.
8. Winkel LP, Hagemans ML, van Doorn PA, et al. The natural course of non-classic Pompe's disease; a review of 225 published cases. *J Neurol*. 2005;252(8):875-884.
9. Thurberg BL, Lynch Maloney C, Vaccaro C, et al. Characterization of pre- and post-treatment pathology after enzyme replacement therapy for Pompe disease. *Lab Invest*. 2006;86(12):1208-1220.
10. Wens SC, Ciet P, Perez-Rovira A, et al. Lung MRI and impairment of diaphragmatic function in Pompe disease. *BMC Pulm Med*. 2015;15:54.
11. Mogalle K, Perez-Rovira A, Ciet P, et al. Quantification of Diaphragm Mechanics in Pompe Disease Using Dynamic 3D MRI. *PLoS One*. 2016;11(7):e0158912.
12. DeRuisseau LR, Fuller DD, Qiu K, et al. Neural deficits contribute to respiratory insufficiency in Pompe disease. *Proc Natl Acad Sci U S A*. 2009;106(23):9419-9424.
13. Sidman RL, Taksir T, Fidler J, et al. Temporal neuropathologic and behavioral phenotype of 6neo/6neo Pompe disease mice. *J Neuropathol Exp Neurol*. 2008;67(8):803-818.
14. Teng YT, Su WJ, Hou JW, Huang SF. Infantile-onset glycogen storage disease type II (Pompe disease): report of a case with genetic diagnosis and pathological findings. *Chang Gung Med J*. 2004;27(5):379-384.
15. Caddell JL, Whittemore R. Observations on generalized glycogenosis with emphasis on electrocardiographic changes. *Pediatrics*. 1962;29:743-763.
16. Crome L, Cumings JN, Duckett S. Neuropathological and Neurochemical Aspects of Generalized Glycogen Storage Disease. *J Neurol Neurosurg Psychiatry*. 1963;26:422-430.
17. Mancall EL, Aponte GE, Berry RG. Pompe's Disease (Diffuse Glycogenosis) with Neuronal Storage. *J Neuropathol Exp Neurol*. 1965;24:85-96.
18. Gambetti P, DiMauro S, Baker L. Nervous system in Pompe's disease. Ultrastructure and biochemistry. *J Neuropathol Exp Neurol*. 1971;30(3):412-430.

19. Martin JJ, de Barsy T, van Hoof F, Palladini G. Pompe's disease: an inborn lysosomal disorder with storage of glycogen. A study of brain and striated muscle. *Acta Neuropathol.* 1973;23(3):229-244.

20. Martini C, Ciana G, Benettoni A, et al. Intractable fever and cortical neuronal glycogen storage in glycogenosis type 2. *Neurology.* 2001;57(5):906-908.

21. Rohrbach M, Klein A, Kohli-Wiesner A, et al. CRIM-negative infantile Pompe disease: 42-month treatment outcome. *J Inherit Metab Dis.* 2010;33(6):751-757.

22. Matsuoka T, Miwa Y, Tajika M, et al. Divergent clinical outcomes of alpha-glucosidase enzyme replacement therapy in two siblings with infantile-onset Pompe disease treated in the symptomatic or pre-symptomatic state. *Mol Genet Metab Rep.* 2016;9:98-105.

23. Ebbink BJ, Aarsen FK, van Gelder CM, et al. Cognitive outcome of patients with classic infantile Pompe disease receiving enzyme therapy. *Neurology.* 2012;78(19):1512-1518.

24. Ebbink BJ, Poelman E, Plug I, et al. Cognitive decline in classic infantile Pompe disease: An underacknowledged challenge. *Neurology.* 2016;86(13):1260-1261.

25. Pardridge WM. The blood-brain barrier: bottleneck in brain drug development. *NeuroRx.* 2005;2(1):3-14.

26. Miranda SR, He X, Simonaro CM, et al. Infusion of recombinant human acid sphingomyelinase into niemann-pick disease mice leads to visceral, but not neurological, correction of the pathophysiology. *Faseb J.* 2000;14(13):1988-1995.

27. Desnick RJ, Schuchman EH. Enzyme replacement therapy for lysosomal diseases: lessons from 20 years of experience and remaining challenges. *Annu Rev Genomics Hum Genet.* 2012;13:307-335.

28. Hemsley KM, Hopwood JJ. Emerging therapies for neurodegenerative lysosomal storage disorders - from concept to reality. *J Inherit Metab Dis.* 2011;34(5):1003-1012.

29. Ahn SY, Chang YS, Sung DK, et al. High-dose enzyme replacement therapy attenuates cerebroventriculomegaly in a mouse model of mucopolysaccharidosis type II. *J Hum Genet.* 2013;58(11):728-733.

30. Ou L, Herzog T, Koniar BL, Gunther R, Whitley CB. High-dose enzyme replacement therapy in murine Hurler syndrome. *Mol Genet Metab.* 2014;111(2):116-122.

31. Cho SY, Lee J, Ko AR, et al. Effect of systemic high dose enzyme replacement therapy on the improvement of CNS defects in a mouse model of mucopolysaccharidosis type II. *Orphanet J Rare Dis.* 2015;10:141.

32. Vellodi A, Tylki-Szymanska A, Davies EH, et al. Management of neuronopathic Gaucher disease: revised recommendations. *J Inherit Metab Dis.* 2009;32(5):660-664.

33. Kakkis E, McEntee M, Vogler C, et al. Intrathecal enzyme replacement therapy reduces lysosomal storage in the brain and meninges of the canine model of MPS I. *Mol Genet Metab.* 2004;83(1-2):163-174.

34. Savas PS, Hemsley KM, Hopwood JJ. Intracerebral injection of sulfamidase delays neuropathology in murine MPS-IIIA. *Mol Genet Metab.* 2004;82(4):273-285.

35. Hemsley KM, Norman EJ, Crawley AC, et al. Effect of cisternal sulfamidase delivery in MPS IIIA Huntaway dogs--a proof of principle study. *Mol Genet Metab.* 2009;98(4):383-392.

36. Stroobants S, Gerlach D, Matthes F, et al. Intracerebroventricular enzyme infusion corrects central nervous system pathology and dysfunction in a mouse model of metachromatic leukodystrophy. *Hum Mol Genet*. 2011;20(14):2760-2769.

37. Vuillemenot BR, Katz ML, Coates JR, et al. Intrathecal tripeptidyl-peptidase 1 reduces lysosomal storage in a canine model of late infantile neuronal ceroid lipofuscinosis. *Mol Genet Metab*. 2011;104(3):325-337.

38. Sohn YB, Lee J, Cho SY, et al. Improvement of CNS defects via continuous intrathecal enzyme replacement by osmotic pump in mucopolysaccharidosis type II mice. *Am J Med Genet A*. 2013;161A(5):1036-1043.

39. Dickson PI, Chen AH. Intrathecal enzyme replacement therapy for mucopolysaccharidosis I: translating success in animal models to patients. *Curr Pharm Biotechnol*. 2011;12(6):946-955.

40. Jones SA, Breen C, Heap F, et al. A phase 1/2 study of intrathecal heparan-N-sulfatase in patients with mucopolysaccharidosis IIIA. *Mol Genet Metab*. 2016;118(3):198-205.

41. Muenzer J, Hendriksz CJ, Fan Z, et al. A phase I/II study of intrathecal idursulfase-IT in children with severe mucopolysaccharidosis II. *Genet Med*. 2016;18(1):73-81.

42. Nestrasil I, Shapiro E, Svatkova A, et al. Intrathecal enzyme replacement therapy reverses cognitive decline in mucopolysaccharidosis type I. *Am J Med Genet A*. 2017;173(3):780-783.

43. Pardridge WM. CSF, blood-brain barrier, and brain drug delivery. *Expert Opin Drug Deliv*. 2016;13(7):963-975.

44. Wiseman JA, Meng Y, Nemtsova Y, et al. Chronic Enzyme Replacement to the Brain of a Late Infantile Neuronal Ceroid Lipofuscinosis Mouse Has Differential Effects on Phenotypes of Disease. *Mol Ther Methods Clin Dev*. 2017;4:204-212.

45. Broadwell RD. Transcytosis of macromolecules through the blood-brain barrier: a cell biological perspective and critical appraisal. *Acta Neuropathol*. 1989;79(2):117-128.

46. Pardridge WM. Drug and gene targeting to the brain with molecular Trojan horses. *Nat Rev Drug Discov*. 2002;1(2):131-139.

47. Pardridge WM. Blood-brain barrier delivery. *Drug Discov Today*. 2007;12(1-2):54-61.

48. Pardridge WM. Drug transport across the blood-brain barrier. *J Cereb Blood Flow Metab*. 2012;32(11):1959-1972.

49. Pardridge WM. Targeted delivery of protein and gene medicines through the blood-brain barrier. *Clin Pharmacol Ther*. 2015;97(4):347-361.

50. Muro S. Strategies for delivery of therapeutics into the central nervous system for treatment of lysosomal storage disorders. *Drug Deliv Transl Res*. 2012;2(3):169-186.

51. Kelly JM, Bradbury A, Martin DR, Byrne ME. Emerging therapies for neuropathic lysosomal storage disorders. *Prog Neurobiol*. 2016.

52. Maga JA, Zhou J, Kambampati R, et al. Glycosylation-independent lysosomal targeting of acid alpha-glucosidase enhances muscle glycogen clearance in pompe mice. *J Biol Chem*. 2013;288(3):1428-1438.

53. Zhao KW, Neufeld EF. Purification and characterization of recombinant human alpha-N-acetylglucosaminidase secreted by Chinese hamster ovary cells. *Protein Expr Purif*. 2000;19(1):202-211.

54. Peng J, Dalton J, Butt M, et al. Reveglucosidase alfa (BMN 701), an IGF2-Tagged rhAcid alpha-Glucosidase, Improves Respiratory Functional Parameters in a Murine Model of Pompe Disease. *J Pharmacol Exp Ther*. 2017;360(2):313-323.

55. Sklar MM, Kiess W, Thomas CL, Nissley SP. Developmental expression of the tissue insulin-like growth factor II/mannose 6-phosphate receptor in the rat. Measurement by quantitative immunoblotting. *J Biol Chem*. 1989;264(28):16733-16738.

56. Ballesteros M, Scott CD, Baxter RC. Developmental regulation of insulin-like growth factor-II/mannose 6-phosphate receptor mRNA in the rat. *Biochem Biophys Res Commun*. 1990;172(2):775-779.

57. Urayama A, Grubb JH, Sly WS, Banks WA. Developmentally regulated mannose 6-phosphate receptor-mediated transport of a lysosomal enzyme across the blood-brain barrier. *Proc Natl Acad Sci U S A*. 2004;101(34):12658-12663.

58. Duffy KR, Pardridge WM, Rosenfeld RG. Human blood-brain barrier insulin-like growth factor receptor. *Metabolism*. 1988;37(2):136-140.

59. Boado RJ, Hui EK, Lu JZ, Pardridge WM. AGT-181: expression in CHO cells and pharmacokinetics, safety, and plasma iduronidase enzyme activity in Rhesus monkeys. *J Biotechnol*. 2009;144(2):135-141.

60. Lu JZ, Hui EK, Boado RJ, Pardridge WM. Genetic engineering of a bifunctional IgG fusion protein with iduronate-2-sulfatase. *Bioconjug Chem*. 2010;21(1):151-156.

61. Boado RJ, Pardridge WM. Brain and Organ Uptake in the Rhesus Monkey in Vivo of Recombinant Iduronidase Compared to an Insulin Receptor Antibody-Iduronidase Fusion Protein. *Mol Pharm*. 2017;14(4):1271-1277.

62. Boado RJ, Ka-Wai Hui E, Zhiqiang Lu J, Pardridge WM. Insulin receptor antibody-iduronate 2-sulfatase fusion protein: pharmacokinetics, anti-drug antibody, and safety pharmacology in Rhesus monkeys. *Biotechnol Bioeng*. 2014;111(11):2317-2325.

63. Boado RJ, Lu JZ, Hui EK, Pardridge WM. Insulin receptor antibody-sulfamidase fusion protein penetrates the primate blood-brain barrier and reduces glycosoaminoglycans in Sanfilippo type A cells. *Mol Pharm*. 2014;11(8):2928-2934.

64. Boado RJ, Lu JZ, Hui EK, Lin H, Pardridge WM. Insulin Receptor Antibody-alpha-N-Acetylglucosaminidase Fusion Protein Penetrates the Primate Blood-Brain Barrier and Reduces Glycosoaminoglycans in Sanfilippo Type B Fibroblasts. *Mol Pharm*. 2016;13(4):1385-1392.

65. Boado RJ, Lu JZ, Hui EK, Sumbria RK, Pardridge WM. Pharmacokinetics and brain uptake in the rhesus monkey of a fusion protein of arylsulfatase a and a monoclonal antibody against the human insulin receptor. *Biotechnol Bioeng*. 2013;110(5):1456-1465.

66. Bockenhoff A, Cramer S, Wolte P, et al. Comparison of five peptide vectors for improved brain delivery of the lysosomal enzyme arylsulfatase A. *J Neurosci*. 2014;34(9):3122-3129.

67. Zhang Y, Pardridge WM. Delivery of beta-galactosidase to mouse brain via the blood-brain barrier transferrin receptor. *J Pharmacol Exp Ther*. 2005;313(3):1075-1081.

68. Boado RJ, Hui EK, Lu JZ, Zhou QH, Pardridge WM. Reversal of lysosomal storage in brain of adult MPS-I mice with intravenous Trojan horse-iduronidase fusion protein. *Mol Pharm*. 2011;8(4):1342-1350.

69. Byrne B, Barohn R, Barshop B, et al. Preliminary clinical efficacy and safety of BMN 701, GILT-tagged recombinant human acid alpha glucosidase (rhGAA), in late-onset Pompe disease: results of an extension study. *Molecular Genetics and Metabolism*. 2014;111(2):S29.

70. Hiwot T, Barohn R, Bratkovic D, et al. G.O.20 - Reveglucosidase alfa (BMN 701), a GILT-tagged recombinant human acid alpha glucosidase (rhGAA), evaluation in late-onset Pompe disease: Preliminary clinical efficacy and safety results of an extension study (72-week results). *Neuromuscular Disorders*. 2015;25, Supplement 2:S313-S314.

71. Boado RJ, Hui EK, Lu JZ, Pardridge WM. Glycemic control and chronic dosing of rhesus monkeys with a fusion protein of iduronidase and a monoclonal antibody against the human insulin receptor. *Drug Metab Dispos*. 2012;40(10):2021-2025.

72. Auer RN. Hypoglycemic brain damage. *Metab Brain Dis*. 2004;19(3-4):169-175.

73. Languren G, Montiel T, Julio-Amilpas A, Massieu L. Neuronal damage and cognitive impairment associated with hypoglycemia: An integrated view. *Neurochem Int*. 2013;63(4):331-343.

74. Banugaria SG, Prater SN, Ng YK, et al. The impact of antibodies on clinical outcomes in diseases treated with therapeutic protein: lessons learned from infantile Pompe disease. *Genet Med*. 2011;13(8):729-736.

75. van Gelder CM, Hoogeveen-Westerveld M, Kroos MA, Plug I, van der Ploeg AT, Reuser AJ. Enzyme therapy and immune response in relation to CRIM status: the Dutch experience in classic infantile Pompe disease. *J Inherit Metab Dis*. 2015;38(2):305-314.

76. Byrne BJ, Falk DJ, Pacak CA, et al. Pompe disease gene therapy. *Hum Mol Genet*. 2011;20(R1):R61-68.

77. Maguire CA, Ramirez SH, Merkel SF, Sena-Esteves M, Breakefield XO. Gene therapy for the nervous system: challenges and new strategies. *Neurotherapeutics*. 2014;11(4):817-839.

78. Aronovich EL, Hackett PB. Lysosomal storage disease: gene therapy on both sides of the blood-brain barrier. *Mol Genet Metab*. 2015;114(2):83-93.

79. Naldini L. Gene therapy returns to centre stage. *Nature*. 2015;526(7573):351-360.

80. Choudhury SR, Hudry E, Maguire CA, Sena-Esteves M, Breakefield XO, Grandi P. Viral vectors for therapy of neurologic diseases. *Neuropharmacology*. 2016.

81. Grimm D, Kay MA. From virus evolution to vector revolution: use of naturally occurring serotypes of adeno-associated virus (AAV) as novel vectors for human gene therapy. *Curr Gene Ther*. 2003;3(4):281-304.

82. Balakrishnan B, Jayandharan GR. Basic biology of adeno-associated virus (AAV) vectors used in gene therapy. *Curr Gene Ther*. 2014;14(2):86-100.

83. Kotterman MA, Schaffer DV. Engineering adeno-associated viruses for clinical gene therapy. *Nat Rev Genet*. 2014;15(7):445-451.

84. Buchlis G, Podsakoff GM, Radu A, et al. Factor IX expression in skeletal muscle of a severe hemophilia B patient 10 years after AAV-mediated gene transfer. *Blood*. 2012;119(13):3038-3041.

85. Summerford C, Samulski RJ. Membrane-associated heparan sulfate proteoglycan is a receptor for adeno-associated virus type 2 virions. *J Virol*. 1998;72(2):1438-1445.

86. Kaludov N, Brown KE, Walters RW, Zabner J, Chiorini JA. Adeno-associated virus serotype 4 (AAV4) and AAV5 both require sialic acid binding for hemagglutination and efficient transduction but differ in sialic acid linkage specificity. *J Virol*. 2001;75(15):6884-6893.

87. Walters RW, Yi SM, Keshavjee S, et al. Binding of adeno-associated virus type 5 to 2,3-linked sialic acid is required for gene transfer. *J Biol Chem*. 2001;276(23):20610-20616.

88. Wu Z, Miller E, Agbandje-McKenna M, Samulski RJ. Alpha2,3 and alpha2,6 N-linked sialic acids facilitate efficient binding and transduction by adeno-associated virus types 1 and 6. *J Virol*. 2006;80(18):9093-9103.

89. Shen S, Bryant KD, Brown SM, Randell SH, Asokan A. Terminal N-linked galactose is the primary receptor for adeno-associated virus 9. *J Biol Chem*. 2011;286(15):13532-13540.

90. Zincarelli C, Soltys S, Rengo G, Rabinowitz JE. Analysis of AAV serotypes 1-9 mediated gene expression and tropism in mice after systemic injection. *Mol Ther*. 2008;16(6):1073-1080.

91. Palomeque J, Chemaly ER, Colosi P, et al. Efficiency of eight different AAV serotypes in transducing rat myocardium in vivo. *Gene Ther*. 2007;14(13):989-997.

92. Chao H, Liu Y, Rabinowitz J, Li C, Samulski RJ, Walsh CE. Several log increase in therapeutic transgene delivery by distinct adeno-associated viral serotype vectors. *Mol Ther*. 2000;2(6):619-623.

93. Gregorevic P, Blankinship MJ, Allen JM, et al. Systemic delivery of genes to striated muscles using adeno-associated viral vectors. *Nat Med*. 2004;10(8):828-834.

94. Nakai H, Fuess S, Storm TA, Muramatsu S, Nara Y, Kay MA. Unrestricted hepatocyte transduction with adeno-associated virus serotype 8 vectors in mice. *J Virol*. 2005;79(1):214-224.

95. Wang L, Wang H, Bell P, et al. Systematic evaluation of AAV vectors for liver directed gene transfer in murine models. *Mol Ther*. 2010;18(1):118-125.

96. Davidson BL, Stein CS, Heth JA, et al. Recombinant adeno-associated virus type 2, 4, and 5 vectors: transduction of variant cell types and regions in the mammalian central nervous system. *Proc Natl Acad Sci U S A*. 2000;97(7):3428-3432.

97. Taymans JM, Vandenberghe LH, Haute CV, et al. Comparative analysis of adeno-associated viral vector serotypes 1, 2, 5, 7, and 8 in mouse brain. *Hum Gene Ther*. 2007;18(3):195-206.

98. Wang C, Wang CM, Clark KR, Sferra TJ. Recombinant AAV serotype 1 transduction efficiency and tropism in the murine brain. *Gene Ther*. 2003;10(17):1528-1534.

99. Foust KD, Nurre E, Montgomery CL, Hernandez A, Chan CM, Kaspar BK. Intravascular AAV9 preferentially targets neonatal neurons and adult astrocytes. *Nat Biotechnol*. 2009;27(1):59-65.

100. Gray SJ, Matagne V, Bachaboina L, Yadav S, Ojeda SR, Samulski RJ. Preclinical differences of intravascular AAV9 delivery to neurons and glia: a comparative study of adult mice and nonhuman primates. *Mol Ther.* 2011;19(6):1058-1069.

101. Saraiva J, Nobre RJ, Pereira de Almeida L. Gene therapy for the CNS using AAVs: The impact of systemic delivery by AAV9. *J Control Release.* 2016;241:94-109.

102. Dehay B, Dalkara D, Dovero S, Li Q, Bezard E. Systemic scAAV9 variant mediates brain transduction in newborn rhesus macaques. *Sci Rep.* 2012;2:253.

103. Samaranch L, Salegio EA, San Sebastian W, et al. Adeno-associated virus serotype 9 transduction in the central nervous system of nonhuman primates. *Hum Gene Ther.* 2012;23(4):382-389.

104. Bevan AK, Duque S, Foust KD, et al. Systemic gene delivery in large species for targeting spinal cord, brain, and peripheral tissues for pediatric disorders. *Mol Ther.* 2011;19(11):1971-1980.

105. Garancis JC. Type II glycogenosis. Biochemical and electron microscopic study. *Am J Med.* 1968;44(2):289-300.

106. Cataldo AM, Broadwell RD. Cytochemical identification of cerebral glycogen and glucose-6-phosphatase activity under normal and experimental conditions. II. Choroid plexus and ependymal epithelia, endothelia and pericytes. *J Neurocytol.* 1986;15(4):511-524.

107. Oe Y, Baba O, Ashida H, Nakamura KC, Hirase H. Glycogen distribution in the microwave-fixed mouse brain reveals heterogeneous astrocytic patterns. *Glia.* 2016;64(9):1532-1545.

108. Brown AM, Tekkok SB, Ransom BR. Glycogen regulation and functional role in mouse white matter. *J Physiol.* 2003;549(Pt 2):501-512.

109. Brown AM, Baltan Tekkok S, Ransom BR. Energy transfer from astrocytes to axons: the role of CNS glycogen. *Neurochem Int.* 2004;45(4):529-536.

110. Brown AM, Ransom BR. Astrocyte glycogen and brain energy metabolism. *Glia.* 2007;55(12):1263-1271.

111. Saez I, Duran J, Sinadinos C, et al. Neurons have an active glycogen metabolism that contributes to tolerance to hypoxia. *J Cereb Blood Flow Metab.* 2014;34(6):945-955.

112. Colangelo AM, Alberghina L, Papa M. Astrogliosis as a therapeutic target for neurodegenerative diseases. *Neurosci Lett.* 2014;565:59-64.

113. Duque S, Joussemet B, Riviere C, et al. Intravenous administration of self-complementary AAV9 enables transgene delivery to adult motor neurons. *Mol Ther.* 2009;17(7):1187-1196.

114. Foust KD, Wang X, McGovern VL, et al. Rescue of the spinal muscular atrophy phenotype in a mouse model by early postnatal delivery of SMN. *Nat Biotechnol.* 2010;28(3):271-274.

115. Pacak CA, Mah CS, Thattaliyath BD, et al. Recombinant adeno-associated virus serotype 9 leads to preferential cardiac transduction in vivo. *Circ Res.* 2006;99(4):e3-9.

116. Inagaki K, Fuess S, Storm TA, et al. Robust systemic transduction with AAV9 vectors in mice: efficient global cardiac gene transfer superior to that of AAV8. *Mol Ther.* 2006;14(1):45-53.

117. Prasad KM, Xu Y, Yang Z, Acton ST, French BA. Robust cardiomyocyte-specific gene expression following systemic injection of AAV: in vivo gene delivery follows a Poisson distribution. *Gene Ther.* 2011;18(1):43-52.

118. Ruzo A, Marco S, Garcia M, et al. Correction of pathological accumulation of glycosaminoglycans in central nervous system and peripheral tissues of MPSIIIA mice through systemic AAV9 gene transfer. *Hum Gene Ther.* 2012;23(12):1237-1246.

119. Fu H, Dirosario J, Killedar S, Zaraspe K, McCarty DM. Correction of neurological disease of mucopolysaccharidosis IIIB in adult mice by rAAV9 trans-blood-brain barrier gene delivery. *Mol Ther.* 2011;19(6):1025-1033.

120. Fu H, Meadows AS, Ware T, Mohney RP, McCarty DM. Near-Complete Correction of Profound Metabolomic Impairments Corresponding to Functional Benefit in MPS IIIB Mice after IV rAAV9-hNAGLU Gene Delivery. *Mol Ther.* 2017;25(3):792-802.

121. Weismann CM, Ferreira J, Keeler AM, et al. Systemic AAV9 gene transfer in adult GM1 gangliosidosis mice reduces lysosomal storage in CNS and extends lifespan. *Hum Mol Genet.* 2015;24(15):4353-4364.

122. Walia JS, Altaleb N, Bello A, et al. Long-term correction of Sandhoff disease following intravenous delivery of rAAV9 to mouse neonates. *Mol Ther.* 2015;23(3):414-422.

123. Miyake N, Miyake K, Asakawa N, Yamamoto M, Shimada T. Long-term correction of biochemical and neurological abnormalities in MLD mice model by neonatal systemic injection of an AAV serotype 9 vector. *Gene Ther.* 2014;21(4):427-433.

124. Murrey DA, Naughton BJ, Duncan FJ, et al. Feasibility and safety of systemic rAAV9-hNAGLU delivery for treating mucopolysaccharidosis IIIB: toxicology, biodistribution, and immunological assessments in primates. *Hum Gene Ther Clin Dev.* 2014;25(2):72-84.

125. Sun B, Zhang H, Franco LM, et al. Efficacy of an adeno-associated virus 8-pseudotyped vector in glycogen storage disease type II. *Mol Ther.* 2005;11(1):57-65.

126. Sun B, Young SP, Li P, et al. Correction of multiple striated muscles in murine Pompe disease through adeno-associated virus-mediated gene therapy. *Mol Ther.* 2008;16(8):1366-1371.

127. Ziegler RJ, Bercury SD, Fidler J, et al. Ability of adeno-associated virus serotype 8-mediated hepatic expression of acid alpha-glucosidase to correct the biochemical and motor function deficits of presymptomatic and symptomatic Pompe mice. *Hum Gene Ther.* 2008;19(6):609-621.

128. Falk DJ, Soustek MS, Todd AG, et al. Comparative impact of AAV and enzyme replacement therapy on respiratory and cardiac function in adult Pompe mice. *Mol Ther Methods Clin Dev.* 2015;2:15007.

129. Doerfler PA, Todd AG, Clement N, et al. Copackaged AAV9 Vectors Promote Simultaneous Immune Tolerance and Phenotypic Correction of Pompe Disease. *Hum Gene Ther.* 2016;27(1):43-59.

130. Boutin S, Monteilhet V, Veron P, et al. Prevalence of serum IgG and neutralizing factors against adeno-associated virus (AAV) types 1, 2, 5, 6, 8, and 9 in the healthy population: implications for gene therapy using AAV vectors. *Hum Gene Ther.* 2010;21(6):704-712.

131. Zaiss AK, Muruve DA. Immune responses to adeno-associated virus vectors. *Curr Gene Ther.* 2005;5(3):323-331.

132. Zaiss AK, Muruve DA. Immunity to adeno-associated virus vectors in animals and humans: a continued challenge. *Gene Ther.* 2008;15(11):808-816.

133. Mingozzi F, Maus MV, Hui DJ, et al. CD8(+) T-cell responses to adeno-associated virus capsid in humans. *Nat Med.* 2007;13(4):419-422.

134. Calcedo R, Wilson JM. Humoral Immune Response to AAV. *Front Immunol.* 2013;4:341.

135. Mingozzi F, High KA. Immune responses to AAV in clinical trials. *Curr Gene Ther.* 2011;11(4):321-330.

136. Manno CS, Pierce GF, Arruda VR, et al. Successful transduction of liver in hemophilia by AAV-Factor IX and limitations imposed by the host immune response. *Nat Med.* 2006;12(3):342-347.

137. Nathwani AC, Rosales C, McIntosh J, et al. Long-term safety and efficacy following systemic administration of a self-complementary AAV vector encoding human FIX pseudotyped with serotype 5 and 8 capsid proteins. *Mol Ther.* 2011;19(5):876-885.

138. Ciesielska A, Hadaczek P, Mittermeyer G, et al. Cerebral infusion of AAV9 vector-encoding non-self proteins can elicit cell-mediated immune responses. *Mol Ther.* 2013;21(1):158-166.

139. Cresawn KO, Fraites TJ, Wasserfall C, et al. Impact of humoral immune response on distribution and efficacy of recombinant adeno-associated virus-derived acid alpha-glucosidase in a model of glycogen storage disease type II. *Hum Gene Ther.* 2005;16(1):68-80.

140. Sun B, Li S, Bird A, et al. Antibody formation and mannose-6-phosphate receptor expression impact the efficacy of muscle-specific transgene expression in murine Pompe disease. *J Gene Med.* 2010;12(11):881-891.

141. Franco LM, Sun B, Yang X, et al. Evasion of immune responses to introduced human acid alpha-glucosidase by liver-restricted expression in glycogen storage disease type II. *Mol Ther.* 2005;12(5):876-884.

142. Sun B, Bird A, Young SP, Kishnani PS, Chen YT, Koeberl DD. Enhanced response to enzyme replacement therapy in Pompe disease after the induction of immune tolerance. *Am J Hum Genet.* 2007;81(5):1042-1049.

143. Sun B, Kulis MD, Young SP, et al. Immunomodulatory gene therapy prevents antibody formation and lethal hypersensitivity reactions in murine pompe disease. *Mol Ther.* 2010;18(2):353-360.

144. Zhang P, Sun B, Osada T, et al. Immunodominant liver-specific expression suppresses transgene-directed immune responses in murine pompe disease. *Hum Gene Ther.* 2012;23(5):460-472.

145. Mingozzi F, Meulenberg JJ, Hui DJ, et al. AAV-1-mediated gene transfer to skeletal muscle in humans results in dose-dependent activation of capsid-specific T cells. *Blood.* 2009;114(10):2077-2086.

146. Kaeppel C, Beattie SG, Fronza R, et al. A largely random AAV integration profile after LPLD gene therapy. *Nat Med.* 2013;19(7):889-891.

147. Donsante A, Miller DG, Li Y, et al. AAV vector integration sites in mouse hepatocellular carcinoma. *Science*. 2007;317(5837):477.

148. Chandler RJ, LaFave MC, Varshney GK, et al. Vector design influences hepatic genotoxicity after adeno-associated virus gene therapy. *J Clin Invest*. 2015;125(2):870-880.

149. Nathwani AC, Reiss UM, Tuddenham EG, et al. Long-term safety and efficacy of factor IX gene therapy in hemophilia B. *N Engl J Med*. 2014;371(21):1994-2004.

150. Dayton RD, Wang DB, Klein RL. The advent of AAV9 expands applications for brain and spinal cord gene delivery. *Expert Opin Biol Ther*. 2012;12(6):757-766.

151. Wang D, El-Amouri SS, Dai M, et al. Engineering a lysosomal enzyme with a derivative of receptor-binding domain of apoE enables delivery across the blood-brain barrier. *Proc Natl Acad Sci U S A*. 2013;110(8):2999-3004.

152. Mingozzi F, High KA. Therapeutic in vivo gene transfer for genetic disease using AAV: progress and challenges. *Nat Rev Genet*. 2011;12(5):341-355.

153. Krivit W, Sung JH, Shapiro EG, Lockman LA. Microglia: the effector cell for reconstitution of the central nervous system following bone marrow transplantation for lysosomal and peroxisomal storage diseases. *Cell Transplant*. 1995;4(4):385-392.

154. Mildner A, Schmidt H, Nitsche M, et al. Microglia in the adult brain arise from Ly-6ChiCCR2+ monocytes only under defined host conditions. *Nat Neurosci*. 2007;10(12):1544-1553.

155. Eglitis MA, Mezey E. Hematopoietic cells differentiate into both microglia and macroglia in the brains of adult mice. *Proc Natl Acad Sci U S A*. 1997;94(8):4080-4085.

156. Kennedy DW, Abkowitz JL. Kinetics of central nervous system microglial and macrophage engraftment: analysis using a transgenic bone marrow transplantation model. *Blood*. 1997;90(3):986-993.

157. Simard AR, Rivest S. Bone marrow stem cells have the ability to populate the entire central nervous system into fully differentiated parenchymal microglia. *Faseb J*. 2004;18(9):998-1000.

158. Lawson LJ, Perry VH, Gordon S. Turnover of resident microglia in the normal adult mouse brain. *Neuroscience*. 1992;48(2):405-415.

159. Massengale M, Wagers AJ, Vogel H, Weissman IL. Hematopoietic cells maintain hematopoietic fates upon entering the brain. *J Exp Med*. 2005;201(10):1579-1589.

160. Ajami B, Bennett JL, Krieger C, Tetzlaff W, Rossi FM. Local self-renewal can sustain CNS microglia maintenance and function throughout adult life. *Nat Neurosci*. 2007;10(12):1538-1543.

161. Prinz M, Mildner A. Microglia in the CNS: immigrants from another world. *Glia*. 2011;59(2):177-187.

162. Diserbo M, Agin A, Lamproglou I, et al. Blood-brain barrier permeability after gamma whole-body irradiation: an in vivo microdialysis study. *Can J Physiol Pharmacol*. 2002;80(7):670-678.

163. Kaya M, Palanduz A, Kalayci R, et al. Effects of lipopolysaccharide on the radiation-induced changes in the blood-brain barrier and the astrocytes. *Brain Res*. 2004;1019(1-2):105-112.

164. Li YQ, Chen P, Haimovitz-Friedman A, Reilly RM, Wong CS. Endothelial apoptosis initiates acute blood-brain barrier disruption after ionizing radiation. *Cancer Res.* 2003;63(18):5950-5956.

165. Linard C, Marquette C, Mathieu J, Pennequin A, Clarencon D, Mathe D. Acute induction of inflammatory cytokine expression after gamma-irradiation in the rat: effect of an NF-kappaB inhibitor. *Int J Radiat Oncol Biol Phys.* 2004;58(2):427-434.

166. Mildner A, Schlevogt B, Kierdorf K, et al. Distinct and non-redundant roles of microglia and myeloid subsets in mouse models of Alzheimer's disease. *J Neurosci.* 2011;31(31):11159-11171.

167. Biffi A, De Palma M, Quattrini A, et al. Correction of metachromatic leukodystrophy in the mouse model by transplantation of genetically modified hematopoietic stem cells. *J Clin Invest.* 2004;113(8):1118-1129.

168. Sano R, Tessitore A, Ingrassia A, d'Azzo A. Chemokine-induced recruitment of genetically modified bone marrow cells into the CNS of GM1-gangliosidosis mice corrects neuronal pathology. *Blood.* 2005;106(7):2259-2268.

169. Ohmi K, Greenberg DS, Rajavel KS, Ryazantsev S, Li HH, Neufeld EF. Activated microglia in cortex of mouse models of mucopolysaccharidoses I and IIIB. *Proc Natl Acad Sci U S A.* 2003;100(4):1902-1907.

170. Capotondo A, Milazzo R, Politi LS, et al. Brain conditioning is instrumental for successful microglia reconstitution following hematopoietic stem cell transplantation. *Proc Natl Acad Sci U S A.* 2012;109(37):15018-15023.

171. Wilkinson FL, Sergijenko A, Langford-Smith KJ, Malinowska M, Wynn RF, Bigger BW. Busulfan conditioning enhances engraftment of hematopoietic donor-derived cells in the brain compared with irradiation. *Mol Ther.* 2013;21(4):868-876.

172. Orchard PJ, Blazar BR, Wagner J, Charnas L, Krivit W, Tolar J. Hematopoietic cell therapy for metabolic disease. *J Pediatr.* 2007;151(4):340-346.

173. Sauer M, Grewal S, Peters C. Hematopoietic stem cell transplantation for mucopolysaccharidoses and leukodystrophies. *Klin Padiatr.* 2004;216(3):163-168.

174. Boelens JJ, van Hasselt PM. Neurodevelopmental Outcome after Hematopoietic Cell Transplantation in Inborn Errors of Metabolism: Current Considerations and Future Perspectives. *Neuropediatrics.* 2016;47(5):285-292.

175. Aldenhoven M, Boelens JJ, de Koning TJ. The clinical outcome of Hurler syndrome after stem cell transplantation. *Biol Blood Marrow Transplant.* 2008;14(5):485-498.

176. Prasad VK, Kurtzberg J. Transplant outcomes in mucopolysaccharidoses. *Semin Hematol.* 2010;47(1):59-69.

177. Whitley CB, Belani KG, Chang PN, et al. Long-term outcome of Hurler syndrome following bone marrow transplantation. *Am J Med Genet.* 1993;46(2):209-218.

178. Peters C, Balthazor M, Shapiro EG, et al. Outcome of unrelated donor bone marrow transplantation in 40 children with Hurler syndrome. *Blood.* 1996;87(11):4894-4902.

179. Peters C, Shapiro EG, Anderson J, et al. Hurler syndrome: II. Outcome of HLA-genotypically identical sibling and HLA-haploidentical related donor bone marrow transplantation in fif-

ty-four children. The Storage Disease Collaborative Study Group. *Blood*. 1998;91(7):2601-2608.

180. Peters C, Shapiro EG, Krivit W. Neuropsychological development in children with Hurler syndrome following hematopoietic stem cell transplantation. *Pediatr Transplant*. 1998;2(4):250-253.
181. Staba SL, Escolar ML, Poe M, et al. Cord-blood transplants from unrelated donors in patients with Hurler's syndrome. *N Engl J Med*. 2004;350(19):1960-1969.
182. Aldenhoven M, Wynn RF, Orchard PJ, et al. Long-term outcome of Hurler syndrome patients after hematopoietic cell transplantation: an international multicenter study. *Blood*. 2015;125(13):2164-2172.
183. Kunin-Batson AS, Shapiro EG, Rudser KD, et al. Long-Term Cognitive and Functional Outcomes in Children with Mucopolysaccharidosis (MPS)-IH (Hurler Syndrome) Treated with Hematopoietic Cell Transplantation. *JIMD Rep*. 2016;29:95-102.
184. Muenzer J, Wraith JE, Clarke LA, International Consensus Panel on M, Treatment of Mucopolysaccharidosis I. Mucopolysaccharidosis I: management and treatment guidelines. *Pediatrics*. 2009;123(1):19-29.
185. de Ru MH, Boelens JJ, Das AM, et al. Enzyme replacement therapy and/or hematopoietic stem cell transplantation at diagnosis in patients with mucopolysaccharidosis type I: results of a European consensus procedure. *Orphanet J Rare Dis*. 2011;6:55.
186. Lorioli L, Biffi A. Hematopoietic stem cell transplantation for metachromatic leukodystrophy. *Expert Opinion on Orphan Drugs*. 2015;3(8):911-919.
187. Martin HR, Poe MD, Provenzale JM, Kurtzberg J, Mendizabal A, Escolar ML. Neurodevelopmental outcomes of umbilical cord blood transplantation in metachromatic leukodystrophy. *Biol Blood Marrow Transplant*. 2013;19(4):616-624.
188. Solders M, Martin DA, Andersson C, et al. Hematopoietic SCT: a useful treatment for late metachromatic leukodystrophy. *Bone Marrow Transplant*. 2014;49(8):1046-1051.
189. Ding XQ, Bley A, Kohlschutter A, Fiehler J, Lanfermann H. Long-term neuroimaging follow-up on an asymptomatic juvenile metachromatic leukodystrophy patient after hematopoietic stem cell transplantation: evidence of myelin recovery and ongoing brain maturation. *Am J Med Genet A*. 2012;158A(1):257-260.
190. van Egmond ME, Pouwels PJ, Boelens JJ, et al. Improvement of white matter changes on neuroimaging modalities after stem cell transplant in metachromatic leukodystrophy. *JAMA Neurol*. 2013;70(6):779-782.
191. Krageloh-Mann I, Groeschel S, Kehrer C, et al. Juvenile metachromatic leukodystrophy 10 years post transplant compared with a non-transplanted cohort. *Bone Marrow Transplant*. 2013;48(3):369-375.
192. Gorg M, Wilck W, Granitzny B, et al. Stabilization of juvenile metachromatic leukodystrophy after bone marrow transplantation: a 13-year follow-up. *J Child Neurol*. 2007;22(9):1139-1142.
193. Bredius RG, Laan LA, Lankester AC, et al. Early marrow transplantation in a pre-symptomatic neonate with late infantile metachromatic leukodystrophy does not halt disease progression. *Bone Marrow Transplant*. 2007;39(5):309-310.

194. Krivit W, Shapiro EG, Peters C, et al. Hematopoietic stem-cell transplantation in globoid-cell leukodystrophy. *N Engl J Med*. 1998;338(16):1119-1126.

195. Escolar ML, Poe MD, Provenzale JM, et al. Transplantation of umbilical-cord blood in babies with infantile Krabbe's disease. *N Engl J Med*. 2005;352(20):2069-2081.

196. McKinnis EJ, Sulzbacher S, Rutledge JC, Sanders J, Scott CR. Bone marrow transplantation in Hunter syndrome. *J Pediatr*. 1996;129(1):145-148.

197. Klein KA, Krivit W, Whitley CB, et al. Poor cognitive outcome of eleven children with Sanfilippo syndrome after bone marrow transplantation and successful engraftment. *Bone Marrow Transplantation*. 1995;15(SUPPL. 1):S176-S181.

198. Shapiro EG, Lockman LA, Balthazor M, Krivit W. Neuropsychological outcomes of several storage diseases with and without bone marrow transplantation. *J Inherit Metab Dis*. 1995;18(4):413-429.

199. Vellodi A, Young E, New M, Pot-Mees C, Hugh-Jones K. Bone marrow transplantation for Sanfilippo disease type B. *J Inherit Metab Dis*. 1992;15(6):911-918.

200. Welling L, Marchal JP, van Hasselt P, van der Ploeg AT, Wijburg FA, Boelens JJ. Early Umbilical Cord Blood-Derived Stem Cell Transplantation Does Not Prevent Neurological Deterioration in Mucopolysaccharidosis Type III. *JIMD Rep*. 2015;18:63-68.

201. Peters C, Steward CG, National Marrow Donor P, International Bone Marrow Transplant R, Working Party on Inborn Errors EBMTG. Hematopoietic cell transplantation for inherited metabolic diseases: an overview of outcomes and practice guidelines. *Bone Marrow Transplant*. 2003;31(4):229-239.

202. Biffi A. Hematopoietic Stem Cell Gene Therapy for Storage Disease: Current and New Indications. *Mol Ther*. 2017.

203. Rodgers NJ, Kaizer AM, Miller WP, Rudser KD, Orchard PJ, Braunlin EA. Mortality after hematopoietic stem cell transplantation for severe mucopolysaccharidosis type I: the 30-year University of Minnesota experience. *J Inherit Metab Dis*. 2017;40(2):271-280.

204. Watson JG, Gardner-Medwin D, Goldfinch ME, Pearson AD. Bone marrow transplantation for glycogen storage disease type II (Pompe's disease). *N Engl J Med*. 1986;314(6):385.

205. Howell JM, Dorling PR, Shelton JN, Taylor EG, Palmer DG, Di Marco PN. Natural bone marrow transplantation in cattle with Pompe's disease. *Neuromuscul Disord*. 1991;1(6):449-454.

206. Naldini L. Ex vivo gene transfer and correction for cell-based therapies. *Nature Reviews Genetics*. 2011;12(5):301-315.

207. Biffi A. Gene therapy for lysosomal storage disorders: a good start. *Hum Mol Genet*. 2016;25(R1):R65-75.

208. Bai Y, Soda Y, Izawa K, et al. Effective transduction and stable transgene expression in human blood cells by a third-generation lentiviral vector. *Gene Ther*. 2003;10(17):1446-1457.

209. Logan AC, Haas DL, Kafri T, Kohn DB. Integrated self-inactivating lentiviral vectors produce full-length genomic transcripts competent for encapsidation and integration. *J Virol*. 2004;78(16):8421-8436.

210. Gieselmann V, Krageloh-Mann I. Metachromatic leukodystrophy--an update. *Neuropediatrics*. 2010;41(1):1-6.

211. Biffi A, Capotondo A, Fasano S, et al. Gene therapy of metachromatic leukodystrophy reverses neurological damage and deficits in mice. *J Clin Invest*. 2006;116(11):3070-3082.

212. Capotondo A, Cesani M, Pepe S, et al. Safety of arylsulfatase A overexpression for gene therapy of metachromatic leukodystrophy. *Hum Gene Ther*. 2007;18(9):821-836.

213. Biffi A, Montini E, Lorioli L, et al. Lentiviral hematopoietic stem cell gene therapy benefits metachromatic leukodystrophy. *Science*. 2013;341(6148):1233158.

214. Sessa M, Lorioli L, Fumagalli F, et al. Lentiviral haemopoietic stem-cell gene therapy in early-onset metachromatic leukodystrophy: an ad-hoc analysis of a non-randomised, open-label, phase 1/2 trial. *Lancet*. 2016;388(10043):476-487.

215. Visigalli I, Delai S, Politi LS, et al. Gene therapy augments the efficacy of hematopoietic cell transplantation and fully corrects mucopolysaccharidosis type I phenotype in the mouse model. *Blood*. 2010;116(24):5130-5139.

216. Wakabayashi T, Shimada Y, Akiyama K, et al. Hematopoietic Stem Cell Gene Therapy Corrects Neuropathic Phenotype in Murine Model of Mucopolysaccharidosis Type II. *Hum Gene Ther*. 2015;26(6):357-366.

217. Langford-Smith A, Wilkinson FL, Langford-Smith KJ, et al. Hematopoietic Stem Cell and Gene Therapy Corrects Primary Neuropathology and Behavior in Mucopolysaccharidosis IIIA Mice. *Mol Ther*. 2012;20(8):1610-1621.

218. Sergijenko A, Langford-Smith A, Liao AY, et al. Myeloid/Microglial driven autologous hematopoietic stem cell gene therapy corrects a neuronopathic lysosomal disease. *Mol Ther*. 2013;21(10):1938-1949.

219. Gentner B, Visigalli I, Hiramatsu H, et al. Identification of hematopoietic stem cell-specific miRNAs enables gene therapy of globoid cell leukodystrophy. *Sci Transl Med*. 2010;2(58):58ra84.

220. Douillard-Guilloux G, Richard E, Batista L, Caillaud C. Partial phenotypic correction and immune tolerance induction to enzyme replacement therapy after hematopoietic stem cell gene transfer of alpha-glucosidase in Pompe disease. *J Gene Med*. 2009;11(4):279-287.

221. van Til NP, Stok M, Aerts Kaya FS, et al. Lentiviral gene therapy of murine hematopoietic stem cells ameliorates the Pompe disease phenotype. *Blood*. 2010;115(26):5329-5337.

222. Raben N, Jatkar T, Lee A, et al. Glycogen stored in skeletal but not in cardiac muscle in acid alpha-glucosidase mutant (Pompe) mice is highly resistant to transgene-encoded human enzyme. *Mol Ther*. 2002;6(5):601-608.

223. Raben N, Fukuda T, Gilbert AL, et al. Replacing acid alpha-glucosidase in Pompe disease: recombinant and transgenic enzymes are equipotent, but neither completely clears glycogen from type II muscle fibers. *Mol Ther*. 2005;11(1):48-56.

224. Moreno-Carranza B, Gentsch M, Stein S, et al. Transgene optimization significantly improves SIN vector titers, gp91phox expression and reconstitution of superoxide production in X-CGD cells. *Gene Ther*. 2009;16(1):111-118.

225. Dull T, Zufferey R, Kelly M, et al. A third-generation lentivirus vector with a conditional packaging system. *J Virol*. 1998;72(11):8463-8471.

226. Zufferey R, Dull T, Mandel RJ, et al. Self-inactivating lentivirus vector for safe and efficient in vivo gene delivery. *J Virol*. 1998;72(12):9873-9880.

227. Schambach A, Zychlinski D, Ehrnstroem B, Baum C. Biosafety features of lentiviral vectors. *Hum Gene Ther.* 2013;24(2):132-142.

228. Cartier N, Hacein-Bey-Abina S, Bartholomae CC, et al. Hematopoietic stem cell gene therapy with a lentiviral vector in X-linked adrenoleukodystrophy. *Science.* 2009;326(5954):818-823.

Chapter 3

Lentiviral gene therapy with IGFII-tagged GAA corrects pathology in heart, skeletal muscle, and the central nervous system in a murine model for Pompe disease

Qiushi Liang, M.D.[1,2,3]; Joon M. Pijnenburg, B.A.Sc.[1,2,3]; Yvette van Helsdingen, B.A.Sc.[4]; Merel Stok, Ph.D.[1,2,3]; Gerard Wagemaker, Ph.D.[4]; Arnold G. Vulto, Pharm.D., Ph.D.[5]; Ans T. van der Ploeg, M.D., Ph.D.[2,3]; Niek P. van Til, Ph.D.[4,6]*; W.W.M. Pim Pijnappel, Ph.D.[1,2,3]*

[1] Molecular Stem Cell Biology, Department of Clinical Genetics, Erasmus University Medical Center, 3015GE Rotterdam, The Netherlands
[2] Department of Pediatrics, Erasmus University Medical Center, 3015GE Rotterdam, The Netherlands
[3] Center for Lysosomal and Metabolic Diseases, Erasmus University Medical Center, 3015GE Rotterdam, The Netherlands
[4] Department of Hematology, Erasmus University Medical Center, 3015GE Rotterdam, The Netherlands
[5] Hospital Pharmacy, Erasmus University Medical Center, 3015GE Rotterdam, The Netherlands
[6] Current address: Laboratory of Translational Immunology, University Medical Center Utrecht, 3584CX Utrecht, The Netherlands

* Correspondence:
Dr. W.W.M. Pim Pijnappel, Erasmus University Medical Center, 3015GE Rotterdam, The Netherlands.
Email: w.pijnappel@erasmusmc.nl.
Dr. N.P. van Til, University Medical Center Utrecht, Heidelberglaan 100, 3584 CX Utrecht, The Netherlands.
Email: N.P.vanTil@umcutrecht.nl.

Manuscript submitted

ABSTRACT

Pompe disease is a lysosomal storage disease caused by deficiency of acid α-glucosidase (GAA). As a result, lysosomal glycogen is accumulated in muscle and the nervous system. This leads to severe cardiac, skeletomuscular and respiratory dysfunction, as well as cognitive decline. Enzyme replacement therapy (ERT) with weekly or biweekly infusion of recombinant human GAA (rhGAA) is currently the only available treatment. It is effective in reducing cardiac hypertrophy but insufficient to improve motor function and respiratory abnormalities, partially due to poor targeting of the rhGAA to affected tissues, and the formation of anti-GAA antibodies. Cognitive decline has been observed more recently in Pompe patients, for which ERT is ineffective due to the blood-brain barrier. Aiming for an alternative treatment option, hematopoietic stem cell mediated lentiviral gene therapy in a Pompe murine model was previously shown to cause partial glycogen reduction in the heart and skeletal muscles but not in the brain. In the current study, we fused insulin-like growth factor II to a codon-optimized version of GAA (LV-IGFIIco.GAAco), with the aim to improve the efficiency by increasing the delivery to target tissues. A quantitative analysis was performed by varying lentiviral vector dosage, transplanted cell number, and irradiation dose. The LV-IGFIIco.GAAco lentiviral vector showed improved efficacy compared to LV-GAAco and fully normalized glycogen levels in the heart and skeletal muscles. *In vitro* analysis indicated that this was caused by increased uptake of IGFII.GAA by skeletal muscle cells. Interestingly, also glycogen accumulation in the brain was close to normalized by LV-IGFIIco.GAAco. We also identified neuroinflammation as a prominent phenotype in the Pompe mouse model. This was characterized by regional astrogliosis and widespread microglia activation which can also be attenuated by LV-IGFIIco.GAAco. These results identify LV-IGFIIco.GAAco as a candidate for the future clinical development of hematopoietic stem cell gene therapy for Pompe disease.

INTRODUCTION

Pompe disease, categorized as a lysosomal storage disorder, is caused by acid-α glucosidase (GAA) deficiency which leads to generalized glycogen accumulation, most prominently in cardiac and skeletal muscles.[1,2] Fatal cardiomyopathy is found primarily in the classic infantile onset form, and without treatment, patients usually die due to cardiorespiratory failure before the age of one.[3,4] Late-onset Pompe patients tend to have a milder phenotype characterized by progressive muscle weakness. They become ventilator-dependent and wheel-chair-bound at a later stage of disease.[5,6] Enzyme replacement treatment (ERT) with recombinant human GAA (rhGAA) derived from Chinese hamster ovary (CHO) cells was approved as registered treatment (Myozyme, Genzyme Corporation) for Pompe patients in 2006. Over a decade, ERT has proven to be effective to relieve life threatening cardiomegaly in classic infantile patients and improve quality of life in late onset patients via effects on skeletal muscles involved in mobility and respiration.[7-13]

However, apart from the extremely high costs and the requirement for life-long (bi)-weekly administration, ERT does not serve as a cure. First, the clinical response of skeletal muscle is highly variable, and sufficient glycogen clearance remains challenging.[14-16] Furthermore, an immune response against infused rhGAA may severely counteract therapeutic outcome. In particular un classic infantile patients, a growing body of evidence indicates attenuated ERT efficacy by high sustained antibody titers against rhGAA.[17,18] Moreover, cognitive decline has been described as a new emerging symptom in long survivors of classic infantile patients,[19-22] but ERT is ineffective in the brain because it cannot pass the blood-brain barrier.

As a curative therapy, hematopoietic stem cell mediated lentiviral gene therapy presents an attractive approach to treat Pompe disease. Previously, we have demonstrated in Pompe mice[23] that by a single intervention, *ex vivo* lentiviral gene therapy ensured the continuous supply of GAA by the hematopoietic system that led to increased GAA enzyme activity in muscle, reduced glycogen storage, and improved cardiac and motor function.[24] Additionally, immune tolerance towards both the transgene product and rhGAA has been established in naïve Pompe mice after receiving gene therapy, which removed one of the major obstacles of ERT (Chapter 6).[24,25] Nevertheless, phenotypic correction was only partial in peripheral organs and glycogen accumulation in the brain was not reduced.[24]

Intracellular GAA transport to the lysosome relies on the binding of mannose 6-phosphate (M6P) residues to the cation-independent mannose 6-phosphate receptor

(CI-MPR), also termed the IGFII receptor (IGFIIR).[26,27] The affinity relies on the level of glycosylation of the M6P residues, which occurs on average at 1 residue in rhGAA as opposed to 7 residues in endogenous GAA.[28] The fusion of a fragment of insulin-like growth factor II (IGFII) to GAA may be able to circumvent the necessity of sufficient posttranslational glycosylation of the GAA protein by exploiting the IGFII binding region of the CI-MPR/IGFIIR for intracellular uptake and subsequent trafficking to the lysosome.[29] Accordingly, IGFII-tagged rhGAA enzyme that was applied intravenously in a Pompe mouse model was delivered more efficiently to target tissues than rhGAA. As a result, glycogen was cleared with higher efficacy and induced a better respiratory improvement.[29,30]

These results led us to modify the previously described lentiviral vector to contain a codon optimized transgene that was tagged with a portion of human insulin-like growth factor II (IGFII) peptide in order to improve lysosomal targeting. *Gaa*$^{-/-}$ mice were engrafted with hematopoietic stem cells that were transduced *ex vivo*, and the effects on metabolic correction, morphology and motor function were analyzed. We also investigated neuroinflammation in the brain and evaluated its rescue by lentiviral gene therapy.

MATERIALS AND METHODS

Experimental animals

Gaa knockout (*Gaa*$^{-/-}$) mice were generated by targeted disruption of *Gaa* gene as previously described.[31] This model recapitulates aspects of human Pompe disease especially the classic infantile form as lack of acid α-glucosidase activity results in generalized glycogen accumulation and pathology.[31-33] Age-matched FVB/N mice were obtained from Charles River as wildtype (WT) control. All mice in experiment were housed under specific pathogen free (SPF) conditions in the Laboratory Animal Science Center (EDC) at the Erasmus MC, and bred according to standard procedures. All animal experiments in this study were approved by the Animal Experiments Committee (DEC) in the Netherlands and these complied with the Dutch legislature to use animals for scientific procedures.

Construction and production of lentiviral vectors

The third generation self-inactivating (SIN)[34] lentiviral vector pRRL.PPT.SF.GAAco.bPRE4*.SIN (LV-GAAco, Figure 1A) containing the codon-optimized human *GAA* sequence (GenScript, Piscataway, NJ) was generated as described (Stok *et al*, submitted). A codon-optimized insulin-like growth factor II (IGFII) cassette (GenScript, Piscataway,

NJ) was then subcloned into this backbone after double digestion of BamHI and SgrAI. The resultant lentiviral vector pRRL.PPT.SF.IGFIIco.GAAco.bPRE4*.SIN (LV-IGFIIco.GAAco) encodes the IGFII signal peptide, residues 1 and 8-67 of codon-optimized human IGFII, a three amino acid spacer, and residues 70-952 of codon-optimized human GAA (Figure 1A).[29] Transgene expression was driven by the spleen focus-forming virus (SF) promoter. High lentiviral titers were generated by calcium phosphatase transfection of 293T cells with the third generation lentiviral vector packaging plasmids.[35,36] Virus concentration and titration was performed as previously detailed.[24] Titers of 10^8 infectious units/ml were routinely obtained for all viruses.

Excretion and uptake of GAA and IGFII.GAA in vitro

HEK293T cells were grown in Ham's F-10 medium (Lonza) supplemented with 10% fetal bovine serum (FBS, Biowest) and 1% penicillin-streptomycin (Gibco) in T175 flask (Greiner bio-one) and transduced with LV-GAAco or LV-IGFIIco.GAAco at a multiplicity of infection (MOI) of 10. Cells were harvested 5 days post transduction and viable frozen as producer cell lines for the *in vitro* assay.

The 293T producer cells were grown at 90% confluency in Ham's F-10 medium consisting of 10% FBS, 1% penicillin-streptomycin, and 3mM PIPES (Sigma) to adjust the pH. After 24 hours, cells and media were collected to determine GAA enzyme activity of excreted GAA. Part of the medium containing GAA (GAA) or IGFII-tagged GAA (IGFII.GAA) enzyme was filtered (0.22 µm filter, Millipore) and used for the uptake assay. Primary myoblasts were isolated from *Gaa*$^{-/-}$ mice as described.[37] And differentiation to myotubes was performed as follows: myoblasts were cultured to 90% confluency on extracellular matrix (ECM, Sigma, 5%) coated 24-well plates, and differentiated into myotubes in differentiation medium (1% penicillin-streptomycin and 2% horse serum (Gibco) in high-glucose Dulbecco's modified Eagle's medium (DMEM, Lonza)) at 37°C with 5% CO_2. Enzyme activity was determined in conditioned medium collected from 293T cells (described above), and GAA protein with an activity of 200 nmol (800 nmol/hr/ml) was incubated on myotubes for 24 hrs. Recombinant human GAA (Myozyme, Genzyme Corporation) was used as positive control. Media and cells were harvested for enzyme assay and Western blotting.

Western blotting

Protein exacts from cell lysates or tissue homogenates were fractionated by SDS-PAGE using 4-15% Criterion TGX (Bio-Rad) and transferred to nitrocellulose blotting membranes (GE Healthcare) according to the manufacturer's protocols (Bio-Rad). The blot was then probed with rabbit anti-GAA (clone EPR4716(2), 1:1000, Abcam) or mouse anti-GAPDH (1:1000, Millipore) antibodies overnight at 4°C. The protein

of interest was detected with secondary IRDye 800CW conjugated goat anti-mouse IgG antibody (926-32210, 1: 10,000, LI-COR Biosciences) or IRDye 680RD conjugated goat anti-rabbit IgG antibody (926-68071, 1: 10,000, LI-COR Biosciences) and visualized with the Odyssey Infrared Imaging System (LI-COR Biosciences) according to the manufacturer's protocols.

Lentiviral hematopoietic stem cell transduction and transplantation

Lentiviral hematopoietic stem cell gene therapy was conducted in two large experiments; one using the LV-GAAco vector and another the LV-IGFIIco.GAAco vector. Untreated *Gaa*$^{-/-}$ and FVB/N wildtype mice were included in each round as internal controls. The experiments were performed by the same investigator (QL) within two weeks using identical procedures. Viral batches were prepared, analyzed, and titrated side by side. A combination of vector dosage (multiplicity of infection (MOI)), number of cells transplanted and irradiation doses was implemented among six gene therapy treated groups as detailed in Table 1. Bone marrow cells were harvested from 8-week old male *Gaa*$^{-/-}$ mice and hematopoietic stem cells and progenitors were sorted out by lineage depletion (Lin^{-}) as previous stated.[24] The Lin^{-} cells were then transduced overnight with lentiviral vectors (either LV-GAAco or LV-IGFIIco.GAAco) at indicated MOIs and transplanted into age matched irradiated female *Gaa*$^{-/-}$ recipients.

Rotarod

Motor function was determined on an accelerating rotarod from 4 to 40 rpm in 300 sec (Panlab, Harvard Apparatus, Holliston, MA).[24] The mice were eight months old, and tested on rotating cylinder for 3 times with 5 minutes interval and endurance was recorded and averaged for each mouse.

GAA enzymatic assay and glycogen content measurement

Before termination at six months after transplantation, mice were fasted overnight and tissues were collected after intracardial perfusion. Tissues were homogenized by TissueLyserII (Qiagen, Venlo, the Netherlands) at 30 Hz for 5 mins and centrifuged for 10 minute at 10,000 rpm. Supernatant was used for GAA and glycogen assays. Bone marrow, leukocytes and cell pellets from *in vitro* experiments were lysed in water by three freeze-thaw cycles. GAA activity was measured using 4-methylumbelliferyl-α-D-glucoside (2.2 mM, Sigma-Aldrich, St. Luis, MO) as substrate.[38] Glycogen was quantified by measuring the amount of glucose released from glycogen after conversion by amyloglucosidase and amylase (Roche Diagnostics, Basel, Switzerland) as previously detailed, and products were measured on Varioskan at 414 nm (Thermo Scientific, Waltham, MA).[39] Results from GAA and glycogen assays were normalized for protein content using the Pierce BCA protein assay kit (Thermo Scientific, Waltham, MA).

Histopathology

Tissue aliquots were either fixed in glutaraldehyde or embedded in OCT compound (Tissue-Tek, Sakura Finetek) that were frozen in isopentane chilled by liquid nitrogen. The glutaraldehyde-fixed samples were further processed in paraffin (heart and tibialis anterior) or glycol methacrylate (GMA)-embedding medium (brain), and sectioned at 4 µm for periodic acid Schiff (PAS) staining according to a standard protocol.[31,40] Acid phosphatase (AP) staining was performed on cryostat sections cut at 8-10 µm as previously described.[31,40] To minimize differences in staining intensity, sections were stained and scanned by NanoZoomer 2.0 (Hamamatsu Photonics, Japan) in one batch.

Immunofluorescent staining in brain

Mice were sacrificed under deep anesthesia by transcardial perfusion with PBS followed by 4% paraformaldehyde (PFA). Brains were fixed in 4% PFA for 4 hours, equilibrated in 20% sucrose overnight and frozen in OCT compound. Sagittal-cut cryostat sections (10 µm) were permeabilized with ice-cold methanol/acetone (4:1, vol:vol) for 10 mins and blocked with 3% bovine serum albumin (BSA) and 0.1% Tween diluted in PBS for 30 minutes at room temperature. Sections were stained with primary antibodies detecting astrocytes (mouse anti-GFAP IgG conjugated to Cy3, 1:300, Sigma-Aldrich), or microglia (rabbit anti-Iba1 IgG, 1:500, Wako Chemicals) and were co-stained with rat anti-LAMP1 IgG (clone 1D4B,1:500, Abcam). After incubation overnight at 4°C, sections were washed with PBS and labeled with the appropriate secondary antibodies conjugated to Alexa Fluor® 488 or Alexa Fluor® 594 (1:500, ThermoFisher Scientific) for 30 mins. All sections were counterstained with Hoechst33258 (1:15000, Life Technologies) for nuclei. The slides were scanned using an LSM 700 confocal microscope (Zeiss) with a 20x objective and analyzed by Adobe Photoshop CS6.

Quantitative polymerase chain reaction of vector integrations

The vector copy number (VCN) and chimerism in bone marrow (BM) was determined by quantitative polymerase chain reaction (qPCR) as described.[24] Briefly, reactions were run on 100 ng of genomic DNA extracted from BM with primers specific for *HIV* (binding to U3 and Psi sequences respectively) or *Sry* locus on the mouse *Y* chromosome. Both VCN and chimerism were normalized using mouse *Gapdh*. Reactions were performed in a CFX96 real-time PCR detection system and analyzed by CFX Manager 3.0 (Bio-Rad, Hercules, CA). Primer sequences are reported in Table S1.

Glucose measurements

Plasma was collected from mice subjected to overnight fasting (15 hours) on a monthly basis. The glucose level was evaluated using a Cobas C311 chemistry ana-

lyzer (Roche/Hitachi) in the Department of Clinical Chemistry of Erasmus University Medical Center.

Statistics

Statistical analyses were performed with SPSS (IBM, version 22). All results are presented as mean ± SEM. The Mann-Whitney U test was used for comparing 2 groups. Multiple comparisons were performed by one-way ANOVA with Bonferroni's correction. Repeated measures ANOVA with Tukey's comparison test was used to detect differences of glucose levels between treatments over time. A P value ≤ 0.05 was considered statistically significant.

An exponential regression model was used to describe the relation between the vector copy number (VCN) and glycogen clearance. This model has two parameters measuring the level at which the curve starts and how fast it declines. To determine whether there is difference in the exponential curves between the LV-GAAco and LV-IGFIIco.GAAco treated groups, we allowed the aforementioned parameters to be group-dependent. The exact definition of the model is as follows: (A0 + group * A1) * EXP((B0 + B1 * group) * VCN), where A0 denotes where the curves starts for the LV-GAAco group; A1 denotes the difference between group LV-IGFIIco.GAAco and LV-GAAco in where the curve starts; B0 quantifies how fast the curve drops for group LV-GAAco; and B1 denotes the difference between groups LV-IGFIIco.GAAco and LV-GAAco in how fast the curve drops. When 95% confidence interval (CI) for estimated value of B1 does not contain zero, the decay in two groups is defined statistically differently. Estimated value of B1 and its 95% CI are listed in Table S2.

RESULTS

Efficient uptake of IGFII.GAA by *Gaa*$^{-/-}$ derived murine myotubes

To investigate whether the addition of the IGFII tag interferes with GAA enzymatic activity, we determined the enzyme activity in HEK 293T producer cells transduced with either LV-GAAco or LV-IGFIIco.GAAco lentiviral vectors (Figure S1A). After correction for VCN (Figure S1B), the GAA activity per integration was comparable between LV-GAAco and LV-IGFIIco.GAAco transduced cells (388.2 ± 4.0 vs 472.8 ± 27.1 nmol/hr/mg/VCN, Figure S1C).

Skeletal muscles are difficult to target with ERT in Pompe patients.[16] To examine whether the uptake of IGFII.GAA protein in muscle fibers was more efficient, GAA-, IGFII.GAA- or rhGAA (Myozyme) containing medium was added to *Gaa*$^{-/-}$ derived murine

myotubes for 24 hours. The quality of the myotubes was assessed using staining with myosin heavy chain (MHC) and by calculating the fusion index (Figure 1B). Myotubes stained positive for MHC showed a very high fusion index of ~80%, and morphology or differentiation was not influenced by incubation with any of the GAA preparations. All conditions contained an initial input of 800 nmol/hr/ml GAA enzymatic activity (Figure 1C). Following incubation of myotubes with GAA enzymes, a significant reduction of GAA activity in the cell culture medium was found for IGFII.GAA compared to GAA and rhGAA (Figure 1C). Immunoblot blot analysis of the cell culture medium after 24 hrs showed that GAA protein remained present as a 110 kDa precursor in all three enzyme preparations (Figure 1H). Analysis of intracellular uptake by myotubes showed that IGFII.GAA protein was taken up with 4-fold higher efficiency (Figure 1E). Immunoblot analysis confirmed the increased uptake of IGFII.GAA protein, and showed that the predominant GAA form was the 76 kDa active protein in all three GAA preparations (Figure 1F). These results show that the IGFII-GAA protein is targeted to the lysosome with superior efficiency compared to GAA or rhGAA, and undergoes proteolytic processing. Taken together, we concluded that intracellular uptake of IGFII.GAA protein in differentiated skeletal muscle cells is improved compared to untagged GAA protein, and that it is processed efficiently in the lysosome into its enzymatically active form.

Efficient long-term reconstitution of LV-transduced hematopoietic cells

To evaluate the therapeutic efficacy of lentiviral gene therapy, LV-GAAco or LV-IGFIIco.GAAco gene modified hematopoietic stem cells (HSCs) were transplanted into irradiated *Gaa*$^{-/-}$ recipient mice. Conditions are presented in Table 1. Six month follow-up showed long-term reconstitution of transplanted gene modified cells occurred in both LV-GAAco and LV-IGFIIco.GAAco treated groups. GAA activities in bone marrow (Figure 2A) and leukocytes (Figure 2B) were higher compared to WT mice. The number of engrafted cells appeared to be an important parameter for GAA enzyme activity, chimerism, and VCN, whereas the impact of multiplicity of infection (MOI) was minor (Figures 2A-D). In addition, the strength of the preconditioning regimen affected all parameters above. For example, 9 Gy treated mice showed 60 to 70% chimerism, while bone marrow from 6 Gy pre-conditioned mice was 10-40% chimeric (Figure 2C). In general, LV-IGFIIco.GAAco showed similar to slightly lower chimerism, and 2-3 fold lower VCN compared to LV-GAAco, possibly due to differences in the quality of the lentiviral preparations. Surprisingly, intracellular GAA enzyme activities from LV-IGFIIco.GAAco transplanted mice in bone marrow and leukocytes were at least 4-5 fold lower compared to LV-GAAco. Although the underlying mechanism is unknown, we speculate that this low intracellular enzyme activity might be related to differences in secretion and/or intracellular distribution.

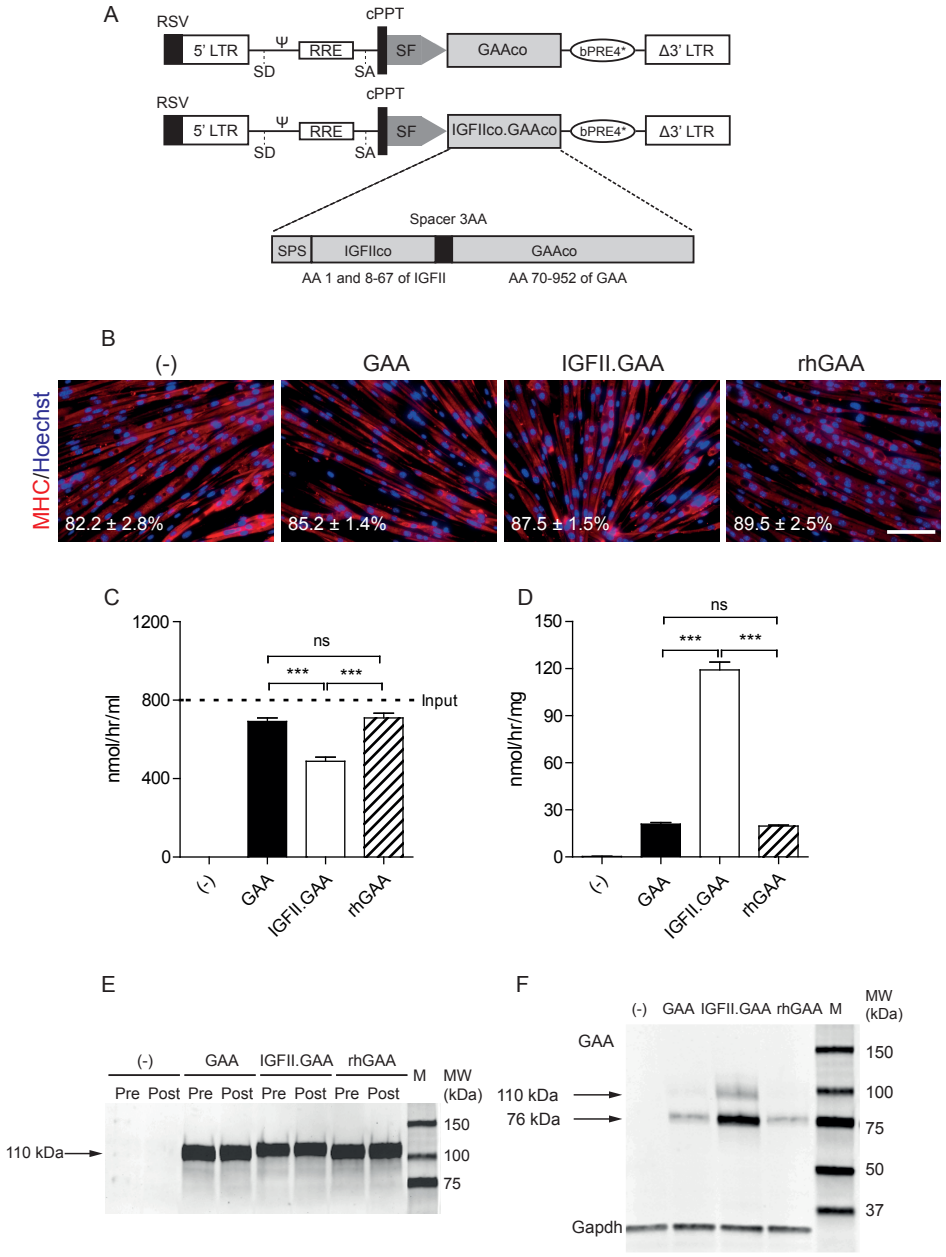

Figure 1. ***In vitro*** **characterization of GAAco and IGFIIco.GAAco proteins.**

Figure 1. *In vitro* characterization of GAAco and IGFIIco.GAAco proteins. (continued) (A) Schematic presentation of the SIN lentiviral vectors. Both vectors contained the spleen focus-forming virus (SF) promoter to drive transgene expression of either codon-optimized GAA (GAAco) or IGFII tagged GAA (the components of IGFIIco.GAAco are shown). LTR indicates long terminal repeat; RSV, enhancer/promoter of Rous Sarcoma Virus replacing the U3 region of LTR; SD, splice donor site; Ψ, packaging signal; RRE, rev response element; SA, splice acceptor site; cPPT, central polypurine tract; bPRE4*, a 600-bp mutant of modified woodchuck posttranslational regulatory element (bPRE4*) devoid of the Woodchuck hepatitis X-protein sequence and ATG sites deleted; Δ3′ LTR, deletion in the U3 region of 3′ LTR to create SIN vector; SPS, signal peptide sequence of IGFII; AA, amino acid. (B-F) Uptake assay in *Gaa*$^{-/-}$ mouse derived myotubes. (B) Myotubes were stained for myogenic differentiation using myosin heavy chain (MHC) in red and counterstained with nuclei marker in blue. Images from five random fields per sample were captured at a 20x magnification using a Zeiss (Thornwood, NY) fluorescence microscope (Axioplan 2 integrated with the AxioCam MR camera), and representative images are shown. Scale bar = 100 μm. Fusion index, shown at the bottom as means ± SEM of five technical replicates, was determined by the percentage of nuclei inside myofibers relative to the total number of nuclei. Representative data from three independent experiments are shown. (-), negative control using culture medium only. (C, E) Enzyme activity in conditioned media (C) and cells (E) 24 hours after co-culturing. Dashed line in (C) represents initial concentration of GAA enzyme in the media. Data represent means ± SEM of three biological replicates and analyzed by one-way ANOVA followed by Bonferroni's multiple testing correction. ***$P \leq 0.001$; ns, not significant. (D, F) Immuno blot analysis of supernatant retrieved from producer cells (D) and target cells (F) to detect GAA protein. Gapdh protein was used in (F) as loading control. Molecular weight (MW) markers (M) are depicted to the right of the panels. Sizes of proteolytic forms of GAA protein (110 and 76 kDa) are indicated. Pre, before uptake; Post, after uptake.

Table 1. Layout of different treatment groups

Group	Treatment	MOI	Cell number	Irradiation (Gy)	Mouse number
1	LV-GAAco/IGFIIco.GAAco	7	1×10^6	9	10
2	LV-GAAco/IGFIIco.GAAco	2	1×10^6	9	10
3	LV-GAAco/IGFIIco.GAAco	7	1×10^6	6	10
4	LV-GAAco/IGFIIco.GAAco	2	1×10^6	6	10
5	LV-GAAco/IGFIIco.GAAco	7	3×10^5	6	10
6	LV-GAAco/IGFIIco.GAAco	2	3×10^5	6	10
7	Untreated KO	*NA*	*NA*	*NA*	6
8	Untreated WT	*NA*	*NA*	*NA*	6

MOI indicates multiplicity of infection; Gy, gray; KO, *Gaa*$^{-/-}$ knockout; WT, FVB/N wildtype; and *NA*, not applicable.

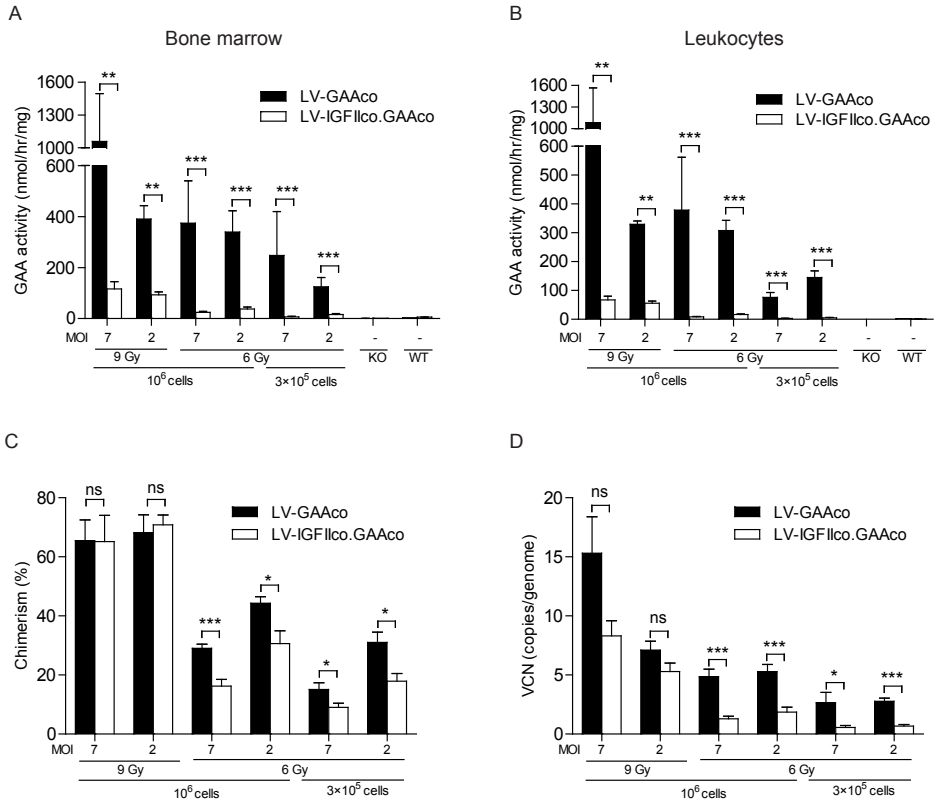

Figure 2. Robust GAA activity in the hematopoietic system after gene therapy. (A, B) Eight-week-old *Gaa*$^{-/-}$ mice were treated with either LV-GAAco or LV-IGFIIco.GAAco. A titration of MOI, donor cell number and total body irradiation was applied to groups for both vectors. Age-matched untreated *Gaa*$^{-/-}$ (KO) and wildtype (WT) mice served as controls. After a six-month follow-up, mice were sacrificed and GAA activity was determined in bone marrow (A) and leukocytes (B). (C) Percentage of reconstituted male donor cells in bone marrow of female recipients. Chimerism was determined by qPCR on *Sry* present on the *Y* chromosome and corrected for *Gapdh*. (D) Lentiviral VCN in bone marrow. VCN was measured in bone marrow by *HIV* qPCR and normalized by *Gapdh*. LV-GAAco and LV-IGFIIco.GAAco, n=7 per group; KO, n=5; and WT, n=5. ns, not significant; **P*≤ 0.05, ***P*≤ 0.01, ****P*≤ 0.001; Mann-Whitney-U test presented as means ± SEM. MOI, multiplicity of infection; Gy, gray; KO, untreated *Gaa*$^{-/-}$ mice; WT, untreated wildtype mice.

Correction of cardiac parameters with LV-IGFIIco.GAAco lentiviral gene therapy

In vivo reconstitution of gene modified cells allowed efficient delivery of functional enzyme to the heart, which is severely affected in classic infantile patients (Figure 3A). GAA activity increased above wildtype levels in LV-GAAco treated groups receiving 9 Gy and the groups receiving a high dose of cells (1×10^6 cells). In contrast, the LV-IGFIIco.GAAco-treated mice had an overall lower activity in the heart tissue (*P*≤ 0.01 or 0.001) compared to WT mice. Significant reduction of glycogen content was

measured in both cohorts receiving gene therapy in a dose-dependent manner, but the effect was much more pronounced in the LV-IGFIIco.GAAco group, in which the storage material was completely cleared in the 9 Gy pre-conditioned groups. ($P \leq 0.001$, Figure 3B) Compared to LV-GAAco, the use of LV-IGFIIco.GAAco vector more dramatically reduced the glycogen at lower VCN (Figure 3C, statistical outcome see Table S2). The significant reduction in glycogen also restored cardiac weight to WT levels, which was reached at lower cell numbers and irradiation intensity in the LV-IGFIIco.GAAco compared to the LV-GAAco treated mice (Figure 3D).

The reduction or complete ablation of glycogen storage in the heart obtained by LV-IGFIIco.GAAco was confirmed by periodic acid Schiff (PAS) staining (Figure 3E, upper row). Strikingly, glycogen-negative cardiac fibers were not observed in KO mice. Both vectors significantly reduced glycogen storage in the heart, but only LV-IGFIIco.GAAco was able to fully normalize glycogen levels to WT levels, consistent with the biochemical findings. Full cardiac sections are shown in Figure S2 with low magnification. Another disease indicator, acid phosphatase (AP), is a lysosomal marker that exhibits increased activity in lysosomal storage diseases[41] as can be observed in cardiac sections of KO mice (Figure 3E, lower row). In LV-GAAco treated mice, the number of AP-positive fibers was reduced but not fully normalized, whereas complete normalization to WT levels was observed in mice treated with LV-IGFIIco.GAAco. We conclude that GAA overexpressed by hematopoietic cells restored enzyme activity in heart muscles, which led to reduction of glycogen that reversed cardiac remodeling and rescued histopathology. Importantly, LV-IGFIIco.GAAco was much more efficient to phenotypically correct the heart compared to LV.GAAco.

Correction of the skeletal muslces with LV-IGFIIco.GAAco lentiviral gene therapy

Skeletal muscle weakness is a prominent symptom of Pompe disease and has a variable response to ERT.[14,15] Therefore, a number of skeletal muscles including the tibialis anterior, quadriceps femoris, gastrocnemius and diaphragm were evaluated after gene therapy. A markedly increased GAA activity was achieved in all LV-GAAco treated mice, whereas the enzyme activity in LV-IGFIIco.GAAco treated mice was often partially restored compared to WT levels (Figure 4A). Conversely, while all gene therapy groups showed significant glycogen reduction in skeletal muscles ($P \leq 0.001$), a more favorable outcome was obtained in LV-IGFIIco.GAAco treated mice, highlighted by near complete glycogen clearance in mice irradiated with 9 Gy (Figure 4B). A correlation between glycogen reduction and VCN was apparent in the tibias anterior by LV-IGFIIco.GAAco treatment, while a higher VCN was required for LV-GAAco to achieve a similar degree of glycogen reduction (Figure 4C, see Table S2 for statistics).

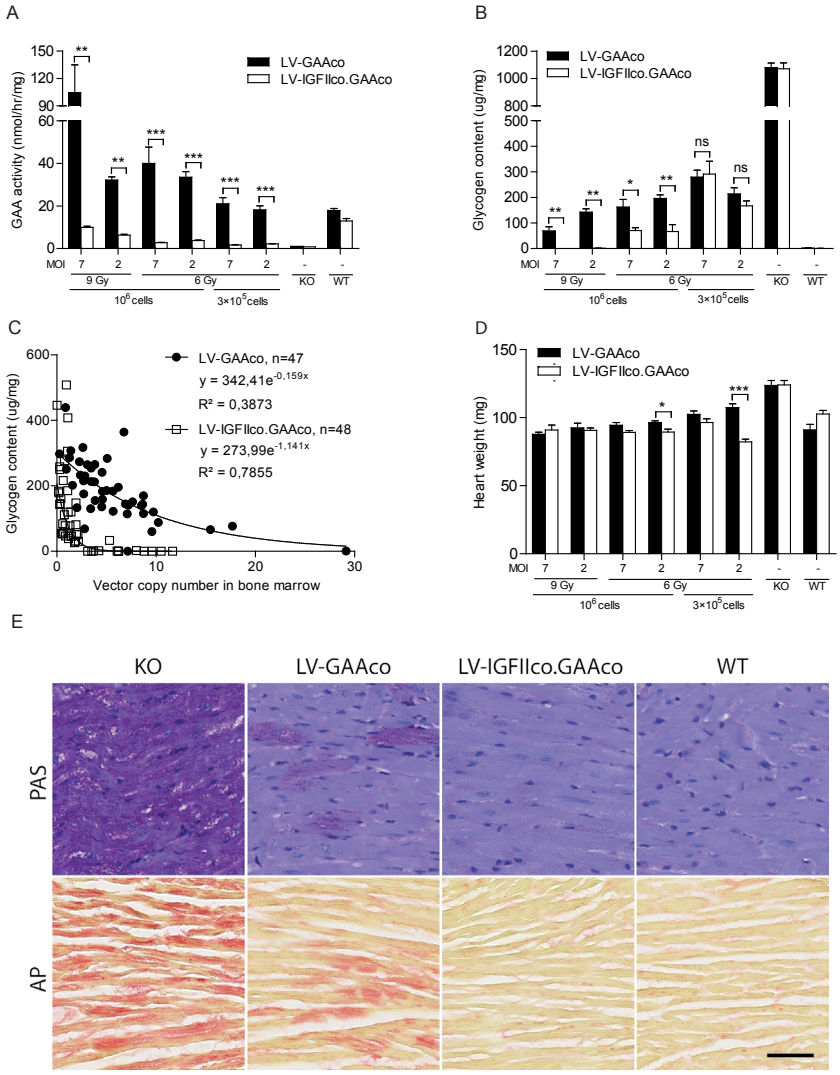

Figure 3. Gene therapy results in correction in heart. Six months after transplantation, mice were sacrificed and GAA activity (A) and glycogen content (B) were determined in cardiac muscles. (C) Correlation between vector copy number and glycogen clearance in heart for each group. VCN in bone marrow was plotted against the corresponding glycogen content. A nonlinear regression model was used to determine the relationship between VCN and glycogen. (D) Cardiac remodeling in response to gene therapy by measurement of heart wet-weight. LV-GAAco and LV-IGFIIco.GAAco, n=7 per group; KO, n=5; and WT, n=5. ns, not significant; *$P \leq 0.05$, **$P \leq 0.01$, ***$P \leq 0.001$; Mann-Whitney-U test. Data are presented as means ± SEM. MOI, multiplicity of infection; Gy, gray; KO, untreated *Gaa*$^{-/-}$ mice; WT, untreated wildtype mice. (E) Morphological analysis of cardiac fibers. At termination, three hearts of 9 Gy-treated mice treated by either LV-GAAco or LV-IGFIIco.GAAco were stained with periodic acid Schiff (PAS, pink, upper panel) and acid phosphatase (AP, red, lower panel). Two mice from untreated *Gaa*$^{-/-}$ and wildtype mice served as controls. Representative images are shown. Scale bar = 50 µm.

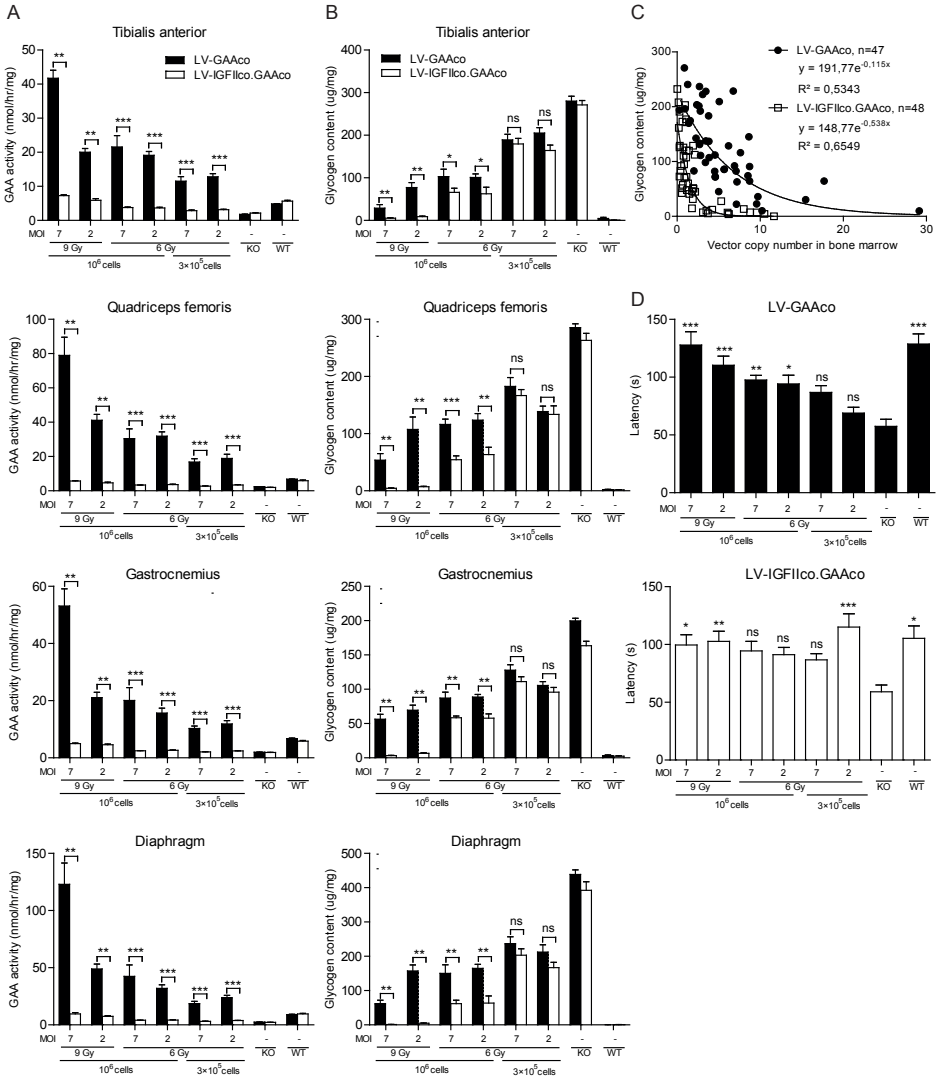

Figure 4. Gene therapy results in correction in skeletal muscles.

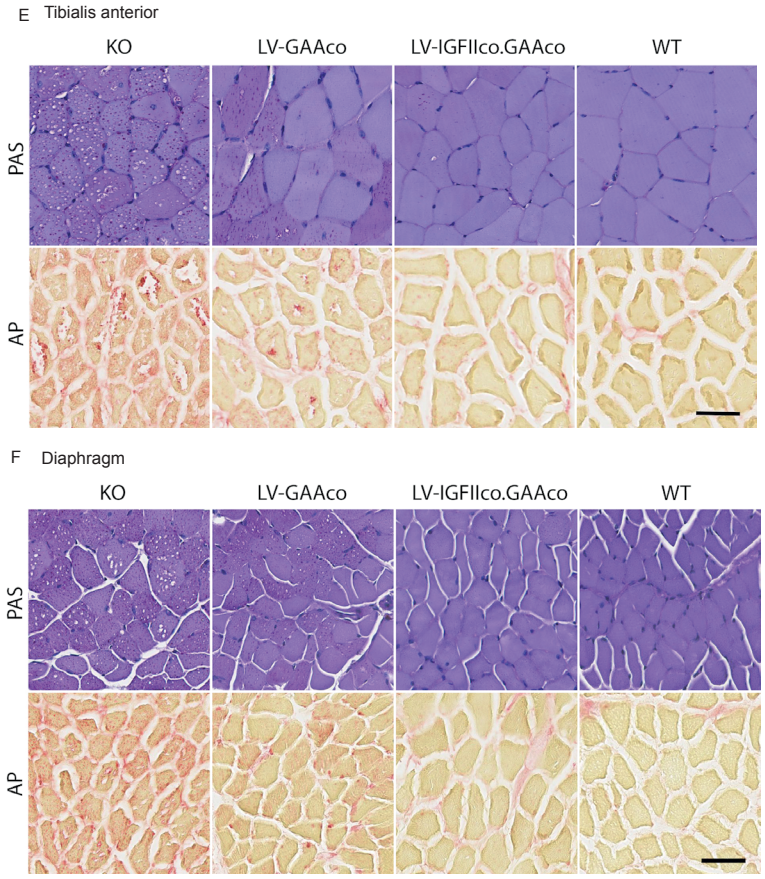

Figure 4. Gene therapy results in correction in skeletal muscles. (continued) (A) Reconstitution of GAA activity in tibialis anterior, quadriceps femoris, gastrocnemius and diaphragm. (B) Glycogen content in skeletal muscles. (C) Correlation between vector copy number and glycogen clearance in tibialis anterior for each gene therapy group. A nonlinear regression model was generated as detailed in material and methods. (D) Latency on a rotarod was evaluated six months after transplantation. LV-GAAco and LV-IGFIIco.GAAco, n=7; KO, n=5; and WT, n=5. ns, not significant; **P*≤ 0.05, ***P*≤ 0.01, ****P*≤0.001; Results are presented as means ± SEM. Significance of the comparison to KO is shown. MOI, multiplicity of infection; Gy, gray; KO, untreated *Gaa*$^{-/-}$ mice; WT, untreated wildtype mice. (E, F) Histopathological analysis in tibialis anterior (E) and diaphragm (F). Periodic acid Schiff (PAS, pink, upper row) and acid phosphatase (AP, red, lower row) were used to stain glycogen and lysosomes respectively. Representative images are shown. Scale bar = 50 μm.

To assess motor function, we performed rotarod measurements six months after transplantation (Figure 4D). Mice treated with LV-GAAco or LV-IGFIIco.GAAco were tested in two separate sessions, and compared to their own internal KO and WT controls. Following gene therapy, all treated mice showed a tendency to remain longer on the accelerating rotarod in comparison to KO mice. Especially, all 9 Gy conditioned mice

showed latency no different than that of WT controls. Of note, one group of LV-IGFIIco.GAAco treated mice with a low number of transplanted cells (3×10^5) stayed clearly longer on the rotarod. This may be explained by the significantly lower average body weight of this group in contrast to the other gene therapy mice (17.0 ± 0.5 g vs 23.6 ± 0.4 g, respectively), which can have an impact on rotarod performance.[42]

Similar to heart tissue, histological improvement by PAS and AP staining was also observed in the tibialis anterior (Figure 4E) and diaphragm (Figure 4F). KO mice exhibited both glycogen deposits and prominent cytoplasmic vacuoles, which represent lysosomes depleted from glycogen during processing (Figures 4E-F, upper row). In AP sections, the muscle fiber appearance was more disrupted in KO mice and AP-positive arrays were present in vacuoles (Figures 4E-F, lower row). After gene therapy, superior alleviation of pathology was achieved in LV-IGFIIco.GAAco treated mice, both when assessed by PAS and by AP staining. Full PAS stained sections are shown in Figure S3 and S4 respectively. In conclusion, the IGFII tagged protein was more efficiently utilized to reduce glycogen in skeletal muscles when compared to GAA, and near-complete glycogen clearance could be obtained and motor deficits were rescued to WT controls.

Correction of the CNS with LV-IGFIIco.GAAco lentiviral gene therapy

Abnormalities in the central nervous system (CNS), including cognitive decline, is a new emerging symptom in classic infantile patients.[21,22] Previously, gene therapy using the native *GAA* sequence[24] was unable to reduce glycogen storage in the brain. Therefore, we tested whether the use of LV-IGFIIco.GAAco for treatment was able to reduce glycogen in brain. Unlike cardiac and skeletal tissues, enzyme activity in cerebrum and cerebellum of LV-GAAco treated mice was only restored to levels reaching 27% and 49% of WT activity respectively (Figure 5A). This limited recovery of enzyme led to, at best, 23% to 38% glycogen reduction accordingly (Figure 5B). In contrast, enzyme activities just above background measurements were detected with the LV-IGFIIco.GAAco cohorts (Figure 5A), but this yielded substantial reduction of glycogen in both cerebrum and cerebellum in all treatment groups, and at 9 Gy conditioning, glycogen was completely eradicated (Figure 5B). This remarkable efficacy of LV-IGFIIco.GAAco in brain was achieved at low VCN (Figure 5C). The estimated VCN needed for 90% glycogen reduction in cerebrum is as low as 1.3. In contrast, the VCN in LV-GAAco treated mice did not correlate with glycogen reduction, although there was some reduction in treated mice compared to KO.(R^2=0.0126, see Table S2 for statistics)

PAS staining on GMA-fixed brain sections of cerebral cortex (layer III/IV), hippocampus (CA1 and dentate gyrus), thalamus and cerebellum revealed distribution of glycogen in various cell types that varied dependent of the cell type and region (Figure 5D), in

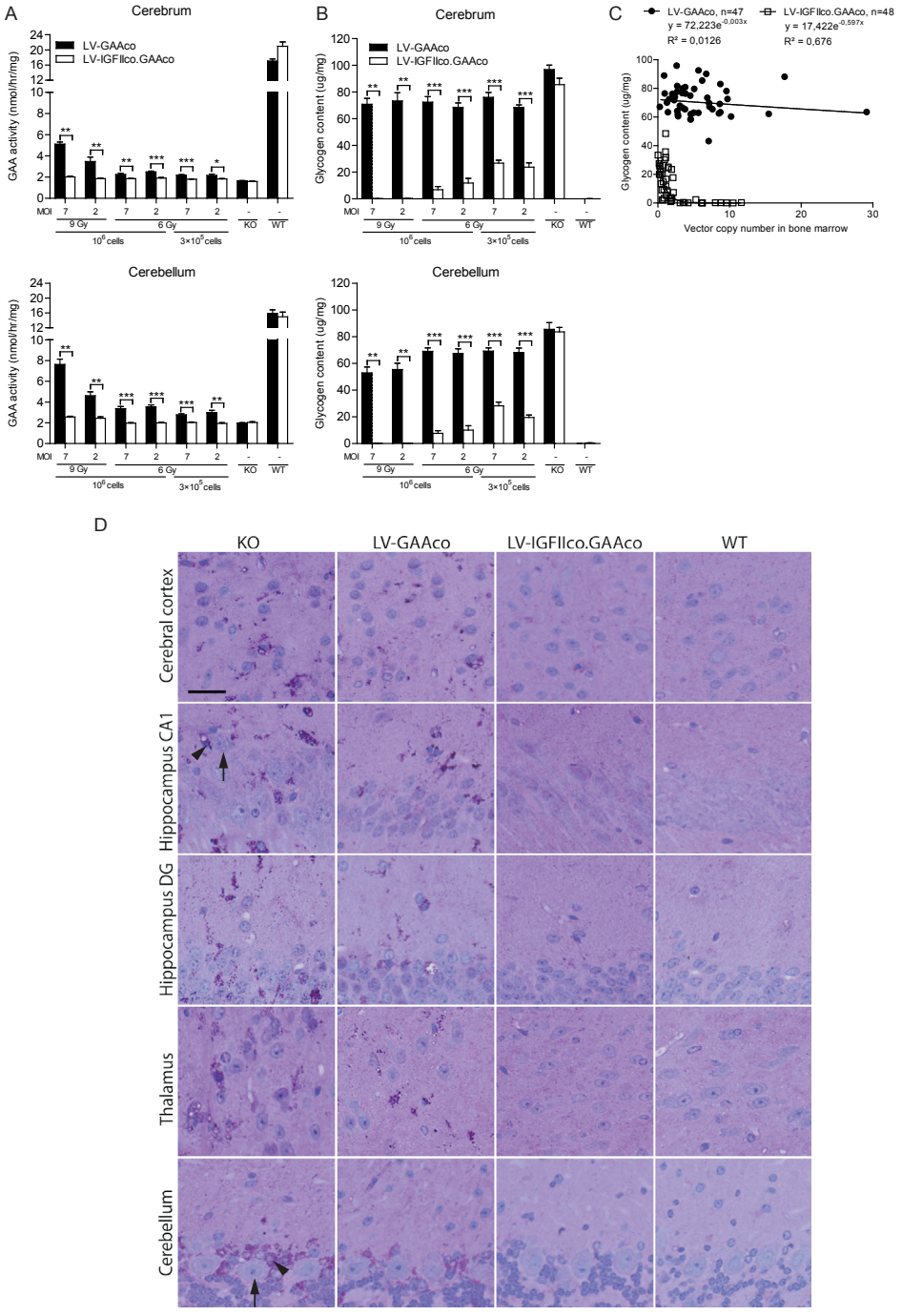

Figure 5. Gene therapy results in correction in brain.

Figure 5. Gene therapy results in correction in brain. (continued) (A) GAA activity in LV-GAAco and LV-IGFIIco.GAAco treated mice in cerebrum and cerebellum. (B) Glycogen reduction in IGFII.GAAco treated mice. LV-GAAco and LV-IGFIIco.GAAco, n=7 per group; KO, n=5; and WT, n=5. **P*≤ 0.05, ***P*≤ 0.01, ****P*≤0.001; Data are presented as means ± SEM. MOI, multiplicity of infection; Gy, gray; KO, untreated *Gaa*$^{-/-}$ mice; WT, untreated wildtype mice. (C) Correlation between vector copy number and glycogen clearance in the cerebrum for LV-GAAco and LV-IGFIIco.GAAco-treated mice. A non-linear regression model was used to determine the relation between VCN and glycogen clearance. (D) Morphologic analysis in brain harvested from the same mice as presented in Fig. 2E. Glycol methacrylate (GMA)-embedded tissues were sectioned sagittally at 6 µm and stained for PAS. Representative images at indicated areas are shown. Black arrows point to pyramidal neurons (in hippocampus CA1) and Purkinje cells (in cerebellum) respectively. Black arrowheads refer to the glial cells surrounding the neurons mentioned above. DG, dentate gyrus; KO, untreated *Gaa*$^{-/-}$ mice; WT, untreated wildtype mice. Scale bar = 25 µm.

agreement with previous studies.[43] For instance, large neurons including pyramidal neurons in the hippocampal area CA1 and cerebellar Purkinje cells (black arrows) were almost free of glycogen deposits whereas adjacent glial cells (black arrow heads) were strongly stained with PAS. Cerebellar white matter and corpus callosum also showed PAS-positive staining (data not shown). After gene therapy, LV-GAAco treated mice showed some reduction of PAS-positive cells, whereas LV-IGFIIco.GAAco treated mice exhibited almost complete absence of PAS-positive cells similar as WT mice. Examples of full sections are shown in Figures S5 and S6. In conclusion, we demonstrated that in the brain, LV-IGFIIco.GAAco was exceptionally effective in normalizing glycogen levels.

Robust alleviation of neuroinflammation by LV-IGFIIco.GAAco lentiviral gene therapy

Neuroinflammation, initiated by astrocytes and microglia activation, plays a well-recognized part in a number of lysosomal storage diseases.[44] However its role in Pompe disease is less well described. By staining astrocytes with GFAP, we first demonstrated regional upregulation of GFAP signals in the brain of KO mice, most strikingly in the corpus callosum, hippocampus, fornix and to a lesser extent, in cerebral cortex, cerebellar white matter and brainstem (Figure S7). A zoom-in at the areas of the hippocampus and corpus callosum confirmed a prominent increase in astrocyte numbers, termed astrogliosis (Figure 6A). Staining of lysosomal associated membrane protein 1 (LAMP1) was additionally included to visualize lysosomal pathology. LAMP1 expression increased in the brain of KO mice due to substrate accumulation and an increase in the number and size of lysosomes (Figure 6A). The high prevalence of LAMP1 in astrocytes indicated that astrocytes were severely affected by aberrant lysosomal accumulation. Upon treatment, LV-IGFIIco.GAAco was more effective in reducing both

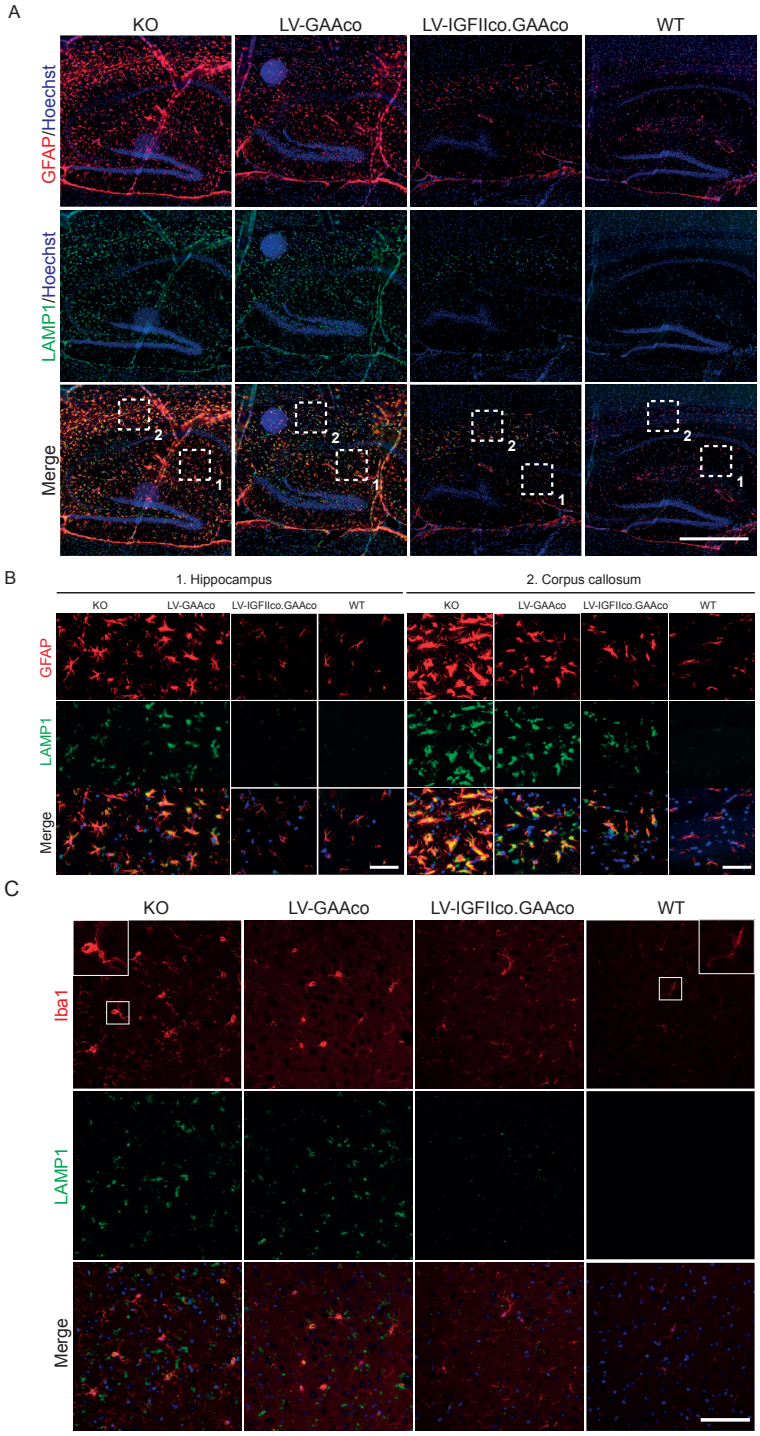

Figure 6. Gene therapy relieves neuroinflammation in brain.

Figure 6. Gene therapy relieves neuroinflammation in brain. (continued) Mice conditioned with 9 Gy and transplanted with either LV-GAAco or LV-IGFIIco.GAAco were sacrificed at six months of age, and sagittal cryosections of the brain were processed for immunofluorescent analysis. Untreated *Gaa*$^{-/-}$ (KO) and wildtype (WT) mice served as controls. (A) Sections of hippocampus and corpus callosum were stained with GFAP for astrocytes (red), LAMP1 for lysosomes (green), and counterstained with Hoechst for nuclei (blue). Scale bar = 500 μm. A higher magnification of the boxed areas numbered 1 (hippocampus) and 2 (corpus callosum) are displayed in (B). Scale bar = 50 μm. (C) Sections of thalamus stained with Iba1 for microglia (red). Microglia in amoeboid shape in *Gaa*$^{-/-}$ (KO) and ramified morphology in wildtype (WT) are boxed and identified in insets with higher magnification. Scale bar = 25 μm. Fluorescent signals are shown individually (bottom panel is merged).

the GFAP and LAMP1 expression to WT levels. Images taken from similar regions in the boxed areas from hippocampus and corpus callosum (1 and 2 in Figure 5A, respectively) were further magnified in Figure 6B. This showed not only an increase in cell number, but also the striking thickening of the cell body and processes of GFAP labeled cells, a typical morphological change for reactive astrocytes.[45,46] Following lentiviral gene therapy, only LV-IGFIIco.GAAco induced major (in corpus callosum) or even complete (in hippocampus) correction of both astrogliosis and lysosomal pathology.

Microglia, another cell type largely involved in neuroinflammation, were marked with Iba1. Unlike the spatial activation of astrocytes, there was widespread increase of microglia in KO brain, i.e. thalamus (Figure 6C) and corpus callosum (Figure S8). Besides a moderate increase of Iba1 positive cells, the most distinctive findings were the altered morphology from a ramified shape in WT brains to a rounded amoeboid-like appearance in KO mice, a typical transformation of microglia upon activation (insets in Figure 6C).[47,48] Microglia activation was barely present in LV-IGFIIco.GAAco treated mice in the majority of brain including thalamus (Figure 6C). However, the treatment was less effective in the corpus callosum where residues of activated LAMP1 positive microglia were still residing (Figure S8).

In conclusion, we demonstrated for the first time that prominent neuroinflammation featured by activation of both astrocytes and microglia was indeed present in Pompe disease, and only with gene therapy using LV-IGFIIco.GAAco, the neuroinflammation and concomitant lysosomal defect could be restored.

Gene therapy using the IGFIIco.GAAco transgene does not affect blood glucose levels

Recent clinical trials using chimeric GAA protein tagged with IGFII in ERT showed a transient hypoglycemia in the majority of Pompe patients.[49,50] This side-effect is related to an insulin-like activity imposed by the IGFII peptide. To investigate whether

long term supraphysiological production of the IGFII.GAA protein by *ex vivo* gene therapy interfere with blood glucose levels, mice with the highest VCN were monitored long-term. Every month, the mice were fasted overnight and plasma glucose levels were determined (Figure 7A). Over the course of the experiment, no significant differences were detected in LV-IGFIIco.GAAco treated mice when compared to either LV-GAAco treated mice or untreated KO and WT controls.

To investigate whether the difference in delivery of ERT and lentiviral gene therapy (intravenous doses (bi)weekly versus continuous endogenous production, respectively) could explain the absence of hypoglycemia in the latter, we compared the GAA activity in plasma. As purified IGFII tagged GAA was not available, we compared the effect of direct injection of rhGAA (Myozyme) to gene therapy with LV-GAAco (Figure 7B). Tail vein injection of 20 mg/kg of rhGAA significantly increased the GAA activity in plasma reaching levels exceeding 40,000 nmol/hr/ml within 5 minutes post-injection.

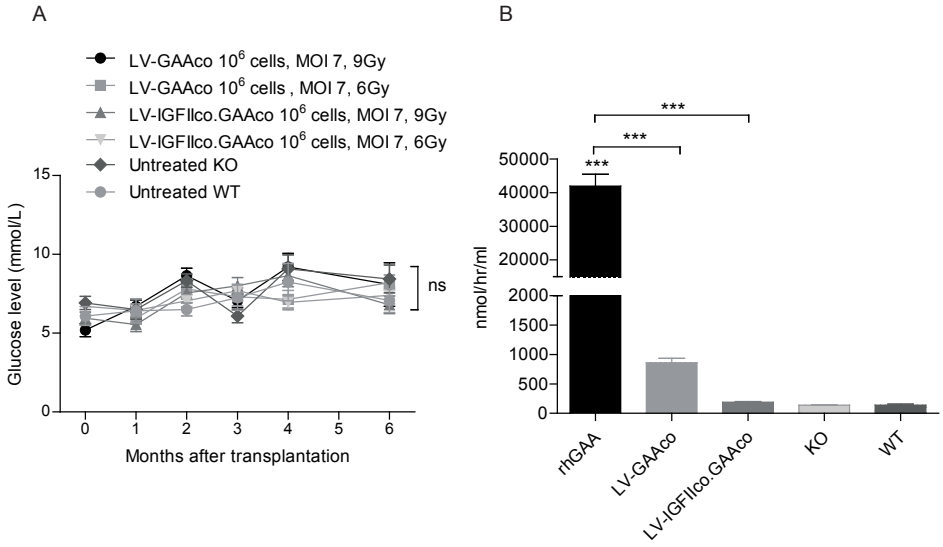

Figure 7. Glucose level is not affected by treatment with the IGFII.GAAco vector. (A) Glucose levels in plasma were determined monthly in gene therapy-treated mice. (B) GAA activity in plasma. Three *Gaa*$^{-/-}$ mice were injected with 20 mg/kg rhGAA (Myozyme) through the tail vein. Plasma was collected five minutes later. Plasma from three LV-GAAco and LV-IGFIIco.GAAco-treated mice treated with 9 Gy, MOI 7 and 1x10^6 cells were compared to untreated *Gaa*$^{-/-}$ (KO) and wildtype (WT) mice. GAA enzyme activity was determined as detailed in materials and methods at a 300-fold dilution. Results are represented as means ± SEM. In panel A, n=10 per gene therapy treated group; n=6 per control groups; All groups were compared using repeated measures ANOVA with post hoc Tukey's analysis. In panel B, n=3 per group; One-way ANOVA with Bonferroni's multiple correction was performed, and statistical comparisons to KO and to ERT are shown. ns, not significant; ***$P \leq$ 0.001.

In contrast, plasma GAA activity in LV-GAAco treated mice was elevated only to 850 nmol/hr/ml which was 50 times lower. The GAA activity in LV-IGFIIco.GAAco treated mice was even lower at 188 nmol/hr/ml, and was comparable to KO and WT values. This supports the notion that high concentration of the IGFII tag caused by an instant influx of protein during ERT is more likely to exert hypoglycemic events compared to a rather low near-physiological supply of IGFII following *ex vivo* lentiviral gene therapy.

DISCUSSION

In this study, we investigated the therapeutic efficacy of hematopoietic stem cell mediated gene therapy using either LV-GAAco or LV-IGFIIco.GAAco in a *Gaa*$^{-/-}$ mouse model for Pompe disease. Our *in vitro* results indicated that the IGFII tag facilitated a four-fold more efficient uptake in primary myotubes, a novel and relevant addition to other widely used cell types, such as fibroblasts or undifferentiated myoblasts.[29,51] Our *in vivo* studies further demonstrated the superior efficiency of LV-IGFIIco.GAAco over LV-GAAco in close to completely eradicating glycogen from major effected tissues including heart, tibialis anterior, quadriceps femoris, gastrocnemius, diaphragm and most prominently the brain, an organ that was poorly targeted by a similar approach previously.[24] Histopathology, as determined by PAS and AP staining, was markedly reduced in LV-IGFIIco.GAAco treated mice. As a result, cardiac hypertrophy was alleviated and motor function was improved to levels of WT mice. Importantly, we confirmed intense neuroinflammation in Pompe mice, which was corrected by gene therapy with LV-IGFIIco.GAAco. These results demonstrate, for the first time, that hematopoietic stem cell mediated lentiviral gene therapy using LV-IGFIIco.GAAco is able to achieve full systemic correction in Pompe disease.

Brain pathology

In our *Gaa*$^{-/-}$ mice, widespread glycogen accumulation was found in all regions of the brain including cerebrum, diencephalon, brainstem and cerebellum. Both neurons and glial cells were compromised with selective severity. Additionally, cerebral and cerebellar white matter and the corpus callosum were also loaded with prominent glycogen metabolites. These findings are in line with comprehensive studies performed in a comparable *Gaa* knockout mouse model for Pompe disease.[43] It was confirmed that the intensity of glycogen accumulation progressed with age, and varied among brain regions and cell types. In general, neurons in the cortex, thalamus and striatum contained less glycogen deposition compared to glial cells. Similarly, Purkinje neurons in the cerebellum and pyramidal neurons in the hippocampus were almost glycogen-free, whereas their neighboring glial cells were almost always intensively stained.

In contrast, motoneurons in the brainstem and spinal cord were heavily filled with glycogen accumulation already at an early age. Additionally, glycogen storage in glial cells residing in the white matter was apparent. The pattern of glycogen involvement in murine Pompe mice is comparable in classic infantile patients. Several autopsy reports corroborated with the region and cell-type specific severity.[52-61] The relative sparing of cortical neurons versus the rather prominent involvement of glial cells is most likely due to the exclusive glycogen synthesis performed by astrocytes,[62-64] which is absent in neurons under physiological circumstances.[65] The rather slow build-up of neuronal glycogen also distinguishes Pompe disease from other LSDs including the neuronopatic forms of mucopolysaccharidosis (MPS) I, II and III where neurodegeneration appears to be the primary and first-emerging neuropathy.[66]

Apart from primary glycogen storage, prominent neuroinflammation was explicitly demonstrated for the first time in Pompe disease mice. Previously, moderate astrogliosis in the white matter tracts was evident only in old mice at the age of 15 months, and the number of microglia remained unaffected. [43] In our study, we showed that regional activation of astrocytes was already clearly present at 8-month of age. Lysosomal dysfunction and astrogliosis were most pronounced in the corpus callosum, hippocampus and fornix, and to a milder extent, in cerebral cortex, cerebellar white matter and brainstem that overlapped with locations described in autopsy findings.[54,56,57] Importantly, an increase of amoeboid typed microglia confirmed the activation of microglia.[67] Similar morphological changes in the basal nuclear masses and the brainstem were also mentioned in a post-mortem report.[56] Collectively, our findings provided solid evidence of neuroinflammation in the Pompe murine model. However, the effect of activated astrocytes and microglia on neuropathology in Pompe disease remains elusive. By creating a neurotoxic environment, neuroinflammation has been linked directly to promote neurodegeneration in the majority of neuropathic LSDs.[44] Indeed, co-localization of gliosis in areas of neuronal loss has been narrated in infantile patients.[54,56,57,60] Neuroinflammation is also suggested to be causative for demyelination in metachromatic leukodystrophy (MLD) mice.[68] This could be clinically relevant for Pompe disease as demyelination was indicated by MRI studies in long survivors of classic infantile Pompe patients.[21,69] Importantly, periventricular white matter abnormalities have been described as being commonly involved, with occasional involvement of internal/external capsule, claustrum, corpus callosum, centrum semiovale and corticospinal tracts in the brainstem,[22,69] that overlaid with areas of gliosis in our studies and other autopsy reports.[54,56] To conclude, further investigation of the spatial and temporal relationship of glycogen storage, neuroinflammation, demyelination and neurodegeneration will aid in fully characterizing the underlying etiology of CNS pathology in Pompe disease, and should provide a better

understanding of the basis of CNS pathology needed to interpret emerging clinical manifestations.

Treatment of CNS pathology

Following sufficient brain conditioning by either total body irradiation[70] or busulfan[71]), circulating hematopoietic progenitor-derived monocytes can be actively recruited to the brain through penetration of the blood-brain barrier and local differentiation as resident microglia.[72,73] Consequently, genetically modified microglia were able to provide the missing enzyme within the brain for the cross-correction of aberrant cells including neurons and glia[74] via CI-MPR mediated endocytosis.[75]

HSC-mediated lentiviral gene therapy has been intensively studied in neuronopathic LSDs, and have been pioneered by the implementation in metachromatic leukodystrophy (MLD), a lysosomal sphingolipid storage disorder caused by the deficiency of arylsulfatase A (ARSA).[76] MLD is characterized by extensive CNS and PNS involvement including motor function decline and cognitive problems, with demyelination being the hallmark.[77] Gene therapy with transduced HSCs encoding the ARSA protein not only prevented but also reversed neuropathological anomalies in presymptomatic and symptomatic MLD mice, respectively,[74,78] which translated successful into clinical trials. Preliminary data obtained from early onset MLD patients treated at presymptomatic or very early symptomatic stage showed stable engraftment of transduced HSCs at high levels, which resulted in supranormal levels of ARSA activity in hematopoietic lineages and, especially, in cerebrospinal fluid, indicative of sufficient enzyme delivery throughout the CNS in humans.[79,80] This resulted in a clear therapeutic benefit.

Previously, restoration of ~6% WT level of GAA enzyme failed to reduce any glycogen storage in the brain.[24] In contrast, an increase of only 10-11% of WT level of the deficient enzyme already sufficed to normalize brain biochemistry and pathology in MLD[74] and MPS IIIA mouse model.[81] As glycogen seemed to be more refractory to degradation than sulfatide in MLD and highly sulfated heparan sulfate (HS) in MPSIIIA, a higher amount and/or more sufficient uptake of the GAA enzyme was expected to better correct the CNS pathology in Pompe disease.

The IGFII.GAA protein showed extraordinary efficiency to remove excessive glycogen in the brain. Strikingly, the difference in therapeutic outcome between the two vectors was especially pronounced in brain when compared to heart and skeletal muscles. The underlying mechanism for the preferential uptake in the CNS is at present unclear. Hereafter we present some possible explanations. First, limited direct transport of IGFII.GAA protein to the brain was suggested by evidence of reduced glycogen stor-

age in the brain following intravenous ERT in Pompe mice.[30] The direct uptake will increase the amount of GAA enzyme in the brain in addition to local excretion from donor-derived microglia. Conceivably, as CI-MPR is developmentally downregulated at the BBB,[82-84] this transcytosis is most likely carried out via the binding of IGFII to the insulin receptor[85] and/or insulin-like growth factor I (IGFI) receptor[86] due to the high degree of homology between the ligands involved. Although the protein expression level of the CI-MPR in the brain was similar to that in muscle or heart,[82,87,88] its molecular weight was particularly smaller than other tissues.[82,88] This was the case in postnatal rat or human samples. Different glycosylation patterns of the receptor were found to be responsible for the size difference,[89] which might suggest the existence of functional differences including differential binding affinity that might be in favor of brain.[90,91]

Safety evaluation of the IGFII-tag

While the use of IGFII significantly improves the efficacy of the therapy, it also raises concern of "off-target" effects as it is capable to bind to insulin receptor (IR), though with lesser affinity, due to the structural similarities as mentioned earlier.[92] Indeed, in clinical trials to treat Pompe patients with IGFII tagged GAA at 20 mg/kg dosing, infusion-associated hypoglycemia was frequently induced during or within one hour of infusion.[49,50,93] This transient hypoglycemia is believed to be caused by insulin-like activity via the cross binding of IGFII to the IR. Intriguingly, in mice receiving IGFII tagged GAA in the form of lentiviral gene therapy, the plasma glucose concentration remained stable, indistinguishable from WT mice. Additionally, the absence of hypoglycemia in gene therapy treated mice might be explained by distinctive delivery of ERT and gene therapy. Plasma GAA activity in rhGAA treated mice was more than 58-fold and 800-fold higher than that in LV-GAAco and LV-IGFIIco.GAAco treated mice when background level of KO mice was exacted.

Additionally, efforts have been made to reduce the IGFII binding affinity to insulin receptor. While maintaining the binding affinity towards CI-MPR, the substitution of Arg to Ala at the amino acid position 37 of the IGFII sequence showed diminished affinity to the IR of 10- or 20- fold relative to the current IGFII tag or wildtype IGFII, respectively.[94] The future incorporation of this IGFII mutant into the lentiviral vector may further increase the safety profile of lentiviral gene therapy for Pompe disease.

Adeno-associated virus gene therapy

Alternatively, *in vivo* adeno-associated virus (AAV) gene therapy has been intensively investigated in a Pompe murine model.[95] Systemic delivery of GAA containing AAV using either a ubiquitous or a muscle-specific promoter was most efficient in clear-

ing glycogen storage in the heart and diaphragm. Other skeletal muscles including quadriceps anterior, tibias anterior and gastrocnemius were relatively refractory to AAV where only partial biochemical reduction was achieved. Nevertheless, motor function was improved compared to KO values.[96-99] Evidence for therapeutic efficacy of AAV in the CNS was limited. Systemic,[99,100] intra-spinal,[101] or intrapleural[102] delivery of AAV showed transduction of spinal cord that partially alleviated respiratory dysfunction. Furthermore, hypoglossal motoneurons in the brainstem can be targeted via retrograde transduction following intralingual injection.[103] However, whether AAV can efficiently transduce the CNS and address CNS pathology deserves further investigation. Compared to AAV gene therapy, the lentiviral gene therapy approach by improved targeting in the present study appears to have higher efficacy not only in addressing abnormalities in skeletal muscles but also in the brain.

Of note, immune response against both AAV capsid and the transgene product can negatively influence the therapeutic efficacy of AAV gene therapy. In Pompe mice,[104] the rapid development of anti-GAA antibodies has shown to impair the overall outcome.[105,106] Although liver-specific transgene expression can establish peripheral immune tolerance to GAA via the induction of regulatory T cells,[100,107-109] CD8(+) T-cell responses against AAV capsid that diminish the efficacy of the treatment remain troublesome in clinical trials.[110,111] Hematopoietic stem cell-mediated lentiviral gene therapy, on the other hand, can generate long-lasting immune tolerance against GAA (Chapter 6),[24,25] likely via establishment of both central and peripheral immune tolerance.[112,113]

CONCLUSION

In this study, we have documented the presence of neuroinflammation as a key feature in brain pathogenesis in Pompe disease. We have also provided strong evidence that a single administration of genetically modified hematopoietic stem cells in Pompe mice can induce (near) complete systemic correction of heart, skeletal muscles and brain, an outcome that is superior to earlier attempts from us[24] and others.[25] These promising preclinical data warrant the continuation of preclinical development of this therapy for the treatment of Pompe patients, especially the classical infantile form.

ACKNOWLEDGEMENTS

We thank Dr.Rizopoulos Dimitris for valuable advice on statistic analysis. This work was supported by The Netherlands Organization for Health Research ZonMw (project number: 40-40300-98-07010) and the Erasmus University Medical Center. Q.L was supported by the China Scholarship Council (File No. 201206240040)

REFERENCES

1. Hirschhorn R, Reuser AJJ. Glycogen storage disease type II: acid α-glucosidase (acid maltase) deficiency. In: Scriver C, Beaudet, AL, Sly, WS and Valle, D ed. The Metabolic and Molecular Basis for Inherited Disease. New York: McGraw-Hill; 2001:3389–3420.
2. van der Ploeg AT, Reuser AJ. Pompe's disease. *Lancet*. 2008;372(9646):1342-1353.
3. van den Hout HM, Hop W, van Diggelen OP, et al. The natural course of infantile Pompe's disease: 20 original cases compared with 133 cases from the literature. *Pediatrics*. 2003;112(2):332-340.
4. Kishnani PS, Hwu WL, Mandel H, Nicolino M, Yong F, Corzo D. A retrospective, multinational, multicenter study on the natural history of infantile-onset Pompe disease. *J Pediatr*. 2006;148(5):671-676.
5. Hagemans ML, Winkel LP, Hop WC, Reuser AJ, Van Doorn PA, Van der Ploeg AT. Disease severity in children and adults with Pompe disease related to age and disease duration. *Neurology*. 2005;64(12):2139-2141.
6. Winkel LP, Hagemans ML, van Doorn PA, et al. The natural course of non-classic Pompe's disease; a review of 225 published cases. *J Neurol*. 2005;252(8):875-884.
7. Kishnani PS, Corzo D, Nicolino M, et al. Recombinant human acid [alpha]-glucosidase: major clinical benefits in infantile-onset Pompe disease. *Neurology*. 2007;68(2):99-109.
8. Kishnani PS, Corzo D, Leslie ND, et al. Early treatment with alglucosidase alpha prolongs long-term survival of infants with Pompe disease. *Pediatr Res*. 2009;66(3):329-335.
9. Nicolino M, Byrne B, Wraith JE, et al. Clinical outcomes after long-term treatment with alglucosidase alfa in infants and children with advanced Pompe disease. *Genet Med*. 2009;11(3):210-219.
10. van Capelle CI, van der Beek NA, Hagemans ML, et al. Effect of enzyme therapy in juvenile patients with Pompe disease: a three-year open-label study. *Neuromuscul Disord*. 2010;20(12):775-782.
11. van der Ploeg AT, Clemens PR, Corzo D, et al. A randomized study of alglucosidase alfa in late-onset Pompe's disease. *N Engl J Med*. 2010;362(15):1396-1406.
12. Gungor D, Kruijshaar ME, Plug I, et al. Impact of enzyme replacement therapy on survival in adults with Pompe disease: results from a prospective international observational study. *Orphanet J Rare Dis*. 2013;8:49.
13. Gungor D, Kruijshaar ME, Plug I, et al. Quality of life and participation in daily life of adults with Pompe disease receiving enzyme replacement therapy: 10 years of international follow-up. *J Inherit Metab Dis*. 2016;39(2):253-260.
14. Van den Hout JM, Kamphoven JH, Winkel LP, et al. Long-term intravenous treatment of Pompe disease with recombinant human alpha-glucosidase from milk. *Pediatrics*. 2004;113(5):e448-457.
15. Kishnani PS, Nicolino M, Voit T, et al. Chinese hamster ovary cell-derived recombinant human acid alpha-glucosidase in infantile-onset Pompe disease. *J Pediatr*. 2006;149(1):89-97.

16. Prater SN, Patel TT, Buckley AF, et al. Skeletal muscle pathology of infantile Pompe disease during long-term enzyme replacement therapy. *Orphanet J Rare Dis.* 2013;8:90.
17. Banugaria SG, Prater SN, Ng YK, et al. The impact of antibodies on clinical outcomes in diseases treated with therapeutic protein: lessons learned from infantile Pompe disease. *Genet Med.* 2011;13(8):729-736.
18. van Gelder CM, Hoogeveen-Westerveld M, Kroos MA, Plug I, van der Ploeg AT, Reuser AJ. Enzyme therapy and immune response in relation to CRIM status: the Dutch experience in classic infantile Pompe disease. *J Inherit Metab Dis.* 2015;38(2):305-314.
19. Rohrbach M, Klein A, Kohli-Wiesner A, et al. CRIM-negative infantile Pompe disease: 42-month treatment outcome. *J Inherit Metab Dis.* 2010;33(6):751-757.
20. Matsuoka T, Miwa Y, Tajika M, et al. Divergent clinical outcomes of alpha-glucosidase enzyme replacement therapy in two siblings with infantile-onset Pompe disease treated in the symptomatic or pre-symptomatic state. *Mol Genet Metab Rep.* 2016;9:98-105.
21. Ebbink BJ, Aarsen FK, van Gelder CM, et al. Cognitive outcome of patients with classic infantile Pompe disease receiving enzyme therapy. *Neurology.* 2012;78(19):1512-1518.
22. Ebbink BJ, Poelman E, Plug I, et al. Cognitive decline in classic infantile Pompe disease: An underacknowledged challenge. *Neurology.* 2016;86(13):1260-1261.
23. Raben N, Nagaraju K, Lee E, et al. Targeted disruption of the acid alpha-glucosidase gene in mice causes an illness with critical features of both infantile and adult human glycogen storage disease type II. *J Biol Chem.* 1998;273(30):19086-19092.
24. van Til NP, Stok M, Aerts Kaya FS, et al. Lentiviral gene therapy of murine hematopoietic stem cells ameliorates the Pompe disease phenotype. *Blood.* 2010;115(26):5329-5337.
25. Douillard-Guilloux G, Richard E, Batista L, Caillaud C. Partial phenotypic correction and immune tolerance induction to enzyme replacement therapy after hematopoietic stem cell gene transfer of alpha-glucosidase in Pompe disease. *J Gene Med.* 2009;11(4):279-287.
26. Kornfeld S. Lysosomal enzyme targeting. *Biochem Soc Trans.* 1990;18(3):367-374.
27. Ghosh P, Dahms NM, Kornfeld S. Mannose 6-phosphate receptors: new twists in the tale. *Nat Rev Mol Cell Biol.* 2003;4(3):202-212.
28. McVie-Wylie AJ, Lee KL, Qiu H, et al. Biochemical and pharmacological characterization of different recombinant acid alpha-glucosidase preparations evaluated for the treatment of Pompe disease. *Mol Genet Metab.* 2008;94(4):448-455.
29. Maga JA, Zhou J, Kambampati R, et al. Glycosylation-independent lysosomal targeting of acid alpha-glucosidase enhances muscle glycogen clearance in pompe mice. *J Biol Chem.* 2013;288(3):1428-1438.
30. Peng J, Dalton J, Butt M, et al. Reveglucosidase alfa (BMN 701), an IGF2-Tagged rhAcid alpha-Glucosidase, Improves Respiratory Functional Parameters in a Murine Model of Pompe Disease. *J Pharmacol Exp Ther.* 2017;360(2):313-323.
31. Bijvoet AG, van de Kamp EH, Kroos MA, et al. Generalized glycogen storage and cardiomegaly in a knockout mouse model of Pompe disease. *Hum Mol Genet.* 1998;7(1):53-62.
32. Bijvoet AG, Van Hirtum H, Vermey M, et al. Pathological features of glycogen storage disease type II highlighted in the knockout mouse model. *J Pathol.* 1999;189(3):416-424.

33. Kamphoven JH, Stubenitsky R, Reuser AJ, Van Der Ploeg AT, Verdouw PD, Duncker DJ. Cardiac remodeling and contractile function in acid alpha-glucosidase knockout mice. *Physiol Genomics*. 2001;5(4):171-179.

34. Zufferey R, Dull T, Mandel RJ, et al. Self-inactivating lentivirus vector for safe and efficient in vivo gene delivery. *J Virol*. 1998;72(12):9873-9880.

35. Naldini L, Blomer U, Gage FH, Trono D, Verma IM. Efficient transfer, integration, and sustained long-term expression of the transgene in adult rat brains injected with a lentiviral vector. *Proc Natl Acad Sci U S A*. 1996;93(21):11382-11388.

36. Dull T, Zufferey R, Kelly M, et al. A third-generation lentivirus vector with a conditional packaging system. *J Virol*. 1998;72(11):8463-8471.

37. Rando TA, Blau HM. Primary mouse myoblast purification, characterization, and transplantation for cell-mediated gene therapy. *J Cell Biol*. 1994;125(6):1275-1287.

38. Okumiya T, Keulemans JL, Kroos MA, et al. A new diagnostic assay for glycogen storage disease type II in mixed leukocytes. *Mol Genet Metab*. 2006;88(1):22-28.

39. Bijvoet AG, Van Hirtum H, Kroos MA, et al. Human acid alpha-glucosidase from rabbit milk has therapeutic effect in mice with glycogen storage disease type II. *Hum Mol Genet*. 1999;8(12):2145-2153.

40. Schaaf GJ, van Gestel TJ, Brusse E, et al. Lack of robust satellite cell activation and muscle regeneration during the progression of Pompe disease. *Acta Neuropathol Commun*. 2015;3:65.

41. Engel AG, Gomez MR, Seybold ME, Lambert EH. The spectrum and diagnosis of acid maltase deficiency. *Neurology*. 1973;23(1):95-106.

42. McFadyen MP, Kusek G, Bolivar VJ, Flaherty L. Differences among eight inbred strains of mice in motor ability and motor learning on a rotorod. *Genes Brain Behav*. 2003;2(4):214-219.

43. Sidman RL, Taksir T, Fidler J, et al. Temporal neuropathologic and behavioral phenotype of 6neo/6neo Pompe disease mice. *J Neuropathol Exp Neurol*. 2008;67(8):803-818.

44. Bosch ME, Kielian T. Neuroinflammatory paradigms in lysosomal storage diseases. *Front Neurosci*. 2015;9:417.

45. Hol EM, Pekny M. Glial fibrillary acidic protein (GFAP) and the astrocyte intermediate filament system in diseases of the central nervous system. *Curr Opin Cell Biol*. 2015;32:121-130.

46. Sun D, Jakobs TC. Structural remodeling of astrocytes in the injured CNS. *Neuroscientist*. 2012;18(6):567-588.

47. Kreutzberg GW. Microglia: a sensor for pathological events in the CNS. *Trends Neurosci*. 1996;19(8):312-318.

48. Hanisch UK, Kettenmann H. Microglia: active sensor and versatile effector cells in the normal and pathologic brain. *Nat Neurosci*. 2007;10(11):1387-1394.

49. Byrne B, Barohn R, Barshop B, et al. Preliminary clinical efficacy and safety of BMN 701, GILT-tagged recombinant human acid alpha glucosidase (rhGAA), in late-onset Pompe disease: results of an extension study. *Molecular Genetics and Metabolism*. 2014;111(2):S29.

50. Hiwot T, Barohn R, Bratkovic D, et al. G.O.20 - Reveglucosidase alfa (BMN 701), a GILT-tagged recombinant human acid alpha glucosidase (rhGAA), evaluation in late-onset Pompe disease: Preliminary clinical efficacy and safety results of an extension study (72-week results). *Neuromuscular Disorders*. 2015;25, Supplement 2:S313-S314.
51. Tiels P, Baranova E, Piens K, et al. A bacterial glycosidase enables mannose-6-phosphate modification and improved cellular uptake of yeast-produced recombinant human lysosomal enzymes. *Nat Biotechnol*. 2012;30(12):1225-1231.
52. Garancis JC. Type II glycogenosis. Biochemical and electron microscopic study. *Am J Med*. 1968;44(2):289-300.
53. Gambetti P, DiMauro S, Baker L. Nervous system in Pompe's disease. Ultrastructure and biochemistry. *J Neuropathol Exp Neurol*. 1971;30(3):412-430.
54. Martin JJ, de Barsy T, van Hoof F, Palladini G. Pompe's disease: an inborn lysosomal disorder with storage of glycogen. A study of brain and striated muscle. *Acta Neuropathol*. 1973;23(3):229-244.
55. Teng YT, Su WJ, Hou JW, Huang SF. Infantile-onset glycogen storage disease type II (Pompe disease): report of a case with genetic diagnosis and pathological findings. *Chang Gung Med J*. 2004;27(5):379-384.
56. Mancall EL, Aponte GE, Berry RG. Pompe's Disease (Diffuse Glycogenosis) with Neuronal Storage. *J Neuropathol Exp Neurol*. 1965;24:85-96.
57. Crome L, Cumings JN, Duckett S. Neuropathological and Neurochemical Aspects of Generalized Glycogen Storage Disease. *J Neurol Neurosurg Psychiatry*. 1963;26:422-430.
58. Pena LD, Proia AD, Kishnani PS. Postmortem Findings and Clinical Correlates in Individuals with Infantile-Onset Pompe Disease. *JIMD Rep*. 2015;23:45-54.
59. Caddell JL, Whittemore R. Observations on generalized glycogenosis with emphasis on electrocardiographic changes. *Pediatrics*. 1962;29:743-763.
60. Martini C, Ciana G, Benettoni A, et al. Intractable fever and cortical neuronal glycogen storage in glycogenosis type 2. *Neurology*. 2001;57(5):906-908.
61. Thurberg BL, Lynch Maloney C, Vaccaro C, et al. Characterization of pre- and post-treatment pathology after enzyme replacement therapy for Pompe disease. *Lab Invest*. 2006;86(12):1208-1220.
62. Brown AM, Tekkok SB, Ransom BR. Glycogen regulation and functional role in mouse white matter. *J Physiol*. 2003;549(Pt 2):501-512.
63. Brown AM, Baltan Tekkok S, Ransom BR. Energy transfer from astrocytes to axons: the role of CNS glycogen. *Neurochem Int*. 2004;45(4):529-536.
64. Brown AM, Ransom BR. Astrocyte glycogen and brain energy metabolism. *Glia*. 2007;55(12):1263-1271.
65. Saez I, Duran J, Sinadinos C, et al. Neurons have an active glycogen metabolism that contributes to tolerance to hypoxia. *J Cereb Blood Flow Metab*. 2014;34(6):945-955.
66. Prada CE, Grabowski GA. Neuronopathic lysosomal storage diseases: clinical and pathologic findings. *Dev Disabil Res Rev*. 2013;17(3):226-246.
67. Neumann H, Kotter MR, Franklin RJ. Debris clearance by microglia: an essential link between degeneration and regeneration. *Brain*. 2009;132(Pt 2):288-295.

68. Stein A, Stroobants S, Gieselmann V, D'Hooge R, Matzner U. Anti-inflammatory Therapy With Simvastatin Improves Neuroinflammation and CNS Function in a Mouse Model of Metachromatic Leukodystrophy. *Mol Ther.* 2015;23(7):1160-1168.

69. Messinger YH, Mendelsohn NJ, Rhead W, et al. Successful immune tolerance induction to enzyme replacement therapy in CRIM-negative infantile Pompe disease. *Genet Med.* 2012;14(1):135-142.

70. Prinz M, Mildner A. Microglia in the CNS: immigrants from another world. *Glia.* 2011;59(2):177-187.

71. Capotondo A, Milazzo R, Politi LS, et al. Brain conditioning is instrumental for successful microglia reconstitution following hematopoietic stem cell transplantation. *Proc Natl Acad Sci U S A.* 2012;109(37):15018-15023.

72. Krivit W, Sung JH, Shapiro EG, Lockman LA. Microglia: the effector cell for reconstitution of the central nervous system following bone marrow transplantation for lysosomal and peroxisomal storage diseases. *Cell Transplant.* 1995;4(4):385-392.

73. Mildner A, Schmidt H, Nitsche M, et al. Microglia in the adult brain arise from Ly-6ChiCCR2+ monocytes only under defined host conditions. *Nat Neurosci.* 2007;10(12):1544-1553.

74. Biffi A, Capotondo A, Fasano S, et al. Gene therapy of metachromatic leukodystrophy reverses neurological damage and deficits in mice. *J Clin Invest.* 2006;116(11):3070-3082.

75. Schluff P, Flott-Rahmel B, Gieselmann V, Zimmer P, Das A, Ullrich K. Localization of receptors for endocytosis of lysosomal enzymes on different brain cells. *J Inherit Metab Dis.* 1998;21(3):313-317.

76. Biffi A. Hematopoietic Stem Cell Gene Therapy for Storage Disease: Current and New Indications. *Mol Ther.* 2017.

77. Gieselmann V, Krageloh-Mann I. Metachromatic leukodystrophy--an update. *Neuropediatrics.* 2010;41(1):1-6.

78. Biffi A, De Palma M, Quattrini A, et al. Correction of metachromatic leukodystrophy in the mouse model by transplantation of genetically modified hematopoietic stem cells. *J Clin Invest.* 2004;113(8):1118-1129.

79. Biffi A, Montini E, Lorioli L, et al. Lentiviral hematopoietic stem cell gene therapy benefits metachromatic leukodystrophy. *Science.* 2013;341(6148):1233158.

80. Sessa M, Lorioli L, Fumagalli F, et al. Lentiviral haemopoietic stem-cell gene therapy in early-onset metachromatic leukodystrophy: an ad-hoc analysis of a non-randomised, open-label, phase 1/2 trial. *Lancet.* 2016;388(10043):476-487.

81. Sergijenko A, Langford-Smith A, Liao AY, et al. Myeloid/Microglial driven autologous hematopoietic stem cell gene therapy corrects a neuronopathic lysosomal disease. *Mol Ther.* 2013;21(10):1938-1949.

82. Sklar MM, Kiess W, Thomas CL, Nissley SP. Developmental expression of the tissue insulin-like growth factor II/mannose 6-phosphate receptor in the rat. Measurement by quantitative immunoblotting. *J Biol Chem.* 1989;264(28):16733-16738.

83. Ballesteros M, Scott CD, Baxter RC. Developmental regulation of insulin-like growth factor-II/mannose 6-phosphate receptor mRNA in the rat. *Biochem Biophys Res Commun.* 1990;172(2):775-779.

84. Urayama A, Grubb JH, Sly WS, Banks WA. Developmentally regulated mannose 6-phosphate receptor-mediated transport of a lysosomal enzyme across the blood-brain barrier. *Proc Natl Acad Sci U S A*. 2004;101(34):12658-12663.

85. Sciacca L, Prisco M, Wu A, Belfiore A, Vigneri R, Baserga R. Signaling differences from the A and B isoforms of the insulin receptor (IR) in 32D cells in the presence or absence of IR substrate-1. *Endocrinology*. 2003;144(6):2650-2658.

86. Duffy KR, Pardridge WM, Rosenfeld RG. Human blood-brain barrier insulin-like growth factor receptor. *Metabolism*. 1988;37(2):136-140.

87. Nissley P, Kiess W, Sklar M. Developmental expression of the IGF-II/mannose 6-phosphate receptor. *Mol Reprod Dev*. 1993;35(4):408-413.

88. Funk B, Kessler U, Eisenmenger W, Hansmann A, Kolb HJ, Kiess W. Expression of the insulin-like growth factor-II/mannose-6-phosphate receptor in multiple human tissues during fetal life and early infancy. *J Clin Endocrinol Metab*. 1992;75(2):424-431.

89. McElduff A, Poronnik P, Baxter RC. The insulin-like growth factor-II (IGF II) receptor from rat brain is of lower apparent molecular weight than the IGF II receptor from rat liver. *Endocrinology*. 1987;121(4):1306-1311.

90. Lowe WL, Jr., Boyd FT, Clarke DW, Raizada MK, Hart C, LeRoith D. Development of brain insulin receptors: structural and functional studies of insulin receptors from whole brain and primary cell cultures. *Endocrinology*. 1986;119(1):25-35.

91. Parrizas M, Maestro MA, Banos N, Navarro I, Planas J, Gutierrez J. Insulin/IGF-I binding ratio in skeletal and cardiac muscles of vertebrates: a phylogenetic approach. *Am J Physiol*. 1995;269(6 Pt 2):R1370-1377.

92. Rinderknecht E, Humbel RE. Primary structure of human insulin-like growth factor II. *FEBS Lett*. 1978;89(2):283-286.

93. Byrne B, Barohn R, Barshop B, et al. POM-001 phase 1/2 study of BMN 701, GILT-tagged recombinant human (rh) GAA in late-onset Pompe disease: Initial experience in 22 patients. *Molecular Genetics and Metabolism*. 2012;108(2):S28.

94. Lebowitz JHN, CA, US), Maga, John (Novato, CA, US). Lysosomal targeting peptides and uses thereof. United States: BioMarin Pharmaceutical Inc. (Novato, CA, US); 2016.

95. Byrne BJ, Falk DJ, Pacak CA, et al. Pompe disease gene therapy. *Hum Mol Genet*. 2011;20(R1):R61-68.

96. Sun B, Zhang H, Franco LM, et al. Efficacy of an adeno-associated virus 8-pseudotyped vector in glycogen storage disease type II. *Mol Ther*. 2005;11(1):57-65.

97. Ziegler RJ, Bercury SD, Fidler J, et al. Ability of adeno-associated virus serotype 8-mediated hepatic expression of acid alpha-glucosidase to correct the biochemical and motor function deficits of presymptomatic and symptomatic Pompe mice. *Hum Gene Ther*. 2008;19(6):609-621.

98. Sun B, Young SP, Li P, et al. Correction of multiple striated muscles in murine Pompe disease through adeno-associated virus-mediated gene therapy. *Mol Ther*. 2008;16(8):1366-1371.

99. Falk DJ, Soustek MS, Todd AG, et al. Comparative impact of AAV and enzyme replacement therapy on respiratory and cardiac function in adult Pompe mice. *Mol Ther Methods Clin Dev*. 2015;2:15007.

100. Doerfler PA, Todd AG, Clement N, et al. Copackaged AAV9 Vectors Promote Simultaneous Immune Tolerance and Phenotypic Correction of Pompe Disease. *Hum Gene Ther*. 2016;27(1):43-59.

101. Qiu K, Falk DJ, Reier PJ, Byrne BJ, Fuller DD. Spinal delivery of AAV vector restores enzyme activity and increases ventilation in Pompe mice. *Mol Ther*. 2012;20(1):21-27.

102. Falk DJ, Mah CS, Soustek MS, et al. Intrapleural administration of AAV9 improves neural and cardiorespiratory function in Pompe disease. *Mol Ther*. 2013;21(9):1661-1667.

103. Elmallah MK, Falk DJ, Nayak S, et al. Sustained correction of motoneuron histopathology following intramuscular delivery of AAV in pompe mice. *Mol Ther*. 2014;22(4):702-712.

104. Zaiss AK, Muruve DA. Immunity to adeno-associated virus vectors in animals and humans: a continued challenge. *Gene Ther*. 2008;15(11):808-816.

105. Cresawn KO, Fraites TJ, Wasserfall C, et al. Impact of humoral immune response on distribution and efficacy of recombinant adeno-associated virus-derived acid alpha-glucosidase in a model of glycogen storage disease type II. *Hum Gene Ther*. 2005;16(1):68-80.

106. Sun B, Li S, Bird A, et al. Antibody formation and mannose-6-phosphate receptor expression impact the efficacy of muscle-specific transgene expression in murine Pompe disease. *J Gene Med*. 2010;12(11):881-891.

107. Franco LM, Sun B, Yang X, et al. Evasion of immune responses to introduced human acid alpha-glucosidase by liver-restricted expression in glycogen storage disease type II. *Mol Ther*. 2005;12(5):876-884.

108. Sun B, Kulis MD, Young SP, et al. Immunomodulatory gene therapy prevents antibody formation and lethal hypersensitivity reactions in murine pompe disease. *Mol Ther*. 2010;18(2):353-360.

109. Zhang P, Sun B, Osada T, et al. Immunodominant liver-specific expression suppresses transgene-directed immune responses in murine pompe disease. *Hum Gene Ther*. 2012;23(5):460-472.

110. Mingozzi F, Maus MV, Hui DJ, et al. CD8(+) T-cell responses to adeno-associated virus capsid in humans. *Nat Med*. 2007;13(4):419-422.

111. Mingozzi F, High KA. Immune responses to AAV vectors: overcoming barriers to successful gene therapy. *Blood*. 2013;122(1):23-36.

112. Kung SK, An DS, Bonifacino A, et al. Induction of transgene-specific immunological tolerance in myeloablated nonhuman primates using lentivirally transduced CD34+ progenitor cells. *Mol Ther*. 2003;8(6):981-991.

113. Tian C, Bagley J, Kaye J, Iacomini J. Induction of T cell tolerance to a protein expressed in the cytoplasm through retroviral-mediated gene transfer. *J Gene Med*. 2003;5(5):359-365.

SUPPLEMENTARY FIGURE LEGENDS

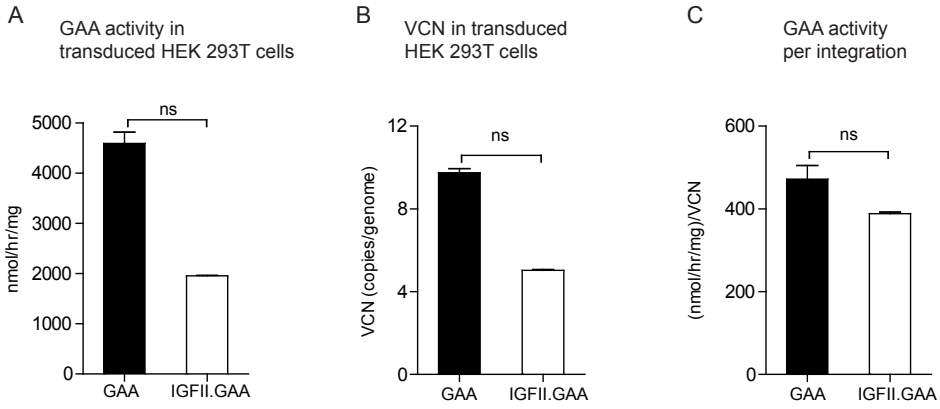

Figure S1. Excretion assay using HEK 293T cells transduced with either LV-GAAco or LV-IGFIIco. GAAco lentiviral vectors. (A) GAA activity in transduced HEK 293T producer cells. (B) Vector copy number in (A) determined by *HIV* qPCR and normalized using *GAPDH*. (C) GAA activity per integration. GAA activity from (A) was corrected by VCN from (B). Data represent means ± SEM of three biological replicates. Mann-Whitney U test was used. ns, not significant.

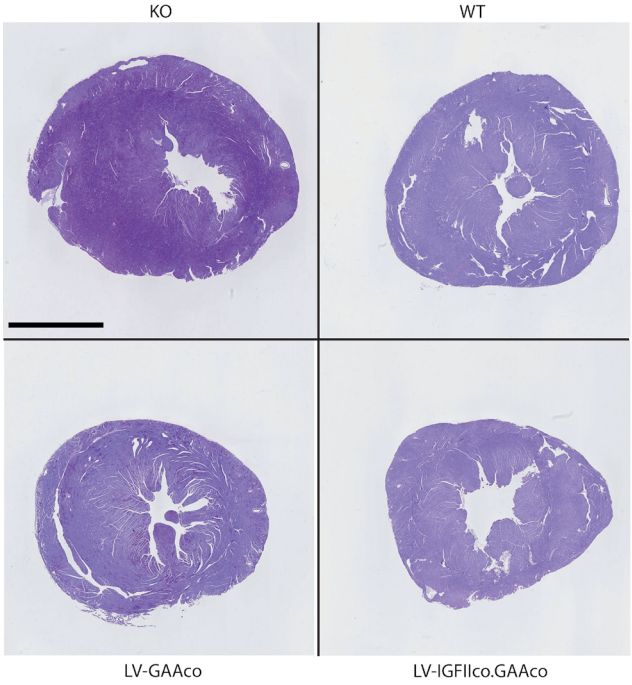

Figure S2. Glycogen reduction in cardiac tissue after gene therapy. Representative full images showing the hearts of 9 Gy irradiated mice treated with either LV-GAAco or LV-IGFIIco.GAAco, and of untreated *Gaa*$^{-/-}$ (KO) and wildtype (WT) mice. Sections were stained with periodic acid Schiff (PAS). Scale bar = 2 mm.

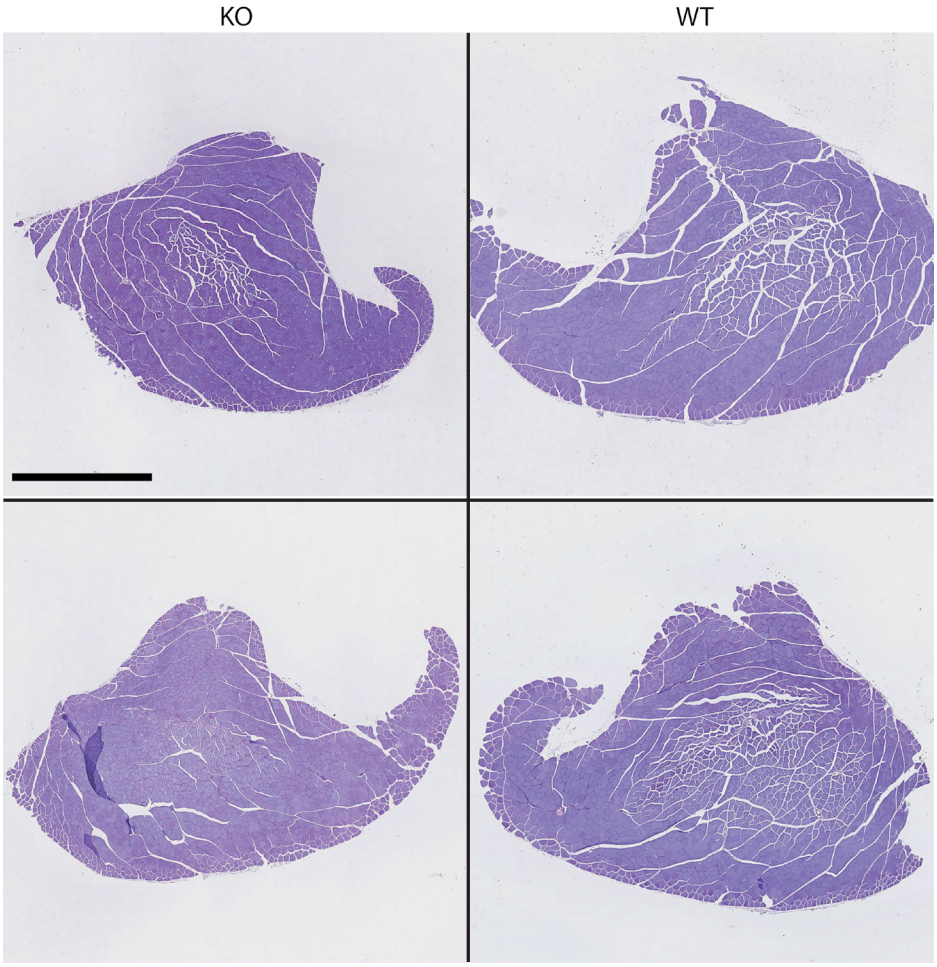

Figure S3. Glycogen reduction in tibialis anterior after gene therapy. Representative full images showing the tibialis anterior of 9 Gy irradiated mice treated with either LV-GAAco or LV-IGFIIco. GAAco, and of untreated *Gaa*$^{-/-}$ (KO) and wildtype (WT) mice. Sections were stained with periodic acid Schiff (PAS). Scale bar = 1 mm.

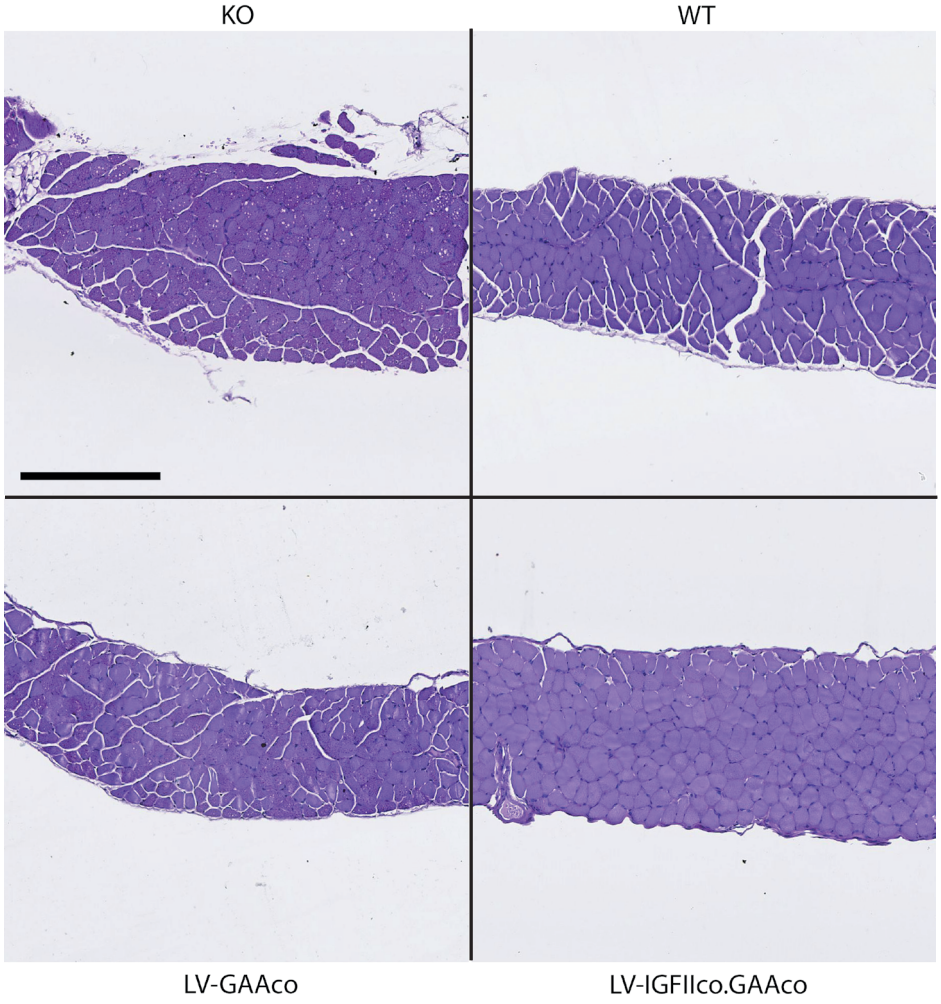

Figure S4. Glycogen reduction in diaphragm after gene therapy. Representative full images showing the diaphragms of 9 Gy irradiated mice treated with either LV-GAAco or LV-IGFIIco.GAAco, and of untreated *Gaa*$^{-/-}$ (KO) and wildtype (WT) mice. Sections were stained with periodic acid Schiff (PAS). Scale bar = 0.25 mm.

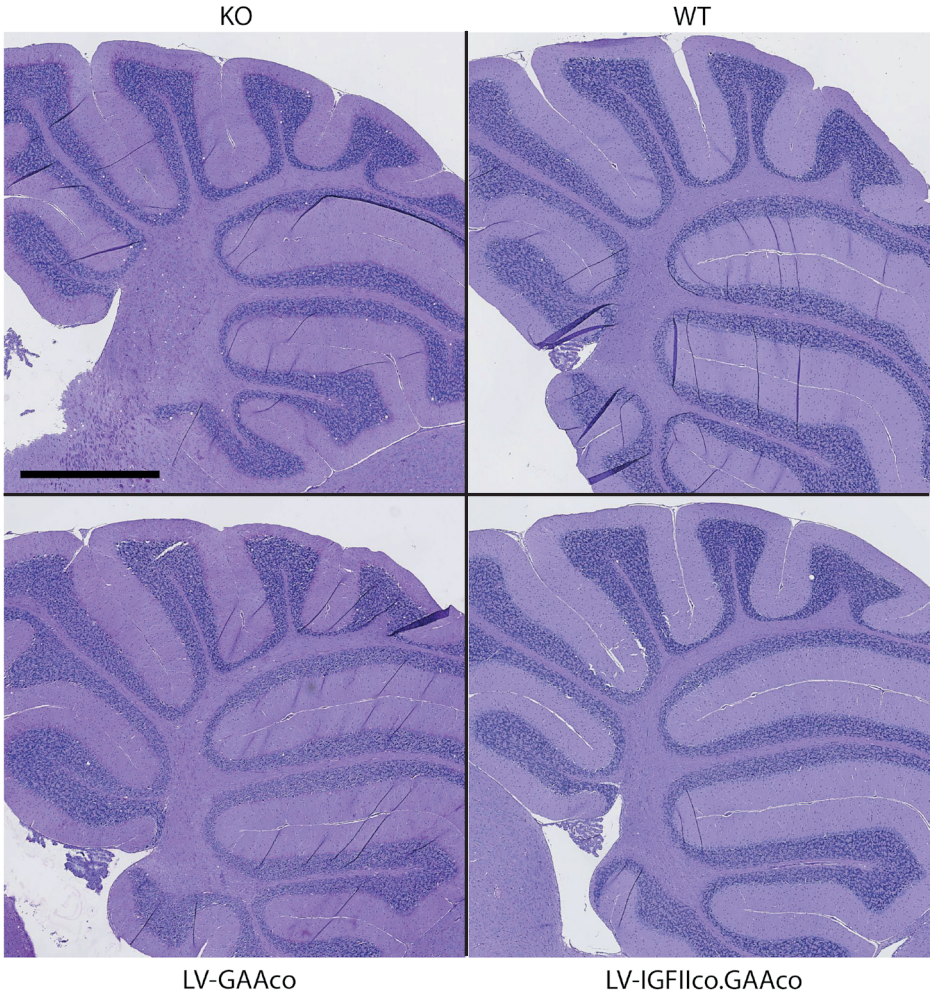

Figure S5. Glycogen reduction in cerebellum after gene therapy. Representative full images showing the brains of 9 Gy irradiated mice treated with either LV-GAAco or LV-IGFIIco.GAAco, and of untreated *Gaa*$^{-/-}$ (KO) and wildtype (WT) mice. Sections were stained with periodic acid Schiff (PAS) and images of cerebellum are shown. Scale bar = 1 mm.

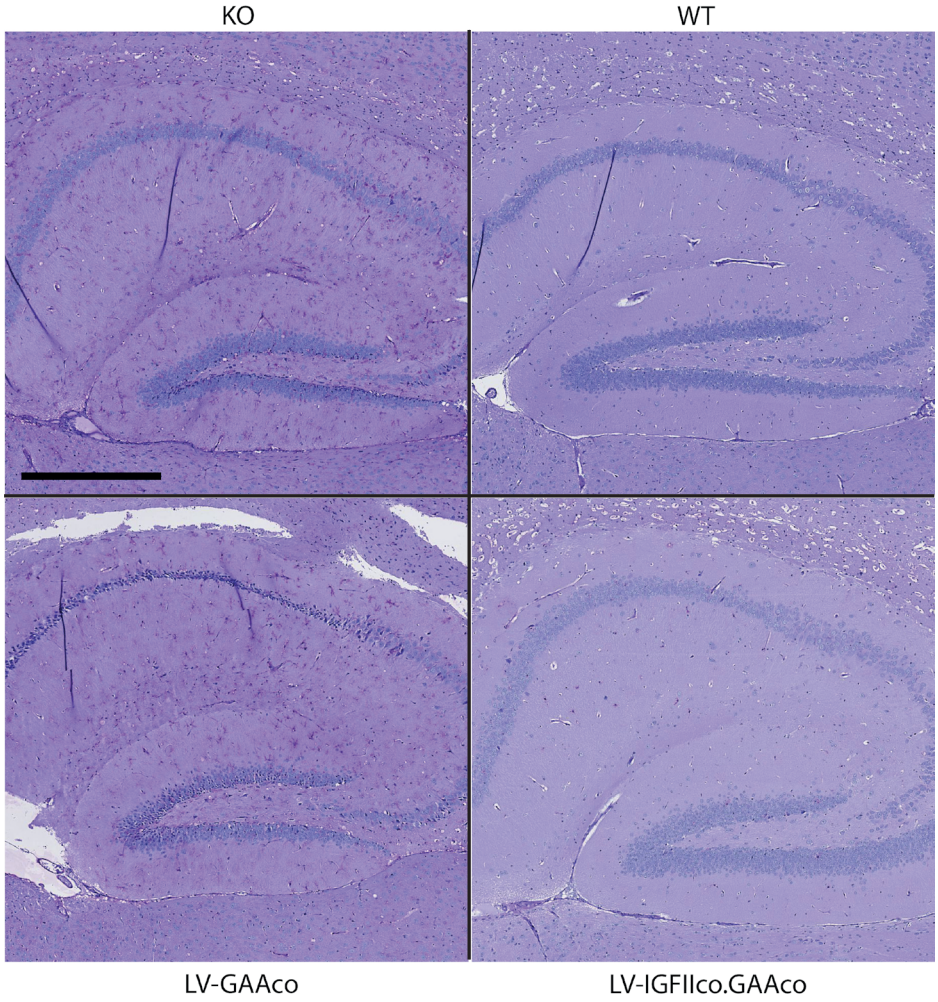

Figure S6. Glycogen reduction in hippocampus after gene therapy. Representative full images showing the brains of 9 Gy irradiated mice treated with either LV-GAAco or LV-IGFIIco.GAAco, and of untreated *Gaa*$^{-/-}$ (KO) and wildtype (WT) mice. Sections were stained with periodic acid Schiff (PAS) and images of hippocampus are shown. Scale bar = 0.5 mm.

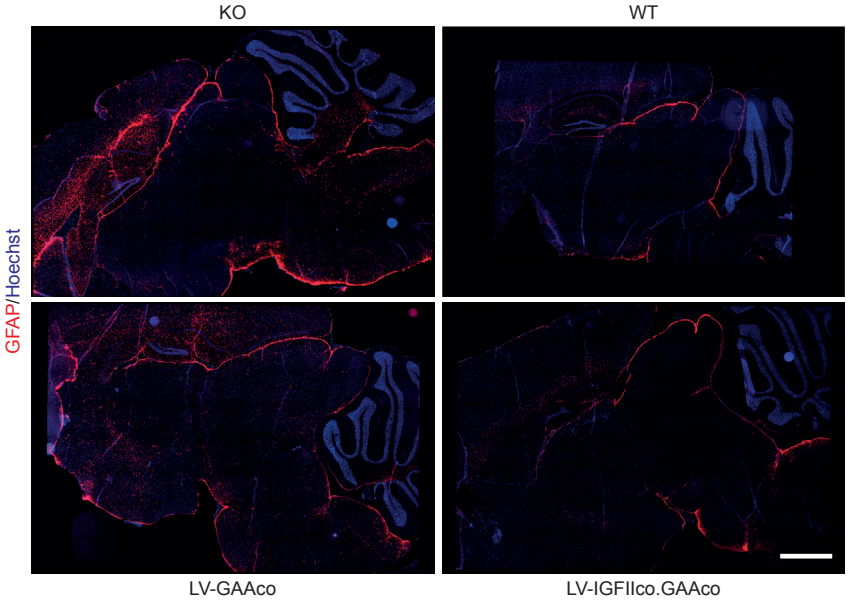

Figure S7. Increased number of astrocytes in brain of Pompe mice corrected by gene therapy. Sagittal cryostat sections from the brains of transplanted mice from 9 Gy cohorts of both LV-GAAco and LV-IGFIIco.GAAco groups were stained with GFAP for astrocytes (red) and counterstained with Hoechst for nuclei (blue) as indicated. Untreated *Gaa*$^{-/-}$ (KO) and wildtype (WT) mice served as controls. Representative images of the whole brain section are shown. Scale bar = 1 mm.

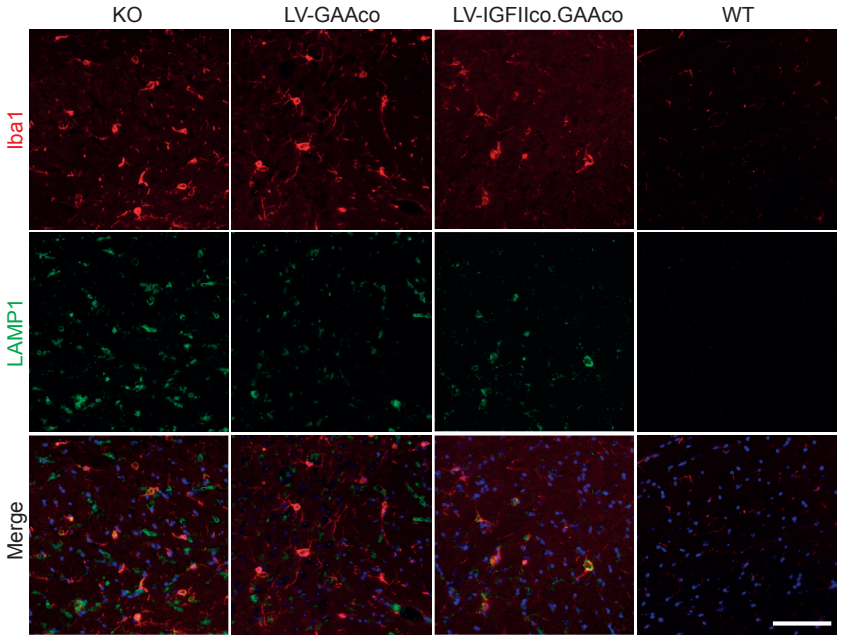

Figure S8. Increased number of microglia in corpus callosum of Pompe mice corrected by gene therapy. Sagittal cryostatic sections from the brains of transplanted mice from 9 Gy cohorts of both LV-GAAco and LV-IGFIIco.GAAco groups were stained with Iba1 for microglia (red), LAMP1 for lysosomal compartment (green) and counterstained with Hoechst for nuclei (blue) as indicated. Untreated *Gaa*$^{-/-}$ (KO) and wildtype (WT) mice served as controls. Representative images in corpus callosum are shown and signals are merged at the bottom panel. Scale bar = 25 µm.

Table S1. Sequence of primers for qPCR

Primers	Sequence
HIV-U3 forward	5′-CTGGAAGGGCTAATTCACTC-3′
HIV-PSI reverse	5′-GGTTTCCCTTTCGCTTTCAG-3′
Sry forward	5′-TCATCGGAGGGCTAAAGTGTCAC-3′
Sry reverse	5′-TGGCATGTGGGTTCCTGTCC-3′
Gapdh forward (mouse)	5′-TAATGGGGAGAGGTTCGATG-3′
Gapdh reverse (mouse)	5′-GCTGCTTCCCGAGTAAAATG-3′
GAPDH forward (human)	5′-CGGTTTCTATAAATTGAGCCCG-3′
GAPDH reverse (human)	5′-GCGACGCAAAAGAAGATGC-3′

Table S2. Parameters estimates for B1 in a nonlinear model for the relation between VCN and glycogen clearance

Tissues	Estimates	Std. Error	95% Confidence Interval		Statistic outcome
			Lower Bound	Upper Bound	
Heart	-0.556	0.183	-0.919	-0.193	Significant
Tibialis anterior	-0.408	0.131	-0.668	-0.148	Significant
Cerebrum	-0.490	0.165	-0.817	-0.163	Significant

The difference between groups LV-IGFIIco.GAAco and LV-GAAco in how fast the curve drops is defined as significant when 95% confidence interval for B1 does not contain zero.

Chapter 4

Effects of hematopoietic stem cell-mediated lentiviral gene therapy on the skeletal muscle proteome in a murine model for Pompe disease

Qiushi Liang, M.D.[1,2,3]; Joon M. Pijnenburg, B.A.Sc.[1,2,3]; Erikjan H.W.J. Rijkers, B.A.Sc.[4]; Jeroen J.A.A. Demmers Ph.D.[4]; Arnold G. Vulto, Pharm.D., Ph.D.[5]; Ans T. van der Ploeg, M.D., Ph.D.[2,3]; Niek P. van Til, Ph.D.[6,7]; W.W.M. Pim Pijnappel, Ph.D.[1,2,3]*

[1] Molecular Stem Cell Biology, Department of Clinical Genetics, Erasmus University Medical Center, 3015GE Rotterdam, The Netherlands
[2] Department of Pediatrics, Erasmus University Medical Center, 3015GE Rotterdam, The Netherlands
[3] Center for Lysosomal and Metabolic Diseases, Erasmus University Medical Center, 3015GE Rotterdam, The Netherlands
[4] Proteomics Center, Erasmus University Medical Center, 3015GE Rotterdam, The Netherlands
[5] Hospital Pharmacy, Erasmus University Medical Center, 3015GE Rotterdam, The Netherlands
[6] Department of Hematology, Erasmus University Medical Center, 3015GE Rotterdam, The Netherlands
[7] Current address: Laboratory of Translational Immunology, University Medical Center Utrecht, 3584CX Utrecht, The Netherlands
* Correspondence: Dr. W.W.M. Pim Pijnappel, Erasmus University Medical Center, 3015GE Rotterdam, The Netherlands.
Email: w.pijnappel@erasmusmc.nl.

Submission in preparation

ABSTRACT

Pompe disease is caused by the deficiency of acid α-glucosidase (GAA) that leads to lysosomal glycogen accumulation. Clinical manifestations include progressive respiratory and motor dysfunction due to skeletal muscle wasting. The currently registered enzyme replacement therapy (ERT) using recombinant human GAA (rhGAA) has a heterogeneous clinical response, warranting the search for an alternative therapy. Hematopoietic stem cell mediated lentiviral gene therapy has been developed as a promising alternative, and promotes systemic glycogen clearance in a mouse model for Pompe disease including the muscles. In this study, we performed a global proteomic analysis of the quadriceps femoris using quantitative mass spectrometry to evaluate the muscle pathology caused by murine Pompe disease and the therapeutic effect of gene therapy. We found dysregulation of proteins involved in skeletal muscle and lysosomal physiology, autophagy and glucose and glycogen metabolism. Importantly, these abnormalities were close to normalized by lentiviral gene therapy using a lentiviral vector with improved targeting of GAA via fusion to an insulin-like growth factor II (IGFII) peptide. We conclude that muscle pathology caused by Pompe disease can be monitored at the proteome level, and that lentiviral gene therapy holds great promise in simultaneously correcting the primary as well as the secondary abnormalities in Pompe disease.

INTRODUCTION

Pompe disease, also called glycogen storage disease type II, is a lysosomal storage disease caused by the deficiency of acid α-glucosidase (GAA), a hydrolase that degrades glycogen within the lysosome.[1,2] The clinical spectrum ranges from life-threatening cardiac hypertrophy and generalized skeletal muscle weakness in classic infantile patients[3,4] to a slower progressing muscle weakness in childhood and adult patients.[5,6]

The primary pathology of Pompe disease is caused by lysosomal glycogen accumulation in virtually all tissues, especially in muscles, causing generalized myopathy.[7] Furthermore, accumulating data have revealed cascades of secondary pathological events including aberrant autophagy, impaired mitochondrial function, dysregulated Ca^{2+} homeostasis and increased reactive oxygen species.[8-10] These are also common hallmarks for other lysosomal storage diseases.[11,12] Transcriptome studies in skeletal muscle from infantile patients showed changed expression patterns characteristic of immature or regenerating muscles, as well as deregulation of markers for inflammation.[13] So far, however, global studies on protein expression levels are lacking in this field.

Enzyme replacement therapy with recombinant human GAA (rhGAA, Myozyme, Genzyme Cooperation) is the only registered therapy and has changed the natural course of infantile patients due to profound reversal of cardiomegaly.[14,15] It can stabilize or even improve the respiratory and motor function in a subset of patients.[16] However, remaining challenges include limited treatment efficacy caused by poor posttranslational modification of the rhGAA enzyme,[17,18] neutralizing effect of anti-GAA antibodies[19,20] and the inability to treat the nervous system.[21] Hematopoietic stem cell (HSC) mediated lentiviral gene therapy has been developed at the preclinical level for Pompe disease. Using a modified lentiviral vector with improved targeting facilitated by the addition of insulin-like growth factor II (IGFII),[22] we have achieved a complete phenotypic correction in heart, skeletal muscles and brain in *Gaa*$^{-/-}$ mice (Chapter 3). However, only glycogen and two other indirect markers, i.e. acid phosphatase and lysosomal-associated membrane protein 1 (LAMP1) were used as biomarkers for therapeutic assessment.

In this study, a global protein expression profiling using quantitative mass spectrometry was performed to identify proteomic changes in skeletal muscle of Pompe mice, and to evaluate the response to HSC mediated lentiviral gene therapy.

MATERIALS AND METHODS

Animals

The *Gaa* knockout (*Gaa*$^{-/-}$) mice and age-matched FVB/N mice obtained from Charles River were bred in the Laboratory Animal Science Center (EDC) at the Erasmus MC according to standard procedures under specific pathogen free (SPF) conditions. All animal experiments in this study were approved by the Animal Experiments Committee (DEC) in the Netherlands.

Transplantation of ex vivo genetically modified hematopoietic stem cells

The third generation self-inactivating (SIN) lentiviral vectors pRRL.PPT.SF.GAAco.bPRE4*.SIN (LV-GAAco) and pRRL.PPT.SF.IGFIIco.GAAco.bPRE4*.SIN (LV-IGFIIco.GAAco) were generated as described in **Chapter 3**. pRRL.PPT.SF.GFP.bPRE4*.SIN (LV-GFP)[23] was included as control. Following the previously published protocol,[23] 8-week old female *Gaa*$^{-/-}$ mice, subjected to 9 Gy irradiation, were transplanted with one million male hematopoietic stem cells (HSCs) transduced overnight with either LV-GAAco or LV-IGFIIco.GAAco at the multiplicity of infection (MOI) of 7. A mock treated group using LV-GFP was infused with 3×10^5 HSCs with a MOI of 2 after 6 Gy irradiation. Age-matched untreated *Gaa*$^{-/-}$ (KO) and FVB/N wildtype (WT) were included as controls (Tables 1, 4).

Tissue collection and protein extraction

Six months after gene therapy, mice were fasted overnight and sacrificed following intracardial perfusion. Three biological replicates of the quadriceps femoris (QF) from three mice per group were processed for proteomic studies.

Tissues were lysed in 1 ml 50 mM Tris/HCl (pH 8.2) supplemented with 0.5 % sodium deoxycholate (SDC) and MS-SAFE™ protease and phosphatase inhibitor using a Bioruptor ultrasonicator (Diagenode). Protein concentrations were measured using the BCA assay (Thermo Scientific). Lysates were reduced with 5 mM dithiothreitol (DTT) and cysteine residues were alkylated with 10 mM iodoacetamide. Protein was extracted by acetone precipitation at -20 °C overnight. Samples were centrifuged at 8,000 g for 10 mins at 4 °C. The acetone was removed and the pellet dried. The protein pellet (~4 mg protein) was dissolved in 1 ml 50 mM Tris/HCl (pH 8.2) with 0.5 % SDC and proteins were digested with LysC (1:200 enzyme:protein ratio) for 4 hrs at 37 °C. Next, trypsin was added (1:100 enzyme:protein ratio) and the digestion proceeded overnight at 30°C. Digests were acidified with 50 µl 10 % formic acid (FA) and centrifuged at 8,000 g for 10 mins at 4 °C to remove the precipitated SDC. The supernatant

was purified with C18 solid phase extraction (Sep-Pak, Waters), lyophilized and stored at -20 °C before further processing.

Tandem Mass Tagging labeling

Isobaric labeling of the peptides was performed using the 10-plex tandem mass tag (TMT) reagents (Thermo Fisher Scientific) as described[24] with some modifications. Peptides were loaded onto 20 mg C18 cartridges prepared in-house. The C18 cartridges were washed once with 1 ml 0.1% trifluoroacetic acid (TFA) and two times with 1 mL of 50 mM KH_2PO_4 (pH 4.5). TMT reagents (0.8 mg) were dissolved in 10 µl of dry acetonitrile (ACN) and diluted with 200 µl 50 mM KH_2PO_4. This TMT solution was immediately loaded onto the column and labeling on column proceeded for 1 hr at room temperature. Each of the 10 samples was labeled with a different TMT tag. After labeling the column was washed two times with 1 ml 2 % ACN / 0.2 % formic acid (FA) and the labeled peptides eluted with 1 ml 50 % ACN. TMT labeled samples were pooled and lyophilized.

High-pH and reversed phase HPLC

TMT labeled peptides were subjected to offline orthogonal high-pH and reverse phase fractionation. TMT labeled peptides were solubilized in 0.1 % TFA and loaded onto a 20 mg polymeric reversed phase (PLRP-S) cartridge made in-house. The cartridge was washed once with 1 ml 0.1 % TFA and three times with 1 ml milliQ water. The peptides were eluted step-wise from column with 0 %, 5 %, 10 %, 15 %, 25 % and 40 % ACN / 10 mM ammonium formate (pH 10). The 6 fractions were dried by vacuum centrifugation and each fraction was reconstituted with 2 % ACN / 0.2 % FA for LC-MS/MS analysis.

LC-MS/MS analysis

Mass spectra were acquired on an Oribtrap Lumos (Thermo) coupled to an EASY-nLC 1200 system (Thermo). Peptides were separated on an in-house packed 75 µm inner diameter column containing 50 cm Waters CSH130 resin (3.5 µm, 130 Å, Waters) with a gradient consisting of 2–20 % (ACN, 0.1 % FA) over 150 min at 300 nl/min. The column was kept at 50 °C in a NanoLC oven - MPI design (MS Wil GmbH). For all experiments, the instrument was operated in the data-dependent acquisition (DDA) mode. MS1 spectra were collected at a resolution of 120,000, with an automated gain control (AGC) target of 2E5 and a max injection time of 50 ms. The most intense ions were selected for MS/MS, top speed method 3 seconds cycle time. Precursors were filtered according to charge state (2-7), and monoisotopic peak assignment. Previously interrogated precursors were dynamically excluded for 70 seconds. Peptide precursors were isolated with a quadrupole mass filter set to a width of 0.7 Th. When

applying the MS3 method, ion trap MS2 spectra were collected at an AGC of 5E4, max injection time of 50 ms and CID collision energy of 35 %. For Orbitrap MS3 spectra, the operation resolution was 60,000, with an AGC setting of 1E5 and a max injection time of 120 ms. The HCD collision energy was set to 65 % to ensure maximal TMT reporter ion yield. Synchronous precursor selection (SPS) was enabled at all times to include up to 10 MS2 fragment ions in the MS3 scan.

Due to the capacity of the machine, samples were run separately in two rounds with three biological replicates from WT group as intergroup controls. See Tables 1 and 4 for detailed sample information.

Data analysis and statistics

Peak lists were automatically created from raw data files using the Proteome Discoverer 2.1 (Thermo) software. The Mascot search algorithm (version 2.2, MatrixScience) was used for searching spectra against the Uniprot database (taxonomy: *Mus musculus*, version from December 2016). The peptide tolerance was set to 10 ppm and the fragment ion tolerance was set to 0.6 Da. A maximum number of 2 missed cleavages were allowed. TMT tags on peptide N termini/lysine residues (+229.162932 Da) and carbamidomethylation of cysteine residues (+57.02146 Da) were set as static modifications. The target FDR for both peptide-spectrum match (PSM) and peptides was set to 0.01. Proteins were marked with 'high confidence' when they fulfilled the requirement for an FDR = 0.01 and were then taken into account for further analysis. The co-isolation threshold was set to 75 % and the minimum signal-to-noise ratio to 10. For TMT quantification, a 0.01 Th window centered on the theoretical m/z value of each reporter ion was queried for the nearest signal intensity. Reporter ion intensities were adjusted to correct for the isotopic impurities of the different TMT reagents (according to the manufacturer's specifications).

Further data analysis was performed using the Perseus software suite (Max Planck Institute of Biochemistry)[25]. Reporter ion abundance data from Proteome Discoverer 2.1 were imported into Perseus, log2 transformed and replicates grouped. Protein groups with less than two valid values in at least one group were removed and missing values were imputed based on normal distribution. Z-scoring was used as additional normalization of the data. Comparison of protein levels between two groups were determined using standard two-sided t-testing (FDR: 0.05, S0: 0.1, number of randomizations: 250). The gene ontology (GO) analysis was performed with Panther using slim term[26] and pathway analysis was executed via Ingenuity Pathway Analysis (QIAGEN Inc.). A P value ≤ 0.05 was considered statistically significant.

RESULTS AND DISCUSSION

Global protein expression in muscle from *Gaa*$^{-/-}$ mice compared to wildtype controls

Global proteomic abnormalities in skeletal muscle in Pompe disease were assessed in Study 1 (see Table 1 for details). To this end, quadriceps femoris (QF) muscles were obtained from untreated *Gaa*$^{-/-}$ (KO) and from FVB/N (WT) mice at the age of 8 months, and processed for TMT-labeling, followed by mass spectrometry analysis. LV-GFP mock-transplanted Pompe mice were also included to evaluate the impact of the transplantation procedure. More than 2,760 proteins were identified in Study 1 with no less than 2 peptides per identified protein (Table 1). A total of 2,544 proteins were successfully quantified (see materials and methods). Scatter plots of the average protein intensity of three biological replicates from each group showed the differences between WT mice and KO mice, and between LV-GFP treated and KO mice (Figure 1A).

In general, differences in protein expression levels caused by GAA deficiency were small, in line with the relatively mild pathology in GAA KO mice. Differentially expressed proteins between the two groups were therefore analyzed using a fold change (FC) ≥ 1.2 and a FDR of 0.05. A total of 480 differentially expressed proteins were identified using these criteria. Among these, 243 proteins were up-regulated and 237 proteins were down-regulated(Figure 1B). Information of these proteins is shown in Table S1. LV-GFP treated mice showed an upregulation of 343 proteins and a downregulated of 300 proteins compared to WT mice (Figure 1C). Importantly, only one protein (Ighg3) was identified to be differentially expressed between KO and LV-GFP treated mice (Figure 1D, arrow). This indicated that at the protein level, the procedures implemented during lentiviral gene therapy including irradiation at sublethal dosage did not cause major disturbances.

Table 1. Sample information and number of proteins identified in Study 1.

Study	Group ID	Treatment	MOI	Cell number	Irradiation (Gy)	Sample ID	No. of Proteins Identified
1	WT	Untreated WT	*NA*	*NA*	*NA*	WT 1	2774
						WT 2	2760
						WT 3	2779
	KO	Untreated KO	*NA*	*NA*	*NA*	KO 1	2782
						KO 2	2780
						KO 3	2784
	LV-GFP	LV-GFP transplanted	2	3×10^5	6	LV-GFP 1	2779
						LV-GFP 2	2777
						LV-GFP 3	2783

MOI indicates multiplicity of infection; Gy, gray; KO, *Gaa*$^{-/-}$ knockout; WT, wildtype; and *NA*, not applicable.

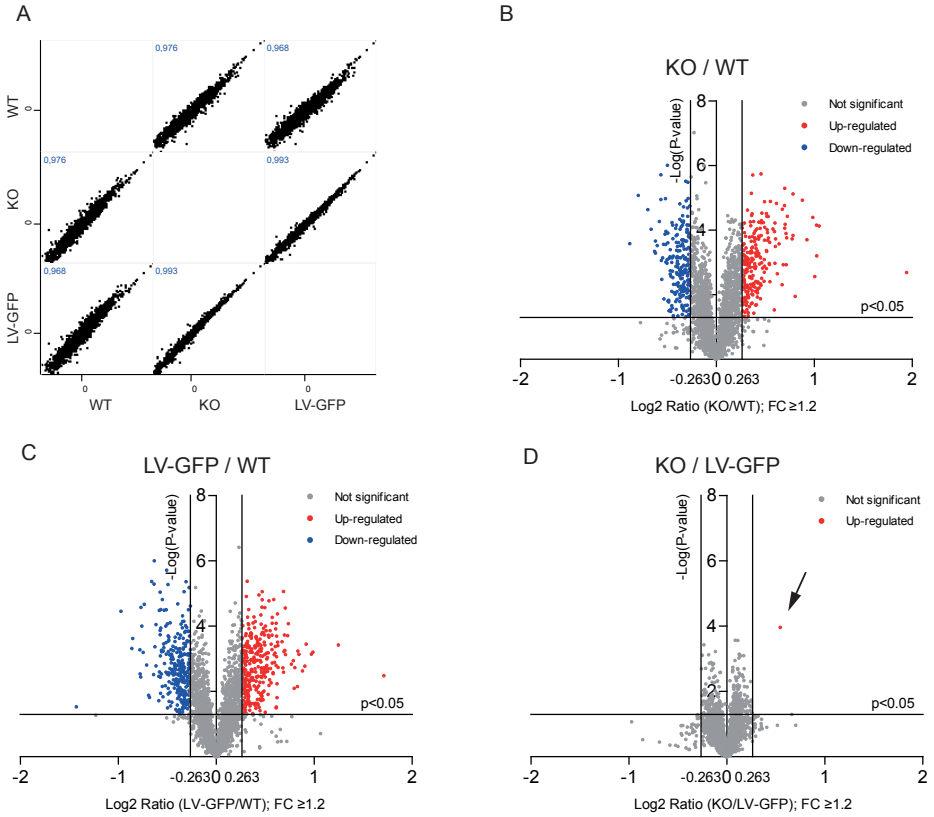

Figure 1. Expression differences in Study 1. (A) Scatter plots of intensities of proteins identified in the three groups indicated. Values from three biological replicates per group were averaged. The Pearson correlation coefficient is displayed. (B-D) Volcano plots showing differentially expressed proteins in KO against WT mice (B), in LV-GFP treated against WT mice (C) and in KO against LV-GFP-treated mice (D). The arrow points to the only differentially regulated protein in (D). FC, fold change.

Gene ontology analysis of the muscle proteome from *Gaa*$^{-/-}$ mice

To gain insight in the biological significance of differentially expressed proteins in GAA KO mice and their possible roles in pathology of Pompe disease, gene ontology (GO) analysis was performed using the Panther and Ingenuity Pathway Analysis (IPA) pipelines. Top 10 GO terms that were significantly enriched (P value<0.05) in the categories molecular function, biological process and cellular components are listed in Table 2 (up-regulated proteins) and Table 3 (down-regulated proteins), respectively. The molecular functions of up-regulated proteins were enriched in "calmodulin binding" and catabolism including "catalytic activity", "hydrolase activity" and "peptidase activity" (Table 2). This is in agreement with previously reported disturbed calcium homeostasis and lysosomal function.[9] Muscle function termed "muscle contraction"

Table 2. Gene ontology slim term enrichment analysis in up-regulated proteins in KO compared to WT.

GO terms	GO ID	Functional category	Count in genome	Count in samples	Expected count	Fold enrichment	P value
Molecular Function	GO:0005200	structural constituent of cytoskeleton	573	34	6.29	5.41	2.14E-15
	GO:0005198	structural molecule activity	924	37	10.14	3.65	1.38E-11
	GO:0004872	receptor activity	2115	2	23.21	< 0.2	9.07E-09
	GO:0005515	protein binding	2863	59	31.42	1.88	1.14E-06
	GO:0008092	cytoskeletal protein binding	263	14	2.89	4.85	1.73E-06
	GO:0005516	calmodulin binding	130	8	1.43	5.61	1.12E-04
	GO:0003779	actin binding	188	9	2.06	4.36	2.72E-04
	GO:0003824	catalytic activity	5143	80	56.45	1.42	3.74E-04
	GO:0016787	hydrolase activity	2160	41	23.71	1.73	3.94E-04
	GO:0008233	peptidase activity	594	15	6.52	2.30	2.63E-03
Biological Process	GO:0006936	muscle contraction	151	14	1.66	8.45	2.16E-09
	GO:0032989	cellular component morphogenesis	529	23	5.81	3.96	3.09E-08
	GO:0006260	DNA replication	146	10	1.60	6.24	6.34E-06
	GO:0006457	protein folding	119	8	1.31	6.13	6.12E-05
	GO:0007010	cytoskeleton organization	154	9	1.69	5.32	6.22E-05
	GO:0006996	organelle organization	767	21	8.42	2.49	1.34E-04
	GO:0042116	macrophage activation	112	7	1.23	5.69	2.73E-04
	GO:0006351	transcription, DNA-dependent	1537	5	16.87	0.30	5.43E-04
	GO:0008152	metabolic process	6955	101	76.34	1.32	5.54E-04
	GO:0015031	protein transport	1000	23	10.98	2.10	7.46E-04
Cellular Component	GO:0005856	cytoskeleton	622	29	6.83	4.25	8.81E-11
	GO:0015629	actin cytoskeleton	234	14	2.57	5.45	4.46E-07
	GO:0005737	cytoplasm	2134	46	23.42	1.96	7.39E-06
	GO:0016021	integral to membrane	1684	6	18.48	0.32	5.27E-04
	GO:0045111	intermediate filament cytoskeleton	72	5	0.79	6.33	1.30E-03
	GO:0045298	tubulin complex	20	3	0.22	13.67	1.48E-03
	GO:0005773	vacuole	92	5	1.01	4.95	3.71E-03
	GO:0031201	SNARE complex	39	3	0.43	7.01	9.43E-03
	GO:0005874	microtubule	128	5	1.40	3.56	1.42E-02
	GO:0005764	lysosome	55	3	0.60	4.97	2.33E-02

Table 3. Gene ontology slim term enrichment analysis in down-regulated proteins in KO compared to WT.

GO terms	GO ID	Functional category	Count in genome	Count in samples	Expected count	Fold enrichment	P value
Molecular Function	GO:0004872	receptor activity	2115	1	22.65	< 0.2	1.21E-09
	GO:0016491	oxidoreductase activity	672	22	7.20	3.06	4.34E-06
	GO:0005198	structural molecule activity	924	26	9.89	2.63	8.44E-06
	GO:0004871	signal transducer activity	1360	2	14.56	< 0.2	4.07E-05
	GO:0016740	transferase activity	1541	33	16.50	2.00	1.21E-04
	GO:0008092	cytoskeletal protein binding	263	11	2.82	3.91	1.51E-04
	GO:0005200	structural constituent of cytoskeleton	573	17	6.14	2.77	1.77E-04
	GO:0003779	actin binding	188	9	2.01	4.47	2.27E-04
	GO:0019203	carbohydrate phosphatase activity	13	3	0.14	21.55	4.00E-04
	GO:0005516	calmodulin binding	130	7	1.39	5.03	5.69E-04
Biological Process	GO:0006936	muscle contraction	151	16	1.62	9.90	1.51E-11
	GO:0032989	cellular component morphogenesis	529	22	5.66	3.88	8.63E-08
	GO:0006096	glycolysis	37	7	0.40	17.67	1.99E-07
	GO:0006520	cellular amino acid metabolic process	253	14	2.71	5.17	8.26E-07
	GO:0050896	response to stimulus	3345	13	35.81	0.36	3.11E-06
	GO:0000910	cytokinesis	111	8	1.19	6.73	3.17E-05
	GO:0006206	pyrimidine nucleobase metabolic process	36	5	0.39	12.97	4.97E-05
	GO:0006094	gluconeogenesis	22	4	0.24	16.98	1.04E-04
	GO:0005975	carbohydrate metabolic process	463	15	4.96	3.03	1.69E-04
	GO:0008152	metabolic process	6955	101	74.47	1.36	1.93E-04
Cellular Component	GO:0015629	actin cytoskeleton	234	21	2.51	8.38	2.12E-13
	GO:0005856	cytoskeleton	622	22	6.66	3.30	1.27E-06
	GO:0005737	cytoplasm	2134	47	22.85	2.06	1.59E-06
	GO:0030054	cell junction	82	7	0.88	7.97	3.48E-05
	GO:0016021	integral to membrane	1684	5	18.03	0.28	2.15E-04
	GO:0005783	endoplasmic reticulum	157	6	1.68	3.57	7.35E-03
	GO:0042175	nuclear outer membrane-endoplasmic reticulum membrane network	98	4	1.05	3.81	2.19E-02
	GO:0005576	extracellular region	953	4	10.20	0.39	2.34E-02
	GO:0016020	membrane	2787	20	29.84	0.67	2.89E-02
	GO:0043234	protein complex	1196	20	12.81	1.56	3.35E-02

was enriched and inflammation-related biological processes including "macrophage activation" also corroborated with previous findings.[13] Cellular components including "vacuoles" and "lysosome" were enriched although the proteins detected were less abundant. Interestingly, the cytoskeleton was strongly represented at all three levels, suggestive of a global disturbance on the cellular level in Pompe disease. While most of the down-regulated proteins were enriched in the similar GO terms, "glycolysis" and "gluconeogenesis" were especially enriched in down-regulated proteins (Table 3). These results were suggestive of a disturbed glucose metabolism in Pompe disease, although hypoglycemia is not a hallmark of Pompe disease.[1]

Next, Ingenuity Pathway Analysis (IPA) was performed (Figure 2). Interesting hits including "autophagy", "phagosome maturation" and "NRF2-mediated oxidative stress response" all pointed to a disturbed cellular homeostasis in line with previous findings (Figure 2A).[8,27] The overrepresentation of proteins, i.e. Gbe1 and Gyg, which promote glycogen biosynthesis, confirmed dysregulation of glycogen metabolism in Pompe disease.[28] Consistent with GO analysis using Panther, down-regulated proteins were mainly involved in glucose metabolism including glycolysis and gluconeogenesis (Figure 2B).

To conclude, compared to WT controls, differentially expressed proteins in KO samples were related to muscle dysfunction, glucose and glycogen metabolism, and autophagy. The abnormalities were not restricted to lysosomes, rather, they extended to the cytoskeleton.

Correction of the proteomic profile by lentiviral gene therapy

In previous experiments (Chapter 3), hematopoietic stem cell (HSC)-mediated gene therapy using a lentiviral vector carrying a codon optimized GAA transgene (LV-GAAco) was able to partially reduce glycogen deposits in Pompe mice. A complete glycogen correction was achieved using vectors encoding GAA with improved targeting by fusion with insulin-like growth factor II (IGFII; LV-IGFIIco.GAAco). To evaluate proteomic correction following gene therapy, the QFs from LV-GAAco and LV-IGFIIco.GAAco-treated mice were analyzed in Study 2 six months after gene therapy (Table 4). The same WT samples from Study 1 were included as intergroup controls. 2,232 proteins (peptides ≥ 2) were identified in Study 2 (Table 4). Of these, 2,158 proteins were quantified, 400 less compared to study 1. The therapeutic effect from gene therapy was compared to WT values within the same study. Scatter plots of averaged protein intensity of three biological replicates in each group demonstrated a higher correlation between WT and LV-IGFIIco.GAAco treated mice in comparison to WT and LV-GAAco treated mice (Figure 3A).

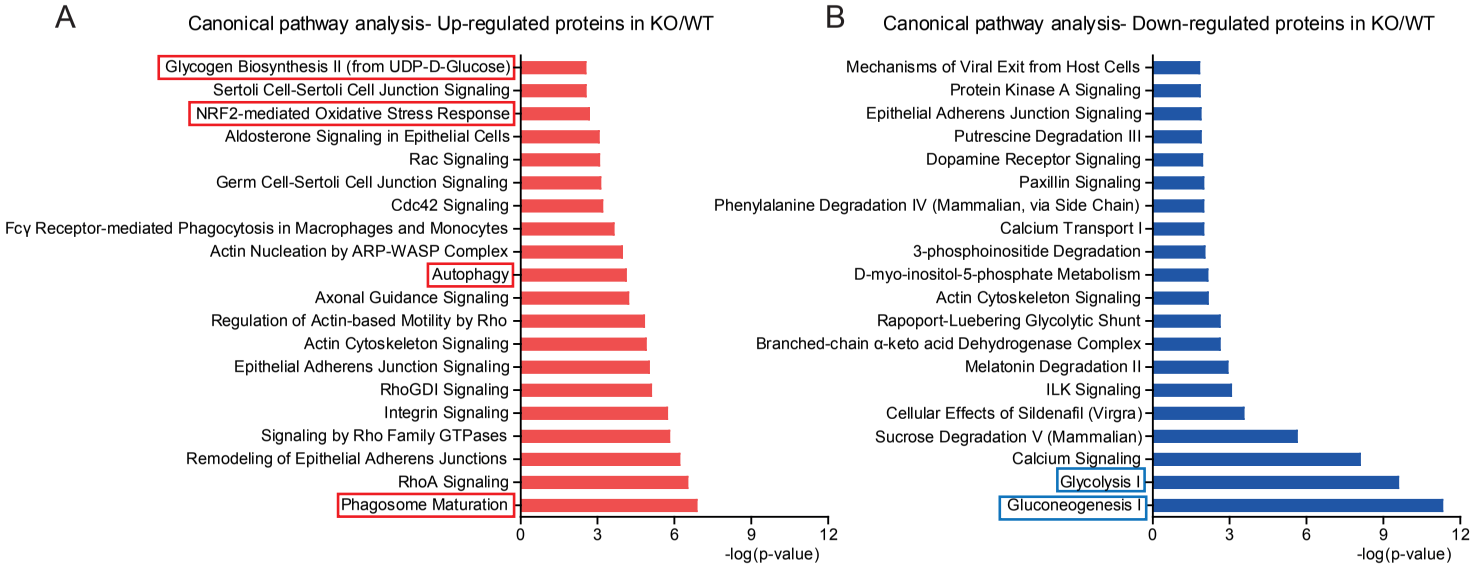

Figure 2. Canonical pathway analysis of proteins affected in KO mice. Bar graphs displaying the top 10 canonical pathways using IPA with up-regulated (A) and down-regulated (B) proteins in samples from KO comparison to WT mice.

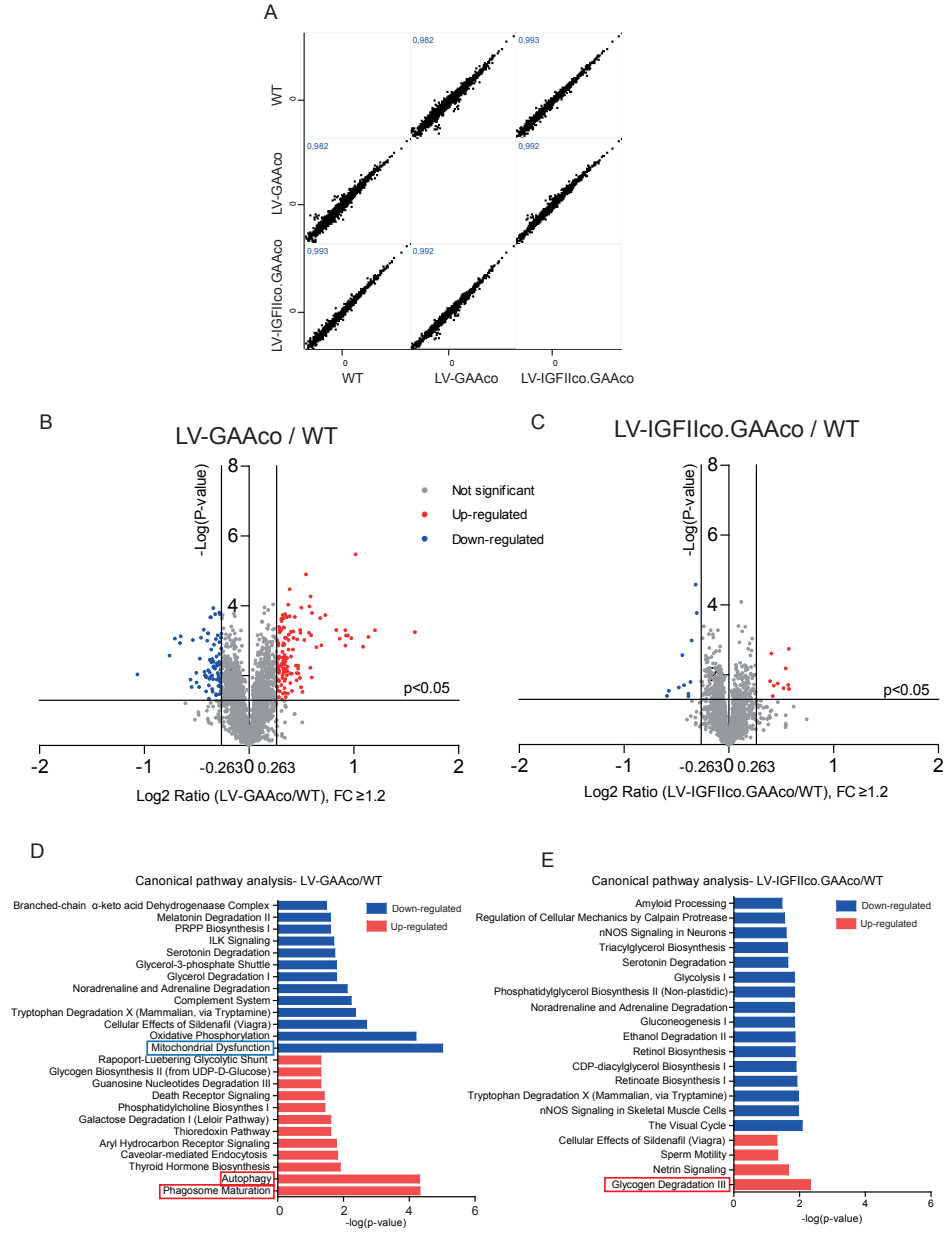

Figure 3. Expression differences in Study 2. (A) Scatter plots of intensities of identified proteins of the three groups indicated. Values from three biological replicates per group were averaged. The Pearson correlation coefficient is displayed. (B,C) Volcano plots showing differentially expressed proteins in LV-GAAco-treated against WT mice (B) and LV-IGFIIco.GAAco-treated against WT mice (C). (D,E) Bar graphs displaying all canonical pathways from differentially expressed proteins in LV-GAAco-treated against WT mice (D) and in LV-IGFIIco.GAAco-treated against WT mice. FC, fold change.

Compared to WT controls, 239 proteins were still differentially expressed (fold change (FC) ≥ 1.2; FDR=0.05) after LV-GAAco gene therapy, among which 135 were up-regulated and 104 were down-regulated (Figure 3B, Table S2). LV-IGFIIco.GAAco, on the other hand, was able to induce a profound correction of protein expression, with only 10 up- and 11 down- regulated proteins relative to WT levels (Figure 3C, Table S3). This dramatic reduction in the number of differentially expressed proteins indicated an almost normalized proteomic status in muscle from LV-IGFIIco.GAAco-treated mice.

Table 4. Sample information and number of proteins identified in Study 2.

Study	Group ID	Treatment	MOI	Cell number	Irradiation (Gy)	Sample ID	No. of Proteins Identified
2	WT	Untreated WT	*NA*	*NA*	*NA*	WT 1	2234
						WT 2	2232
						WT 3	2240
	LV-GAAco	LV-GAAco transplanted	7	1×10^6	9	LV-GAAco 1	2242
						LV-GAAco 2	2242
						LV-GAAco 3	2240
	LV-IGFIIco. GAAco	LV-IGFIIco.GAAco transplanted	7	1×10^6	9	LV-IGFIIco.GAAco 1	2241
						LV-IGFIIco.GAAco 2	2238
						LV-IGFIIco.GAAco 3	2239

MOI indicates multiplicity of infection; Gy, gray; KO, *Gaa*$^{-/-}$ knockout; WT, wildtype; and *NA*, not applicable.

GO terms shown in Tables 5-6 and pathway analysis shown in Figure 3D of differentially expressed proteins in LV-GAAco-treated samples showed similar hits compared to KO samples. However, the number of proteins involved in the same GO or pathways were significantly decreased, indicating that LV-GAAco can partially reverse pathology at the proteome level. Proteins involved in autophagy and mitochondrial dysfunction remained not fully corrected. GO terms shown in Tables 7-8 were analyzed and pathway analysis shown in Figure 3E was performed on the 21 differentially expressed proteins in LV-IGFIIco.GAAco treated samples. Essentially, this yielded inconclusive results as the number of proteins involved in each term or pathway was not more than two, and P values indicated insignificance. This result further confirmed correction of pathology in Pompe disease following gene therapy with LV-IGFIIco.GAAco.

Taken together, we demonstrated that LV-GAAco was able to induce a partial correction, whereas LV-IGFIIco.GAAco almost completely corrected the aberrant proteomics

Table 5. Gene ontology slim term enrichment analysis in up-regulated proteins in LV-GAAco treated mice compared to WT.

GO terms	GO ID	Functional category	Count in genome	Count in samples	Expected count	Fold enrichment	P value
Molecular Function	GO:0004872	receptor activity	2115	1	13.83	< 0.2	7.94E-06
	GO:0005515	protein binding	2863	33	18.73	1.76	7.81E-04
	GO:0008092	cytoskeletal protein binding	263	7	1.72	4.07	1.84E-03
	GO:0003824	catalytic activity	5143	48	33.64	1.43	4.25E-03
	GO:0005200	structural constituent of cytoskeleton	573	10	3.75	2.67	4.66E-03
	GO:0030234	enzyme regulator activity	590	10	3.86	2.59	5.69E-03
	GO:0019212	phosphatase inhibitor activity	25	2	0.16	12.23	1.19E-02
	GO:0016491	oxidoreductase activity	672	10	4.40	2.28	1.34E-02
	GO:0005198	structural molecule activity	924	12	6.04	1.99	1.87E-02
	GO:0003677	DNA binding	1631	18	10.67	1.69	2.05E-02
Biological Process	GO:0006996	organelle organization	767	24	5.02	4.78	2.39E-10
	GO:0016043	cellular component organization	1627	34	10.64	3.20	1.20E-09
	GO:0006325	chromatin organization	279	14	1.82	7.67	5.85E-09
	GO:0006936	muscle contraction	151	8	0.99	8.10	8.07E-06
	GO:0007010	cytoskeleton organization	154	7	1.01	6.95	7.82E-05
	GO:0008152	metabolic process	6955	64	45.49	1.41	8.55E-04
	GO:0006629	lipid metabolic process	595	11	3.89	2.83	1.96E-03
	GO:0006098	pentose-phosphate shunt	11	2	0.07	27.80	2.45E-03
	GO:0032989	cellular component morphogenesis	529	10	3.46	2.89	2.67E-03
	GO:0050789	regulation of biological process	2647	7	17.31	0.40	2.93E-03
Cellular Component	GO:0005856	cytoskeleton	622	11	4.07	2.70	2.75E-03
	GO:0043005	neuron projection	46	3	0.30	9.97	3.57E-03
	GO:0016021	integral to membrane	1684	3	11.01	0.27	3.82E-03
	GO:0030054	cell junction	82	3	0.54	5.59	1.71E-02
	GO:0005773	vacuole	92	3	0.60	4.99	2.30E-02
	GO:0031201	SNARE complex	39	2	0.26	7.84	2.74E-02
	GO:0030425	dendrite	5	1	0.03	30.58	3.22E-02
	GO:0005578	proteinaceous extracellular matrix	46	2	0.30	6.65	3.70E-02
	GO:0042995	cell projection	111	3	0.73	4.13	3.70E-02
	GO:0016020	membrane	2787	11	18.23	0.60	3.95E-02

Table 6. Gene ontology slim term enrichment analysis in down-regulated proteins in LV-GAAco treated mice compared to WT.

GO terms	GO ID	Functional category	Count in genome	Count in samples	Expected count	Fold enrichment	P value
Molecular Function	GO:0016491	oxidoreductase activity	672	15	3.07	4.88	4.43E-07
	GO:0003824	catalytic activity	5143	45	23.50	1.91	2.10E-06
	GO:0016829	lyase activity	212	5	0.97	5.16	3.00E-03
	GO:0005200	structural constituent of cytoskeleton	573	8	2.62	3.06	4.88E-03
	GO:0019239	deaminase activity	29	2	0.13	15.09	7.98E-03
	GO:0004872	receptor activity	2115	3	9.66	0.31	1.03E-02
	GO:0004871	signal transducer activity	1360	1	6.21	< 0.2	1.25E-02
	GO:0003700	sequence-specific DNA binding transcription factor activity	1352	1	6.18	< 0.2	1.29E-02
	GO:0003677	DNA binding	1631	2	7.45	0.27	1.79E-02
	GO:0016787	hydrolase activity	2160	17	9.87	1.72	1.85E-02
Biological Process	GO:0006091	generation of precursor metabolites and energy	238	10	1.09	9.20	1.66E-07
	GO:0006119	oxidative phosphorylation	51	5	0.23	21.46	4.31E-06
	GO:0022904	respiratory electron transport chain	165	7	0.75	9.28	1.21E-05
	GO:0006936	muscle contraction	151	6	0.69	8.70	7.41E-05
	GO:0006206	pyrimidine nucleobase metabolic process	36	3	0.16	18.24	6.39E-04
	GO:0008152	metabolic process	6955	47	31.78	1.48	1.12E-03
	GO:0006520	cellular amino acid metabolic process	253	6	1.16	5.19	1.13E-03
	GO:0007067	mitosis	355	7	1.62	4.32	1.27E-03
	GO:0000910	cytokinesis	111	4	0.51	7.89	1.76E-03
	GO:0016070	RNA metabolic process	2072	2	9.47	0.21	3.16E-03
Cellular Component	GO:0015629	actin cytoskeleton	234	6	1.07	5.61	7.57E-04
	GO:0042611	MHC protein complex	12	2	0.05	36.47	1.44E-03
	GO:0005737	cytoplasm	2134	19	9.75	1.95	3.52E-03
	GO:0005622	intracellular	4104	30	18.75	1.60	4.54E-03
Cellular Component	GO:0005783	endoplasmic reticulum	157	4	0.72	5.58	6.02E-03
	GO:0044464	cell part	4186	30	19.13	1.57	6.08E-03
	GO:0005856	cytoskeleton	622	8	2.84	2.81	7.85E-03
	GO:0005635	nuclear envelope	71	2	0.32	6.16	4.23E-02
	GO:0043226	organelle	2770	19	12.66	1.50	4.53E-02

Table 7. Gene ontology slim term enrichment analysis in up-regulated proteins in LV-IGFIIco.GAAco treated mice compared to WT.

GO terms	GO ID	Functional category	Count in genome	Count in samples	Expected count	Fold enrichment	P value
Molecular Function	GO:0015926	glucosidase activity	11	1	0.00	> 100	4.92E-03
	GO:0005253	anion channel activity	51	1	0.02	43.77	2.26E-02
	GO:0004553	hydrolase activity, hydrolyzing O-glycosyl compounds	54	1	0.02	41.34	2.39E-02
Biological Process	GO:0006936	muscle contraction	151	2	0.07	29.57	1.99E-03
	GO:0000910	cytokinesis	111	1	0.05	20.11	4.86E-02
	GO:0007067	mitosis	355	2	0.16	12.58	1.05E-02
	GO:0006928	cellular component movement	403	2	0.18	11.08	1.33E-02
Cellular Component	GO:0030054	cell junction	82	1	0.04	27.22	3.61E-02

Table 8. Gene ontology slim term enrichment analysis in down-regulated proteins in LV-IGFIIco.GAAco treated mice compared to WT.

GO terms	GO ID	Functional category	Count in genome	Count in samples	Expected count	Fold enrichment	P value
Molecular Function	GO:0019203	hydrolase activity, acting on ester bonds	622	3	0.31	9.79	3.02E-03
	GO:0016788	carbohydrate phosphatase activity	13	1	0.01	> 100	6.39E-03
	GO:0019212	phosphatase inhibitor activity	25	1	0.01	81.17	1.23E-02
	GO:0003743	translation initiation factor activity	57	1	0.03	35.60	2.77E-02
	GO:0045182	translation regulator activity	85	1	0.04	23.87	4.11E-02
	GO:0008234	cysteine-type peptidase activity	100	1	0.05	20.29	4.82E-02
Biological Process	GO:0006094	gluconeogenesis	22	1	0.01	92.24	1.08E-02
	GO:0031497	chromatin assembly	26	1	0.01	78.05	1.27E-02
	GO:0006096	glycolysis	37	1	0.02	54.85	1.81E-02
	GO:0043066	negative regulation of apoptotic process	83	1	0.04	24.45	4.01E-02
Cellular Component	GO:0032993	protein-DNA complex	37	1	0.02	54.85	1.81E-02

profile induced by GAA deficiency. This observation correlated with the degrees of glycogen reduction induced by two vectors that we observed previously (Chapter 3).

Correction of novel biomarkers by ex vivo lentiviral gene therapy

In the above analysis, the fold change to define differentially expressed proteins was set at 1.2. We then made a more stringent cutoff at a fold change of 1.5 in search of

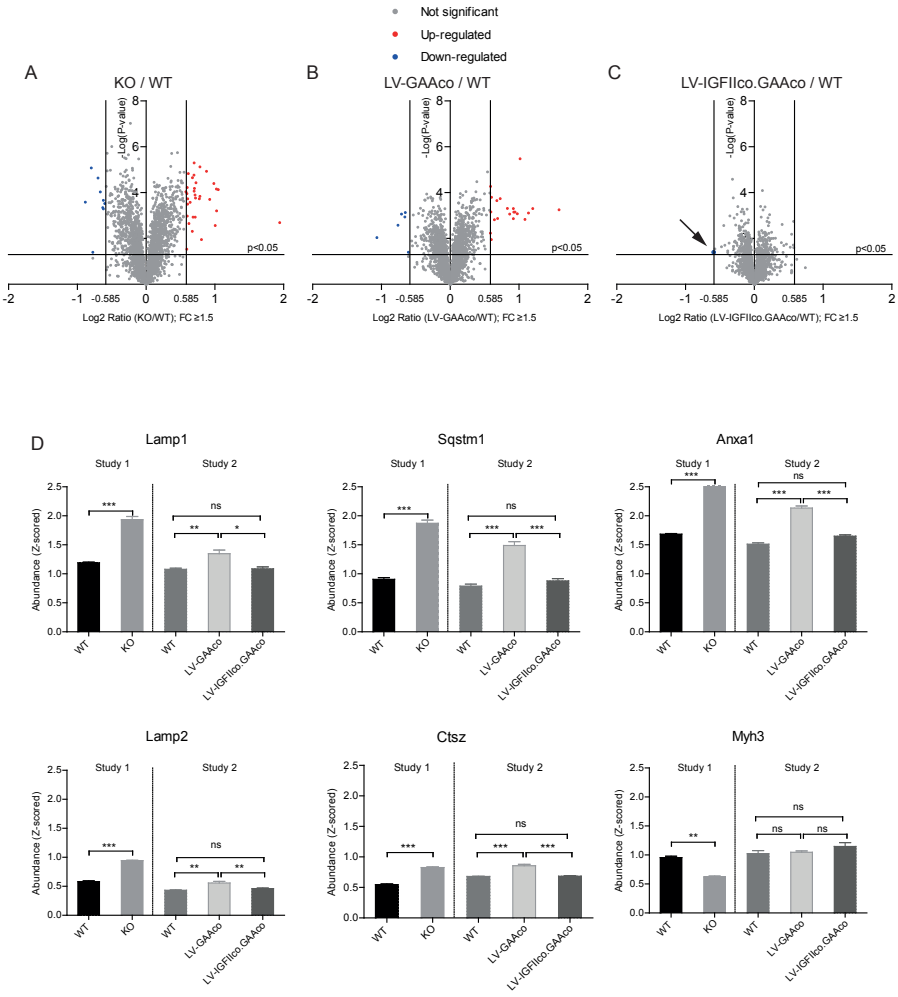

Figure 4. Efficacy of *ex vivo* lentiviral gene therapy with a fold change ≥ 1.5. (A-C) Volcano plots showing differentially expressed proteins in KO against WT mice (A), in LV-GAAco-treated against WT mice (B) and in LV-IGFIIco.GAAco-treated against LV-GFP-treated mice (C). Fold change (FC) is set at 1.5. Arrow points to the only differentially regulated protein in (C). (D) Protein abundance of six selected markers. Data are presented as means ± SEM; n=3. ns, not significant; **P*≤ 0.05, ***P*≤ 0.01, ****P*≤ 0.001.

more robust disease markers. Compared to WT samples, 32 proteins were up-regulated in KO samples, while 21 proteins were still up-regulated in LV-GAAco-treated samples (Figures 4A-B). The count of down-regulated proteins was 9 and 6 in those two groups, respectively. Strikingly, only one protein (Gpam, arrow) was differentially expressed after LV-IGFIIco.GAAco gene therapy (Figure 4C). Differentially expressed proteins from the above comparisons were marked with an asterisk in Tables S1, 2 and 3 respectively.

To investigate whether gene therapy restored levels of differentially expressed proteins, six biomarkers that were differentially expressed in KO against WT samples (FC≥1.5) were chosen based on their presence in two studies and their biological function. Abundance values (after normalized through z-scoring) were compared (Figure 4D). Note that data of WT from both studies were included. In Study 1, markers for lysosomal storage disease (Lamp1, Lamp2), autophagy (Sqstm1, Ctsz) and immunity (Anxa1) were overexpressed in KO mice. As the absolute expression levels varied between two studies, the abundance in gene therapy-treated samples was compared to WT levels from Study 2. While the abundance of the indicated proteins remained significantly higher after LV-GAAco gene therapy, they were all completely reversed to wildtype levels in LV-IGFIIco.GAAco-treated samples. The muscle contraction marker (Myoh3), on the other hand, was down-regulated in KO mice and gene therapy with both vectors managed to normalize it to WT levels.

In conclusion, lentiviral gene therapy with LV-IGFIIco.GAAco not only cleared glycogen accumulation (Chapter 3), but also achieved to normalize WT levels of the proteome in skeletal muscle. The results also suggest that secondary pathological events can be reversed once the primary abnormality is sufficiently corrected. These data, complemented with the previous normalization of glycogen levels and morphological correction, provide additional evidence on the safety and efficacy of lentiviral gene therapy, further advocating the clinical development of this treatment for Pompe disease.

ACKNOWLEDGEMENTS

We thank Dr.Rizopoulos Dimitris for valuable advice on statistic analysis. This work was supported by The Netherlands Organization for Health Research ZonMw (project number: 40-40300-98-07010) and the Erasmus University Medical Center. Q.L. was additionally supported by the China Scholarship Council (File No. 201206240040).

REFERENCES

1. Hirschhorn R, Reuser AJJ. Glycogen storage disease type II: acid α-glucosidase (acid maltase) deficiency. In: Scriver C, Beaudet, AL, Sly, WS and Valle, D ed. The Metabolic and Molecular Basis for Inherited Disease. New York: McGraw-Hill; 2001:3389–3420.
2. van der Ploeg AT, Reuser AJ. Pompe's disease. *Lancet*. 2008;372(9646):1342-1353.
3. van den Hout HM, Hop W, van Diggelen OP, et al. The natural course of infantile Pompe's disease: 20 original cases compared with 133 cases from the literature. *Pediatrics*. 2003;112(2):332-340.
4. Kishnani PS, Hwu WL, Mandel H, Nicolino M, Yong F, Corzo D. A retrospective, multinational, multicenter study on the natural history of infantile-onset Pompe disease. *J Pediatr*. 2006;148(5):671-676.
5. Hagemans ML, Winkel LP, Van Doorn PA, et al. Clinical manifestation and natural course of late-onset Pompe's disease in 54 Dutch patients. *Brain*. 2005;128(Pt 3):671-677.
6. Winkel LP, Hagemans ML, van Doorn PA, et al. The natural course of non-classic Pompe's disease; a review of 225 published cases. *J Neurol*. 2005;252(8):875-884.
7. Thurberg BL, Lynch Maloney C, Vaccaro C, et al. Characterization of pre- and post-treatment pathology after enzyme replacement therapy for Pompe disease. *Lab Invest*. 2006;86(12):1208-1220.
8. Raben N, Wong A, Ralston E, Myerowitz R. Autophagy and mitochondria in Pompe disease: nothing is so new as what has long been forgotten. *Am J Med Genet C Semin Med Genet*. 2012;160C(1):13-21.
9. Lim JA, Li L, Kakhlon O, Myerowitz R, Raben N. Defects in calcium homeostasis and mitochondria can be reversed in Pompe disease. *Autophagy*. 2015;11(2):385-402.
10. Lim JA, Kakhlon O, Li L, Myerowitz R, Raben N. Pompe disease: Shared and unshared features of lysosomal storage disorders. *Rare Dis*. 2015;3(1):e1068978.
11. Cox TM, Cachon-Gonzalez MB. The cellular pathology of lysosomal diseases. *J Pathol*. 2012;226(2):241-254.
12. Platt FM, Boland B, van der Spoel AC. The cell biology of disease: lysosomal storage disorders: the cellular impact of lysosomal dysfunction. *J Cell Biol*. 2012;199(5):723-734.
13. Palermo AT, Palmer RE, So KS, et al. Transcriptional response to GAA deficiency (Pompe disease) in infantile-onset patients. *Mol Genet Metab*. 2012;106(3):287-300.
14. Kishnani PS, Nicolino M, Voit T, et al. Chinese hamster ovary cell-derived recombinant human acid alpha-glucosidase in infantile-onset Pompe disease. *J Pediatr*. 2006;149(1):89-97.
15. Kishnani PS, Corzo D, Nicolino M, et al. Recombinant human acid [alpha]-glucosidase: major clinical benefits in infantile-onset Pompe disease. *Neurology*. 2007;68(2):99-109.
16. van der Ploeg AT, Clemens PR, Corzo D, et al. A randomized study of alglucosidase alfa in late-onset Pompe's disease. *N Engl J Med*. 2010;362(15):1396-1406.
17. Zhao KW, Neufeld EF. Purification and characterization of recombinant human alpha-N-acetylglucosaminidase secreted by Chinese hamster ovary cells. *Protein Expr Purif*. 2000;19(1):202-211.

18. Togawa T, Takada M, Aizawa Y, Tsukimura T, Chiba Y, Sakuraba H. Comparative study on mannose 6-phosphate residue contents of recombinant lysosomal enzymes. *Mol Genet Metab*. 2014;111(3):369-373.
19. Banugaria SG, Prater SN, Ng YK, et al. The impact of antibodies on clinical outcomes in diseases treated with therapeutic protein: lessons learned from infantile Pompe disease. *Genet Med*. 2011;13(8):729-736.
20. van Gelder CM, Hoogeveen-Westerveld M, Kroos MA, Plug I, van der Ploeg AT, Reuser AJ. Enzyme therapy and immune response in relation to CRIM status: the Dutch experience in classic infantile Pompe disease. *J Inherit Metab Dis*. 2015;38(2):305-314.
21. Falk DJ, Mah CS, Soustek MS, et al. Intrapleural administration of AAV9 improves neural and cardiorespiratory function in Pompe disease. *Mol Ther*. 2013;21(9):1661-1667.
22. Maga JA, Zhou J, Kambampati R, et al. Glycosylation-independent lysosomal targeting of acid alpha-glucosidase enhances muscle glycogen clearance in pompe mice. *J Biol Chem*. 2013;288(3):1428-1438.
23. van Til NP, Stok M, Aerts Kaya FS, et al. Lentiviral gene therapy of murine hematopoietic stem cells ameliorates the Pompe disease phenotype. *Blood*. 2010;115(26):5329-5337.
24. Bohm G, Prefot P, Jung S, et al. Low-pH Solid-Phase Amino Labeling of Complex Peptide Digests with TMTs Improves Peptide Identification Rates for Multiplexed Global Phosphopeptide Analysis. *J Proteome Res*. 2015;14(6):2500-2510.
25. Tyanova S, Temu T, Sinitcyn P, et al. The Perseus computational platform for comprehensive analysis of (prote)omics data. *Nat Methods*. 2016;13(9):731-740.
26. Thomas PD, Campbell MJ, Kejariwal A, et al. PANTHER: a library of protein families and subfamilies indexed by function. *Genome Res*. 2003;13(9):2129-2141.
27. Raben N, Roberts A, Plotz PH. Role of autophagy in the pathogenesis of Pompe disease. *Acta Myol*. 2007;26(1):45-48.
28. Taylor KM, Meyers E, Phipps M, et al. Dysregulation of multiple facets of glycogen metabolism in a murine model of Pompe disease. *PLoS One*. 2013;8(2):e56181.

Table S1. Identification of differentially expressed proteins in *Gaa*$^{-/-}$ knockout mice compared to WT mice. (Entries with * refers to proteins with fold change ≥ 1.5)

Assession No.	Gene name	Peptides	Log_2(Fold change)	Description
			Up-regulated	
P02798*	Mt2*	2	1,943*	Metallothionein-2
Q64337*	Sqstm1*	10	1,049*	Sequestosome-1
P54116*	Stom*	7	1,025*	Erythrocyte band 7 integral membrane protein
P46425*	Gstp2*	5	1,023*	Glutathione S-transferase P 2
Q52KR3*	Prune2*	2	1,006*	Protein prune homolog 2
Q9D154*	Serpinb1a*	19	0,985*	Leukocyte elastase inhibitor A
P13595*	Ncam1*	13	0,927*	Neural cell adhesion molecule 1
Q60854*	Serpinb6*	20	0,878*	Serpin B6
Q91VW3*	Sh3bgrl3*	5	0,805*	SH3 domain-binding glutamic acid-rich-like protein 3
O35640*	Anxa8*	6	0,784*	Annexin A8
P13745*	Gsta1*	5	0,783*	Glutathione S-transferase A1
Q62009*	Postn*	23	0,773*	Periostin
Q9QYR6*	Map1a*	13	0,725*	Microtubule-associated protein 1A
A2AWA9*	Rabgap1*	2	0,719*	Rab GTPase-activating protein 1
Q8K354*	Cbr3*	2	0,714*	Carbonyl reductase [NADPH] 3
P97429*	Anxa4*	14	0,712*	Annexin A4
P17047*	Lamp2*	4	0,702*	Lysosome-associated membrane glycoprotein 2
P19157*	Gstp1*	7	0,700*	Glutathione S-transferase P 1
P11438*	Lamp1*	2	0,699*	Lysosome-associated membrane glycoprotein 1
Q8VCB3*	Gys2*	8	0,696*	Glycogen [starch] synthase, liver
E9PYB0*	Ahnak2*	10	0,684*	Protein Ahnak2 (Fragment)
P10126*	Eef1a1*	15	0,674*	Elongation factor 1-alpha 1
O70456*	Sfn*	4	0,671*	14-3-3 protein sigma
Q9DCN2*	Cyb5r3*	10	0,640*	NADH-cytochrome b5 reductase 3
P35385*	Hspb7*	4	0,623*	Heat shock protein beta-7
P10107*	Anxa1*	18	0,615*	Annexin A1
Q9DBS1*	Tmem43*	5	0,606*	Transmembrane protein 43
B1AVZ0*	Uprt*	3	0,603*	Uracil phosphoribosyltransferase homolog
Q9WUU7*	Ctsz*	4	0,598*	Cathepsin Z
Q9CQI6*	Cotl1*	3	0,598*	Coactosin-like protein
P97352*	S100a13*	5	0,595*	Protein S100-A13
Q8K0G5*	Eipr1*	2	0,593*	Protein TSSC1
Q9R1Q7	Plp2	2	0,578	Proteolipid protein 2
P09470	Ace	9	0,552	Angiotensin-converting enzyme
Q9EP75	Cyp4f14	4	0,549	Leukotriene-B4 omega-hydroxylase 3

Table S1. Identification of differentially expressed proteins in *Gaa*$^{-/-}$ knockout mice compared to WT mice. (Entries with * refers to proteins with fold change ≥ 1.5) (*continued*)

Assession No.	Gene name	Peptides	Log_2(Fold change)	Description
Q922F4	Tubb6	17	0,546	Tubulin beta-6 chain
P0C605	Prkg1	6	0,543	cGMP-dependent protein kinase 1
P23927	Cryab	11	0,541	Alpha-crystallin B chain
O08739	Ampd3	5	0,536	AMP deaminase 3
P14602	Hspb1	13	0,532	Heat shock protein beta-1
E9Q616	Ahnak	160	0,531	Protein Ahnak
P48036	Anxa5	16	0,525	Annexin A5
Q6WVG3	Kctd12	4	0,523	BTB/POZ domain-containing protein KCTD12
P48722	Hspa4l	6	0,520	Heat shock 70 kDa protein 4L
Q8CI59	Steap3	4	0,516	Metalloreductase STEAP3
E9Q3M9	2010300C02Rik	2	0,516	Protein 2010300C02Rik
Q9D1L9	Lamtor5	2	0,515	Ragulator complex protein LAMTOR5
Q9R0P3	Esd	11	0,513	S-formylglutathione hydrolase
Q64314	Cd34	5	0,512	Hematopoietic progenitor cell antigen CD34
Q8K2T4	Uqcc3	2	0,512	Ubiquinol-cytochrome-c reductase complex assembly factor 3
Q9EQK5	Mvp	25	0,494	Major vault protein
Q9CQ22	Lamtor1	4	0,493	Ragulator complex protein LAMTOR1
Q8C854	Myef2	2	0,493	Myelin expression factor 2
Q9CQE5	Rgs10	2	0,492	Regulator of G-protein signaling 10
P56565	S100a1	2	0,492	Protein S100-A1
P01872	Ighm	7	0,490	Ig mu chain C region
Q6P3D0	Nudt16	2	0,489	U8 snoRNA-decapping enzyme
Q3ULW8	Parp3	4	0,488	Poly [ADP-ribose] polymerase
Q8VEK0	Tmem30a	4	0,480	Cell cycle control protein 50A
Q5EBG6	Hspb6	5	0,472	Heat shock protein beta-6
Q64669	Nqo1	10	0,466	NAD(P)H dehydrogenase [quinone] 1
P16406	Enpep	6	0,464	Glutamyl aminopeptidase
Q80UG5	Sept9	3	0,463	Septin-9
Q9EPM5	Sync	12	0,460	Syncoilin
P56394	Cox17	4	0,459	Cytochrome c oxidase copper chaperone
Q921H8	Acaa1a	9	0,458	3-ketoacyl-CoA thiolase A, peroxisomal
Q62465	Vat1	6	0,456	Synaptic vesicle membrane protein VAT-1 homolog
Q68FL4	Ahcyl2	2	0,456	Putative adenosylhomocysteinase 3
O09161	Casq2	7	0,453	Calsequestrin-2
Q61599	Arhgdib	4	0,453	Rho GDP-dissociation inhibitor 2
P33434	Mmp2	2	0,450	72 kDa type IV collagenase

Table S1. Identification of differentially expressed proteins in *Gaa*$^{-/-}$ knockout mice compared to WT mice. (Entries with * refers to proteins with fold change ≥ 1.5) (*continued*)

Assession No.	Gene name	Peptides	Log_2(Fold change)	Description
P10605	Ctsb	8	0,448	Cathepsin B
P10833	Rras	3	0,448	Ras-related protein R-Ras
Q6P5H2	Nes	19	0,441	Nestin
P17710	Hk1	14	0,438	Hexokinase-1
Q9D711	Pir	3	0,436	Pirin
P61161	Actr2	11	0,435	Actin-related protein 2
Q61578	Fdxr	4	0,435	NADPH:adrenodoxin oxidoreductase, mitochondrial
P31428	Dpep1	3	0,433	Dipeptidase 1
Q61207	Psap	16	0,432	Prosaposin
Q9WTK5	Nfkb2	2	0,425	Nuclear factor NF-kappa-B p100 subunit
Q8BMD8	Slc25a24	6	0,425	Calcium-binding mitochondrial carrier protein SCaMC-1
P29391	Ftl1	5	0,425	Ferritin light chain 1
Q8CGE8	Ifi205a	3	0,422	Interferon-activable protein 205-A
P51655	Gpc4	3	0,421	Glypican-4
P0C5K1	Sbk2	3	0,420	Serine/threonine-protein kinase SBK2
Q91VI7	Rnh1	20	0,419	Ribonuclease inhibitor
Q9D1I2	Card19	4	0,419	Caspase recruitment domain-containing protein 19
O08804	Serpinb6b	2	0,419	NK13
Q9R0X4	Acot9	13	0,414	Acyl-coenzyme A thioesterase 9, mitochondrial
Q6PHZ2	Camk2d	15	0,411	Calcium/calmodulin-dependent protein kinase type II subunit delta
Q91YP2	Nln	2	0,410	Neurolysin, mitochondrial
O35604	Npc1	2	0,407	Niemann-Pick C1 protein
P35762	Cd81	2	0,406	CD81 antigen
P14069	S100a6	2	0,403	Protein S100-A6
Q8VHX6	Flnc	111	0,403	Filamin-C
O70373	Xirp1	39	0,402	Xin actin-binding repeat-containing protein 1
Q99LM3	Smtnl1	7	0,402	Smoothelin-like protein 1
Q8CIN4	Pak2	4	0,400	Serine/threonine-protein kinase PAK 2
Q91V61	Sfxn3	5	0,400	Sideroflexin-3
Q9JL62	Gltp	3	0,397	Glycolipid transfer protein
Q9D379	Ephx1	8	0,397	Epoxide hydrolase 1
Q8BMK4	Ckap4	12	0,397	Cytoskeleton-associated protein 4
P51637	Cav3	2	0,396	Caveolin-3

Table S1. Identification of differentially expressed proteins in *Gaa*$^{-/-}$ knockout mice compared to WT mice. (Entries with * refers to proteins with fold change ≥ 1.5) (*continued*)

Assession No.	Gene name	Peptides	Log_2(Fold change)	Description
Q8BGK2	Adprhl1	7	0,394	[Protein ADP-ribosylarginine] hydrolase-like protein 1
P62317	Snrpd2	5	0,393	Small nuclear ribonucleoprotein Sm D2
O70439	Stx7	3	0,391	Syntaxin-7
Q9JM14	Nt5c	3	0,391	5(3)-deoxyribonucleotidase, cytosolic type
P28798	Grn	6	0,386	Granulins
O08917	Flot1	8	0,384	Flotillin-1
P07091	S100a4	3	0,384	Protein S100-A4
P51863	Atp6v0d1	4	0,383	V-type proton ATPase subunit d 1
P24270	Cat	14	0,382	Catalase
P21844	Cma1	2	0,380	Chymase
Q91XV3	Basp1	2	0,380	Brain acid soluble protein 1
Q9D666	Sun1	4	0,377	SUN domain-containing protein 1
Q3TLH4	Prrc2c	2	0,375	Protein PRRC2C
P70290	Mpp1	5	0,374	55 kDa erythrocyte membrane protein
P55096	Abcd3	4	0,374	ATP-binding cassette sub-family D member 3
Q66K08	Cilp	14	0,372	Cartilage intermediate layer protein 1
Q9D783	Klhl40	17	0,372	Kelch-like protein 40
Q91VC9	Ghitm	3	0,371	Growth hormone-inducible transmembrane protein
P62962	Pfn1	8	0,367	Profilin-1
P40336	Vps26a	4	0,366	Vacuolar protein sorting-associated protein 26A
Q8C3X2	Ccdc90b	2	0,366	Coiled-coil domain-containing protein 90B, mitochondrial
P27546	Map4	25	0,365	Microtubule-associated protein 4
Q9CVB6	Arpc2	11	0,364	Actin-related protein 2/3 complex subunit 2
P99024	Tubb5	26	0,364	Tubulin beta-5 chain
P11352	Gpx1	6	0,363	Glutathione peroxidase 1
Q9JHS3	Lamtor2	2	0,363	Ragulator complex protein LAMTOR2
Q60766	Irgm1	5	0,363	Immunity-related GTPase family M protein 1
P10639	Txn	4	0,362	Thioredoxin
Q9ESE1	Lrba	5	0,361	Lipopolysaccharide-responsive and beige-like anchor protein
Q9QYB1	Clic4	11	0,360	Chloride intracellular channel protein 4
P48678	Lmna	43	0,359	Prelamin-A/C
Q6PDL0	Dync1li2	6	0,359	Cytoplasmic dynein 1 light intermediate chain 2
P61028	Rab8b	7	0,358	Ras-related protein Rab-8B
P26645	Marcks	10	0,357	Myristoylated alanine-rich C-kinase substrate

Table S1. Identification of differentially expressed proteins in *Gaa*$^{-/-}$ knockout mice compared to WT mice. (Entries with * refers to proteins with fold change ≥ 1.5) (*continued*)

Assession No.	Gene name	Peptides	Log_2(Fold change)	Description
P16110	Lgals3	2	0,357	Galectin-3
Q08857	Cd36	8	0,355	Platelet glycoprotein 4
Q7TMB8	Cyfip1	8	0,353	Cytoplasmic FMR1-interacting protein 1
Q3UHZ5	Lmod2	6	0,352	Leiomodin-2
Q60634	Flot2	7	0,349	Flotillin-2
Q99KC8	Vwa5a	17	0,349	von Willebrand factor A domain-containing protein 5A
Q9DCD0	Pgd	17	0,347	6-phosphogluconate dehydrogenase, decarboxylating
P11276	Fn1	20	0,345	Fibronectin
P68369	Tuba1a	25	0,345	Tubulin alpha-1A chain
Q60605	Myl6	12	0,342	Myosin light polypeptide 6
Q8VEE1	Lmcd1	21	0,342	LIM and cysteine-rich domains protein 1
P18760	Cfl1	9	0,341	Cofilin-1
P97449	Anpep	12	0,340	Aminopeptidase N
P14094	Atp1b1	7	0,337	Sodium/potassium-transporting ATPase subunit beta-1
P18242	Ctsd	11	0,336	Cathepsin D
Q9Z1G4	Atp6v0a1	5	0,336	V-type proton ATPase 116 kDa subunit a isoform 1
P26041	Msn	36	0,330	Moesin
P01869	Ighg1	3	0,329	Ig gamma-1 chain C region, membrane-bound form
P46660	Ina	3	0,329	Alpha-internexin
O89053	Coro1a	3	0,328	Coronin-1A
Q9R062	Gyg1	8	0,327	Glycogenin-1
O55143	Atp2a2	37	0,326	Sarcoplasmic/endoplasmic reticulum calcium ATPase 2
P59999	Arpc4	4	0,325	Actin-related protein 2/3 complex subunit 4
Q9EQU5	Set	6	0,325	Protein SET
O70591	Pfdn2	3	0,323	Prefoldin subunit 2
Q3URD3	Slmap	6	0,323	Sarcolemmal membrane-associated protein
Q8BJ03	Cox15	2	0,322	Cytochrome c oxidase assembly protein COX15 homolog
Q9EPL9	Acox3	4	0,320	Peroxisomal acyl-coenzyme A oxidase 3
E9QA62	Lmod3	6	0,320	Protein Lmod3
E9PYF4	Lmo7	13	0,319	Protein Lmo7
P70452	Stx4	6	0,319	Syntaxin-4

Table S1. Identification of differentially expressed proteins in *Gaa*$^{-/-}$ knockout mice compared to WT mice. (Entries with * refers to proteins with fold change ≥ 1.5) (*continued*)

Assession No.	Gene name	Peptides	Log_2(Fold change)	Description
Q9WVE8	Pacsin2	8	0,318	Protein kinase C and casein kinase substrate in neurons protein 2
P39061	Col18a1	4	0,318	Collagen alpha-1(XVIII) chain
Q05816	Fabp5	5	0,318	Fatty acid-binding protein, epidermal
Q63844	Mapk3	7	0,317	Mitogen-activated protein kinase 3
P27659	Rpl3	11	0,314	60S ribosomal protein L3
Q07076	Anxa7	12	0,314	Annexin A7
Q9D6Y9	Gbe1	21	0,313	1,4-alpha-glucan-branching enzyme
Q9CQQ8	Lsm7	2	0,313	U6 snRNA-associated Sm-like protein LSm7
Q9CYR0	Ssbp1	3	0,313	Single-stranded DNA-binding protein, mitochondrial
O08585	Clta	2	0,312	Clathrin light chain A
O88447	Klc1	11	0,311	Kinesin light chain 1
Q9JM76	Arpc3	4	0,310	Actin-related protein 2/3 complex subunit 3
P24452	Capg	5	0,310	Macrophage-capping protein
P63024	Vamp3	3	0,308	Vesicle-associated membrane protein 3
O88569	Hnrnpa2b1	19	0,307	Heterogeneous nuclear ribonucleoproteins A2/B1
P16125	Ldhb	16	0,305	L-lactate dehydrogenase B chain
Q8K019	Bclaf1	3	0,304	Bcl-2-associated transcription factor 1
Q9WVA4	Tagln2	9	0,303	Transgelin-2
Q04447	Ckb	4	0,303	Creatine kinase B-type
P97927	Lama4	7	0,301	Laminin subunit alpha-4
Q9EQW7	Kif13a	2	0,299	Kinesin-like protein KIF13A
P03987	Ighg3	5	0,299	Ig gamma-3 chain C region
Q60598	Cttn	9	0,298	Src substrate cortactin
P97447	Fhl1	14	0,297	Four and a half LIM domains protein 1
P68433	Hist1h3a	6	0,297	Histone H3,1
Q6ZWQ9	Myl12a	9	0,297	MCG5400
P31001	Des	42	0,296	Desmin
O70252	Hmox2	4	0,296	Heme oxygenase 2
P29788	Vtn	5	0,295	Vitronectin
Q9Z1Z0	Uso1	19	0,295	General vesicular transport factor p115
Q3TW96	Uap1l1	9	0,293	UDP-N-acetylhexosamine pyrophosphorylase-like protein 1
P21107	Tpm3	31	0,293	Tropomyosin alpha-3 chain
Q9QYI5	Dnajb2	2	0,293	DnaJ homolog subfamily B member 2
P84084	Arf5	9	0,292	ADP-ribosylation factor 5

Table S1. Identification of differentially expressed proteins in *Gaa*$^{-/-}$ knockout mice compared to WT mice. (Entries with * refers to proteins with fold change ≥ 1.5) (*continued*)

Assession No.	Gene name	Peptides	Log_2(Fold change)	Description
Q8BVL3	Snx17	2	0,289	Sorting nexin-17
Q99MN1	Kars	12	0,289	Lysine--tRNA ligase
Q9Z2D6	Mecp2	7	0,288	Methyl-CpG-binding protein 2
Q9D883	U2af1	3	0,287	Splicing factor U2AF 35 kDa subunit
Q00493	Cpe	2	0,287	Carboxypeptidase E
O35075	Dscr3	2	0,287	Down syndrome critical region protein 3 homolog
P43275	Hist1h1a	2	0,286	Histone H1,1
Q9Z2Q5	Mrpl40	3	0,286	39S ribosomal protein L40, mitochondrial
P82349	Sgcb	5	0,286	Beta-sarcoglycan
Q9CWS0	Ddah1	10	0,285	N(G),N(G)-dimethylarginine dimethylaminohydrolase 1
Q6IRU2	Tpm4	18	0,283	Tropomyosin alpha-4 chain
A2AMM0	Murc	7	0,282	Muscle-related coiled-coil protein
P42208	Sept2	9	0,282	Septin-2
Q8VCH8	Ubxn4	4	0,282	UBX domain-containing protein 4
P26039	Tln1	73	0,281	Talin-1
Q3UW53	Fam129a	7	0,281	Protein Niban
Q9D5T0	Atad1	8	0,280	ATPase family AAA domain-containing protein 1
Q8K0E8	Fgb	11	0,280	Fibrinogen beta chain
P60229	Eif3e	10	0,280	Eukaryotic translation initiation factor 3 subunit E
P97493	Txn2	2	0,278	Thioredoxin, mitochondrial
P28656	Nap1l1	5	0,278	Nucleosome assembly protein 1-like 1
Q9ESD7	Dysf	65	0,276	Dysferlin
Q9CT10	Ranbp3	2	0,275	Ran-binding protein 3
P82348	Sgcg	4	0,275	Gamma-sarcoglycan
Q62048	Pea15	4	0,274	Astrocytic phosphoprotein PEA-15
P63260	Actg1	27	0,273	Actin, cytoplasmic 2
Q91WJ8	Fubp1	6	0,273	Far upstream element-binding protein 1
Q9DB15	Mrpl12	3	0,272	39S ribosomal protein L12, mitochondrial
P07901	Hsp90aa1	37	0,271	Heat shock protein HSP 90-alpha
P08207	S100a10	3	0,270	Protein S100-A10
Q62523	Zyx	4	0,270	Zyxin
Q9DBR7	Ppp1r12a	4	0,269	Protein phosphatase 1 regulatory subunit 12A
Q9WTR5	Cdh13	12	0,267	Cadherin-13
P51855	Gss	4	0,266	Glutathione synthetase
Q6PB93	Galnt2	2	0,266	Polypeptide N-acetylgalactosaminyltransferase 2

Table S1. Identification of differentially expressed proteins in *Gaa*$^{-/-}$ knockout mice compared to WT mice. (Entries with * refers to proteins with fold change ≥ 1.5) (*continued*)

Assession No.	Gene name	Peptides	Log_2(Fold change)	Description
Q99P72	Rtn4	22	0,266	Reticulon-4
O08529	Capn2	18	0,265	Calpain-2 catalytic subunit
Q80XB4	Nrap	62	0,264	Nebulin-related-anchoring protein
P14873	Map1b	9	0,263	Microtubule-associated protein 1B
Q8BLF1	Nceh1	4	0,263	Neutral cholesterol ester hydrolase 1
Down-regulated				
Q69ZS0*	Pdzrn3*	2	-0,883*	E3 ubiquitin-protein ligase PDZRN3
P50431*	Shmt1*	2	-0,796*	Serine hydroxymethyltransferase, cytosolic
A6ZI46*	Aldoart1*	20	-0,773*	Fructose-bisphosphate aldolase
Q3V1D3*	Ampd1*	25	-0,700*	AMP deaminase 1
Q8R1G2*	Cmbl*	4	-0,665*	Carboxymethylenebutenolidase homolog
Q8K003*	Tma7*	2	-0,630*	Translation machinery-associated protein 7
P70695*	Fbp2*	7	-0,621*	Fructose-1,6-bisphosphatase isozyme 2
P13541*	Myh3*	82	-0,621*	Myosin-3
Q8VCT4*	Ces1d*	12	-0,602*	Carboxylesterase 1D
Q91XD6	Vps36	2	-0,580	Vacuolar protein-sorting-associated protein 36
P12710	Fabp1	4	-0,574	Fatty acid-binding protein, liver
P70266	Pfkfb1	5	-0,566	6-phosphofructo-2-kinase/fructose-2,6-bisphosphatase 1
Q8CHS7	Dhrs7c	9	-0,565	Dehydrogenase/reductase SDR family member 7C
Q3TMP8	Tmem38a	4	-0,561	Trimeric intracellular cation channel type A
Q91Y97	Aldob	3	-0,560	Fructose-bisphosphate aldolase B
Q9DBB5	Eif4e3	2	-0,556	Eukaryotic translation initiation factor 4E type 3
P52760	Hrsp12	4	-0,548	Ribonuclease UK114
Q9D1F9	Slc37a4	4	-0,539	Protein Slc37a4
P70663	Sparcl1	2	-0,534	SPARC-like protein 1
Q921R8	Slc41a3	2	-0,524	Solute carrier family 41 member 3
Q8VCR8	Mylk2	19	-0,520	Myosin light chain kinase 2, skeletal/cardiac muscle
P15327	Bpgm	4	-0,516	Bisphosphoglycerate mutase
Q5XKE0	Mybpc2	70	-0,515	Myosin-binding protein C, fast-type
Q3U962	Col5a2	3	-0,515	Collagen alpha-2(V) chain
Q02357	Ank1	8	-0,514	Ankyrin-1
Q3TJD7	Pdlim7	7	-0,504	PDZ and LIM domain protein 7
Q9ER35	Fn3k	3	-0,504	Fructosamine-3-kinase
Q8C494	Prr33	9	-0,503	Proline-rich protein 33
P10711	Tcea1	2	-0,502	Transcription elongation factor A protein 1

Table S1. Identification of differentially expressed proteins in *Gaa*$^{-/-}$ knockout mice compared to WT mice. (Entries with * refers to proteins with fold change ≥ 1.5) (*continued*)

Assession No.	Gene name	Peptides	Log_2(Fold change)	Description
P70236	Map2k6	9	-0,499	Dual specificity mitogen-activated protein kinase kinase 6
B1AR69	Myh13	63	-0,495	Protein Myh13
P31254	Uba1y	10	-0,495	Ubiquitin-like modifier-activating enzyme 1 Y
P13707	Gpd1	21	-0,494	Glycerol-3-phosphate dehydrogenase [NAD(+)], cytoplasmic
Q60739	Bag1	4	-0,486	BAG family molecular chaperone regulator 1
B2RQC6	Cad	6	-0,484	CAD protein
P63248	Pkia	3	-0,483	cAMP-dependent protein kinase inhibitor alpha
Q8CAA7	Pgm2l1	3	-0,483	Glucose 1,6-bisphosphate synthase
Q8CI70	Lrrc20	6	-0,473	Leucine-rich repeat-containing protein 20
P62204	Calm1	6	-0,471	Calmodulin
P47968	Rpia	2	-0,470	Ribose-5-phosphate isomerase
G3UXL2	Prps1l3	10	-0,470	Protein Prps1l3
P13542	Myh8	149	-0,469	Myosin-8
Q8VE47	Uba5	2	-0,466	Ubiquitin-like modifier-activating enzyme 5
Q9DC77	Smpx	2	-0,465	Small muscular protein
P47754	Capza2	8	-0,464	F-actin-capping protein subunit alpha-2
Q8R0X7	Sgpl1	3	-0,455	Sphingosine-1-phosphate lyase 1
Q8VD04	Gripap1	2	-0,455	GRIP1-associated protein 1
Q8BWZ3	Naa25	4	-0,453	N-alpha-acetyltransferase 25, NatB auxiliary subunit
Q5XKN4	Jagn1	2	-0,452	Protein jagunal homolog 1
Q8K3R3	Plcd4	2	-0,451	1-phosphatidylinositol 4,5-bisphosphate phosphodiesterase delta-4
P11798	Camk2a	9	-0,449	Calcium/calmodulin-dependent protein kinase type II subunit alpha
Q9QZ23	Nfu1	2	-0,447	NFU1 iron-sulfur cluster scaffold homolog, mitochondrial
Q06335	Aplp2	3	-0,446	Amyloid-like protein 2
P68033	Actc1	31	-0,444	Actin, alpha cardiac muscle 1
Q922Y1	Ubxn1	5	-0,443	UBX domain-containing protein 1
Q8BSS9	Ppfia2	2	-0,440	Liprin-alpha-2
Q99246	Cacna1d	5	-0,439	Voltage-dependent L-type calcium channel subunit alpha-1D
Q01149	Col1a2	12	-0,439	Collagen alpha-2(I) chain
P03888	Mtnd1	2	-0,437	NADH-ubiquinone oxidoreductase chain 1
P15626	Gstm2	18	-0,437	Glutathione S-transferase Mu 2
O88207	Col5a1	2	-0,435	Collagen alpha-1(V) chain

Table S1. Identification of differentially expressed proteins in *Gaa*$^{-/-}$ knockout mice compared to WT mice. (Entries with * refers to proteins with fold change ≥ 1.5) (*continued*)

Assession No.	Gene name	Peptides	Log_2(Fold change)	Description
Q61545	Ewsr1	3	-0,431	RNA-binding protein EWS
V9GX06	Gm11214	5	-0,429	Protein Gm11214 (Fragment)
Q99JR1	Sfxn1	3	-0,419	Sideroflexin-1
Q63ZW6	Col4a5	3	-0,419	Col4a5 protein
P17183	Eno2	10	-0,415	Gamma-enolase
Q80X82	Sympk	2	-0,414	Symplekin
Q8R4E4	Myoz3	8	-0,414	Myozenin-3
E9Q5C9	Nolc1	2	-0,412	Protein Nolc1
Q8BGU0	Cyp4f39	2	-0,411	Protein Cyp4f39
O70622	Rtn2	5	-0,410	Reticulon-2
P70402	Mybph	16	-0,408	Myosin-binding protein H
Q9ER60	Scn4a	5	-0,407	Sodium channel protein type 4 subunit alpha
P62267	Rps23	4	-0,406	40S ribosomal protein S23
P07310	Ckm	31	-0,405	Creatine kinase M-type
Q8R5A0	Smyd2	5	-0,405	N-lysine methyltransferase SMYD2
Q9WUZ7	Sh3bgr	7	-0,402	SH3 domain-binding glutamic acid-rich protein
P41317	Mbl2	2	-0,402	Mannose-binding protein C
Q8BH86	C14orf159	3	-0,401	UPF0317 protein C14orf159 homolog, mitochondrial
Q9Z172	Sumo3	2	-0,399	Small ubiquitin-related modifier 3
P52196	Tst	5	-0,398	Thiosulfate sulfurtransferase
O70250	Pgam2	16	-0,398	Phosphoglycerate mutase 2
P17563	Selenbp1	9	-0,398	Selenium-binding protein 1
O35551	Rabep1	2	-0,397	Rab GTPase-binding effector protein 1
P58771	Tpm1	38	-0,397	Tropomyosin alpha-1 chain
Q8BUZ1	Abra	3	-0,395	Actin-binding Rho-activating protein
Q9QXZ0	Macf1	6	-0,393	Microtubule-actin cross-linking factor 1
P49813	Tmod1	17	-0,393	Tropomodulin-1
P06801	Me1	15	-0,392	NADP-dependent malic enzyme
Q921M7	Fam49b	5	-0,390	Protein FAM49B
Q8BGT5	Gpt2	2	-0,390	Alanine aminotransferase 2
A6H630	Armt1	4	-0,387	Protein-glutamate O-methyltransferase
Q7M729	Scn4b	3	-0,385	Sodium channel subunit beta-4
Q9WV35	Apobec2	9	-0,383	C->U-editing enzyme APOBEC-2
Q99LJ6	Gpx7	2	-0,373	Glutathione peroxidase 7
Q8BZJ7	Dcun1d2	5	-0,373	DCN1-like protein 2
Q8CG72	Adprhl2	2	-0,373	Poly(ADP-ribose) glycohydrolase ARH3

Table S1. Identification of differentially expressed proteins in *Gaa*$^{-/-}$ knockout mice compared to WT mice. (Entries with * refers to proteins with fold change ≥ 1.5) (*continued*)

Assession No.	Gene name	Peptides	Log_2(Fold change)	Description
P97328	Khk	2	-0,373	Ketohexokinase
Q8R0P4	Aamdc	7	-0,373	Mth938 domain-containing protein
Q99JT9	Adi1	2	-0,372	1,2-dihydroxy-3-keto-5-methylthiopentene dioxygenase
E9Q9K5	Trdn	13	-0,371	Triadin
Q80ZX0	Sec24b	3	-0,371	Protein Sec24b
Q9WUR9	Ak4	7	-0,371	Adenylate kinase 4, mitochondrial
Q9JK37	Myoz1	16	-0,371	Myozenin-1
Q9Z1Q2	Abhd16a	4	-0,370	Protein ABHD16A
Q9Z191	Eya4	2	-0,369	Eyes absent homolog 4
O54734	Ddost	5	-0,369	Dolichyl-diphosphooligosaccharide--protein glycosyltransferase 48 kDa subunit
Q9QXD8	Limd1	2	-0,365	LIM domain-containing protein 1
Q02566	Myh6	103	-0,365	Myosin-6
Q8BW75	Maob	8	-0,364	Amine oxidase [flavin-containing] B
Q0VF55	Atp2b3	6	-0,362	Calcium-transporting ATPase
O09165	Casq1	9	-0,361	Calsequestrin-1
Q9JLH8	Tmod4	11	-0,358	Tropomodulin-4
Q3UMW7	Mapkapk3	3	-0,354	MAP kinase-activated protein kinase 3
Q6PD26	Pigs	2	-0,354	GPI transamidase component PIG-S
Q9R0Y5	Ak1	19	-0,353	Adenylate kinase isoenzyme 1
Q920E5	Fdps	4	-0,352	Farnesyl pyrophosphate synthase
Q9WUB3	Pygm	69	-0,352	Glycogen phosphorylase, muscle form
Q3KNY0	Igfn1	15	-0,351	Immunoglobulin-like and fibronectin type III domain-containing protein 1
Q8K2C6	Sirt5	4	-0,350	NAD-dependent protein deacylase sirtuin-5, mitochondrial
Q8VED9	Lgalsl	2	-0,347	Galectin-related protein
P63087	Ppp1cc	12	-0,347	Serine/threonine-protein phosphatase PP1-gamma catalytic subunit
Q9JLT4	Txnrd2	2	-0,347	Thioredoxin reductase 2, mitochondrial
Q922B1	Macrod1	7	-0,347	O-acetyl-ADP-ribose deacetylase MACROD1
E9Q6E5	Srsf11	2	-0,346	Protein Srsf11
Q8R3Q2	Ppp6r2	2	-0,344	Serine/threonine-protein phosphatase 6 regulatory subunit 2
Q64133	Maoa	6	-0,344	Amine oxidase [flavin-containing] A
Q05BC3	Eml1	12	-0,344	Echinoderm microtubule-associated protein-like 1

Table S1. Identification of differentially expressed proteins in *Gaa*$^{-/-}$ knockout mice compared to WT mice. (Entries with * refers to proteins with fold change ≥ 1.5) (*continued*)

Assession No.	Gene name	Peptides	Log_2(Fold change)	Description
P42230	Stat5a	7	-0,343	Signal transducer and activator of transcription 5A
Q8BU85	Msrb3	4	-0,343	Methionine-R-sulfoxide reductase B3, mitochondrial
P85094	Isoc2a	3	-0,342	Isochorismatase domain-containing protein 2A
Q9QXD6	Fbp1	3	-0,342	Fructose-1,6-bisphosphatase 1
Q2NL51	Gsk3a	4	-0,342	Glycogen synthase kinase-3 alpha
P47757	Capzb	14	-0,341	F-actin-capping protein subunit beta
Q6TEK5	Vkorc1l1	3	-0,340	Vitamin K epoxide reductase complex subunit 1-like protein 1
Q8CI12	Smtnl2	7	-0,339	Smoothelin-like protein 2
Q6P3A8	Bckdhb	6	-0,339	2-oxoisovalerate dehydrogenase subunit beta, mitochondrial
Q80UM7	Mogs	4	-0,339	Mannosyl-oligosaccharide glucosidase
P50136	Bckdha	7	-0,337	2-oxoisovalerate dehydrogenase subunit alpha, mitochondrial
Q8C166	Cpne1	3	-0,337	Copine-1
Q14BI5	Myom2	90	-0,337	Myomesin 2
Q3TDQ1	Stt3b	4	-0,337	Dolichyl-diphosphooligosaccharide--protein glycosyltransferase subunit STT3B
P13634	Ca1	3	-0,335	Carbonic anhydrase 1
P45376	Akr1b1	14	-0,335	Aldose reductase
P68134	Acta1	33	-0,334	Actin, alpha skeletal muscle
Q8C0M9	Asrgl1	10	-0,334	Isoaspartyl peptidase/L-asparaginase
Q6NXN1	Szrd1	2	-0,334	SUZ domain-containing protein 1
Q9ES74	Nek7	3	-0,333	Serine/threonine-protein kinase Nek7
Q9DAK9	Phpt1	6	-0,331	14 kDa phosphohistidine phosphatase
Q5SX39	Myh4	209	-0,331	Myosin-4
Q91WM2	Cecr5	3	-0,330	Cat eye syndrome critical region protein 5 homolog
P05063	Aldoc	7	-0,328	Fructose-bisphosphate aldolase C
Q9CQ80	Vps25	4	-0,327	Vacuolar protein-sorting-associated protein 25
P12367	Prkar2a	12	-0,327	cAMP-dependent protein kinase type II-alpha regulatory subunit
P54731	Faf1	3	-0,326	FAS-associated factor 1
P13412	Tnni2	7	-0,324	Troponin I, fast skeletal muscle
Q8BGH4	Reep1	3	-0,322	Receptor expression-enhancing protein 1
P97370	Atp1b3	2	-0,320	Sodium/potassium-transporting ATPase subunit beta-3

Table S1. Identification of differentially expressed proteins in *Gaa*$^{-/-}$ knockout mice compared to WT mice. (Entries with * refers to proteins with fold change ≥ 1.5) (*continued*)

Assession No.	Gene name	Peptides	Log_2(Fold change)	Description
Q9D358	Acp1	5	-0,320	Low molecular weight phosphotyrosine protein phosphatase
E9Q1W3	Neb	406	-0,316	Protein Neb
Q8CGF5	Tmem56	2	-0,316	Transmembrane protein 56
Q8VI75	Ipo4	3	-0,316	Importin-4
S4R1W1	Gm3839	20	-0,315	Glyceraldehyde-3-phosphate dehydrogenase
Q62087	Pon3	5	-0,313	Serum paraoxonase/lactonase 3
Q8VI36	Pxn	3	-0,312	Paxillin
P50171	Hsd17b8	4	-0,312	Estradiol 17-beta-dehydrogenase 8
O55013	Trappc3	4	-0,309	Trafficking protein particle complex subunit 3
Q8VE22	Mrps23	2	-0,308	28S ribosomal protein S23, mitochondrial
P23475	Xrcc6	4	-0,308	X-ray repair cross-complementing protein 6
Q9DD02	L7rn6	2	-0,305	Protein Hikeshi
Q6ZWZ2	Ube2r2	3	-0,305	Ubiquitin-conjugating enzyme E2 R2
O88952	Lin7c	3	-0,303	Protein lin-7 homolog C
Q8VCK3	Tubg2	4	-0,303	Tubulin gamma-2 chain
Q99J99	Mpst	8	-0,303	3-mercaptopyruvate sulfurtransferase
Q91V64	Isoc1	6	-0,302	Isochorismatase domain-containing protein 1
Q62234	Myom1	92	-0,301	Myomesin-1
Q99JW2	Acy1	4	-0,300	Aminoacylase-1
Q8R3Z5	Cacnb1	13	-0,298	Voltage-dependent L-type calcium channel subunit beta-1
Q3UBX0	Tmem109	3	-0,298	Transmembrane protein 109
P20801	Tnnc2	10	-0,298	Troponin C, skeletal muscle
O88990	Actn3	68	-0,298	Alpha-actinin-3
Q3UE37	Ube2z	2	-0,296	Ubiquitin-conjugating enzyme E2 Z
Q9Z0V7	Timm17b	2	-0,295	Mitochondrial import inner membrane translocase subunit Tim17-B
Q8K010	Oplah	16	-0,295	5-oxoprolinase
I3ITR1	AK157302	2	-0,294	MCG50313
Q9WTU6	Mapk9	6	-0,294	Mitogen-activated protein kinase 9
Q8R429	Atp2a1	57	-0,293	Sarcoplasmic/endoplasmic reticulum calcium ATPase 1
P34914	Ephx2	6	-0,292	Bifunctional epoxide hydrolase 2
Q8CJG0	Ago2	7	-0,291	Protein argonaute-2
Q91YN5	Uap1	6	-0,291	UDP-N-acetylhexosamine pyrophosphorylase
Q5XPI3	Rnf123	8	-0,290	E3 ubiquitin-protein ligase RNF123
Q9CYH2	Fam213a	7	-0,289	Redox-regulatory protein FAM213A

Table S1. Identification of differentially expressed proteins in *Gaa*$^{-/-}$ knockout mice compared to WT mice. (Entries with * refers to proteins with fold change ≥ 1.5) (*continued*)

Assession No.	Gene name	Peptides	Log_2(Fold change)	Description
Q6A4J8	Usp7	5	-0,288	Ubiquitin carboxyl-terminal hydrolase 7
Q9Z1J3	Nfs1	4	-0,287	Cysteine desulfurase, mitochondrial
Q9D024	Ccdc47	6	-0,287	Coiled-coil domain-containing protein 47
Q8BVF2	Pdcl3	4	-0,286	Phosducin-like protein 3
Q9R0G6	Comp	12	-0,286	Cartilage oligomeric matrix protein
P00920	Ca2	2	-0,285	Carbonic anhydrase 2
P70288	Hdac2	2	-0,285	Histone deacetylase 2
Q9Z2C5	Mtm1	8	-0,284	Myotubularin
Q61247	Serpinf2	5	-0,284	Alpha-2-antiplasmin
P16460	Ass1	6	-0,284	Argininosuccinate synthase
Q8VE97	Srsf4	3	-0,282	Serine/arginine-rich splicing factor 4
Q04735	Cdk16	2	-0,282	Cyclin-dependent kinase 16
Q64691	Capn3	12	-0,282	Calpain-3
O35083	Agpat1	2	-0,281	1-acyl-sn-glycerol-3-phosphate acyltransferase alpha
Q8CCF0	Prpf31	3	-0,281	U4/U6 small nuclear ribonucleoprotein Prp31
P21550	Eno3	25	-0,281	Beta-enolase
A2A432	Cul4b	10	-0,281	Cullin-4B
A2ARP1	Ppip5k1	4	-0,281	Inositol hexakisphosphate and diphosphoinositol-pentakisphosphate kinase 1
P82198	Tgfbi	8	-0,281	Transforming growth factor-beta-induced protein ig-h3
Q6PA06	Atl2	9	-0,280	Atlastin-2
Q9CY27	Tecr	8	-0,280	Very-long-chain enoyl-CoA reductase
Q61655	Ddx19a	6	-0,278	ATP-dependent RNA helicase DDX19A
Q9JLR1	Sec61a2	6	-0,278	Protein transport protein Sec61 subunit alpha isoform 2
Q8VCP8	Ak6	2	-0,277	Adenylate kinase isoenzyme 6
P56501	Ucp3	6	-0,277	Mitochondrial uncoupling protein 3
O35435	Dhodh	2	-0,276	Dihydroorotate dehydrogenase (quinone), mitochondrial
P35285	Rab22a	2	-0,275	Ras-related protein Rab-22A
Q9D7H3	RtcA	3	-0,274	RNA 3-terminal phosphate cyclase
P05064	Aldoa	35	-0,274	Fructose-bisphosphate aldolase A
Q8BFZ3	Actbl2	12	-0,273	Beta-actin-like protein 2
Q8C5Q4	Grsf1	2	-0,273	G-rich sequence factor 1
Q8VEL0	Mospd1	4	-0,272	Motile sperm domain-containing protein 1
P56375	Acyp2	6	-0,272	Acylphosphatase-2

Table S1. Identification of differentially expressed proteins in *Gaa*$^{-/-}$ knockout mice compared to WT mice. (Entries with * refers to proteins with fold change ≥ 1.5) (*continued*)

Assession No.	Gene name	Peptides	Log_2(Fold change)	Description
Q9JKB1	Uchl3	8	-0,272	Ubiquitin carboxyl-terminal hydrolase isozyme L3
Q8R2G4	Art3	6	-0,272	Ecto-ADP-ribosyltransferase 3
Q9JI46	Nudt3	2	-0,271	Diphosphoinositol polyphosphate phosphohydrolase 1
Q8VCA8	Scrn2	3	-0,270	Secernin-2
Q9ET78	Jph2	17	-0,270	Junctophilin-2
Q9JJI8	Rpl38	4	-0,267	60S ribosomal protein L38
P97443	Smyd1	17	-0,267	Histone-lysine N-methyltransferase Smyd1
Q9QYI4	Dnajb12	3	-0,267	DnaJ homolog subfamily B member 12
Q9Z0J0	Npc2	3	-0,267	Epididymal secretory protein E1
Q8R105	Vps37c	2	-0,265	Vacuolar protein sorting-associated protein 37C
Q9D7N9	Apmap	7	-0,265	Adipocyte plasma membrane-associated protein
Q8BWA5	Klhl31	6	-0,263	Kelch-like protein 31

Table S2. Identification of differentially expressed proteins in LV-GAAco treated mice compared to WT mice. (Entries with * refers to proteins with fold change ≥ 1.5)

Assession No.	Gene name	Peptides	Log2(Fold change)	Description
			Up-regulated	
P70699*	Gaa*	2	1,58275*	Lysosomal alpha-glucosidase
P46425*	Gstp2*	5	1,2013*	Glutathione S-transferase P 2
E9PYB0*	Ahnak2*	7	1,13837*	Protein Ahnak2 (Fragment)
P19973*	Lsp1*	2	1,08792*	Lymphocyte-specific protein 1
P13745*	Gsta1*	5	1,01557*	Glutathione S-transferase A1
Q8VCB3*	Gys2*	5	0,97758*	Glycogen [starch] synthase, liver
P0C605*	Prkg1*	4	0,94349*	cGMP-dependent protein kinase 1
P13595*	Ncam1*	10	0,92489*	Neural cell adhesion molecule 1
P54116*	Stom*	2	0,91815*	Erythrocyte band 7 integral membrane protein
Q64337*	Sqstm1*	9	0,91789*	Sequestosome-1
Q62009*	Postn*	7	0,86646*	Periostin
P07091*	S100a4*	2	0,83294*	Protein S100-A4
Q9D154*	Serpinb1a*	17	0,7288*	Leukocyte elastase inhibitor A
P19157*	Gstp1*	7	0,69039*	Glutathione S-transferase P 1
Q60854*	Serpinb6*	19	0,67927*	Serpin B6
P97352*	S100a13*	6	0,64276*	Protein S100-A13
Q9EQK5*	Mvp*	20	0,60086*	Major vault protein
P33175*	Kif5a*	6	0,59812*	Kinesin heavy chain isoform 5A
P35385*	Hspb7*	5	0,59135*	Heat shock protein beta-7
Q66K08*	Cilp*	12	0,58773*	Cartilage intermediate layer protein 1
Q9CQV1*	Pam16*	3	0,58527*	Mitochondrial import inner membrane translocase subunit TIM16
Q64669	Nqo1	6	0,57775	NAD(P)H dehydrogenase [quinone] 1
Q9WTQ5	Akap12	8	0,57215	A-kinase anchor protein 12
Q9DCN2	Cyb5r3	8	0,54269	NADH-cytochrome b5 reductase 3
Q3TW96	Uap1l1	4	0,52825	UDP-N-acetylhexosamine pyrophosphorylase-like protein 1
P84084	Arf5	4	0,50892	ADP-ribosylation factor 5
P63321	Rala	2	0,50807	Ras-related protein Ral-A
P10107	Anxa1	12	0,49819	Annexin A1
Q3UHZ5	Lmod2	3	0,49686	Leiomodin-2
O70578	Cacng1	3	0,48973	Voltage-dependent calcium channel gamma-1 subunit
P14602	Hspb1	14	0,48764	Heat shock protein beta-1
Q9D1L9	Lamtor5	2	0,48649	Ragulator complex protein LAMTOR5
A2AQP0	Myh7b	19	0,47265	Myosin-7B
A2AJ76	Hmcn2	2	0,46794	Hemicentin-2

Table S2. Identification of differentially expressed proteins in LV-GAAco treated mice compared to WT mice. (Entries with * refers to proteins with fold change ≥ 1.5) (*continued*)

Assession No	Gene name	Peptides	Log2(Fold change)	Description
P04925	Prnp	2	0,46727	Major prion protein
O70373	Xirp1	32	0,4578	Xin actin-binding repeat-containing protein 1
B2RPU8	Zbed5	2	0,45464	MCG130675
Q9D8X2	Ccdc124	3	0,45434	Coiled-coil domain-containing protein 124
Q9CQH7	Btf3l4	4	0,44673	Transcription factor BTF3 homolog 4
E9Q616	Ahnak	132	0,43614	Protein Ahnak
Q9D404	Oxsm	4	0,43541	3-oxoacyl-[acyl-carrier-protein] synthase, mitochondrial
O35381	Anp32a	3	0,43405	Acidic leucine-rich nuclear phosphoprotein 32 family member A
Q9R0P3	Esd	10	0,4224	S-formylglutathione hydrolase
Q9R0P9	Uchl1	9	0,42223	Ubiquitin carboxyl-terminal hydrolase isozyme L1
P62806	Hist1h4a	6	0,41927	Histone H4
Q61739	Itga6	2	0,40968	Integrin alpha-6
Q6P9J9	Ano6	2	0,40743	Anoctamin-6
Q8VCH8	Ubxn4	2	0,40117	UBX domain-containing protein 4
Q9QYB1	Clic4	4	0,40014	Chloride intracellular channel protein 4
V9GX38	Gm17190	2	0,39419	Protein Gm17190
Q99JX3	Gorasp2	2	0,39221	Golgi reassembly-stacking protein 2
Q60634	Flot2	6	0,38824	Flotillin-2
Q62465	Vat1	5	0,38681	Synaptic vesicle membrane protein VAT-1 homolog
P27546	Map4	24	0,37987	Microtubule-associated protein 4
Q9WTR5	Cdh13	15	0,37628	Cadherin-13
P97315	Csrp1	4	0,37585	Cysteine and glycine-rich protein 1
Q5NBX1	Cobl	7	0,37411	Protein cordon-bleu
Q62048	Pea15	2	0,36951	Astrocytic phosphoprotein PEA-15
Q921H8	Acaa1a	9	0,36794	3-ketoacyl-CoA thiolase A, peroxisomal
P17047	Lamp2	2	0,36406	Lysosome-associated membrane glycoprotein 2
P56394	Cox17	2	0,36395	Cytochrome c oxidase copper chaperone
P29391	Ftl1	4	0,36208	Ferritin light chain 1
Q62165	Dag1	6	0,36099	Dystroglycan
P19246	Nefh	5	0,35328	Neurofilament heavy polypeptide
P31786	Dbi	2	0,35136	Acyl-CoA-binding protein
P23927	Cryab	9	0,35129	Alpha-crystallin B chain
P01921	H2-Ab1	2	0,34971	H-2 class II histocompatibility antigen, A-D beta chain

Table S2. Identification of differentially expressed proteins in LV-GAAco treated mice compared to WT mice. (Entries with * refers to proteins with fold change ≥ 1.5) (*continued*)

Assession No	Gene name	Peptides	Log2(Fold change)	Description
P11352	Gpx1	8	0,34797	Glutathione peroxidase 1
Q9JLJ2	Aldh9a1	3	0,3459	4-trimethylaminobutyraldehyde dehydrogenase
A2A9K7	Cnksr1	3	0,34552	Protein Cnksr1
Q9DCD0	Pgd	12	0,34546	6-phosphogluconate dehydrogenase, decarboxylating
Q91XV3	Basp1	2	0,34521	Brain acid soluble protein 1
Q9Z2X1	Hnrnpf	3	0,34435	Heterogeneous nuclear ribonucleoprotein F
Q61599	Arhgdib	4	0,34413	Rho GDP-dissociation inhibitor 2
O70209	Pdlim3	10	0,34277	PDZ and LIM domain protein 3
P23198	Cbx3	2	0,34143	Chromobox protein homolog 3
Q9DBJ1	Pgam1	8	0,33999	Phosphoglycerate mutase 1
P35762	Cd81	2	0,33964	CD81 antigen
D3Z5G7	Ces1b	7	0,33944	Carboxylic ester hydrolase
Q9CWS0	Ddah1	7	0,33939	N(G),N(G)-dimethylarginine dimethylaminohydrolase 1
P99024	Tubb5	23	0,3358	Tubulin beta-5 chain
Q91V61	Sfxn3	4	0,33538	Sideroflexin-3
P28656	Nap1l1	3	0,33508	Nucleosome assembly protein 1-like 1
P70290	Mpp1	4	0,33381	55 kDa erythrocyte membrane protein
P10126	Eef1a1	12	0,33286	Elongation factor 1-alpha 1
O35114	Scarb2	4	0,33172	Lysosome membrane protein 2
P48036	Anxa5	12	0,33151	Annexin A5
Q9WUU7	Ctsz	3	0,32949	Cathepsin Z
P82349	Sgcb	8	0,32889	Beta-sarcoglycan
P28798	Grn	6	0,32871	Granulins
Q61233	Lcp1	5	0,32849	Plastin-2
Q9EPL9	Acox3	2	0,32701	Peroxisomal acyl-coenzyme A oxidase 3
P63158	Hmgb1	5	0,32489	High mobility group protein B1
P18242	Ctsd	12	0,32417	Cathepsin D
P63024	Vamp3	2	0,32403	Vesicle-associated membrane protein 3
P51885	Lum	11	0,3216	Lumican
P10639	Txn	3	0,32089	Thioredoxin
P16015	Ca3	16	0,31928	Carbonic anhydrase 3
Q61207	Psap	17	0,31923	Prosaposin
P11438	Lamp1	2	0,31854	Lysosome-associated membrane glycoprotein 1
Q8VEE1	Lmcd1	18	0,31693	LIM and cysteine-rich domains protein 1

Table S2. Identification of differentially expressed proteins in LV-GAAco treated mice compared to WT mice. (Entries with * refers to proteins with fold change ≥ 1.5) (*continued*)

Assession No	Gene name	Peptides	Log2(Fold change)	Description
P17225	Ptbp1	3	0,31642	Polypyrimidine tract-binding protein 1
Q9D6Y9	Gbe1	18	0,31102	1,4-alpha-glucan-branching enzyme
Q9CWZ3	Rbm8a	2	0,31083	RNA-binding protein 8A
Q9Z0F7	Sncg	6	0,30811	Gamma-synuclein
P49586	Pcyt1a	3	0,30684	Choline-phosphate cytidylyltransferase A
Q8BGK2	Adprhl1	6	0,30682	[Protein ADP-ribosylarginine] hydrolase-like protein 1
Q8CI59	Steap3	2	0,30457	Metalloreductase STEAP3
Q6PDL0	Dync1li2	3	0,3025	Cytoplasmic dynein 1 light intermediate chain 2
P07724	Alb	44	0,29271	Serum albumin
P97449	Anpep	10	0,29259	Aminopeptidase N
O08917	Flot1	3	0,29245	Flotillin-1
Q9D020	Nt5c3a	12	0,29182	Cytosolic 5-nucleotidase 3A
A2AMM0	Murc	5	0,28868	Muscle-related coiled-coil protein
Q921I1	Tf	38	0,28816	Serotransferrin
O89053	Coro1a	2	0,28647	Coronin-1A
P10637	Mapt	11	0,28509	Microtubule-associated protein tau
O88653	Lamtor3	2	0,28447	Ragulator complex protein LAMTOR3
Q62188	Dpysl3	9	0,28427	Dihydropyrimidinase-related protein 3
P01831	Thy1	2	0,27934	Thy-1 membrane glycoprotein
P51637	Cav3	2	0,27837	Caveolin-3
Q9EQP2	Ehd4	8	0,27824	EH domain-containing protein 4
Q91VI7	Rnh1	18	0,27819	Ribonuclease inhibitor
Q8VCM7	Fgg	7	0,27812	Fibrinogen gamma chain
O89086	Rbm3	3	0,27739	RNA-binding protein 3
Q8BK84	Dupd1	7	0,27658	Dual specificity phosphatase DUPD1
Q8K157	Galm	2	0,27337	Aldose 1-epimerase
Q6P5H2	Nes	9	0,27174	Nestin
P40336	Vps26a	3	0,27171	Vacuolar protein sorting-associated protein 26A
E9PV24	Fga	10	0,27002	Fibrinogen alpha chain
Q8BH61	F13a1	5	0,26946	Coagulation factor XIII A chain
Q9D666	Sun1	2	0,2691	SUN domain-containing protein 1
Q6P1B1	Xpnpep1	3	0,26883	Xaa-Pro aminopeptidase 1
Q8K354	Cbr3	2	0,26524	Carbonyl reductase [NADPH] 3
Q9ER00	Stx12	3	0,26432	Syntaxin-12
			Down-regulated	

Table S2. Identification of differentially expressed proteins in LV-GAAco treated mice compared to WT mice. (Entries with * refers to proteins with fold change ≥ 1.5) (*continued*)

Assession No	Gene name	Peptides	Log2(Fold change)	Description
Q9ERT9*	Ppp1r1a*	2	-1,0655*	Protein phosphatase 1 regulatory subunit 1A
P17183*	Eno2*	9	-0,7592*	Gamma-enolase
P50431*	Shmt1*	4	-0,7073*	Serine hydroxymethyltransferase, cytosolic
E9Q3M9*	2010300C02Rik*	2	-0,6584*	Protein 2010300C02Rik
Q9D1F9*	Slc37a4*	2	-0,6532*	Protein Slc37a4
Q61586*	Gpam*	2	-0,6078*	Glycerol-3-phosphate acyltransferase 1, mitochondrial
Q9EP53	Tsc1	2	-0,5586	Hamartin
Q9ERI6	Rdh14	2	-0,548	Retinol dehydrogenase 14
P43023	Cox6a2	2	-0,5374	Cytochrome c oxidase subunit 6A2, mitochondrial
Q9D820	Prorsd1	2	-0,5157	Prolyl-tRNA synthetase associated domain-containing protein 1
Q8BJU0	Sgta	3	-0,5027	Small glutamine-rich tetratricopeptide repeat-containing protein alpha
Q80VJ2	Sra1	2	-0,5015	Steroid receptor RNA activator 1
Q9CR29	Ccdc43	2	-0,4831	Coiled-coil domain-containing protein 43
E9PVA8	Gcn1	2	-0,482	eIF-2-alpha kinase activator GCN1
Q8BGR9	Ublcp1	2	-0,4776	Ubiquitin-like domain-containing CTD phosphatase 1
Q6QD59	Bnip1	4	-0,4708	Vesicle transport protein SEC20
Q61129	Cfi	2	-0,4579	Complement factor I
P70236	Map2k6	8	-0,4313	Dual specificity mitogen-activated protein kinase kinase 6
Q9Z1R4	D17h6s53e	2	-0,4256	Uncharacterized protein C6orf47 homolog
Q63739	Ptp4a1	2	-0,421	Protein tyrosine phosphatase type IVA 1
Q8CGP0	Hist3h2bb	6	-0,4123	Histone H2B type 3-B
Q9CR67	Tmem33	2	-0,4108	Transmembrane protein 33
E9Q3C1	C2cd2	2	-0,4099	Protein C2cd2
P01942	Hba	6	-0,4029	Hemoglobin subunit alpha
Q6P6M7	Sepsecs	2	-0,3995	O-phosphoseryl-tRNA(Sec) selenium transferase
P13542	Myh8	145	-0,3942	Myosin-8
Q8R1G2	Cmbl	9	-0,3922	Carboxymethylenebutenolidase homolog
Q9QY06	Myo9b	2	-0,3908	Unconventional myosin-IXb
P02089	Hbb-b2	12	-0,3901	Hemoglobin subunit beta-2
Q80W22	Thnsl2	2	-0,3898	Threonine synthase-like 2
Q9CXV1	Sdhd	2	-0,3892	Succinate dehydrogenase [ubiquinone] cytochrome b small subunit, mitochondrial

Table S2. Identification of differentially expressed proteins in LV-GAAco treated mice compared to WT mice. (Entries with * refers to proteins with fold change ≥ 1.5) (*continued*)

Assession No	Gene name	Peptides	Log2(Fold change)	Description
O55003	Bnip3	3	-0,3842	BCL2/adenovirus E1B 19 kDa protein-interacting protein 3
O35071	Kif1c	4	-0,3838	Kinesin-like protein KIF1C
P06909	Cfh	4	-0,3799	Complement factor H
Q6P9Q6	Fkbp15	2	-0,3763	FK506-binding protein 15
Q3V1D3	Ampd1	28	-0,3752	AMP deaminase 1
Q8VEL0	Mospd1	5	-0,3698	Motile sperm domain-containing protein 1
P61080	Ube2d1	2	-0,3693	Ubiquitin-conjugating enzyme E2 D1
Q9R0Q3	Tmed2	5	-0,3663	Transmembrane emp24 domain-containing protein 2
Q9Z0P5	Twf2	5	-0,3623	Twinfilin-2
O54734	Ddost	3	-0,3617	Dolichyl-diphosphooligosaccharide--protein glycosyltransferase 48 kDa subunit
P57787	Slc16a3	4	-0,3612	Monocarboxylate transporter 4
P15331	Prph	3	-0,3526	Peripherin
Q9CRD0	Ociad1	4	-0,3516	OCIA domain-containing protein 1
P56382	Atp5e	2	-0,3496	ATP synthase subunit epsilon, mitochondrial
O08759	Ube3a	5	-0,3475	Ubiquitin-protein ligase E3A
Q8R105	Vps37c	2	-0,3428	Vacuolar protein sorting-associated protein 37C
Q9CU62	Smc1a	2	-0,3428	Structural maintenance of chromosomes protein 1A
Q9CZX9	Emc4	2	-0,3409	ER membrane protein complex subunit 4
Q9D8W7	Ociad2	3	-0,3406	OCIA domain-containing protein 2
Q8K3J1	Ndufs8	8	-0,3389	NADH dehydrogenase [ubiquinone] iron-sulfur protein 8, mitochondrial
B2RUR8	Otud7b	2	-0,3389	OTU domain-containing protein 7B
P03911	Mtnd4	3	-0,3341	NADH-ubiquinone oxidoreductase chain 4
Q8BGH4	Reep1	3	-0,328	Receptor expression-enhancing protein 1
P70695	Fbp2	4	-0,3257	Fructose-1,6-bisphosphatase isozyme 2
G3UXL2	Prps1l3	9	-0,3232	Protein Prps1l3
E9Q401	Ryr2	11	-0,3179	Ryanodine receptor 2
Q91V79	Fitm1	3	-0,3163	Fat storage-inducing transmembrane protein 1
Q9WUA5	Epm2a	3	-0,3147	Laforin
Q9JLT4	Txnrd2	4	-0,3146	Thioredoxin reductase 2, mitochondrial
Q8BH58	Tiprl	3	-0,3139	TIP41-like protein
P13707	Gpd1	22	-0,3107	Glycerol-3-phosphate dehydrogenase [NAD(+)], cytoplasmic

Table S2. Identification of differentially expressed proteins in LV-GAAco treated mice compared to WT mice. (Entries with * refers to proteins with fold change ≥ 1.5) (*continued*)

Assession No	Gene name	Peptides	Log2(Fold change)	Description
Q8CG72	Adprhl2	3	-0,3098	Poly(ADP-ribose) glycohydrolase ARH3
Q921R8	Slc41a3	6	-0,3076	Solute carrier family 41 member 3
Q8VHW3	Cacng6	3	-0,3053	Voltage-dependent calcium channel gamma-6 subunit
Q8CHS7	Dhrs7c	12	-0,2999	Dehydrogenase/reductase SDR family member 7C
Q8VDI7	Ubac1	6	-0,2979	Ubiquitin-associated domain-containing protein 1
Q08093	Cnn2	3	-0,2956	Calponin-2
G5E8J6	Hrc	12	-0,2946	Histidine rich calcium binding protein, isoform CRA_a
Q80X68	Csl	9	-0,2945	Citrate synthase
Q9WV35	Apobec2	9	-0,2922	C->U-editing enzyme APOBEC-2
P35283	Rab12	2	-0,2921	Ras-related protein Rab-12
Q8BRK9	Man2a2	5	-0,2887	Alpha-mannosidase 2x
Q8QZR5	Gpt	8	-0,2886	Alanine aminotransferase 1
P68033	Actc1	32	-0,2858	Actin, alpha cardiac muscle 1
Q6TEK5	Vkorc1l1	4	-0,2855	Vitamin K epoxide reductase complex subunit 1-like protein 1
Q8CI12	Smtnl2	8	-0,2852	Smoothelin-like protein 2
Q8CGF5	Tmem56	2	-0,2844	Transmembrane protein 56
P0DN34	Ndufb1	2	-0,2844	NADH dehydrogenase [ubiquinone] 1 beta subcomplex subunit 1
Q91WD5	Ndufs2	11	-0,2839	NADH dehydrogenase [ubiquinone] iron-sulfur protein 2, mitochondrial
Q9CY45	N6amt2	2	-0,283	Protein-lysine N-methyltransferase N6amt2
Q8BFZ3	Actbl2	12	-0,2829	Beta-actin-like protein 2
Q6P3A8	Bckdhb	5	-0,2805	2-oxoisovalerate dehydrogenase subunit beta, mitochondrial
P17665	Cox7c	2	-0,2802	Cytochrome c oxidase subunit 7C, mitochondrial
Q8JZN7	Rhot2	3	-0,2773	Mitochondrial Rho GTPase 2
Q2TPA8	Hsdl2	3	-0,2764	Hydroxysteroid dehydrogenase-like protein 2
P68181	Prkacb	8	-0,2762	cAMP-dependent protein kinase catalytic subunit beta
A0A140T8K6	Rpl36-ps3	3	-0,2761	60S ribosomal protein L36
Q8CCJ3	Ufl1	4	-0,2745	E3 UFM1-protein ligase 1
Q99KP3	Cryl1	3	-0,2731	Lambda-crystallin homolog
P61620	Sec61a1	4	-0,2725	Protein transport protein Sec61 subunit alpha isoform 1

Table S2. Identification of differentially expressed proteins in LV-GAAco treated mice compared to WT mice. (Entries with * refers to proteins with fold change ≥ 1.5) (*continued*)

Assession No	Gene name	Peptides	Log2(Fold change)	Description
Q920E5	Fdps	5	-0,2712	Farnesyl pyrophosphate synthase
Q9CQS8	Sec61b	2	-0,2694	Protein transport protein Sec61 subunit beta
Q921H9	Coa7	5	-0,2676	Cytochrome c oxidase assembly factor 7
Q9EQH2	Erap1	7	-0,267	Endoplasmic reticulum aminopeptidase 1
Q3TMP8	Tmem38a	5	-0,2664	Trimeric intracellular cation channel type A
Q6P9R2	Oxsr1	8	-0,2663	Serine/threonine-protein kinase OSR1
Q9R059	Fhl3	6	-0,2656	Four and a half LIM domains protein 3
Q9D8T7	Slirp	2	-0,2651	SRA stem-loop-interacting RNA-binding protein, mitochondrial
O70622	Rtn2	5	-0,265	Reticulon-2
Q8C494	Prr33	8	-0,2647	Proline-rich protein 33
Q8BW75	Maob	11	-0,264	Amine oxidase [flavin-containing] B
Q921M4	Golga2	2	-0,2635	Golgin subfamily A member 2
Q9WUR9	Ak4	6	-0,2634	Adenylate kinase 4, mitochondrial

Table S3. Identification of differentially expressed proteins in LV-IGFIIco.GAAco treated mice compared to WT mice. (Entries with * refers to proteins with fold change ≥ 1.5)

Assession No.	Gene name	Peptides	Log2(Fold change)	Description
			Up-regulated	
P70699	Gaa	2	0,57367	Lysosomal alpha-glucosidase
A2AJ76	Hmcn2	2	0,57143	Hemicentin-2
P19973	Lsp1	2	0,56889	Lymphocyte-specific protein 1
P0C605	Prkg1	4	0,54376	cGMP-dependent protein kinase 1
A2AQP0	Myh7b	19	0,52313	Myosin-7B
Q9D8X2	Ccdc124	3	0,46776	Coiled-coil domain-containing protein 124
P46425	Gstp2	5	0,42996	Glutathione S-transferase P 2
Q9WTQ5	Akap12	8	0,40466	A-kinase anchor protein 12
E9PYB0	Ahnak2	7	0,39524	Protein Ahnak2 (Fragment)
Q9QYB1	Clic4	4	0,30675	Chloride intracellular channel protein 4
			Down-regulated	
Q61586*	Gpam*	2	-0,5908*	Glycerol-3-phosphate acyltransferase 1, mitochondrial
Q9ERT9	Ppp1r1a	2	-0,572	Protein phosphatase 1 regulatory subunit 1A
P17183	Eno2	9	-0,4767	Gamma-enolase
E9Q3C1	C2cd2	2	-0,4437	Protein C2cd2
Q9ERI6	Rdh14	2	-0,4275	Retinol dehydrogenase 14
Q9D1F9	Slc37a4	2	-0,3666	Protein Slc37a4
Q8CGP0	Hist3h2bb	6	-0,3534	Histone H2B type 3-B
P50431	Shmt1	4	-0,3164	Serine hydroxymethyltransferase, cytosolic
Q91VK1	Bzw2	7	-0,306	Basic leucine zipper and W2 domain-containing protein 2
Q64691	Capn3	13	-0,2927	Calpain-3
P70695	Fbp2	4	-0,2698	Fructose-1,6-bisphosphatase isozyme 2

Chapter 5

Comparison of promoters for expression of acid α-glucosidase using self-inactivating lentiviral vectors in a murine model for Pompe disease

Qiushi Liang, M.D.[1,2,3]; Joon M. Pijnenburg, B.A.Sc.[1,2,3]; Arnold G. Vulto, Pharm.D., Ph.D.[4];
Ans T. van der Ploeg, M.D., Ph.D.[2,3]; Niek P. van Til, Ph.D.[5,6];
W.W.M. Pim Pijnappel, Ph.D.[1,2,3]*

[1] Molecular Stem Cell Biology, Department of Clinical Genetics, Erasmus University Medical Center, 3015GE Rotterdam, The Netherlands
[2] Department of Pediatrics, Erasmus University Medical Center, 3015GE Rotterdam, The Netherlands
[3] Center for Lysosomal and Metabolic Diseases, Erasmus University Medical Center, 3015GE Rotterdam, The Netherlands
[4] Hospital Pharmacy, Erasmus University Medical Center, 3015GE Rotterdam, The Netherlands
[5] Department of Hematology, Erasmus University Medical Center, 3015GE Rotterdam, The Netherlands
[6] Current address: Laboratory of Translational Immunology, University Medical Center Utrecht, 3584CX Utrecht, The Netherlands
* Correspondence: Dr. W.W.M. Pim Pijnappel, Erasmus University Medical Center, 3015GE Rotterdam, The Netherlands.
Email: w.pijnappel@erasmusmc.nl.

Submission in preparation

ABSTRACT

Deficiency of lysosomal acid α-glucosidase (GAA) leads to glycogen accumulation in Pompe disease featured by progressive cardiomyopathy and skeletal muscle weakness. Previously, it was demonstrated that a self-inactivating (SIN) lentiviral vector (LV) with a spleen focus-forming virus (SF) promoter provided robust hematopoietic GAA production that ameliorates symptoms in Pompe mice. However, an alternative promoter with an improved safety profile is preferred for clinical application to minimize genotoxic risks. In this study, we compared the *in vivo* therapeutic outcome of SIN LVs using three candidate promoters that are currently used in ongoing gene therapy trials, i.e. the cellular human phosphoglycerate kinase (PGK) promoter, and two myeloproliferative sarcoma virus enhancer, negative control region deleted, dl587rev primer-binding site substituted (MND)-derived promoter fragments: a long (MND-L) and short version (MND-S). We applied sub-therapeutic dosing of the LVs in order to detect differences within the dynamic range. Compared to the expression driven by the SF promoter, a promoter that was able to provide near-complete correction of muscle function, the MND promoters exhibited similar GAA production in the hematopoietic system with a significant reduction of glycogen to levels comparable to that of the SF-driven LV. Although safety analysis is still required, our findings suggest that the MND promoter may be a valid alternative to the SF promoter.

INTRODUCTION

Pompe disease, also termed glycogen storage disease type II (GSDII, OMIM 232300) or acid maltase deficiency (AMD), is an inherited metabolic disorder caused by the lack of acid α-glucosidase (GAA), resulting in lysosomal glycogen accumulation in all tissues.[1,2] Clinical manifestation in classic infantile patients is characterized by cardiomegaly and progressive myopathy within the first months of life. , These patients die within 1-year of age due to cardiorespiratory failure.[3,4] In late-onset patients, a broad spectrum of symptoms is observed that mainly includes skeletal muscle weakness and respiratory problems, and patients eventually become wheelchair-bound and ventilator-dependent.[5,6]

Enzyme replacement therapy (ERT, Myozyme) obtained market approval in 2006 and has since shown improved ventilator-free survival and cardiomyopathy in classic infantile Pompe patients,[7-9] as well as improved walking distance, stabilized pulmonary function and improved life quality in late-onset patients.[10-13] However, the weekly or biweekly administration of recombinant human GAA (rhGAA) enzyme is insufficient to restore symptoms in many patients with Pompe disease with the underlying problems, including: 1) impaired targeting of rhGAA due to low abundance of mannose-6-phosphatase residues,[14] 2) hampered efficacy of ERT by the formation of high sustained anti-rhGAA antibodies,[15-17] and 3) no improvement of white matter abnormalities in classical infantile patients due to limitations to reach the brain.[18-20]

For life-long correction of Pompe disease, transplantation of genetically modified autologous hematopoietic stem progenitor cells into the patients is an attractive clinical option. *Ex vivo* gene therapy using γ-retroviral vectors (γ-RV) has been successfully implemented in primary immunodeficiencies (PIDs), such as X-linked severe combined immunodeficiency (SCID-X1). This resulted in the generation of functional T-lymphocytes in 19 out of 20 patients in two clinical trials, and demonstrated a sustained immune reconstitution after 10 years-of follow-up.[21,22] However, 5 patients developed T-cell leukemia following gene therapy due to the insertional activation by RVs of the LIM domain only 2 (LMO2) proto-oncogene in combination of an acquired second genomic lesion.[23,24] Consequently, extensive studies to profile the integration pattern of RVs showed its preference to insert in the vicinity of promoter and enhancer regions (i.e. transcriptional start sites),[25-29] with highly enriched hotspots in proto-oncogenes, cancer-associated common insertion sites (CISs), and growth-controlling genes.[30,31] To improve efficacy and safety, HIV-derived lentiviral vectors (LVs) were developed. These vectors exhibit lower genotoxicity, in part by their different integration pattern which favors actively transcribed genes[32,33] but without

specific oncogenic targeting,[34] suggesting that LVs are a safer choice in comparison to RVs. Furthermore, LVs also facilitate higher transduction efficiencies of HSCs than RVs.[35] Deletion of the U3 region of 3' long terminal repeats (LTRs) to generate a self-inactivation configuration (SIN) further reduced the genotoxicity by 1) preventing generation of replication-competent virus upon integration;[36,37] and 2) directly reducing the risk of insertional upregulation of adjacent genes by incorporating cellular promoters.[31,38,39] SIN lentiviral vectors have since become a relatively safe platform for gene delivery with recent success in clinical trials for treating patients with immune deficiency, i.e. SCID-X1 and Wiskott-Aldrich syndrome;[40-42] metabolic disorders such as X-linked adrenoleukodystrophy (ALD)[43,44] and metachromatic leukodystrophy (MLD), a lysosomal storage disease.[45,46] No vector-associated oncogenesis has been reported in these ongoing clinical trials so far after a follow up of up to 7 years.[47]

As a proof-of-principle, we previously reported amelioration of the disease in Pompe mice by using a lentiviral vector driven by a strong viral spleen focus-forming virus (SF) promoter that achieved supranormal GAA activity levels.[48] This resulted in partial glycogen reduction in heart and the skeletal muscles.[49] In order to further increase GAA production, the native GAA sequence was replaced by a codon optimized version (GAAco). As a result, a more complete clearance of glycogen was obtained that was accompanied by normalized motor function in *Gaa*$^{-/-}$ mice (Stok *et al*, submitted). For clinical application, the choice of the exogenous promoter inserted in the vector to drive the expression cassette appeared to be a critical factor for biosafety regarding its propensity for activating neighboring genes.[39,50,51] While the application of SIN LV may already reduce potential genotoxicity, the SF promoter was still able to transform cells *in vitro* even when the vectors contained a SIN configuration.[38,52] These observations collectively initiated a search for alternative promoters that are more suitable for clinical development.

In this study, we have used *Gaa*$^{-/-}$ mice to test the therapeutic outcome of three candidate promoters that drive the GAA transgene from a SIN LV: (1) the human phosphoglycerate kinase (PGK) promoter, (2) the Moloney murine leukemic virus (MoMuLV)-derived myeloproliferative sarcoma virus enhancer, negative control region deleted, dl587rev primer-binding site substituted (MND) promoter (MND-long) and (3) a shorter version of the MND promoter (MND-short). The PGK promoter is a ubiquitously expressed housekeeping promoter that provides robust expression in the hematopoietic system. This promoter has recently been successfully implemented in a lentiviral gene therapy clinical trial for the lysosomal storage disease MLD.[45,46] The MND promoter (long) is a synthetic promoter[53] that is highly active in the hematopoietic system.[54,55] It has been used in a clinical trial for gene therapy of the peroxisomal storage disease

ALD, and is resulted in stabilization of disease progression.[43] The MND-short promoter consists of an approximately 174bp deletion at the 5' end of the MND-long promoter. These three LVs were compared to a previously described LV containing a strong SF promoter[48] that harbored a codon optimized GAA transgene at sub-therapeutic dosing. GAA activity and glycogen levels were used as read-out.

MATERIALS AND METHODS

Animals

Gaa knockout (*Gaa*$^{-/-}$) mice have been described.[48] Age-matched FVB/N mice were obtained from Charles River as wildtype control. Mice were housed under specific pathogen free (SPF) conditions according to the standard procedures. All animal experiments were approved by Animal Experiments Committee (DEC) in the Netherlands.

Vector construction and production

The construction of self-inactivating (SIN)[36] lentiviral vector pRRL.PPT.SF.GAAco.bPRE4*.SIN (LV-SF, Figure 1A) has been described previously.[56] It harbors an internal spleen focusing-forming virus (SF) promoter,[57,58] the codon-optimized human *GAA* sequence (*GAAco*, GenScript, Piscataway, NJ), and a modified woodchuck posttranslational regulatory element (bPRE4*) devoid of the Woodchuck hepatitis X-protein sequence to improve vector titers and transgene expression.[59] The SF promoter was then substituted by the phosphoglycerate kinase (PGK) promoter,[45,46] the Moloney murine leukemia virus-derived MND (myeloproliferative sarcoma virus enhancer, negative control region deleted, dl587rev primer-binding site substituted) promoter (MND-long)[43] (kindly provided by Dr. Laure Caccavelli) and its modified version with a 174bp deletion upstream (MND-short) (kindly provided by Dr. FTJ Staal) respectively, through XhoI/AgeI restriction sites, thus generating pRRL.PPT.PGK.GAAco.bPRE4*.SIN (LV-PGK, Figure 1B), pRRL.PPT.MND-L.GAAco.bPRE4*.SIN (LV-MND-L, Figure 1C) and pRRL.PPT.MND-S.GAAco.bPRE4*.SIN (LV-MND-S, Figure 1D). The difference between the MND-L and MND-S promoters is depicted in Figure 1E.

Lentiviruses were produced by calcium phosphate transfection of 293T cells with a third generation packaging system according to standard procedures.[60,61] Vectors were then concentrated by ultracentrifugation (20,000 rpm, 4°C, 2 hrs) and titers were determined as previously described.[49] Titers ranging from 10^8 to 10^9 transduction units/ml were routinely obtained for all viruses.

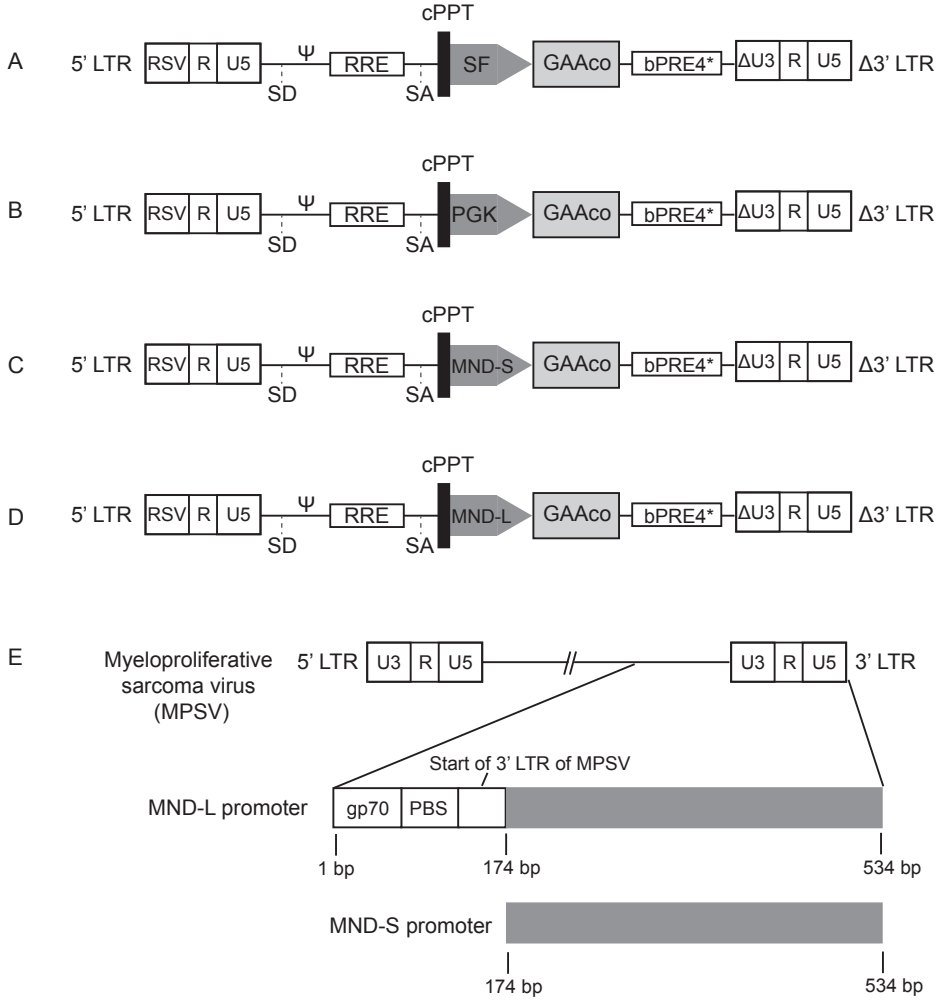

Figure 1. Schematic representation of the lentiviral vectors. The figure shows self-inactivating (SIN) lentiviral vectors expressing codon optimized GAA (GAAco) driven by different internal promoters. (A) pRRL.PPT.SF.GAAco.bPRE4*.SIN (referred as LV-SF) contains the spleen focus-forming virus (SF) promoter. (B) pRRL.PPT.PGK.GAAco.bPRE4*.SIN (referred as LV-PGK) contains the human phosphoglycerate kinase (PGK) promoter. (C) pRRL.PPT.MND_long.GAAco.bPRE4*.SIN (referred as LV-MND-L) contains the murine leukemia virus-derived MND promoter. (D) pRRL.PPT.MND_short.GAAco.bPRE4*.SIN (referred as LV-MND-S) contains the above MND promoter with a 174bp deletion at the 5' end. (E) The MND-L promoter was derived from 3' LTR of myeloproliferative sarcoma virus (MPSV). The difference between the MND long and short promoter is a 174bp upstream fragment including sequences encoding the gp70 envelope protein, the primary binding site (PBS) and the beginning of 3' LTR of MPSV. LTR indicates long terminal repeat; RSV, enhancer and promoter from the U3 region of Rous sarcoma virus; SD, splice donor site; Ψ, packaging signal; RRE, rev response element; SA, splice acceptor site; cPPT, central polypurine tract; bPRE4*, a modified woodchuck posttranslational regulatory element devoid of the Woodchuck hepatitis X-protein sequence and ATG sites deleted; ΔU3, deletion in the U3 region of 3' LTR to create SIN vector.

Transduction of hematopoietic stem cells and transplantation

Bone marrow cells were extracted from male *Gaa*$^{-/-}$ donor mice at the age of 8-weeks, and hematopoietic stem cells were enriched through lineage depletion (Lin$^-$) using the Mouse Hematopoietic Progenitor Cell Enrichment Kit (BD Sciences, San Jose, CA). After enrichment, Lin$^-$ cells were cultured in StemMACS HSC expansion media (Miltenyi Biotec, Leiden, the Netherlands), supplemented with 3 growth factors: murine thrombopoietin (Tpo, 100 ng/mL), murine stem cell factor (SCF, 100 ng/mL) and human FMS-like tyrosine kinase 3 murine ligand (Flt3-L, 50 ng/mL) as previously described.[49] The cells were then transduced with the concentrated lentivirus vectors at a multiplicity of infection (MOI) of 7 and incubated at 37°C with 5% CO_2 overnight. On the following day, 10^6 transduced Lin$^-$ cells were transplanted through the tail vein into age-matched female *Gaa*$^{-/-}$ recipients, subjected to 6 Gy sublethal irradiation using a Gammacell 40 (Atomic Energy of Canada LTD., Ontario, Canada) one day before transplantation. Parameters for each group are detailed in Table 1.

Table 1. Layout of experimental groups

Group	Treatment	Cell number	MOI	Irradiation (Gy)	Number of mice
1	LV-PGK	10^6	7	6	4
2	LV-MND-S	10^6	7	6	5
3	LV-MND-L	10^6	7	6	5
4	LV-SF	10^6	7	6	5
5	Untreated KO	*NA*	*NA*	*NA*	5
6	Untreated WT	*NA*	*NA*	*NA*	5

MOI indicates multiplicity of infection; Gy, gray; KO, *Gaa*$^{-/-}$ knockout; WT, wildtype.

Rotarod

Motor function was evaluated on a rotarod accelerating from 4 to 40 rpm in 300 sec (Panlab, Harvard Apparatus, Holliston, MA) according to the protocol detailed previously.[49] The latency was recorded and averaged for each mouse after 3 runs.

GAA and glycogen assays

Five months after gene therapy, mice were sacrificed by intracardiac perfusion after overnight fasting.[62] Heart, skeletal muscles and brain were harvested and immediately snap-frozen in liquid nitrogen and stored at -80 until further analysis. Tissues were lysed as previously described[49] and the resultant supernatant was used for assays to determine GAA enzymatic activity[63] and glycogen content.[62] Both GAA activity and glycogen content were corrected for total protein concentration using the Pierce BCA protein assay kit (Thermo Scientific, Waltham, MA).

Quantification of lentiviral vector copy numbers

The vector copy number (VCN) and chimerism were determined in genomic DNA from bone marrow by quantitative polymerase chain reaction (qPCR) as previously described.[49] Both VCN and chimerism were normalized for mouse *Gapdh*. Reactions were carried out in CFX96 real-time PCR detection system and analyzed by CFX Manager 3.0 (Bio-Rad, Hercules, CA). Primers sequences are reported in Table S1.

Statistics

Statistical analysis was performed with SPSS (IBM, version 22). All results were presented by mean ± SEM. Mann-Whitney U test was used for comparison of two groups. Multiple comparisons were analyzed by one-way ANOVA followed by Bonferroni's multiple testing correction. Repeated measures ANOVA was applied to detect differences of enzyme activity in leukocytes between treatment over the course of gene therapy, with Tukey's comparison test for individual comparisons among groups. *P* value ≤ 0.05 was considered statistically significant.

RESULTS

GAA expression in the hematopoietic system

To test the strength of the promoters *in vivo*, 10^6 transduced Lin- cells were injected into sublethally irradiated *Gaa*$^{-/-}$ mice (see Table 1 for transplantation conditions). Five months after transplantation, bone marrow (BM) was extracted for analysis of donor engraftment and LV integrations by qPCR (Figures 2A-B). An average of 20.0~49.5% chimerism was detected in BM, indicating long-term engraftment of the donor cells (Figure 2A). LVs with the PGK and MND-L promoters showed similar chimerism compared to LV-SF, whereas LV containing MND-S promoter showed 2-fold lower chimerism. The vector copy number (VCN) per genome, as determined by *HIV* qPCR, was similar between LV-MND-L and LV-SF (4.7 vs 5.4, Figure 2B). An average of 12.1 copies per genome was detected in the LV-PGK treated group. In contrast, the LV with MND-S promoter showed a 2-fold lower VCN at an average of 2 copies per genome, which was consistent with the 50% lower chimerism (Figure 2A).

Sufficient gene marking in the BM led to robust restoration of GAA activity in the hematopoietic system by all four constructs (Figure 2C). In order to eliminate influence from different integration frequencies from the vectors, the transgene expression of each vector was further corrected by VCN (Figure 2D). Per vector copy, GAA expression driven by the cellular PGK promoter was at least 10- to 20- fold lower than the expression produced by the other three viral promoters. Encouragingly, activity per VCN was

similar between LVs with MND-L and MND-S promoters, both of which demonstrated comparable strength with their SF-driven counterparts on a per-copy basis.

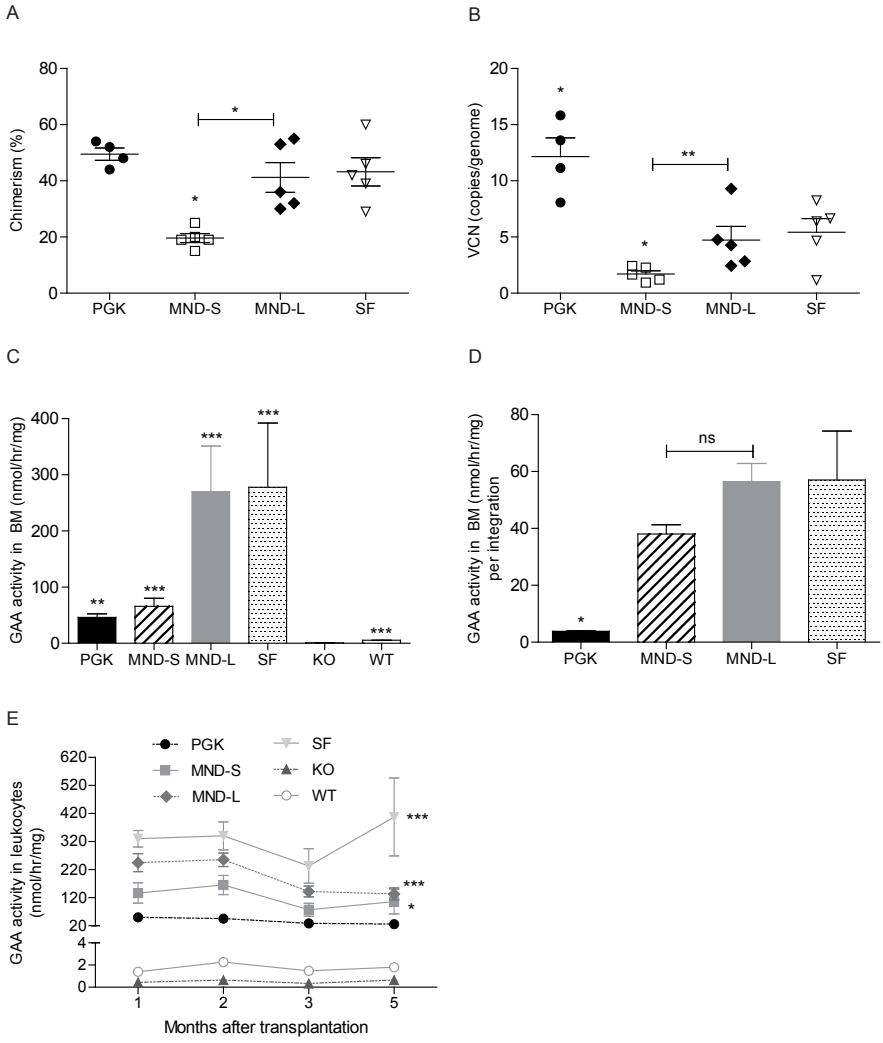

Figure 2. Reconstituted GAA activity in hematopoietic system. (A) Percentage of the engrafted donor cells in BM of the recipients (chimerism) five months post-gene therapy. This chimerism was determined by *Sry* qPCR and normalized using *Gapdh*. (B) Copies of lentiviral vector in BM assessed by qPCR using primers against *HIV* and normalized using *Gapdh*. (C) GAA activity in BM five months post-transplantation. (D) Relative promoter strength in BM. GAA activity in BM was divided by VCN (B). (E) GAA expression in peripheral leukocytes at 1, 2, 3, and 5 months after transplantation. Data are represented as means ± SEM; n=4 for the PGK group and n=5 for the other groups in all panels. Statistical comparisons that are only indicated by asterisks refer to a comparison to the LV-SF group in panels A, B, D, and comparison to the KO group in panels C and E. **P*≤ 0.05; ***P*≤ 0.01; ****P*≤ 0.001; ns, not significant.

The enzyme activity was also monitored on a monthly basis in the peripheral leukocytes (Figure 2E). Compared to the untreated KO mice, all vector treated mice exhibited overexpression of GAA consistent with the findings in BM. Similarly, the LV-SF provided the highest enzyme activities whereas the LV-PGK showed the lowest enzyme activities. The LVs with two MND promoters generated relatively high expression similar to that containing the SF promoter, especially when corrected for VCN.

To conclude, all lentiviral vectors provided high GAA enzyme activities in the hematopoietic system, i.e. bone marrow and peripheral leukocytes. The transgene expression was greatest when driven by the SF promoter and least by the PGK promoter. Importantly, the two versions of MND promoters demonstrated equal promoter strength as their SF counterpart in the hematopoietic system, suggesting that the MND is a promising promoter to replace the SF without compromising therapeutic efficacy.

Phenotypic correction in heart

Cardiac hypertrophy is a characteristic symptom in classic infantile Pompe patients. To assess whether secreted enzyme from the genetically modified hematopoietic system could lead to therapeutic rescue, hearts were harvested for biochemical analysis five months post-gene therapy. There was very limited GAA activity in mice treated by the PGK construct, whereas the LVs containing two MND promoters exhibited a 1.5-fold higher and the SF promoter 2.8-fold higher GAA activity compared to WT levels (Figure 3A). Consequently, no glycogen reduction was observed in the LV-PGK treated mice, in contrast to 80~90% glycogen clearance achieved by all the LVs with other viral promoters (Figure 3B). The efficacy in the LV-MND-S treated mice was slightly lower than the LV-MND-L version, but the VCN was also 50% lower.

To evaluate whether reduced glycogen content led to normalization of cardiac hypertrophy, wet-weight of hearts were measured (Figure 3C). The reduction in heart mass correlated with the glycogen clearance in LVs with two MND and SF promoters treated Pompe mice.

Therefore, we conclude that the MND- and SF- driven constructs produced GAA sufficiently to restore enzyme activities in the heart resulting in reduction of glycogen and heart weight close to WT level. In contrast, the cellular PGK promoter provided too low expression to induce any therapeutic effect in the heart.

Phenotypic correction in skeletal muscles

Skeletal muscles are severely affected in Pompe disease. Therefore, quadriceps femoris (QF), tibialis anterior (TA), gastrocnemius (GA) and diaphragm (DA) were analyzed

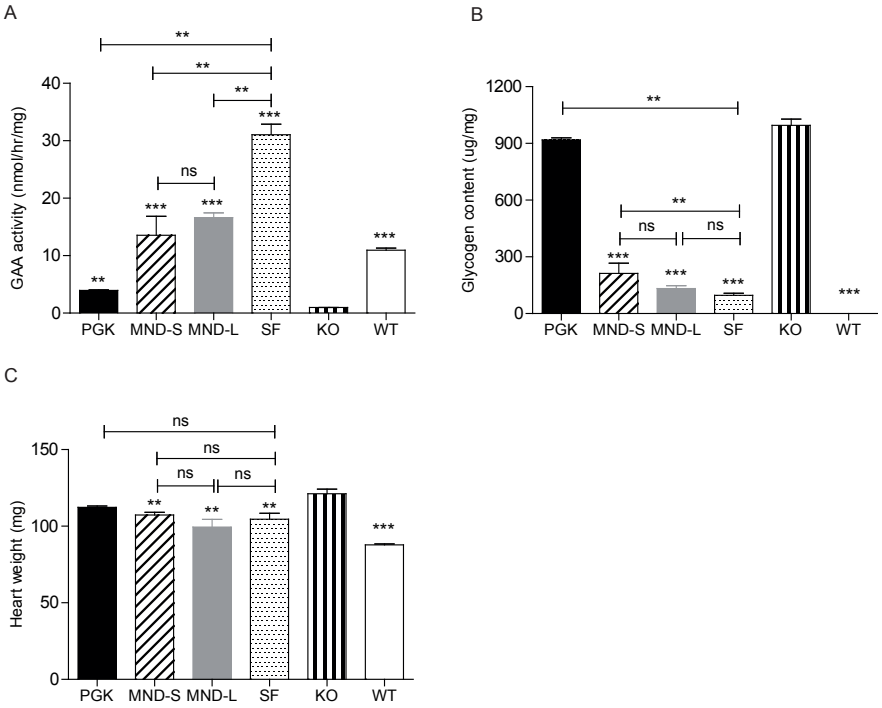

Figure 3. Therapeutic effect in heart after lentiviral gene therapy. Five months after transplantation, mice were sacrificed and hearts were analyzed. (A) Restoration of GAA activity in heart. (B) Correction of glycogen storage in heart. (C) Correction of cardiac hypertrophy. The whole heart (wet-weight) was measured. Data are represented as means ± SEM; n=4 for PGK group and n=5 for the other groups in all panels. The statistical comparison that is only indicated by asterisks refers to comparison to KO group in all panels. $^{**}P \leq 0.01$; $^{***}P \leq 0.001$; ns, not significant.

to evaluate the effect of lentiviral gene therapy in the skeletal muscle system. Five months after transplantation, all gene therapy treated groups showed significant restoration of enzyme activity compared to the untreated KO mice (Figure 4A). As expected, the LV-SF presented the highest transgene expression reaching up to 5-fold of WT level, while the MND promoter containing constructs reached approximately 2-fold of WT level. The PGK-driven construct provided 50 to 90% of WT GAA activity. Lysosomal glycogen levels in the corresponding tissues were then determined, and in the LV-PGK treated mice, there was no difference in the lysosomal glycogen content compared to untreated KO mice (Figure 4B). In contrast, the LV-SF led to 30% to 70% glycogen reduction in the muscles with the best clearance in DA and the poorest in GA. Intriguingly, the LV-MND-L showed comparable efficiency in clearing the glycogen content compared to the SF promoter-containing vector even with 50% lower GAA activity. Similarly, despite the comparable enzyme levels, the LV-MND-S construct was less effective in clearing glycogen in QF and TA compared to the LV-MND-L.

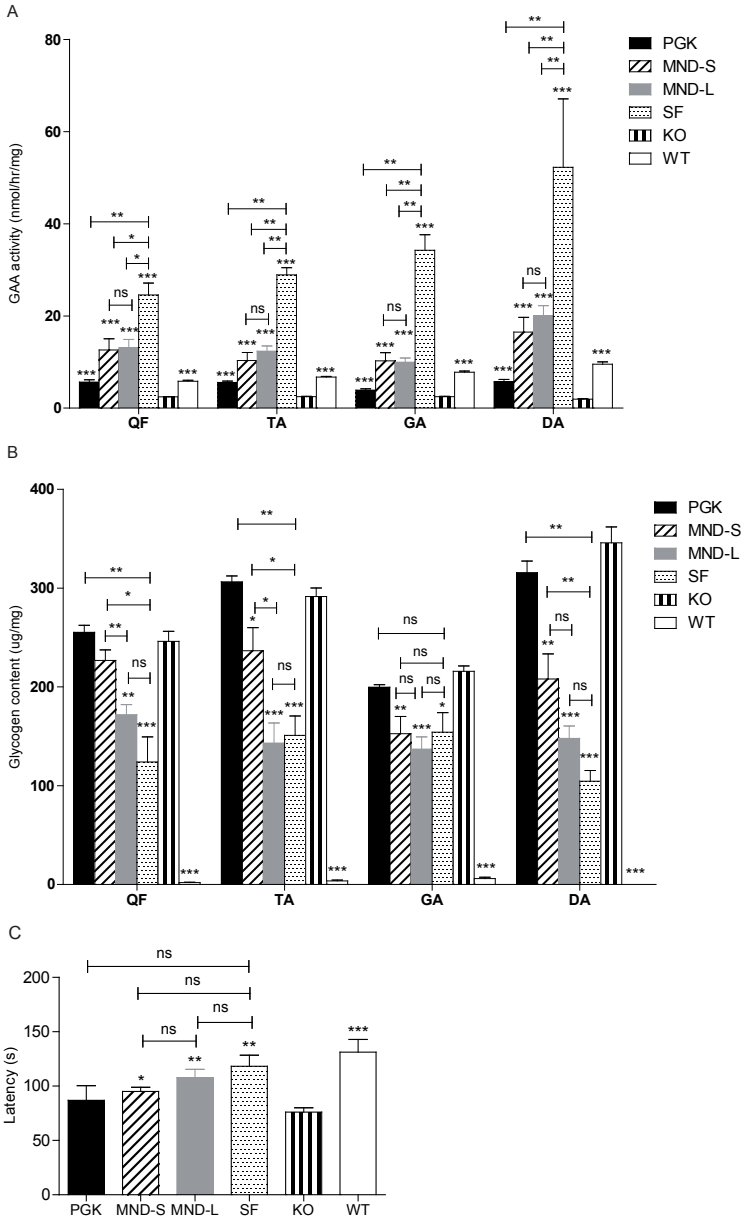

Figure 4. Therapeutic effect in skeletal muscles after lentiviral gene therapy. Five months after lentiviral gene therapy, mice were sacrificed and four skeletal muscle types were analyzed. (A) Restoration of GAA activity in skeletal muscles. (B) Glycogen correction in corresponding skeletal muscles in (A). (C) Motor function determined by rotarod. Data are represented as means ± SEM; n=4 for PGK group and n=5 for the other groups in all panels. The statistical comparison that is only indicated by asterisks refers to comparison to the KO group in all panels. *$P \leq 0.05$; **$P \leq 0.01$; ***$P \leq 0.001$; ns, not significant. QF indicates quadriceps femoris; TA, tibialis anterior; GA, gastrocnemius; DA, diaphragm.

Motor function was assessed on an accelerating rotarod at five months after transplantation (Figure 4C). Consistent with the poor elimination of glycogen load, the LV-PGK treated mice rapidly fell off the rotarod, similar as the untreated KO control mice. Latency was significantly prolonged after treatment with MND-L, MND-S, and SF promoter containing vectors, in line with the improved glycogen clearance obtained with these constructs.

To summarize, these results showed that under the conditions employed, the cellular PGK-driven construct had no therapeutic effect in skeletal muscles as evidenced by low levels of GAA activity and lack of significant glycogen reduction. The SF- and MND-L-driven constructs displayed comparable efficiency in ameliorating glycogen accumulation, and both accounted for improved motor function. The LV-MND-S treated mice seemed to be less efficient compared to its LV-MND-L counterparts, although the VCN was on average two-fold lower (Figure 2A).

Phenotypic correction in brain

Recent clinical studies have revealed cognitive decline as a new emerging symptom in long survivors of classic infantile disease,[18,20,64,65] which is accompanied by structural abnormalities in the brain including delayed myelination[66] and periventricular white matter abnormalities.[18,20,64] Therefore, brain is one of the important target tissues for therapy. Five months after transplantation, only LV-SF treated mice showed a small but significant increase of GAA activity in both the cerebrum and the cerebellum compared to untreated KO mice (Figure 5A). Consequently, this limited elevation of GAA enzyme failed to reduce glycogen accumulation (Figure 5B). Hence, we conclude that the lentiviral constructs tested in the current study at sub-therapeutic dosing are unable to address abnormalities in the brain.

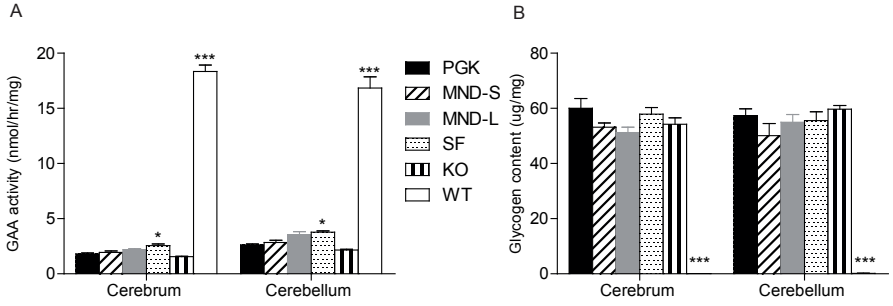

Figure 5. Therapeutic effect in brain after lentiviral gene therapy. Five months after lentiviral gene therapy, mice were sacrificed and brains (separated as cerebrum and cerebellum) were further analyzed. (A) GAA activity in brain. (B) Glycogen content in brain. Data are represented as means ± SEM; n=4 for PGK group and n=5 for the other groups. The statistical comparison that is only indicated by asterisks refers to comparison to KO group in all panels. *$P \leq 0.05$; ***$P \leq 0.001$.

DISCUSSION

The aim of this study was to test promoters in a lentiviral gene therapy approach that are suitable for clinical development, and that provide sufficient expression to effectively treat Pompe disease in a mouse model. The promoters included the housekeeping gene promoter PGK, and two versions of the MND promoter. These promoters have been validated for safety, i.e. insertional oncogenesis and no adverse events have been associated with the use of these promoters.[43,45,46] We found that the PGK promoter was too weak to generate therapeutic levels of GAA in the target tissues. Under the conditions employed. In contrast, two versions of the MND promoter were capable of driving high levels of GAA transgene expression that resulted in glycogen reductions that were comparable to those achieved by SF promoter constructs.

The SF promoter was used as a reference promoter, since we previously showed that this promoter could ameliorate the phenotype of Pompe mice.[49] The native GAA transgene in this lentiviral vector as applied in ref 49 was replaced in the present study by a codon-optimized GAA sequence (GAAco) (Stok *et al*, submitted). Although the SF promoter was also successfully applied for the γ-RV gene therapy trial for treating adenosine deaminase-severe combined immunodeficiency patients (ADA-SCID),[58,67] in another trial, two patients with chronic granulomatous disease (GCD) were found to have developed myelodysplastic syndrome (MDS) with monosomy 7 due to insertional activation of ectopic viral integration site 1 (EVI1).[57,68] Although the choice of γ-RV for gene delivery may have largely contributed to those adverse events, the potent SF promoter may still reinforce the transcriptional activation of flanking endogenous genes by its strong enhancer elements.[38] An alternative promoter is thus preferred to substitute the rather strong SF promoter.

The PGK promoter is a cellular promoter with weak enhancer promiscuity, which accounts for its inability to induce clonal dominance in cultured cells,[39] and therefore, it is an ideal choice in terms of safety. This promoter has been successfully applied in preclinical models for Gaucher type 1,[69] Krabbe disease,[70] mucopolysaccharidosis type I[71] and MLD[72] with sufficient enzyme reconstitution for metabolic correction in affected tissues. However, we showed in this study that with a relatively high VCN of 12.2 in BM, a PGK-driven LV failed to restore adequate GAA activity in the hematopoietic system, and consequently showed no therapeutic effect in all assessed tissues including heart (Figure 3B) and the skeletal muscles (Figure 4B). This is largely due to a 15-fold less promoter strength determined on per-copy basis when comparing to SF promoter (Figure 2D). Furthermore, glycogen seemed to be more refractory to degradation than for instance, sulfatide in MLD and highly sulfated heparan sulfate

(HS) in MPSIIIA. This was suggested by the finding that an increase of only 10-11 % of the WT level of the deficient enzyme activity already sufficed to normalize brain biochemistry and pathology in MLD[72] and MPS IIIA mouse models.[73] In contrast, with a similar amount of increase, no glycogen was reduced in the brain of Pompe mice (Figure 5). Collectively, these findings suggested that a higher amount of GAA is needed for sufficient phenotypic correction of Pompe disease in the mouse.

The viral-derived MND promoter stands out as compared to other physiological promoters (e.g. the human proximal *WAS* promoter or the elongation factor 1α (EF1α) promoter), as it can induce high-level gene expression in the hematopoietic system that almost fully corrected the immune deficiency in a murine model of Wiskott-Aldrich syndrome (WAS).[74,75] We have shown in Pompe mice that at similar VCN, the MND-L promoter showed similar promoter strength compared to the strong SF promoter in the BM (Figures 2A-D), which eventually resulted in comparable glycogen reduction in heart and skeletal muscles (Figures 3B, 4B). Alternatively, a shortened MND promoter lacking additional sequences without promoter activity was also tested (MND-S). Regrettably, a 2-fold lower engraftment efficiency (Figure 2A) led to equivalently lower VCNs obtained by this vector (Figure 2B) which makes the side-by-side comparison of the efficacy less accurate. Nevertheless, the MND-S promoter provided similar promoter strength in BM when corrected for VCN compared to its MND-L counterpart (Figure 2D). This suggests that the sequences removed from the MND-S promoter do not contribute to promoter activity.[53] A more careful *in vitro* titration of both MND-L and MND-S promoters should be performed in order to make an informed choice.

Naturally, consistent with other virus-derived enhancer/promoters (e.g. SF promoter), the MND promoter may also possess transactivation potential when used as an internal promoter for SIN LV. A clonal expansion correlated with the integration site at the *atf7ip* proto-oncogene was detected in one animal from the abovementioned preclinical studies in WAS mice.[74] Currently, a side by side comparison of SF and MND promoters is lacking. Only in one *in vitro* experiment using cultured thymocytes, SF driven LV seemed to have a relatively higher oncogenic insertion frequency than that of MND driven LV.[76] In addition, the same MND promoter was first approved for γ-RV gene therapy for ADA-SCID patients,[77] and was then successfully implemented in gene therapy for ALD patients with the improved SIN LV backbone.[43] In both cases, there was no progressive clonal expansion in the hematopoietic system after 10-year follow-up, further pointing to the relative safe profile of the MND promoter. Importantly, unlike the SF promoter, which is prone to methylation[68,78] as seen in the ADA-SCID trial,[58] the MND promoter has been engineered to resist DNA methylation,[54,55] assuring a long-term stable expression of the transgene.

The MND promoter seemed to be a promising promoter choice to substitute the SF promoter because it has a reduced genotoxicity profile, while it provides a comparable therapeutic outcome. In addition, it has been used in gene therapy trials without adverse events. In this study, we applied a sub-therapeutic dosing (MOI 7) of the LVs in order to detect differences in promoters within the dynamic range. An increased dose of LV-SF at MOI 20 can lead to near-complete glycogen clearance in the heart and skeletal muscles (Stok *et al*, submitted). However, the higher integration load also increases the risk of insertional mutagenesis, which appears to be dose-dependent,[79] and may directly correlate with the insertion frequency per cell.[80,81] Accordingly, an attractive solution for minimizing the VCN is to enhance the targeting of GAA enzyme so that expression of less transgene product is required. In our recent attempt, a portion of insulin-like growth factor II (IGFII) was attached to GAA to facilitate the uptake by mannose-6-phosphatase receptor after binding to IGFII binding domain.[82,83] With the resultant vector, SF.IGFIIco.GAAco, a complete clearance was achieved in all relevant tissues. This also included the brain, which is difficult to reach by ERT and refractory to treatment by previous versions of GAA containing lentiviral vectors through the hematopoietic system even with a high MOI (Stok *et al*, submitted).[49] More importantly, at least a 5-fold enhanced efficiency was observed in comparison with the untagged version, suggesting a clinical relevant VCN capable of full phenotypic correction (Liang *et al*, manuscript in preparation; Chapter 3).

In summary, the balance between therapeutic benefit and biosafety of the vectors remains challenging in gene therapy. We showed that the physiological promoter PGK is not applicable in Pompe disease due to too low GAA transgene expression to allow phenotypic correction, even at high VCN. The MND promoter, on the other hand, showed great potential to drive robust transgene expression similar to the SF promoter. Although no adverse events have been observed for the MND promoter in preclinical and clinical studies, comprehensive safety monitoring is required before deciding on the final lentiviral vector of choice that may be developed for Pompe disease.

ACKNOWLEDGEMENTS

The authors thank Dr. Laure Caccavelli (Biotherapy Department, Necker Children's Hospital, Assistance Publique–Hôpitaux de Paris, Paris, France) for providing the MND-L promoter and Dr. FTJ Staal (The molecular stem cells biology laboratory, Leiden University Medical Center, Leiden, The Netherlands) for providing the MND-S promoter. This work was supported by The Netherlands Organization for Health Research ZonMw

(project number: 40-40300-98-07010) and the Erasmus Medical Center. Q.L was additionally supported by the China Scholarship Council (File No. 201206240040)

REFERENCES

1. Hirschhorn R, Reuser AJJ. Glycogen storage disease type II: acid α-glucosidase (acid maltase) deficiency. In: Scriver C, Beaudet, AL, Sly, WS and Valle, D ed. The Metabolic and Molecular Basis for Inherited Disease. New York: McGraw-Hill; 2001:3389–3420.
2. van der Ploeg AT, Reuser AJ. Pompe's disease. *Lancet*. 2008;372(9646):1342-1353.
3. van den Hout HM, Hop W, van Diggelen OP, et al. The natural course of infantile Pompe's disease: 20 original cases compared with 133 cases from the literature. *Pediatrics*. 2003;112(2):332-340.
4. Kishnani PS, Hwu WL, Mandel H, Nicolino M, Yong F, Corzo D. A retrospective, multinational, multicenter study on the natural history of infantile-onset Pompe disease. *J Pediatr*. 2006;148(5):671-676.
5. Hagemans ML, Winkel LP, Van Doorn PA, et al. Clinical manifestation and natural course of late-onset Pompe's disease in 54 Dutch patients. *Brain*. 2005;128(Pt 3):671-677.
6. Winkel LP, Hagemans ML, van Doorn PA, et al. The natural course of non-classic Pompe's disease; a review of 225 published cases. *J Neurol*. 2005;252(8):875-884.
7. Kishnani PS, Corzo D, Nicolino M, et al. Recombinant human acid [alpha]-glucosidase: major clinical benefits in infantile-onset Pompe disease. *Neurology*. 2007;68(2):99-109.
8. Kishnani PS, Corzo D, Leslie ND, et al. Early treatment with alglucosidase alpha prolongs long-term survival of infants with Pompe disease. *Pediatr Res*. 2009;66(3):329-335.
9. Nicolino M, Byrne B, Wraith JE, et al. Clinical outcomes after long-term treatment with alglucosidase alfa in infants and children with advanced Pompe disease. *Genet Med*. 2009;11(3):210-219.
10. van Capelle CI, van der Beek NA, Hagemans ML, et al. Effect of enzyme therapy in juvenile patients with Pompe disease: a three-year open-label study. *Neuromuscul Disord*. 2010;20(12):775-782.
11. van der Ploeg AT, Clemens PR, Corzo D, et al. A randomized study of alglucosidase alfa in late-onset Pompe's disease. *N Engl J Med*. 2010;362(15):1396-1406.
12. Gungor D, Kruijshaar ME, Plug I, et al. Impact of enzyme replacement therapy on survival in adults with Pompe disease: results from a prospective international observational study. *Orphanet J Rare Dis*. 2013;8:49.
13. Gungor D, Kruijshaar ME, Plug I, et al. Quality of life and participation in daily life of adults with Pompe disease receiving enzyme replacement therapy: 10 years of international follow-up. *J Inherit Metab Dis*. 2016;39(2):253-260.
14. Zhu Y, Li X, Kyazike J, et al. Conjugation of mannose 6-phosphate-containing oligosaccharides to acid alpha-glucosidase improves the clearance of glycogen in pompe mice. *J Biol Chem*. 2004;279(48):50336-50341.
15. Kishnani PS, Goldenberg PC, DeArmey SL, et al. Cross-reactive immunologic material status affects treatment outcomes in Pompe disease infants. *Molecular Genetics and Metabolism*. 2010;99(1):26-33.

16. Banugaria SG, Prater SN, Ng YK, et al. The impact of antibodies on clinical outcomes in diseases treated with therapeutic protein: lessons learned from infantile Pompe disease. *Genet Med*. 2011;13(8):729-736.

17. van Gelder CM, Hoogeveen-Westerveld M, Kroos MA, Plug I, van der Ploeg AT, Reuser AJ. Enzyme therapy and immune response in relation to CRIM status: the Dutch experience in classic infantile Pompe disease. *J Inherit Metab Dis*. 2015;38(2):305-314.

18. Ebbink BJ, Aarsen FK, van Gelder CM, et al. Cognitive outcome of patients with classic infantile Pompe disease receiving enzyme therapy. *Neurology*. 2012;78(19):1512-1518.

19. Spiridigliozzi GA, Heller JH, Kishnani PS. Cognitive and adaptive functioning of children with infantile Pompe disease treated with enzyme replacement therapy: long-term follow-up. *Am J Med Genet C Semin Med Genet*. 2012;160C(1):22-29.

20. Ebbink BJ, Poelman E, Plug I, et al. Cognitive decline in classic infantile Pompe disease: An underacknowledged challenge. *Neurology*. 2016;86(13):1260-1261.

21. Hacein-Bey-Abina S, Hauer J, Lim A, et al. Efficacy of gene therapy for X-linked severe combined immunodeficiency. *N Engl J Med*. 2010;363(4):355-364.

22. Gaspar HB, Cooray S, Gilmour KC, et al. Long-term persistence of a polyclonal T cell repertoire after gene therapy for X-linked severe combined immunodeficiency. *Sci Transl Med*. 2011;3(97):97ra79.

23. Hacein-Bey-Abina S, Garrigue A, Wang GP, et al. Insertional oncogenesis in 4 patients after retrovirus-mediated gene therapy of SCID-X1. *J Clin Invest*. 2008;118(9):3132-3142.

24. Howe SJ, Mansour MR, Schwarzwaelder K, et al. Insertional mutagenesis combined with acquired somatic mutations causes leukemogenesis following gene therapy of SCID-X1 patients. *J Clin Invest*. 2008;118(9):3143-3150.

25. Rohdewohld H, Weiher H, Reik W, Jaenisch R, Breindl M. Retrovirus integration and chromatin structure: Moloney murine leukemia proviral integration sites map near DNase I-hypersensitive sites. *J Virol*. 1987;61(2):336-343.

26. Wu X, Li Y, Crise B, Burgess SM. Transcription start regions in the human genome are favored targets for MLV integration. *Science*. 2003;300(5626):1749-1751.

27. Mitchell RS, Beitzel BF, Schroder AR, et al. Retroviral DNA integration: ASLV, HIV, and MLV show distinct target site preferences. *PLoS Biol*. 2004;2(8):E234.

28. Felice B, Cattoglio C, Cittaro D, et al. Transcription factor binding sites are genetic determinants of retroviral integration in the human genome. *PLoS One*. 2009;4(2):e4571.

29. De Ravin SS, Su L, Theobald N, et al. Enhancers are major targets for murine leukemia virus vector integration. *J Virol*. 2014;88(8):4504-4513.

30. Cattoglio C, Facchini G, Sartori D, et al. Hot spots of retroviral integration in human CD34+ hematopoietic cells. *Blood*. 2007;110(6):1770-1778.

31. Montini E, Cesana D, Schmidt M, et al. The genotoxic potential of retroviral vectors is strongly modulated by vector design and integration site selection in a mouse model of HSC gene therapy. *J Clin Invest*. 2009;119(4):964-975.

32. De Palma M, Montini E, Santoni de Sio FR, et al. Promoter trapping reveals significant differences in integration site selection between MLV and HIV vectors in primary hematopoietic cells. *Blood*. 2005;105(6):2307-2315.

33. Montini E, Cesana D, Schmidt M, et al. Hematopoietic stem cell gene transfer in a tumor-prone mouse model uncovers low genotoxicity of lentiviral vector integration. *Nat Biotechnol.* 2006;24(6):687-696.
34. Biffi A, Bartolomae CC, Cesana D, et al. Lentiviral vector common integration sites in preclinical models and a clinical trial reflect a benign integration bias and not oncogenic selection. *Blood.* 2011;117(20):5332-5339.
35. Naldini L, Blomer U, Gallay P, et al. In vivo gene delivery and stable transduction of nondividing cells by a lentiviral vector. *Science.* 1996;272(5259):263-267.
36. Zufferey R, Dull T, Mandel RJ, et al. Self-inactivating lentivirus vector for safe and efficient in vivo gene delivery. *J Virol.* 1998;72(12):9873-9880.
37. Bukovsky AA, Song JP, Naldini L. Interaction of human immunodeficiency virus-derived vectors with wild-type virus in transduced cells. *J Virol.* 1999;73(8):7087-7092.
38. Modlich U, Bohne J, Schmidt M, et al. Cell-culture assays reveal the importance of retroviral vector design for insertional genotoxicity. *Blood.* 2006;108(8):2545-2553.
39. Maruggi G, Porcellini S, Facchini G, et al. Transcriptional enhancers induce insertional gene deregulation independently from the vector type and design. *Mol Ther.* 2009;17(5):851-856.
40. Aiuti A, Biasco L, Scaramuzza S, et al. Lentiviral hematopoietic stem cell gene therapy in patients with Wiskott-Aldrich syndrome. *Science.* 2013;341(6148):1233151.
41. Hacein-Bey Abina S, Gaspar HB, Blondeau J, et al. Outcomes following gene therapy in patients with severe Wiskott-Aldrich syndrome. *Jama.* 2015;313(15):1550-1563.
42. De Ravin SS, Wu X, Moir S, et al. Lentiviral hematopoietic stem cell gene therapy for X-linked severe combined immunodeficiency. *Sci Transl Med.* 2016;8(335):335ra357.
43. Cartier N, Hacein-Bey-Abina S, Bartholomae CC, et al. Hematopoietic stem cell gene therapy with a lentiviral vector in X-linked adrenoleukodystrophy. *Science.* 2009;326(5954):818-823.
44. Cartier N, Hacein-Bey-Abina S, Bartholomae CC, et al. Lentiviral hematopoietic cell gene therapy for X-linked adrenoleukodystrophy. *Methods Enzymol.* 2012;507:187-198.
45. Biffi A, Montini E, Lorioli L, et al. Lentiviral hematopoietic stem cell gene therapy benefits metachromatic leukodystrophy. *Science.* 2013;341(6148):1233158.
46. Sessa M, Lorioli L, Fumagalli F, et al. Lentiviral haemopoietic stem-cell gene therapy in early-onset metachromatic leukodystrophy: an ad-hoc analysis of a non-randomised, open-label, phase 1/2 trial. *Lancet.* 2016;388(10043):476-487.
47. Biasco L, Pellin D, Scala S, et al. In Vivo Tracking of Human Hematopoiesis Reveals Patterns of Clonal Dynamics during Early and Steady-State Reconstitution Phases. *Cell Stem Cell.* 2016;19(1):107-119.
48. Bijvoet AG, van de Kamp EH, Kroos MA, et al. Generalized glycogen storage and cardiomegaly in a knockout mouse model of Pompe disease. *Hum Mol Genet.* 1998;7(1):53-62.
49. van Til NP, Stok M, Aerts Kaya FS, et al. Lentiviral gene therapy of murine hematopoietic stem cells ameliorates the Pompe disease phenotype. *Blood.* 2010;115(26):5329-5337.
50. Modlich U, Schambach A, Brugman MH, et al. Leukemia induction after a single retroviral vector insertion in Evi1 or Prdm16. *Leukemia.* 2008;22(8):1519-1528.

51. Modlich U, Navarro S, Zychlinski D, et al. Insertional transformation of hematopoietic cells by self-inactivating lentiviral and gammaretroviral vectors. *Mol Ther*. 2009;17(11):1919-1928.

52. Zychlinski D, Schambach A, Modlich U, et al. Physiological promoters reduce the genotoxic risk of integrating gene vectors. *Mol Ther*. 2008;16(4):718-725.

53. Challita PM, Skelton D, el-Khoueiry A, Yu XJ, Weinberg K, Kohn DB. Multiple modifications in cis elements of the long terminal repeat of retroviral vectors lead to increased expression and decreased DNA methylation in embryonic carcinoma cells. *J Virol*. 1995;69(2):748-755.

54. Robbins PB, Skelton DC, Yu XJ, Halene S, Leonard EH, Kohn DB. Consistent, persistent expression from modified retroviral vectors in murine hematopoietic stem cells. *Proc Natl Acad Sci U S A*. 1998;95(17):10182-10187.

55. Halene S, Wang L, Cooper RM, Bockstoce DC, Robbins PB, Kohn DB. Improved expression in hematopoietic and lymphoid cells in mice after transplantation of bone marrow transduced with a modified retroviral vector. *Blood*. 1999;94(10):3349-3357.

56. Stok M. Stem cell based gene therapy for Pompe's disease. Hematology: Erasmus Medical Center, Erasmus University of Rotterdam; 2013.

57. Ott MG, Schmidt M, Schwarzwaelder K, et al. Correction of X-linked chronic granulomatous disease by gene therapy, augmented by insertional activation of MDS1-EVI1, PRDM16 or SETBP1. *Nat Med*. 2006;12(4):401-409.

58. Gaspar HB, Bjorkegren E, Parsley K, et al. Successful reconstitution of immunity in ADA-SCID by stem cell gene therapy following cessation of PEG-ADA and use of mild preconditioning. *Mol Ther*. 2006;14(4):505-513.

59. Schambach A, Bohne J, Baum C, et al. Woodchuck hepatitis virus post-transcriptional regulatory element deleted from X protein and promoter sequences enhances retroviral vector titer and expression. *Gene Ther*. 2006;13(7):641-645.

60. Naldini L, Blomer U, Gage FH, Trono D, Verma IM. Efficient transfer, integration, and sustained long-term expression of the transgene in adult rat brains injected with a lentiviral vector. *Proc Natl Acad Sci U S A*. 1996;93(21):11382-11388.

61. Dull T, Zufferey R, Kelly M, et al. A third-generation lentivirus vector with a conditional packaging system. *J Virol*. 1998;72(11):8463-8471.

62. Bijvoet AG, Van Hirtum H, Kroos MA, et al. Human acid alpha-glucosidase from rabbit milk has therapeutic effect in mice with glycogen storage disease type II. *Hum Mol Genet*. 1999;8(12):2145-2153.

63. Okumiya T, Keulemans JL, Kroos MA, et al. A new diagnostic assay for glycogen storage disease type II in mixed leukocytes. *Mol Genet Metab*. 2006;88(1):22-28.

64. Rohrbach M, Klein A, Kohli-Wiesner A, et al. CRIM-negative infantile Pompe disease: 42-month treatment outcome. *J Inherit Metab Dis*. 2010;33(6):751-757.

65. Matsuoka T, Miwa Y, Tajika M, et al. Divergent clinical outcomes of alpha-glucosidase enzyme replacement therapy in two siblings with infantile-onset Pompe disease treated in the symptomatic or pre-symptomatic state. *Mol Genet Metab Rep*. 2016;9:98-105.

66. Chien YH, Lee NC, Peng SF, Hwu WL. Brain development in infantile-onset Pompe disease treated by enzyme replacement therapy. *Pediatr Res.* 2006;60(3):349-352.

67. Gaspar HB, Cooray S, Gilmour KC, et al. Hematopoietic stem cell gene therapy for adenosine deaminase-deficient severe combined immunodeficiency leads to long-term immunological recovery and metabolic correction. *Sci Transl Med.* 2011;3(97):97ra80.

68. Stein S, Ott MG, Schultze-Strasser S, et al. Genomic instability and myelodysplasia with monosomy 7 consequent to EVI1 activation after gene therapy for chronic granulomatous disease. *Nat Med.* 2010;16(2):198-204.

69. Dahl M, Doyle A, Olsson K, et al. Lentiviral gene therapy using cellular promoters cures type 1 Gaucher disease in mice. *Mol Ther.* 2015;23(5):835-844.

70. Gentner B, Visigalli I, Hiramatsu H, et al. Identification of hematopoietic stem cell-specific miRNAs enables gene therapy of globoid cell leukodystrophy. *Sci Transl Med.* 2010;2(58):58ra84.

71. Visigalli I, Delai S, Politi LS, et al. Gene therapy augments the efficacy of hematopoietic cell transplantation and fully corrects mucopolysaccharidosis type I phenotype in the mouse model. *Blood.* 2010;116(24):5130-5139.

72. Biffi A, Capotondo A, Fasano S, et al. Gene therapy of metachromatic leukodystrophy reverses neurological damage and deficits in mice. *J Clin Invest.* 2006;116(11):3070-3082.

73. Sergijenko A, Langford-Smith A, Liao AY, et al. Myeloid/Microglial driven autologous hematopoietic stem cell gene therapy corrects a neuronopathic lysosomal disease. *Mol Ther.* 2013;21(10):1938-1949.

74. Astrakhan A, Sather BD, Ryu BY, et al. Ubiquitous high-level gene expression in hematopoietic lineages provides effective lentiviral gene therapy of murine Wiskott-Aldrich syndrome. *Blood.* 2012;119(19):4395-4407.

75. Koldej RM, Carney G, Wielgosz MM, et al. Comparison of insulators and promoters for expression of the Wiskott-Aldrich syndrome protein using lentiviral vectors. *Hum Gene Ther Clin Dev.* 2013;24(2):77-85.

76. Zhou S, Fatima S, Ma Z, et al. Evaluating the Safety of Retroviral Vectors Based on Insertional Oncogene Activation and Blocked Differentiation in Cultured Thymocytes. *Mol Ther.* 2016;24(6):1090-1099.

77. Candotti F, Shaw KL, Muul L, et al. Gene therapy for adenosine deaminase-deficient severe combined immune deficiency: clinical comparison of retroviral vectors and treatment plans. *Blood.* 2012;120(18):3635-3646.

78. Herbst F, Ball CR, Tuorto F, et al. Extensive methylation of promoter sequences silences lentiviral transgene expression during stem cell differentiation in vivo. *Mol Ther.* 2012;20(5):1014-1021.

79. Modlich U, Kustikova OS, Schmidt M, et al. Leukemias following retroviral transfer of multidrug resistance 1 (MDR1) are driven by combinatorial insertional mutagenesis. *Blood.* 2005;105(11):4235-4246.

80. King W, Patel MD, Lobel LI, Goff SP, Nguyen-Huu MC. Insertion mutagenesis of embryonal carcinoma cells by retroviruses. *Science.* 1985;228(4699):554-558.

81. Stocking C, Bergholz U, Friel J, et al. Distinct classes of factor-independent mutants can be isolated after retroviral mutagenesis of a human myeloid stem cell line. *Growth Factors*. 1993;8(3):197-209.

82. LeBowitz JH, Grubb JH, Maga JA, Schmiel DH, Vogler C, Sly WS. Glycosylation-independent targeting enhances enzyme delivery to lysosomes and decreases storage in mucopolysaccharidosis type VII mice. *Proc Natl Acad Sci U S A*. 2004;101(9):3083-3088.

83. Maga JA, Zhou J, Kambampati R, et al. Glycosylation-independent lysosomal targeting of acid alpha-glucosidase enhances muscle glycogen clearance in pompe mice. *J Biol Chem*. 2013;288(3):1428-1438.

Table S1. Sequences of primers for qPCR

Primers	Sequence
HIV-U3 forward	5′-CTGGAAGGGCTAATTCACTC-3′
HIV-PSI reverse	5′-GGTTTCCCTTTCGCTTTCAG-3′
Sry forward	5′-TCATCGGAGGGCTAAAGTGTCAC-3′
Sry reverse	5′-TGGCATGTGGGTTCCTGTCC-3′
Gapdh forward	5′- TAATGGGGAGAGGTTCGATG -3′
Gapdh reverse	5′- GCTGCTTCCCGAGTAAAATG -3′

Chapter 6

Immune tolerance against human acid α-glucosidase achieved in a gene therapy model for Pompe disease

Qiushi Liang, M.D.[1,2,3]; Joon M. Pijnenburg, B.A.Sc.[1,2,3]; Yvette van Helsdingen, B.A.Sc.[4]; Gerard Wagemaker, Ph.D.[4]; Arnold G. Vulto, Pharm.D., Ph.D.[5]; Ans T. van der Ploeg, M.D., Ph.D.[2,3]; W.W.M. Pim Pijnappel, Ph.D.[1,2,3]*; Niek P. van Til, Ph.D.[4,6]*

[1] Molecular Stem Cell Biology, Department of Clinical Genetics, Erasmus University Medical Center, 3015GE Rotterdam, The Netherlands
[2] Department of Pediatrics, Erasmus University Medical Center, 3015GE Rotterdam, The Netherlands
[3] Center for Lysosomal and Metabolic Diseases, Erasmus University Medical Center, 3015GE Rotterdam, The Netherlands
[4] Department of Hematology, Erasmus University Medical Center, 3015GE Rotterdam, The Netherlands
[5] Hospital Pharmacy, Erasmus University Medical Center, 3015GE Rotterdam, The Netherlands
[6] Current address: Laboratory of Translational Immunology, University Medical Center Utrecht, 3584CX Utrecht, The Netherlands

* Correspondence:
Dr. N.P. van Til, University Medical Center Utrecht, Heidelberglaan 100, 3584 CX Utrecht, The Netherlands.
Email: N.P.vanTil@umcutrecht.nl.
Dr. W.W.M. Pim Pijnappel, Erasmus University Medical Center, 3015GE Rotterdam, The Netherlands.
Email: w.pijnappel@erasmusmc.nl.

Manuscript submitted

ABSTRACT

The current standard of care for Pompe disease, a lysosomal storage disease due to deficiency of acid α-glucosidase (GAA), is enzyme replacement therapy (ERT). While ERT has shown to improve life expectancy, major drawbacks include poor enzyme delivery to target tissues, the enzyme's inability to cross the blood-brain barrier, and the development of neutralizing antibodies. Hematopoietic stem cell-mediated lentiviral gene therapy provides a novel, potentially life-long therapy via a single intervention. It can also induce immune tolerance, but little is known on its robustness and its compatibility with ERT. In a *Gaa* knockout mouse model for Pompe disease, we found that lentiviral expression of a low, sub-therapeutic dose of recombinant human GAA was sufficient to induce immune tolerance to the transgene product and as well as to complementary ERT within 4 weeks after transplantation of transduced hematopoietic progenitor cells. ERT was tolerated up to doses 5-fold higher than the standard dosing at 20 mg/kg. At sub-therapeutic gene therapy treatment, the induction of immune tolerance resulted in survival of mice that would have otherwise died from ERT-induced anaphylactic shock. In these mice, ERT corrected glycogen accumulation in cardiac and skeletal muscle, and to normalized their performance on a rotarod. Collectively, our data demonstrate that hematopoietic stem cell-mediated lentiviral gene therapy can induce a complete and robust humoral immune tolerance to both the transgene product and to ERT. These properties eliminate a major drawback of ERT, and warrant further investigations of lentiviral gene therapy as a treatment option for Pompe disease.

INTRODUCTION

Pompe disease, also termed glycogen storage disease type II (GSDII, OMIM 232300), is an autosomal recessive metabolic disorder caused by deficiency of the lysosomal enzyme acid alpha-glucosidase (GAA). This leads to glycogen accumulation that eventually results in tissue damage and loss of function.[1,2] Classic infantile Pompe disease is the most severe form and is caused by a complete GAA enzyme deficiency. It is featured by left ventricle cardiomyopathy and general skeletal muscle weakness at birth. Without treatment, classic infantile Pompe patients die within the first year of life due to cardiorespiratory failure.[3,4] A milder and more slowly progressive phenotype also exists and is explained by a partial deficiency with residual GAA activity.[5,6] These patients have progressive skeletal muscle weakness while cardiac abnormalities are more rare, and the age of symptom onset can vary from early childhood to late adult.[7,8]

Clinical trials for enzyme replacement therapy (ERT) with recombinant human acid alpha-glucosidase (rhGAA) derived from either rabbit milk[9-13] or Chinese hamster ovary cells (CHO)[14,15] have shown reversal of cardiomyopathy, improved skeletal muscle function, and enhanced survival in classic infantile Pompe patients. Improved skeletal muscle strength and function were also observed in late-onset Pompe patients after 3 years of treatment.[16] These findings paved the way for approval of ERT for Pompe disease (Myozyme, Genzyme Corporation) in 2006 and since then, ERT has shown to be effective in prolonging lifespan and improving muscle function.[17-23]

Despite the promise of ERT, there are a number of drawbacks. The response to ERT is heterogeneous. In addition, slowly progressing white matter abnormalities have been observed in the central nervous system (CNS) of classic infantile patients.[24-26] Reasons for this include the poor delivery of systemically applied rhGAA to target tissues, as delivery to skeletal muscle is inefficient,[27,28] while the blood-brain barrier prevents delivery to the CNS. Another complication of ERT is antibody formation to rhGAA. This may counteract ERT by blocking entry of GAA into the cells or lysosomes through the mannose-6-phophate receptor, or by blocking the catalytic domain of rhGAA and thereby reduce its enzymatic activity.[29-32] Accumulating evidence indicates that in classic infantile patients, the efficacy of ERT is attenuated when high sustained antibody (Ab) titers against rhGAA are formed.[14,15,17,18,33,34] This has now initiated the development of immunomodulatory protocols aimed to reduce antibody formation in classic infantile Pompe patients.[35-37] In particular, CRIM negative patients, in which GAA protein is not detectable, are at risk for formation of high sustained antibody titers. These patients have a poor prognosis and have the highest risk of early death due to cardiorespiratory insufficiency.[34,38]

Hematopoietic stem cell mediated lentiviral gene therapy provides an attractive potential alternative treatment for lysosomal storage disease (LSD). Clinical trials have been initiated for several disorders including Wiskott–Aldrich syndrome,[39,40] β-Thalassemia major,[41] X-linked adrenoleukodystrophy,[42,43] and metachromatic leukodystrophy[44,45] resulting in improved clinical outcomes.[46,47] While previous trials using retroviral backbones resulted in several cases of insertional mutagenesis-induced leukemia,[48,49] current lentiviral backbones have proven to be safe in trials up to 7 years of follow up.[45]

Previously, our laboratory generated *Gaa* knockout (*Gaa*$^{-/-}$) mice that have complete absence of GAA resulting in a generalized lysosomal glycogen accumulation. Symptoms and tissue pathology were indicative of classic infantile Pompe disease.[50-52] Using this mouse model, it was demonstrated that hematopoietic stem cell mediated lentiviral gene therapy with human GAA resulted in increased GAA enzyme activity in host tissues, reduction of glycogen accumulation, and improvement of cardiac and skeletal muscle function.[53] While intravenous treatment with rhGAA results in a strong immune response in *Gaa*$^{-/-}$ mice, evidenced by high anti-rhGAA antibody titers and anaphylactic shock,[54,55] hematopoietic stem cell mediated lentiviral gene therapy induced immune tolerance to the GAA transgene for at least 2 challenges with rhGAA.[53] This was further confirmed by others using an extended protocol with 5 weekly infusions.[56] This approach was also successfully applied to induce tolerance to factor VIII and IX in hemophilia A[57,58] and hemophilia B[59-61] mouse models, respectively.

As the extra beneficial role for *ex vivo* lentiviral gene therapy as an immunomodulatory regimen in Pompe patients has now become evident, it is important to gain a better understanding of the requirements to successfully establish immune tolerance. Here, we have investigated the relationship between ERT and immune tolerance induction for several parameters including timing, viral dose, robustness at high ERT doses, and reversal of disease symptoms.

METHODS

Animals

Immunocompetent *Gaa* knockout (*Gaa*$^{-/-}$) mice were used.[50] Age-matched FVB/N mice were purchased from Charles River as wildtype control. All mice were housed under specific pathogen free (SPF) conditions in the Animal Experimental Center at the Erasmus MC (EDC) according to standard procedures, including a 12-hour light-dark cycle and *ad libitum* diet. All animal experiments conformed to the Dutch law for the

protection of animals used for scientific procedures and were approved by Animal Experiments Committee (DEC) in the Netherlands.

Lentiviral vector construction and production

Codon-optimized human *GAA* sequence (*GAAco*, GenScript, Piscataway, NJ) was cloned into the previously described[53] third generation self-inactivating (SIN)[62] lentiviral vector pRRL.PPT.SF.GFP.bPRE4*.SIN (LV-SF-GFP) by replacing GFP using AgeI and SbfI restriction sites. Expression of the transgene was driven by the spleen focus forming virus (SF) promoter. Lentiviruses were produced by calcium phosphate transfection of 293T cells with plasmids pMDL-g/pRRE, pMD2-VSVg and pRSV-Rev and concentrated according to standard procedures.[63,64]

Lentiviral hematopoietic stem cell transduction, transplantation, and ERT

Bone marrow cells were extracted from male *Gaa*$^{-/-}$ donor mice at the age of 8 weeks, enriched through lineage depletion (Lin$^-$) using the mouse hematopoietic progenitor cell enrichment kit (BD Sciences, San Jose, CA), and transduced overnight. On the following day, 5×10^5 transduced Lin$^-$ cells were transplanted intravenously through the tail vein into 8-week-old female *Gaa*$^{-/-}$ recipients, previously subjected to 6 Gy (or 2 Gy in one setting) sublethal irradiation using a Gammacell 40 (Atomic Energy of Canada LTD., Ontario, Canada). ERT with recombinant human acid α-glucosidase (rhGAA, Myozyme, Genzyme corporation, Cambridge, MA) was administered through the tail vein.

Molecular and functional assays

Enzyme-linked immunosorbent assay (ELISA) of plasma was performed as described[38,53] with adjustments. Motor function was evaluated on a rotarod.[53] GAA enzyme activity[65] and glycogen content[66] were measured as described. The vector copy number (VCN) and chimerism was determined by quantitative polymerase chain reaction (qPCR) [53] with few modifications.

Statistics

Statistical analysis was performed with SPSS (IBM, version 22). Repeated measures ANOVA was applied to detect differences of antibody titer between treatment over the course of ERT, with Tukey's comparison test for individual comparisons among groups. Multiple comparisons were analyzed by one-way ANOVA followed by Bonferroni's multiple testing correction. Mann-Whitney U test was used for comparison of two groups. A P value ≤ 0.05 was considered statistically significant.

Additional information can be found in the supplementary Methods.

RESULTS

Effect of viral gene dosage on immune tolerance induction

It has been shown previously that hematopoietic stem cell mediated lentiviral gene therapy can induce immune tolerance to rhGAA in *Gaa*$^{-/-}$ mice.[53,56] Immune tolerance was induced to the transgene product as well as to subsequent intravenously applied rhGAA. The relation of lentiviral dosage to effectively induce immune tolerance is however unknown. To test this, we compared MOI 2, which has only partial efficacy in our Pompe mouse model (see below), with MOI 20 (see Figure 1A for the treatment schedule). MOI 20 corresponded to an average vector copy number (VCN) of 8 copies per genome and 43% chimerism (Figures S1A-B). At MOI 2, these values were on average 3 copies per genome and 64% chimerism (Figures S1A-B). Twelve weeks were used as interval between the start of gene therapy and the start of ERT to ensure full hematopoietic reconstitution following transplantation.[67,68] LV-SF-GAAco-treated mice were treated weekly with ERT at 20 mg/kg for 10 weeks, whereas only 2 injections were administered in LV-SF-GFP treated mice to avoid anaphylactic shock.[54,66,69,70] Mice that underwent gene therapy with the LV-SF-GFP vector developed a high sustained antibody titer to rhGAA when treated with ERT (Figure 1B, open squares). Gene therapy with the LV-SF-GAAco vector at MOI 20 prevented anti-rhGAA antibody formation in response to ERT (Figure 1B, open triangles, titers were ≤1:300, which is within the background levels of the assay, indicated in grey). At MOI 2, prevention of anti-rhGAA antibody formation in response to ERT was also achieved. At both MOIs, anti-rhGAA antibody formation was not detected in the absence of ERT treatment. We conclude that a low dose of LV-SF-GAAco can induce immune tolerance to both the transgene specific product and to rhGAA supplied as ERT. We therefore applied the low lentiviral vector dose in all subsequent experiments.

Timing of immune tolerance induction

The timing by which lentiviral gene therapy can induce immune tolerance was investigated by shortening the interval between gene therapy and the start of ERT from 12 weeks to 4 or 1 week (for experimental design see Figures 1C and 1E). At an interval of 4 weeks and MOI of 2, ERT treatment did not elicit antibody formation in LV-SF-GAAco-treated mice, whereas it caused significant antibody formation in LV-SF-GFP-treated mice (Figure 1D). The VCN in LV-SF-GAAco-treated mice was 3 copies per genome, while chimerism was 39% (Figures S1C-D), comparable to the results obtained at a 12-week interval. This indicates that immune tolerance can already be induced during incomplete immune reconstitution of the hematopoietic system, which takes 8-12 weeks in the mouse to complete.[67,68] When the interval was shortened to 1 week, anti-rhGAA antibodies were formed in both LV-SF-GFP and LV-SF-GAAco-treated mice (both at MOI 2), but at

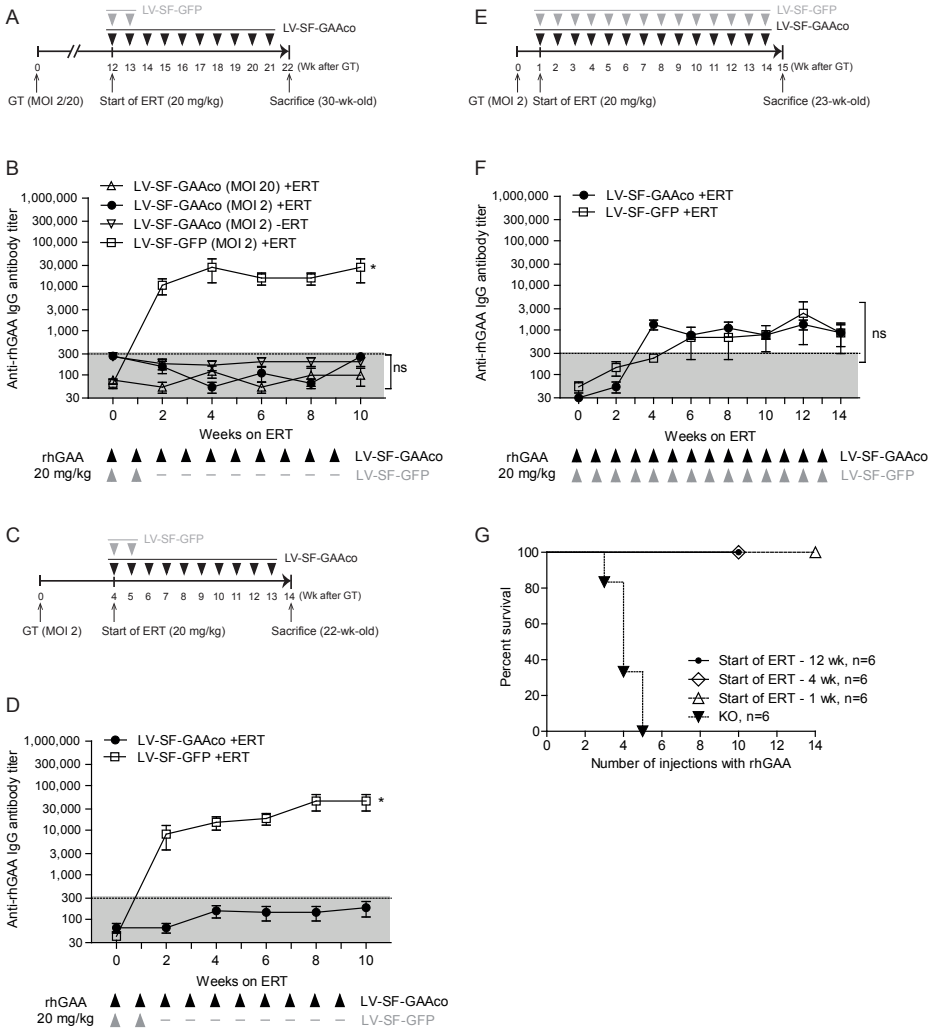

Figure 1. Timing of immune tolerance induction by HSC-mediated lentiviral gene therapy. (A, C, E): experimental set ups. (B, D, E): anti-rhGAA antibody titers as determined by ELISA. Grey zones indicate technical background of the ELISA assay, which was up to 1:300. Lentiviral gene therapy was started in 8-week-old immunocompetent *Gaa*$^{-/-}$ mice with the vectors indicated. ERT (weekly 20 mg/kg, i.v.) was started 12 weeks (A, B), 4 weeks (C, D), or 1 week (E, F) after gene therapy. Administration of ERT is indicated by arrowheads. The number of ERT doses in mice treated with LV-SF-GFP was adjusted based on preliminary experiments that indicated anaphylactic shock and death in response to ERT treatment. (G) Effect of immune tolerance induction on ERT-induced anaphylactic shock and death. Mice were treated with gene therapy using LV-SF-GAAco at MOI 2 following the schemes shown in (A, C, and E). *Gaa*$^{-/-}$ mice that did not receive gene therapy served as controls and died in response to ERT. Data are means ± SEM; n=6 per group. All groups were compared using repeated measures ANOVA with post hoc Tukey's analysis. *$P \leq 0.05$; ns, not significant. GT, gene therapy; MOI, multiplicity of infection; ERT, enzyme replacement therapy; wk, week; rhGAA, recombinant human acid α-glucosidase; IgG, immunoglobin G. ▲, injections in LV-SF-GAAco mice; ▲, injections in LV-SF-GFP mice; ▬, no injections.

low titers of up to 1:3,000, and these stabilized until the endpoint (Figure 1F) (compare to previous titers of 1:30,000). An expanded ERT scheme with 14 injections was applied in both groups to exclude any delayed immune response, which did not occur. These results had two implications: first, at an interval of 1 week, only partial immune tolerance induction to rhGAA was achieved, and second, partial tolerance was likely induced by systemically supplied rhGAA rather than lentiviral expressed GAA, because LV-SF-GFP treated mice obtained a similar immune tolerance to rhGAA as LV-SF-GAAco treated mice. The short interval between partial ablation of the hematopoietic system and the systemic administration of rhGAA likely allowed the immune system to recognize part of the systemically supplied rhGAA as being self. However, the VCN in LV-SF-GAAco treated mice was significantly lower than in LV-SF-GFP treated mice (1.7 vs 7; Figure S1E), or when compared to VCN obtained at 12- and 4- week intervals (3 and 3, respectively) with similar bone marrow chimerism (see Figures S1B,D,F). These results suggested a cytotoxic T cell mediated-response to cells expressing GAAco.[71] We conclude that lentiviral gene therapy starting at least 4 weeks prior to ERT can prevent formation of anti-rhGAA antibodies in the mouse. This interval was used in subsequent experiments.

Prevention of mortality in immune tolerant mice

In *Gaa*$^{-/-}$ mice without lentiviral gene therapy, up to three injections with rhGAA were tolerated. More than three injections resulted in death within 1 hour from anaphylactic shock.[55,69,72] All mice died after 5 injections (Figure 1G). Gene therapy with LV-SF-GAAco under conditions that prevented anti-rhGAA antibody formation allowed 100% survival (Figure 1G). In addition, mice that received LV-SF-GAAco and ERT at an interval of 1 week survived all 14 injections despite the formation of low anti-rhGAA antibody titers, indicating that the immune response was sufficiently reduced to prevent anaphylactic shock.

Dosing of ERT in immune tolerance induction

Recent studies suggest that a higher dosing of ERT may improve outcome in CRIM negative classic infantile Pompe patients.[73] No consistent effects of a higher dosing on antibody formation were observed but the number of patients analyzed so far remains small. On one hand, one could argue that exposure to higher concentration of antigen may increase the likelihood of antibody formation. On the other hand, in other disorders treated with recombinant proteins, higher dosing results in a gradual acquirement of immune tolerance.[74] To investigate the effect of ERT dosing on immune tolerance induction by lentiviral gene therapy, mice were treated with a dose of 100 mg/kg rhGAA on a weekly basis (see Figure 2A for experimental setup). Full suppression of antibody formation was observed in the LV-SF-GAAco-treated mice (Figure 2B). Mice treated with LV-SF-GFP showed antibody formation to rhGAA dosed at 100 mg/kg, although the titers

were lower (up to 1:10,000) compared to treatment with rhGAA dosed at 20 mg/kg. This may indicate that a higher dose of rhGAA weakens the immune response, which should be explored in future studies. The VCN in LV-SF-GAAco-treated mice was around 4 with 49% chimerism (Figures S2A-B), similar to the results obtained with the 20 mg/kg dosing scheme. We conclude that lentiviral gene therapy induces immune tolerance to ERT both when given at 20 mg/kg and at 100 mg/kg.

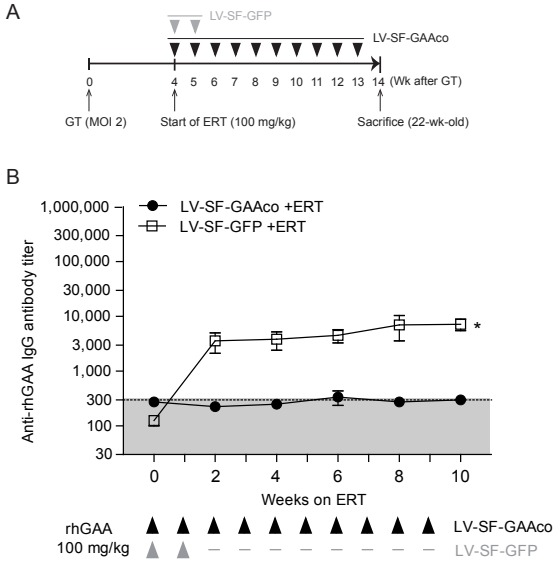

Figure 2. Effect of ERT dosing on immune tolerance induction. (A) Experimental set up. (B) Anti rhGAA antibody titers by ELISA. The experiment was identical as described in Figure 1C and D, except that now ERT was given at a dose of 100 mg/kg (weekly, i.v.). *$P \leq 0.05$.

Therapeutic efficacy of ERT after immune tolerance induction

Future lentiviral gene therapy may show heterogeneous efficacy, with a subset of treated patients that show subclinical benefit, for example due to insufficient engraftment efficiency. Those patients would require additional treatment with ERT to improve survival and clinical outcome. The current drawback of ERT, in particular in classic infantile Pompe patients, is formation of neutralizing anti-rhGAA antibodies. These can severely interfere with treatment outcome and survival. It is therefore important to test whether immune tolerance induction by subclinical lentiviral gene therapy allows ERT to be effective in the long term by preventing antibody formation. To test this, mice treated with a low MOI of LV-SF-GAAco were treated with ERT at a dose of 20 mg/kg or 100 mg/kg 4 weeks after gene therapy (See Figure 1C and Figure 2A for experimental set-up, respectively). PBS injections were used as control for ERT treatment. Without ERT, LV-SF-GAAco treatment at low MOI resulted in increased GAA enzymatic activity in the heart, quadriceps femoris, and diaphragm (Figures. 3A-B), but only in a partial reduction of glycogen levels in these tissues (Figures 3C-D) and

a partial restoration of rotarod function (Figures 3E-F). Treatment with ERT 4 weeks after gene therapy provided additional efficacy. At a dose of 20 mg/kg, efficacy was improved but was still incomplete compared to wild type mice (Figures 3A,C,E), in line with previously reports on the partial efficacy of ERT in mice at this dose.[54] At 100 mg/kg ERT, full correction of glycogen levels and rotarod performance was achieved (Figures 3D,F). We conclude that immune tolerance induction by lentiviral gene therapy allowed ERT to be effective in normalization of glycogen levels in heart and skeletal muscles and in restoration of skeletal muscle motor function.

Effect of conditioning for lentiviral gene therapy on immune responses

To test the effect of the pre-transplant conditioning regimen on immune tolerance induction, we applied total body irradiation (TBI) at 2 Gy instead of 6 Gy (Figure 4A). Four weeks after transplantation, all LV-SF-GAAco treated mice died within the first hour after the first injection with rhGAA due to anaphylactic shock (data not shown). Therefore, at a second attempt, we tested antibody levels prior to the start of ERT (Figure 4B), and these titers were 1:100,000 already at two weeks after gene therapy and in the absence of any challenges from rhGAA. Notably, these titers were higher than in mice treated with LV-SF-GFP (1:30,000). After 4 weeks, titers plateaued at 1:1,000,000. Anti-rhGAA titers in mice treated with LV-SF-GFP and ERT were up to 1:30,000, similar as in Fig. 1. This indicated that 2 Gy conditioning was intolerable to infusion of gene modified cells expressing GAAco. Analysis of the VCN and chimerism in bone marrow confirmed this idea, as both were very low to undetectable (Figures 4C-D).

Failure of immune tolerance induction after start of ERT

To investigate whether lentiviral gene therapy can also induce immune tolerance after the start of ERT, we administered rhGAA to naïve mice 2 days before gene therapy, and resumed administration of rhGAA 1 week later (Figure 5A). After 5 injections, ERT was stopped because several mice died, notably 1 mouse treated with LV-SF-GAAco and 2 mice treated with LV-SF-GFP. Antibody titers were measured in the surviving mice and ranged from 1:3000 to 1:1,000,000, starting at 2 weeks post-gene therapy (Figure 5B). The VCN in bone marrow from LV-SF-GAAco treated mice was undetectable (Figure 5C), while chimerism was 25-45% (Figure 5D). In contrast, the surviving mouse treated with LV-SF-GFP showed a VCN of 6 and a chimerism of 29%. The failure to detect bone marrow cells that contained integration of LV-SF-GAAco suggest an effective immune response against such cells, possibly caused by cytotoxic T cell-mediated destruction.[71] These results indicate that gene therapy was unable to prevent antibody formation when ERT was given in advance.

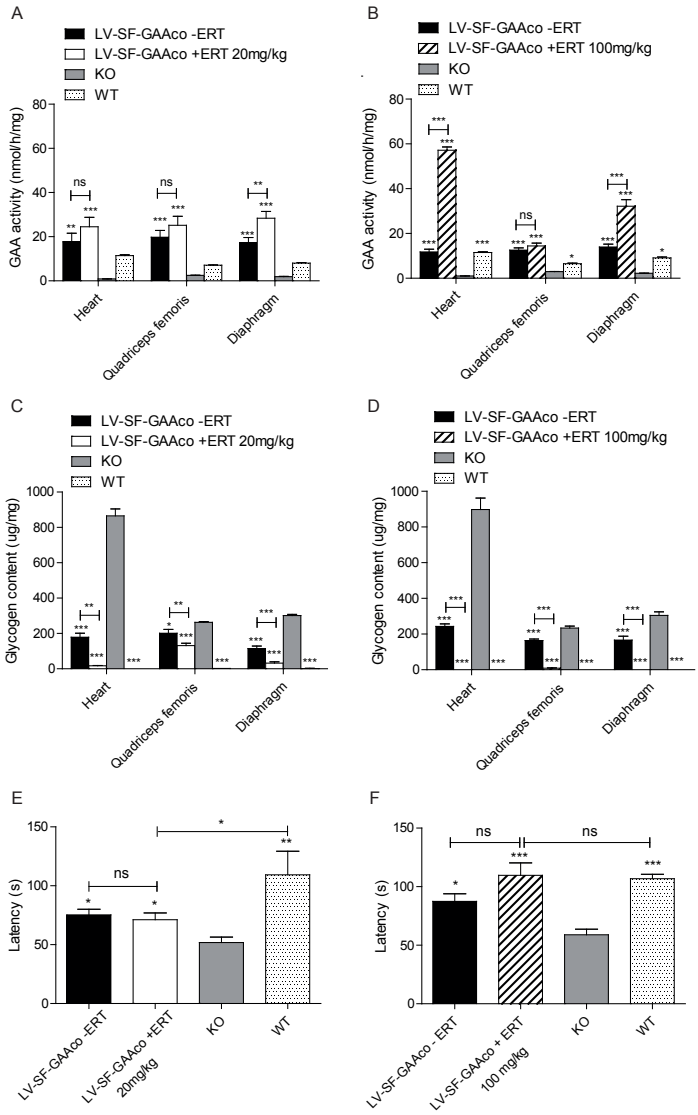

Figure 3. Efficacy of ERT following immune tolerance induction. (A, C, E): therapeutic efficacy in immune-tolerant mice treated with 20 mg/kg rhGAA (weekly, i.v.). (B, D, F): therapeutic efficacy in immune-tolerant mice treated with 100 mg/kg rhGAA (weekly, i.v.). The scheme shown in Figures 1C and 2A was used. Tissues indicated were collected for analysis 1 week after the last injection with rhGAA. LV-SF-GAAco treated mice that received weekly PBS injections were included to evaluate the effect of gene therapy alone. These mice were derived from independent experiments at two different dosing to guarantee a uniform background level from lentiviral gene therapy. Age-matched untreated *Gaa*$^{-/-}$ and wildtype mice served as controls. (A, B) GAA enzymatic activity. (C, D) Glycogen levels. (E, F) Motor function as measured by rotarod. Latency on the rotarod was evaluated after the 10th injection. Data are represented as means ± SEM; n=6 per group in panels A,C,E; n=5 per group in panels B,D; n=8 per group in panel F. Asterisks without bar indicated comparison to KO mice and additional comparison is indicated with bars. *P≤ 0.05; **P≤ 0.01; ***P≤ 0.001; ns, not significant.

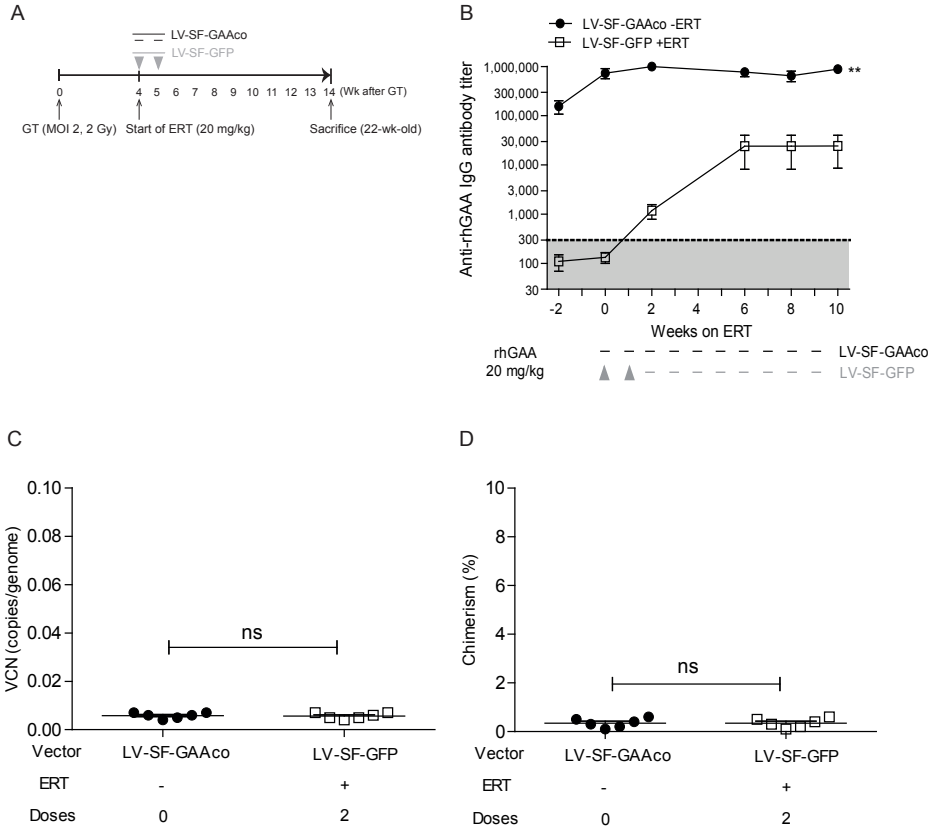

Figure 4. Immune tolerance induction is dependent on conditioning. (A) Experimental design. The experiment was comparable to that depicted in Figures 1C and D, except that recipient mice received a total body irradiation dose of 2 Gy instead of 6 Gy, and that rhGAA was not administered to LV-GAAco treated mice because these already developed very high anti-rhGAA antibody titers to lentiviral-expressed rhGAA (see B). (B) Anti-rhGAA IgG titers as determined by ELISA. (C) Vector copy number was determined in bone marrow by qPCR to the *HIV* gene and normalized to mouse *Gapdh*. (D) Chimerism, the percentage of male donor cells in female recipient bone marrow, as determined by *Sry* qPCR and corrected for mouse *Gapdh*. Data are represented as means ± SEM; n=6 per group. $^{**}P \leq 0.01$; ns, not significant.

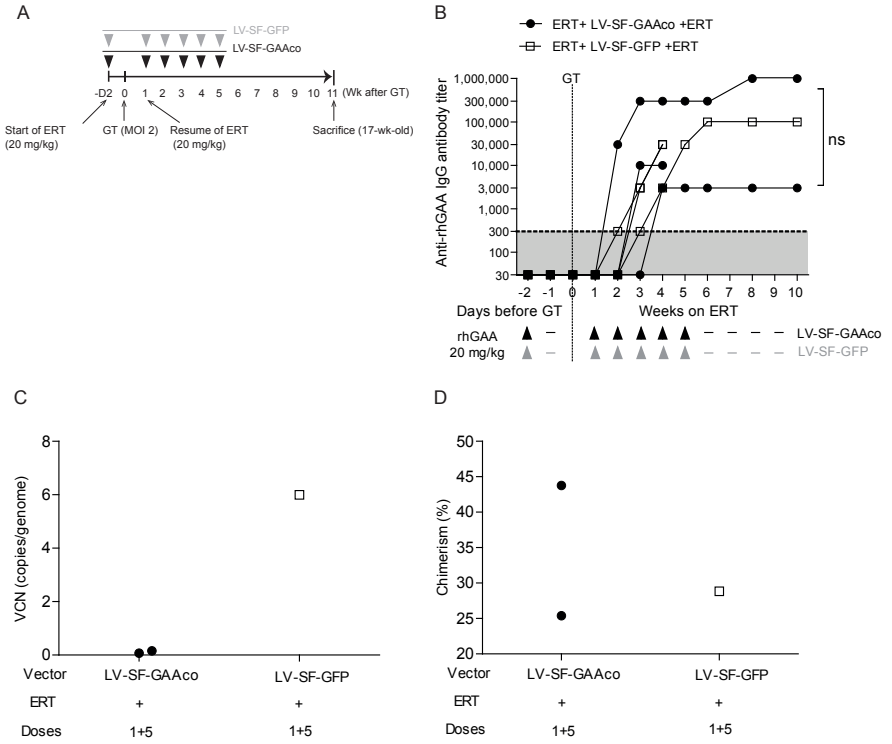

Figure 5. Immune reactions in mice treated with rhGAA prior to lentiviral gene therapy. (A) Sequence of treatment events. One injection of rhGAA (20 mg/kg, i.v.) was given to 8-week-old naïve *Gaa*$^{-/-}$ mice (n=3 per group). Two days later, lentiviral gene therapy was initiated with the vectors indicated. ERT (weekly 20 mg/kg, i.v.) was started 1 week after gene therapy and halted after 5 injections due to anaphylactic shock-induced death in both groups (see below) (1 from the LV-SF-GAAco and 2 from the LV-SF-GFP treated cohort). (B) Anti-rhGAA IgG titers. Data are shown for each individual mouse. Vector copy number (C) and chimerism (D) were determined in bone marrow as in Figure 4. In panels C and D, n=2 in the LV-SF-GAAco group (1 mouse died, see above) and n=1 in the LV-SF-GFP group (2 mice died, see above). ns, not significant.

DISCUSSION

We have investigated conditions for immune tolerance induction by hematopoietic stem cell mediated gene therapy in a *Gaa*$^{-/-}$ mouse model for Pompe disease. Our results indicate that this approach prevents antibody formation to the GAA transgene product, and that in addition, it allows efficacy of intravenously applied rhGAA (ERT). Partial immune tolerance to ERT is already in place at least 1 week following sublethal conditioning and gene therapy, and effective prevention of humoral immunity to rhGAA immune tolerance was achieved 4 weeks after gene therapy. Challenges with ERT at doses that were 5 times higher than clinically used doses did not impede gene

therapy-induced tolerance. Sub-therapeutic gene therapy treatment allowed long-term efficacy of ERT, enabling full phenotypic correction of skeletal muscle pathology and function. In the absence of gene therapy, ERT induced immune-mediated death. These results show that hematopoietic stem cell mediated lentiviral gene therapy induces robust immune tolerance to the transgene product and to ERT. In this respect, it removes an important drawback associated with current ERT treatment that is especially relevant for classic infantile Pompe patients.

Central versus peripheral immune tolerance

Two major strategies for gene therapy for Pompe disease have been reported, and each of these induces immune tolerance. The strategy described in this report uses hematopoietic stem cells that are transduced *ex vivo* with a lentivirus expressing a GAA transgene, and has been previously described by us and Douillard-Guilloux et al.[53,56] Another approach is to use adeno-associated virus (AAV) vectors that can deliver *GAA*. AAV has been applied systemically or intramuscularly, using a GAA transgene driven by a liver-specific promoter, and/or muscle specific promoter.[75-77] Interestingly, selective expression of GAA in the liver also induces immune tolerance.[69,78,79] However, there are important differences between these two strategies that may be explained by different mechanisms of action of immune tolerance induction.

In hematopoietic stem cell mediated lentiviral gene therapy, autologous gene-modified stem cell progenitors are used to deliver the missing gene. A series of experiments has indicated that this procedure results in both central and peripheral immune tolerance.[80,81] Central tolerance is induced by elimination of alloreactive CD8+ T cells in the thymus.[82-85] Although alloreactive CD4+ cells are not completely eliminated, tolerance induction is complete, as judged from the ability for long-term allogenic skin engraftment.[86] In addition, peripheral immune tolerance is also induced via formation of regulatory T cells.[87] In AAV-mediated gene therapy for Pompe disease, immune tolerance can be induced by liver-specific transgene expression via establishment of peripheral immune tolerance involving the induction of regulatory T cells.[55,88] However, variable therapeutic efficacy of such approach has been reported.[88-90] To improve efficacy, ubiquitous transgene expression or direct delivery to the skeletal muscle in the diaphragm have been tested, but these procedures could not prevent an immune response to the transgene product that interfered with therapeutic efficacy.[88,91] Recently, co-packaging of liver-specific and muscle-specific AAV particles has been described that combined immune tolerance induction and therapeutic efficacy in mice.[90] Achievement of peripheral immune tolerance is an advantage, however, this type of tolerance can be temporarily, as CD4+CD25+FoxP3+Tregs can lose FoxP3 expression, and worse, these cells have the ability to become memory T cells capable of recogniz-

ing previously tolerant antigens and act as effector T cells that generate an immune response.[92,93] In contrast, central immune tolerance induced by lentiviral gene therapy is thought to be permanent.[80,85] These reports highlight the importance of immune regulation against the transgene product in gene therapy, and the potential impact of the gene therapy approach taken on immune tolerance induction.

LV gene therapy versus ERT

The timing of immune tolerance induction and the combination with ERT treatment is of crucial importance when this therapy would be applied to classic infantile Pompe patients. The reason for this is that in the absence of treatment these patients rapidly deteriorate and die within 1 year of age. When a patient is diagnosed with classic infantile Pompe disease, it would be highly desirable to start treatment immediately to prevent irreversible muscle damage and to improve the condition of the patient prior to gene therapy. Newborn screening will be important for early diagnosis of classic infantile patients [94]. We showed that ERT before gene therapy prevents immune tolerance induction (Figure 5), highlighting the importance of applying gene therapy to naïve patients or to use immunosuppression until gene therapy has been applied. Immune tolerance to ERT was partial one week after lentiviral gene therapy (Figures 1E,F). Interestingly, a similar level of immune tolerance to ERT was observed when a mock lentiviral transduction was used and the mice were challenged with ERT one week later. This suggests that early exposure to a 'foreign' protein during early hematopoietic reconstitution can induce partial immune tolerance to that protein, similar to other studies.[95,96] This would be an important clinical benefit of the approach. No detectable anti-rhGAA antibodies were formed 4 weeks after gene-modified HSC transplantation. This indicates that full reconstitution of the hematopoietic stem cell compartment, which takes 8-12 weeks in the mouse,[67,68] is not required to induce efficient immune tolerance. In human Pompe patients the optimal timing of immune tolerance induction using this approach remains to be determined.

Robustness of immune tolerance induction

It remains possible that when it comes to clinical implementation, certain Pompe patients will have insufficient engraftment of transduced hematopoietic stem cells. Therefore, these patients would need additional ERT to treat symptoms. Recent work has suggested that the recommended dosing in classic infantile patients (20 mg/kg, biweekly) is insufficient and that increased dosing (e.g. 40 mg/kg weekly) provides a better prognosis.[73] Similarly to Pompe patients, 20 mg/kg cannot fully reverse the phenotype in *Gaa*$^{-/-}$ mice even when given weekly.[54] This raises the question whether increased dosing would result in altered antibody titers, and whether it affects immune tolerance induction. In hemophilia A, prolonged treatment with higher doses

of factor VIII provides gradual immune tolerance over a period of several years.[97,98] In classic infantile Pompe patients, anti-rhGAA antibody titers were similarly high in patients treated with 20 mg/kg (biweekly) as with 40 mg/kg weekly.[73] Lentiviral gene therapy in Pompe mice showed prevention of humoral immunity to even higher ERT doses (100 mg/kg weekly), highlighting the robustness of its immune tolerance induction effects. This was also evident from the fact that Pompe *Gaa*$^{-/-}$ mice, which normally die in response to ERT due to anaphylactic reactions,[55,69,72] now remained alive and showed full therapeutic response to ERT treatment at 100 mg/kg/week.

CONCLUSION

While clinical development of lentiviral gene therapy for Pompe disease seems promising, it will be a challenge to perform a tolerable conditioning regimen in severely disabled classic infantile patients to achieve engraftment levels that are safe yet provide sufficient clinical efficacy. But when it can be successfully applied in these patients, lentiviral gene therapy has major benefits by providing long-term therapeutic efficacy with immune tolerance induction. Therefore, even if gene therapy would result in sub-therapeutic efficacy, it does not disqualify patients to receive complementary ERT to be fully effective.

ACKNOWLEDGEMENTS

This work was supported by The Netherlands Organization for Health Research ZonMW (project number: 40-40300-98-07010) and the Erasmus Medical Center. Q.L was additionally supported by the China Scholarship Council (File No. 201206240040)

REFERENCES

1. Hirschhorn R, Reuser AJJ. Glycogen storage disease type II: acid α-glucosidase (acid maltase) deficiency. In: Scriver C, Beaudet, AL, Sly, WS and Valle, D ed. The Metabolic and Molecular Basis for Inherited Disease. New York: McGraw-Hill; 2001:3389–3420.
2. van der Ploeg AT, Reuser AJ. Pompe's disease. *Lancet.* 2008;372(9646):1342-1353.
3. van den Hout HM, Hop W, van Diggelen OP, et al. The natural course of infantile Pompe's disease: 20 original cases compared with 133 cases from the literature. *Pediatrics.* 2003;112(2):332-340.
4. Kishnani PS, Hwu WL, Mandel H, et al. A retrospective, multinational, multicenter study on the natural history of infantile-onset Pompe disease. *J Pediatr.* 2006;148(5):671-676.
5. Wokke JH, Ausems MG, van den Boogaard MJ, et al. Genotype-phenotype correlation in adult-onset acid maltase deficiency. *Ann Neurol.* 1995;38(3):450-454.
6. Kroos M, Hoogeveen-Westerveld M, van der Ploeg A, Reuser AJ. The genotype-phenotype correlation in Pompe disease. *Am J Med Genet C Semin Med Genet.* 2012;160C(1):59-68.
7. Hagemans ML, Winkel LP, Van Doorn PA, et al. Clinical manifestation and natural course of late-onset Pompe's disease in 54 Dutch patients. *Brain.* 2005;128(Pt 3):671-677.
8. Winkel LP, Hagemans ML, van Doorn PA, et al. The natural course of non-classic Pompe's disease; a review of 225 published cases. *J Neurol.* 2005;252(8):875-884.
9. Van den Hout H, Reuser AJ, Vulto AG, Loonen MC, Cromme-Dijkhuis A, Van der Ploeg AT. Recombinant human alpha-glucosidase from rabbit milk in Pompe patients. *Lancet.* 2000;356(9227):397-398.
10. Van den Hout JM, Reuser AJ, de Klerk JB, Arts WF, Smeitink JA, Van der Ploeg AT. Enzyme therapy for pompe disease with recombinant human alpha-glucosidase from rabbit milk. *J Inherit Metab Dis.* 2001;24(2):266-274.
11. Van den Hout JM, Kamphoven JH, Winkel LP, et al. Long-term intravenous treatment of Pompe disease with recombinant human alpha-glucosidase from milk. *Pediatrics.* 2004;113(5):e448-457.
12. Klinge L, Straub V, Neudorf U, et al. Safety and efficacy of recombinant acid alpha-glucosidase (rhGAA) in patients with classical infantile Pompe disease: results of a phase II clinical trial. *Neuromuscul Disord.* 2005;15(1):24-31.
13. Klinge L, Straub V, Neudorf U, Voit T. Enzyme replacement therapy in classical infantile pompe disease: results of a ten-month follow-up study. *Neuropediatrics.* 2005;36(1):6-11.
14. Amalfitano A, Bengur AR, Morse RP, et al. Recombinant human acid alpha-glucosidase enzyme therapy for infantile glycogen storage disease type II: results of a phase I/II clinical trial. *Genet Med.* 2001;3(2):132-138.
15. Kishnani PS, Nicolino M, Voit T, et al. Chinese hamster ovary cell-derived recombinant human acid alpha-glucosidase in infantile-onset Pompe disease. *J Pediatr.* 2006;149(1):89-97.
16. Winkel LP, Van den Hout JM, Kamphoven JH, et al. Enzyme replacement therapy in late-onset Pompe's disease: a three-year follow-up. *Ann Neurol.* 2004;55(4):495-502.

17. Kishnani PS, Corzo D, Nicolino M, et al. Recombinant human acid [alpha]-glucosidase: major clinical benefits in infantile-onset Pompe disease. *Neurology*. 2007;68(2):99-109.
18. Kishnani PS, Corzo D, Leslie ND, et al. Early treatment with alglucosidase alpha prolongs long-term survival of infants with Pompe disease. *Pediatr Res*. 2009;66(3):329-335.
19. Nicolino M, Byrne B, Wraith JE, et al. Clinical outcomes after long-term treatment with alglucosidase alfa in infants and children with advanced Pompe disease. *Genet Med*. 2009;11(3):210-219.
20. van Capelle CI, van der Beek NA, Hagemans ML, et al. Effect of enzyme therapy in juvenile patients with Pompe disease: a three-year open-label study. *Neuromuscul Disord*. 2010;20(12):775-782.
21. van der Ploeg AT, Clemens PR, Corzo D, et al. A randomized study of alglucosidase alfa in late-onset Pompe's disease. *N Engl J Med*. 2010;362(15):1396-1406.
22. Gungor D, Kruijshaar ME, Plug I, et al. Impact of enzyme replacement therapy on survival in adults with Pompe disease: results from a prospective international observational study. *Orphanet J Rare Dis*. 2013;8:49.
23. Gungor D, Kruijshaar ME, Plug I, et al. Quality of life and participation in daily life of adults with Pompe disease receiving enzyme replacement therapy: 10 years of international follow-up. *J Inherit Metab Dis*. 2016;39(2):253-260.
24. Ebbink BJ, Aarsen FK, van Gelder CM, et al. Cognitive outcome of patients with classic infantile Pompe disease receiving enzyme therapy. *Neurology*. 2012;78(19):1512-1518.
25. Spiridigliozzi GA, Heller JH, Kishnani PS. Cognitive and adaptive functioning of children with infantile Pompe disease treated with enzyme replacement therapy: long-term follow-up. *Am J Med Genet C Semin Med Genet*. 2012;160C(1):22-29.
26. Ebbink BJ, Poelman E, Plug I, et al. Cognitive decline in classic infantile Pompe disease: An underacknowledged challenge. *Neurology*. 2016;86(13):1260-1261.
27. Raben N, Fukuda T, Gilbert AL, et al. Replacing acid alpha-glucosidase in Pompe disease: recombinant and transgenic enzymes are equipotent, but neither completely clears glycogen from type II muscle fibers. *Mol Ther*. 2005;11(1):48-56.
28. Raben N, Jatkar T, Lee A, et al. Glycogen stored in skeletal but not in cardiac muscle in acid alpha-glucosidase mutant (Pompe) mice is highly resistant to transgene-encoded human enzyme. *Mol Ther*. 2002;6(5):601-608.
29. Brooks DA. Immune response to enzyme replacement therapy in lysosomal storage disorder patients and animal models. *Mol Genet Metab*. 1999;68(2):268-275.
30. Brooks DA, Kakavanos R, Hopwood JJ. Significance of immune response to enzyme-replacement therapy for patients with a lysosomal storage disorder. *Trends Mol Med*. 2003;9(10):450-453.
31. Wang J, Lozier J, Johnson G, et al. Neutralizing antibodies to therapeutic enzymes: considerations for testing, prevention and treatment. *Nat Biotechnol*. 2008;26(8):901-908.
32. Matzner U, Matthes F, Weigelt C, et al. Non-inhibitory antibodies impede lysosomal storage reduction during enzyme replacement therapy of a lysosomal storage disease. *J Mol Med (Berl)*. 2008;86(4):433-442.

33. Kishnani PS, Goldenberg PC, DeArmey SL, et al. Cross-reactive immunologic material status affects treatment outcomes in Pompe disease infants. *Molecular Genetics and Metabolism.* 2010;99(1):26-33.

34. Berrier KL, Kazi ZB, Prater SN, et al. CRIM-negative infantile Pompe disease: characterization of immune responses in patients treated with ERT monotherapy. *Genet Med.* 2015;17(11):912-918.

35. Broomfield A, Jones SA, Hughes SM, Bigger BW. The impact of the immune system on the safety and efficiency of enzyme replacement therapy in lysosomal storage disorders. *J Inherit Metab Dis.* 2016;39(4):499-512.

36. Stenger EO, Kazi Z, Lisi E, Gambello MJ, Kishnani P. Immune Tolerance Strategies in Siblings with Infantile Pompe Disease-Advantages for a Preemptive Approach to High-Sustained Antibody Titers. *Mol Genet Metab Rep.* 2015;4:30-34.

37. Elder ME, Nayak S, Collins SW, et al. B-Cell depletion and immunomodulation before initiation of enzyme replacement therapy blocks the immune response to acid alpha-glucosidase in infantile-onset Pompe disease. *J Pediatr.* 2013;163(3):847-854 e841.

38. van Gelder CM, Hoogeveen-Westerveld M, Kroos MA, Plug I, van der Ploeg AT, Reuser AJ. Enzyme therapy and immune response in relation to CRIM status: the Dutch experience in classic infantile Pompe disease. *J Inherit Metab Dis.* 2015;38(2):305-314.

39. Aiuti A, Biasco L, Scaramuzza S, et al. Lentiviral hematopoietic stem cell gene therapy in patients with Wiskott-Aldrich syndrome. *Science.* 2013;341(6148):1233151.

40. Hacein-Bey Abina S, Gaspar HB, Blondeau J, et al. Outcomes following gene therapy in patients with severe Wiskott-Aldrich syndrome. *Jama.* 2015;313(15):1550-1563.

41. Cavazzana-Calvo M, Payen E, Negre O, et al. Transfusion independence and HMGA2 activation after gene therapy of human beta-thalassaemia. *Nature.* 2010;467(7313):318-322.

42. Cartier N, Hacein-Bey-Abina S, Bartholomae CC, et al. Hematopoietic stem cell gene therapy with a lentiviral vector in X-linked adrenoleukodystrophy. *Science.* 2009;326(5954):818-823.

43. Cartier N, Hacein-Bey-Abina S, Bartholomae CC, et al. Lentiviral hematopoietic cell gene therapy for X-linked adrenoleukodystrophy. *Methods Enzymol.* 2012;507:187-198.

44. Biffi A, Montini E, Lorioli L, et al. Lentiviral hematopoietic stem cell gene therapy benefits metachromatic leukodystrophy. *Science.* 2013;341(6148):1233158.

45. Sessa M, Lorioli L, Fumagalli F, et al. Lentiviral haemopoietic stem-cell gene therapy in early-onset metachromatic leukodystrophy: an ad-hoc analysis of a non-randomised, open-label, phase 1/2 trial. *Lancet.* 2016;388(10043):476-487.

46. Naldini L, Trono D, Verma IM. Lentiviral vectors, two decades later. *Science.* 2016;353(6304):1101-1102.

47. Naldini L. Gene therapy returns to centre stage. *Nature.* 2015;526(7573):351-360.

48. Hacein-Bey-Abina S, Von Kalle C, Schmidt M, et al. LMO2-associated clonal T cell proliferation in two patients after gene therapy for SCID-X1. *Science.* 2003;302(5644):415-419.

49. Hacein-Bey-Abina S, Garrigue A, Wang GP, et al. Insertional oncogenesis in 4 patients after retrovirus-mediated gene therapy of SCID-X1. *J Clin Invest.* 2008;118(9):3132-3142.

50. Bijvoet AG, van de Kamp EH, Kroos MA, et al. Generalized glycogen storage and cardiomegaly in a knockout mouse model of Pompe disease. *Hum Mol Genet.* 1998;7(1):53-62.
51. Bijvoet AG, Van Hirtum H, Vermey M, et al. Pathological features of glycogen storage disease type II highlighted in the knockout mouse model. *J Pathol.* 1999;189(3):416-424.
52. Kamphoven JH, Stubenitsky R, Reuser AJ, Van Der Ploeg AT, Verdouw PD, Duncker DJ. Cardiac remodeling and contractile function in acid alpha-glucosidase knockout mice. *Physiol Genomics.* 2001;5(4):171-179.
53. van Til NP, Stok M, Aerts Kaya FS, et al. Lentiviral gene therapy of murine hematopoietic stem cells ameliorates the Pompe disease phenotype. *Blood.* 2010;115(26):5329-5337.
54. Raben N, Danon M, Gilbert AL, et al. Enzyme replacement therapy in the mouse model of Pompe disease. *Mol Genet Metab.* 2003;80(1-2):159-169.
55. Sun B, Kulis MD, Young SP, et al. Immunomodulatory gene therapy prevents antibody formation and lethal hypersensitivity reactions in murine pompe disease. *Mol Ther.* 2010;18(2):353-360.
56. Douillard-Guilloux G, Richard E, Batista L, Caillaud C. Partial phenotypic correction and immune tolerance induction to enzyme replacement therapy after hematopoietic stem cell gene transfer of alpha-glucosidase in Pompe disease. *J Gene Med.* 2009;11(4):279-287.
57. Schroeder JA, Chen Y, Fang J, Wilcox DA, Shi Q. In vivo enrichment of genetically manipulated platelets corrects the murine hemophilic phenotype and induces immune tolerance even using a low multiplicity of infection. *J Thromb Haemost.* 2014;12(8):1283-1293.
58. Evans GL, Morgan RA. Genetic induction of immune tolerance to human clotting factor VIII in a mouse model for hemophilia A. *Proc Natl Acad Sci U S A.* 1998;95(10):5734-5739.
59. Chen Y, Schroeder JA, Kuether EL, Zhang G, Shi Q. Platelet gene therapy by lentiviral gene delivery to hematopoietic stem cells restores hemostasis and induces humoral immune tolerance in FIX(null) mice. *Mol Ther.* 2014;22(1):169-177.
60. Martinet J, Bourdenet G, Meliani A, et al. Induction of Hematopoietic Microchimerism by Gene-Modified BMT Elicits Antigen-Specific B and T Cell Unresponsiveness toward Gene Therapy Products. *Front Immunol.* 2016;7:360.
61. Bigger BW, Siapati EK, Mistry A, et al. Permanent partial phenotypic correction and tolerance in a mouse model of hemophilia B by stem cell gene delivery of human factor IX. *Gene Ther.* 2006;13(2):117-126.
62. Zufferey R, Dull T, Mandel RJ, et al. Self-inactivating lentivirus vector for safe and efficient in vivo gene delivery. *J Virol.* 1998;72(12):9873-9880.
63. Naldini L, Blomer U, Gage FH, Trono D, Verma IM. Efficient transfer, integration, and sustained long-term expression of the transgene in adult rat brains injected with a lentiviral vector. *Proc Natl Acad Sci U S A.* 1996;93(21):11382-11388.
64. Dull T, Zufferey R, Kelly M, et al. A third-generation lentivirus vector with a conditional packaging system. *J Virol.* 1998;72(11):8463-8471.
65. Okumiya T, Keulemans JL, Kroos MA, et al. A new diagnostic assay for glycogen storage disease type II in mixed leukocytes. *Mol Genet Metab.* 2006;88(1):22-28.

66. Bijvoet AG, Van Hirtum H, Kroos MA, et al. Human acid alpha-glucosidase from rabbit milk has therapeutic effect in mice with glycogen storage disease type II. *Hum Mol Genet.* 1999;8(12):2145-2153.

67. Leshem B, Tsuberi BZ, Lebendiker Z, et al. Bone marrow transplantation with T-cell-depleted grafts. II. Reconstitution of immunohemopoietic functions in lethally irradiated mice transplanted with unseparated or T-cell-depleted bone marrow grafts disparate at minor histocompatibility antigens. *Transplantation.* 1987;43(6):814-817.

68. Filip S, Mokry J, Vavrova J, et al. The peripheral chimerism of bone marrow-derived stem cells after transplantation: regeneration of gastrointestinal tissues in lethally irradiated mice. *J Cell Mol Med.* 2014;18(5):832-843.

69. Sun B, Bird A, Young SP, Kishnani PS, Chen YT, Koeberl DD. Enhanced response to enzyme replacement therapy in Pompe disease after the induction of immune tolerance. *Am J Hum Genet.* 2007;81(5):1042-1049.

70. Raben N, Nagaraju K, Lee A, et al. Induction of tolerance to a recombinant human enzyme, acid alpha-glucosidase, in enzyme deficient knockout mice. *Transgenic Res.* 2003;12(2):171-178.

71. Rosenzweig M, Connole M, Glickman R, et al. Induction of cytotoxic T lymphocyte and antibody responses to enhanced green fluorescent protein following transplantation of transduced CD34(+) hematopoietic cells. *Blood.* 2001;97(7):1951-1959.

72. Nayak S, Doerfler PA, Porvasnik SL, et al. Immune responses and hypercoagulation in ERT for Pompe disease are mutation and rhGAA dose dependent. *PLoS One.* 2014;9(6):e98336.

73. van Gelder CM, Poelman E, Plug I, et al. Effects of a higher dose of alglucosidase alfa on ventilator-free survival and motor outcome in classic infantile Pompe disease: an open-label single-center study. *J Inherit Metab Dis.* 2016;39(3):383-390.

74. Kubisz P, Plamenova I, Holly P, Stasko J. Successful immune tolerance induction with high-dose coagulation factor VIII and intravenous immunoglobulins in a patient with congenital hemophilia and high-titer inhibitor of coagulation factor VIII despite unfavorable prognosis for the therapy. *Med Sci Monit.* 2009;15(6):CS105-111.

75. Sun B, Zhang H, Franco LM, et al. Correction of glycogen storage disease type II by an adeno-associated virus vector containing a muscle-specific promoter. *Mol Ther.* 2005;11(6):889-898.

76. Sun B, Li S, Bird A, Koeberl DD. Hydrostatic isolated limb perfusion with adeno-associated virus vectors enhances correction of skeletal muscle in Pompe disease. *Gene Ther.* 2010;17(12):1500-1505.

77. Falk DJ, Soustek MS, Todd AG, et al. Comparative impact of AAV and enzyme replacement therapy on respiratory and cardiac function in adult Pompe mice. *Mol Ther Methods Clin Dev.* 2015;2:15007.

78. Franco LM, Sun B, Yang X, et al. Evasion of immune responses to introduced human acid alpha-glucosidase by liver-restricted expression in glycogen storage disease type II. *Mol Ther.* 2005;12(5):876-884.

79. Sun B, Li S, Bird A, et al. Antibody formation and mannose-6-phosphate receptor expression impact the efficacy of muscle-specific transgene expression in murine Pompe disease. *J Gene Med*. 2010;12(11):881-891.

80. Kung SK, An DS, Bonifacino A, et al. Induction of transgene-specific immunological tolerance in myeloablated nonhuman primates using lentivirally transduced CD34+ progenitor cells. *Mol Ther*. 2003;8(6):981-991.

81. Tian C, Bagley J, Kaye J, Iacomini J. Induction of T cell tolerance to a protein expressed in the cytoplasm through retroviral-mediated gene transfer. *J Gene Med*. 2003;5(5):359-365.

82. Kang ES, Iacomini J. Induction of central deletional T cell tolerance by gene therapy. *J Immunol*. 2002;169(4):1930-1935.

83. Krenger W, Blazar BR, Hollander GA. Thymic T-cell development in allogeneic stem cell transplantation. *Blood*. 2011;117(25):6768-6776.

84. Nossal GJ. Negative selection of lymphocytes. *Cell*. 1994;76(2):229-239.

85. Bagley J, Tian C, Sachs DH, Iacomini J. Induction of T-cell tolerance to an MHC class I alloantigen by gene therapy. *Blood*. 2002;99(12):4394-4399.

86. Forman D, Kang ES, Tian C, Paez-Cortez J, Iacomini J. Induction of alloreactive CD4 T cell tolerance in molecular chimeras: a possible role for regulatory T cells. *J Immunol*. 2006;176(6):3410-3416.

87. Chidgey AP, Layton D, Trounson A, Boyd RL. Tolerance strategies for stem-cell-based therapies. *Nature*. 2008;453(7193):330-337.

88. Zhang P, Sun B, Osada T, et al. Immunodominant liver-specific expression suppresses transgene-directed immune responses in murine pompe disease. *Hum Gene Ther*. 2012;23(5):460-472.

89. Sun B, Zhang H, Franco LM, et al. Efficacy of an adeno-associated virus 8-pseudotyped vector in glycogen storage disease type II. *Mol Ther*. 2005;11(1):57-65.

90. Doerfler PA, Todd AG, Clement N, et al. Copackaged AAV9 Vectors Promote Simultaneous Immune Tolerance and Phenotypic Correction of Pompe Disease. *Hum Gene Ther*. 2016;27(1):43-59.

91. Rucker M, Fraites TJ, Jr., Porvasnik SL, et al. Rescue of enzyme deficiency in embryonic diaphragm in a mouse model of metabolic myopathy: Pompe disease. *Development*. 2004;131(12):3007-3019.

92. Zhou X, Bailey-Bucktrout S, Jeker LT, Bluestone JA. Plasticity of CD4(+) FoxP3(+) T cells. *Curr Opin Immunol*. 2009;21(3):281-285.

93. da Silva Martins M, Piccirillo CA. Functional stability of Foxp3+ regulatory T cells. *Trends Mol Med*. 2012;18(8):454-462.

94. Chien YH, Chiang SC, Zhang XK, et al. Early detection of Pompe disease by newborn screening is feasible: results from the Taiwan screening program. *Pediatrics*. 2008;122(1):e39-45.

95. Murphy KM, Heimberger AB, Loh DY. Induction by antigen of intrathymic apoptosis of CD4+CD8+TCRlo thymocytes in vivo. *Science*. 1990;250(4988):1720-1723.

96. Liblau RS, Tisch R, Shokat K, et al. Intravenous injection of soluble antigen induces thymic and peripheral T-cells apoptosis. *Proc Natl Acad Sci U S A*. 1996;93(7):3031-3036.

97. Brackmann HH, Oldenburg J, Schwaab R. Immune tolerance for the treatment of factor VIII inhibitors--twenty years' 'bonn protocol'. *Vox Sang.* 1996;70 Suppl 1:30-35.

98. Hausl C, Ahmad RU, Sasgary M, et al. High-dose factor VIII inhibits factor VIII-specific memory B cells in hemophilia A with factor VIII inhibitors. *Blood.* 2005;106(10):3415-3422.

SUPPLEMENTARY DATA

METHODS

Lentiviral vector concentration and titration

Vectors were concentrated by ultracentrifugation (20,000 rpm, 4°C, 2 hrs). Lentiviral titers were determined in 2×10^5 HeLa cells, in which the vector copy numbers (VCNs) were determined 5 days after transduction by quantitative PCR (qPCR) using primers targeting the U3 and Psi sequences of *HIV* (listed in Table S1). A standard curve was prepared using HeLa cells carrying on average 1 copy of integrated lentiviral vector per genome. The final titers were determined by the average VCNs multiplied by the cell number (2×10^5) and fold dilution. Titers of approximately 10^8 transduction units/ml were routinely obtained for all virus vectors.

Lentiviral hematopoietic stem cell transduction

After enrichment, Lin^- cells were seeded in 6-well plates at a density of 10^6 cells/ml in StemMACS HSC expansion media (Miltenyl Biotec, Leiden, the Netherlands), supplemented with 3 growth factors: murine thrombopoietin (100 ng/mL), murine stem cell factor (100 ng/mL) and human FMS-like tyrosine kinase 3 murine ligand (50 ng/mL).[1] The cells were then transduced overnight with concentrated LV-SF-GAAco at various multiplicity of infections (MOIs, as specified in the figures) or with LV-SF-GFP at MOI 2 as control, and incubated at 37℃ with 10% CO^2.

Enzyme replacement therapy in *Gaa*$^{-/-}$ mice

Preceding or following lentiviral gene therapy, LV-SF-GAAco and LV-SF-GFP treated mice were divided into two groups: one group received enzyme replacement therapy (+ERT) with recombinant human acid α-glucosidase (rhGAA, Myozyme, Genzyme corporation, Cambridge, MA) through the tail vain at either 20 mg/kg or 100 mg/kg body weight; the other group was subjected to phosphate-buffered saline (PBS) alone (-ERT) using the same procedure. Plasma was collected at baseline and every other week during the course of ERT to monitor antibody titers, and mice were sacrificed 1 week after the last injection to evaluate the therapeutic effect.

Enzyme-linked immunosorbent assay (ELISA)

Samples were diluted 30 to 1,000,000 fold in 3-fold dilution series and analyzed in duplicate. Control plasma were incubated on uncoated plates to determine background levels of this method, which ranged between 1:30 and 1:300.[2] In each experiment, rabbit anti-GAA serum was included as positive control and plasma from

age-matched untreated FVB/N mouse as negative control. Titers were defined as the highest dilution at which absorbance was at least twice as high as the averaged value of the negative control plus 10%.

Rotarod

Motor function was evaluated on a rotarod accelerating from 4 to 40 rpm in 300 sec (Panlab, Harvard Apparatus, Holliston, MA). Prior to the experiment, mice were kept in the testing room to adjust to the environment for at least 15 min. A test session including 3 trials was then conducted for the mice to adjust to the apparatus, followed by 3 runs with intervals of 5 min. The latency before falling off the rotarod was recorded and averaged for each mouse.

GAA activity and glycogen content measurement

Mice were deprived of food overnight (15 hours) to deplete cytoplasmic glycogen.[3] They were then anesthetized by ketamine (10%, Alfasan, Woerden, the Netherlands) and sedator (1mg/ml, Eurovet, Bladel, the Netherlands) and sacrificed by intracardiac perfusion with 50ml PBS to remove blood. Tissues of interest including heart, diaphragm and quadriceps anterior were harvested and snap-frozen in liquid nitrogen and stored at -80°C until further analysis.

Tissue aliquots were homogenized completely in 300 µl distilled water using a TissueLyserII (Qiagen, Venlo, the Netherlands) for 5 mins at 30 Hz. Debris was pelleted by centrifugation at 10,000 rpm for 5 min, and the supernatant was used for assays of enzymatic activity and glycogen content. GAA enzymatic activity was determined using 4-methylumbelliferyl-α-D-glucoside (Sigma-Aldrich, St. Luis, MO) as substrate as decribed.[4] Glycogen content was quantified by the amount of glucose released from glycogen after conversion by amyloglucosidase and amylase (Roche Diagnostics, Basel, Switzerland) as previously detailed.[3] Both GAA activity and glycogen content were normalized to total protein levels using the Pierce BCA protein assay kit (Thermo Scientific, Waltham, MA).

Quantitative polymerase chain reaction of LV integrations

Genomic DNA, extracted from bone marrow (BM) using NucleoSpin tissue kit (Macherey-Nagel, Düren, Germany), was used at 100 ng per reaction. Reactions were performed using iTaq Universal Sybr Green Supermix (Bio-Rad, Hercules, CA). A standard curve for VCNs was prepared using serial dilutions of genomic DNA from transduced mouse 3T3 cells carrying 1 copy of integrated lentiviral vector per genome. Chimerism was determined using primers specific for the *Sry* locus on the mouse *Y* chromosome. Both VCN and chimerism were normalized by mouse *Gapdh*. BM DNA from untreated male

Gaa$^{-/-}$ donor mice were used to establish reference standard in *Sry* and *Gapdh* qPCR. Reactions were carried out in CFX96 real-time PCR detection system and analyzed by CFX Manager 3.0 (Bio-Rad, Hercules, CA). Primers sequences are reported in Table S1.

REFERENCES FOR SUPPLEMENTARY DATA

1. van Til NP, Stok M, Aerts Kaya FS, et al. Lentiviral gene therapy of murine hematopoietic stem cells ameliorates the Pompe disease phenotype. *Blood*. 2010;115(26):5329-5337.
2. de Vries JM, Kuperus E, Hoogeveen-Westerveld M, et al. Pompe disease in adulthood: effects of antibody formation on enzyme replacement therapy. *Genet Med*. 2016.
3. Bijvoet AG, Van Hirtum H, Kroos MA, et al. Human acid alpha-glucosidase from rabbit milk has therapeutic effect in mice with glycogen storage disease type II. *Hum Mol Genet*. 1999;8(12):2145-2153.
4. Okumiya T, Keulemans JL, Kroos MA, et al. A new diagnostic assay for glycogen storage disease type II in mixed leukocytes. *Mol Genet Metab*. 2006;88(1):22-28.

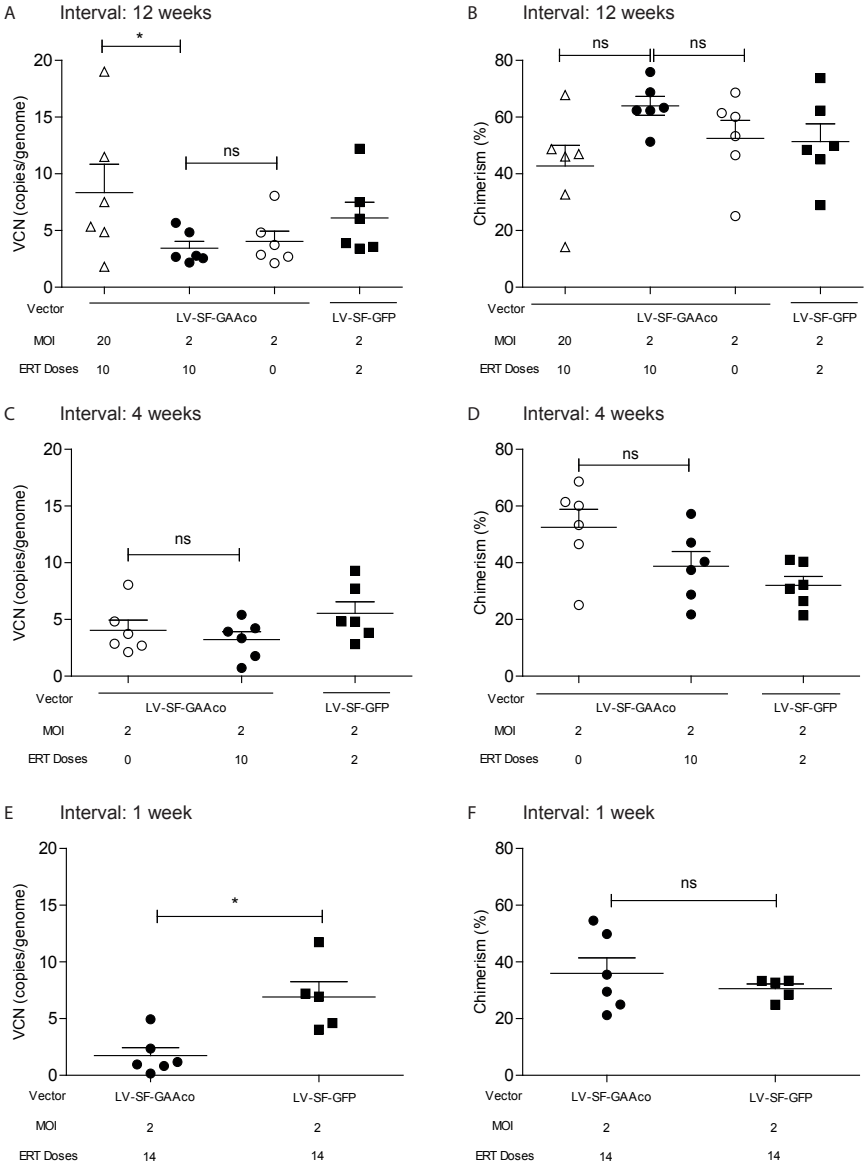

Figure S1. Timing of immune tolerance induction: vector copy number and chimerism. The data correspond to the experiments shown in Figure 1. ERT was started 12 weeks (A, B), 4 weeks (C, D), or 1 week (E, F) after gene therapy. Bone marrow was collected at the end of the experiment and vector copy number and chimerism were determined by *HIV* and *Sry* qPCR, respectively, and normalized using *Gapdh*. Data are means ± SEM; n=5 in LV-SF-GFP treated mice in panels E and F; the rest: n=6 per group. **P*≤ 0.05; ns, not significant.

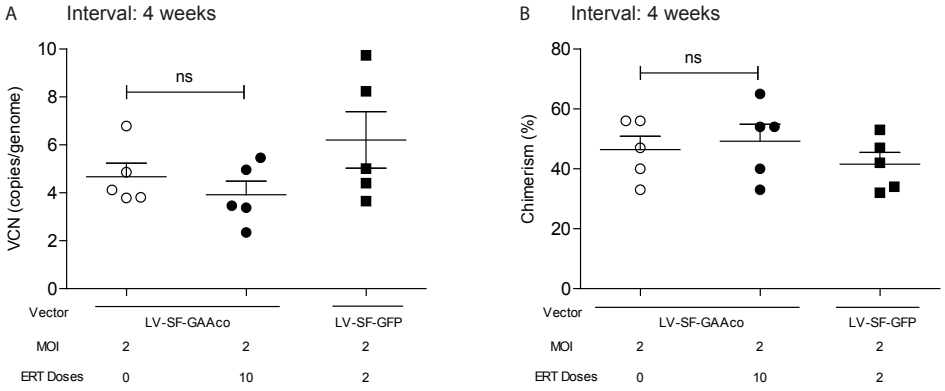

Figure S2. Dosing with ERT at 100 mg/kg: vector copy number and chimersm. The data correspond to the experiment shown in Figure 2. Vector copy number and chimerism were determined as in Figure S1. Data are means ± SEM; n=5 per group.

Table S1. Sequences of primers for qPCR

Primers	Sequence
HIV-U3 forward	5′-CTGGAAGGGCTAATTCACTC-3′
HIV-PSI reverse	5′-GGTTTCCCTTTCGCTTTCAG-3′
Sry forward	5′-TCATCGGAGGGCTAAAGTGTCAC-3′
Sry reverse	5′-TGGCATGTGGGTTCCTGTCC-3′
Gapdh forward	5′- TAATGGGGAGAGGTTCGATG -3′
Gapdh reverse	5′- GCTGCTTCCCGAGTAAAATG -3′

Chapter 7

General discussion

In this thesis, we have defined conditions for hematopoietic stem cell-mediated lentiviral gene therapy that mediate near-complete phenotypic correction in a mouse model for Pompe disease, including heart, skeletal muscle, and the central nervous system. The reversal of skeletal muscle pathology was confirmed at the proteomic level. Additionally, we have tested three promoters to replace the SF promoter. These promoters have been previously used in lentiviral gene therapy trials for other metabolic disorders resulting in significant efficacy. Furthermore, we have investigated immune tolerance induction to complementary recombinant GAA protein infusions. Below, we discuss consequences of our findings, future directions towards clinical application, as well as potential implementation of more recently developed state-of-the-art techniques.

1. THE ROLE OF NEUROINFLAMMATION IN CNS PATHOLOGY IN POMPE DISEASE

Neuroinflammation, typified by microglial and astrocyte activation, is a hallmark of the majority of neuronopathic lysosomal storage diseases (LSDs).[1-5] In Pompe disease, gliosis has been described in autopsies, and this co-localized with areas of neuronal loss in classic infantile patients, highly suggestive of its active role contributing to neurodegeneration in Pompe disease.[6-9] In **Chapter 3**, we also have demonstrated prominent regional astrocyte proliferation and widespread microglial activation in a Pompe murine model. As the impairment of CNS in Pompe disease has become recently evident, the possible role of neuroinflammation in the CNS pathology in Pompe disease requires further exploration.

Neuroinflammation and neurodegeneration

A transient inflammatory response is usually a protective mechanism in the CNS following trauma, infection or disease, with the purpose to evoke a swift response to control and defend the insult. However, prolonged and excessive inflammation as seen in LSDs can exert detrimental effects on brain function by creating a neurotoxic environment and by further perpetuating an inflammatory cycle.[10,11]

Although the initial mechanism that activates microglia and astrocytes in LSDs is still not elucidated, it has been proposed that dying or dysfunctional neurons,[12] chronic stimulation of primary storage material,[13-15] disruption of lysosomal membrane integrity with resultant release of lysosomal contents, including hydrolases and metabolites into the cytosol,[16-18] and infiltration of intracellular components into the extracellular milieu[19-21] can contribute to danger-associated molecular patterns (DAMPs) activating microglia. Furthermore, cellular dysfunction, including elevated intracellular Ca^{2+} and

ER stress that are secondary to primary storage, can also trigger multiple immune pathways in microglia.[22-26] Similarly, cytoplasmic DAMPs can activate astrocytes due to primary accumulation of storage material, impaired autophagy and dysfunctional mitochondria.[27-29] There is also extensive cross-talk between microglia and astrocytes, such that dysfunction of either population can trigger the activation of the other.[30,31]

Activated microglia and astrocytes can generate a severe neurotoxic environment via secretion of nitric oxide (NO) together with superoxide (SO),[32,33] and are major reservoirs of chemokines and pro-inflammatory cytokines that initiate innate and adaptive immune response in the CNS[34-39] that are toxic to neurons.[40-42] Those cytotoxic mediators can also act upon neighboring microglia, astrocytes and neurons that further perpetuate the inflammatory circle, eventually triggering neuronal death. To further aggravate, chronic neuroinflammation impairs neurotrophic support by astrocytes, further increasing the neuronal vulnerability to cytotoxic events.[43,44] The proposed vicious circle of neuroinflammation is depicted in Figure 1.

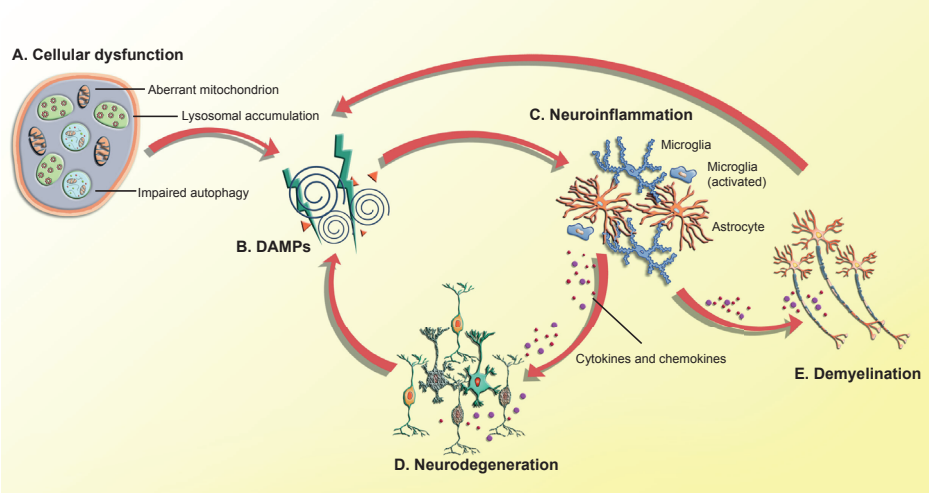

Figure 1. Cartoon of a model for the CNS pathology in Pompe disease. Cellular dysfunction (A) caused by lysosomal glycogen accumulation, dysfunctional autophagy and aberrant mitochondrion is the source of danger-associated molecular patterns (DAMPs) in (B). This further activates microglia and astrocytes, causing neuroinflammation (C). As a result, harmful cytokines and chemokines are released that are detrimental to the survival of neurons and oligodendrocytes, causing neurodegeneration (D) and demyelination (E), which in turn, are forms of DAMP by themselves, thereby, further perpetuating pathology.

In several LSDs including Sandhoff disease,[45] Niemann-Pick type C,[46] Gaucher disease[4] and neuronal ceroid lipofuscinosis,[47-49] a temporal and spatial relationship between neuroinflammation and neuronal loss has been described, in which glial activation

and neuroinflammation precede neurodegeneration and can predict regions where eventual neuronal loss will occur. This phenomenon further highlights the negative impact of inflammation on neuronal survival and ongoing neurodegeneration.[50] On the other hand, neurodegeneration in mucopolysaccharidosis (MPS) is primarily cell-autonomous, and neuronal damage provokes a subsequent inflammatory response.[19,51] In Pompe disease, it remains elusive whether inflammation is triggered by intracellular storage in glial cells or is a response to neuronal damage, and whether neuronal loss is cell-autonomous due to an intrinsic defect or induced by inflammation. Typically, in multiple sulfatase-deficient mice, a selective deletion of the target gene in astrocytes alone led to neuronal loss.[29] In the central nervous system, glycogen is exclusively distributed in astrocytes throughout the brain,[52,53] which serve as a buffer to deliver energy to neurons on demand for a limited amount of time.[54-56] Only a low but traceable amount of glycogen is present in neurons that contributes to neuronal tolerance to hypoxia.[57] Given this distinctive glycogen metabolism in brain, resulting in glycogen accumulation mainly in astrocytes, we hypothesize that the defective astrocytes are the major contributors that trigger a cascade of pathological events. Since neurodegeneration has a rather late-onset in Pompe patients, longer follow-up is required to monitor possible neurodegeneration and its correlation with inflammation.

Demyelination

Oligodendrocytes are myelinating glial cells of the CNS and also provide metabolic support to axons.[58-61] The myelin sheath surrounding the axons is required to ensure rapid nerve conduction that allows impulse propagation,[62,63] and is therefore critical for functional motor, sensory and cognitive abilities.[64-66]

Using T2-weighed MRI, classic infantile Pompe patients manifested hyperintensified signals mainly in the periventricular white matter with occasionally involvement of internal/external capsule, claustrum, corpus callosum, centrum semiovale and corticospinal tracts in the brainstem.[67,68] Information processing speed[68-70] attributed to decreased neuronal conduction was particularly impaired in Pompe patients, similarly as seen in multiple sclerosis, a disease featured by widespread demyelination.[71]

So far, there are no studies on the mechanism by which demyelination occurs in Pompe disease, other than a few autopsy reports describing glycogen deposits in oligodendrocytes or myelinated axons.[6-8,72] Possible cytotoxicity from excessive primary storage and chronic neuroinflammation are plausible factors that can negatively influence oligodendrogenesis, survival of oligodendrocytes, proper myelination and homeostasis of the myelin sheath, leading to eventual loss of oligodendrocytes and

breakdown of myelin (Figure 1).[10,73-77] It is worth noting that, similar to metachromatic leukodystrophy (MLD),[78] subcortical U-fibers are relatively spared[67,79] even in a patient with extensive subcortical white matter involvement.[68] This feature strongly suggests that the initial pathology is not directly damaging to oligodendrocytes, but rather related to disturbed myelin metabolism and turnover. The relatively normal myelination reported in autopsies is in line with the slowly progressive nature of white matter abnormalities in classic infantile patients.[7,80] Nevertheless, investigation of the cause of demyelination in Pompe disease is required to clarify the underlying mechanism.

To summarize, the pathogenesis of CNS abnormalities in Pompe disease is still poorly understood. Nevertheless, current evidence suggests a combined paradigm featured by prominent neuroinflammation, developing white matter changes mimicking leukodystrophy, and a minimal neurodegeneration. Extensive mechanistic research in combination with long-term clinical follow-up are required to further understand the links between pathophysiology in the CNS and the underlying molecular defect.

2. SAFETY PROFILE OF LENTIVIRAL GENE THERAPY

Genotoxicity assessment is an important aspect for translation of lentiviral gene therapy to the clinic. Lentiviral vectors integrate into the host genome providing permanent gene expression; on the other hand, the risk of insertion near proto-oncogenes might lead to insertional oncogenesis. As a multifactorial risk, insertional mutagenesis depends on the integration pattern of the vector and its *cis*-activating elements including enhancer and promoter.[81] It also requires the acquisition of secondary mutations in time that are not vector-related.[82] Importantly, the disease background in combination with the vector and gene used largely determines the risk to develop insertional oncogenesis. For instance, the use of a γ-retroviral vector (γ-RV) was associated with hematological malignancies, occurring in 5 out of 20 patients with X-linked severe combined immunodeficiency (SCID-X1),[82,83] and 7 out of 10 patients with Wiskott-Aldrich syndrome (WAS)[84] In contrast, in a larger cohort of ADA-SCID patients clonal expansions were not observed despite the use of the same viral vector backbone.[85,86] As a matter of fact, gene therapy with the exact same vector backbone has gained market approval in Europe in 2016 to treat ADA-SCID.[87] Therefore, it has been speculated that the expression pattern and the gene of interest contributes significantly: in contrast to IL2RG and WASp, which are involved in the cellular responses to proliferative stimuli, and are exclusively expressed in the hematopoietic system, ADA is a metabolic "housekeeping" protein that is constitutively expressed in all cell types, similar to *GAA* expression.

Compared to the previously mentioned γ-RV, the lentiviral vector used in our studies has been shown to have an improved safety profile. Lentiviral vectors exhibit a semi-random integration pattern with no preference for oncogenes.[88] This is in direct contrast to the preferential integration of γ-RV within highly enriched hotspots in proto-oncogenes, cancer-associated common insertion sites (CISs), and growth-controlling genes.[89-91] Furthermore, the third generation lentiviral vector system has deleted crucial elements for viral transcription activation and replication. It also reassigned the production of lentiviral vectors with four separate plasmids that strongly reduced the possibility for the generation of wild-type virus via recombination.[92] Hence, the construction of self-inactivating (SIN) lentiviral vector created by the deletion of the U3 region of 3' long terminal repeats (LTRs) prevented the generation of replication-competent virus upon integration.[93,94] It also renders the control of transgene expression to an internal promoter of choice, which can further reduce the risk of unwanted regulation of adjacent genes, because cell-type specific promoters can be incorporated. So far, no genotoxicity has been observed using the third generation of SIN lentiviral vectors during 10 years of follow-up in the clinic in X-linked adrenoleukodystrophy.[95] Lentiviral gene therapy could also be a valid treatment option for Pompe disease, which preferably can be applied with the use of a modestly strong promoter in combination with a lower vector copy number, thereby improving the biosafety profile.

Additional approaches have been developed that can be applied to further improve biosafety. The HIV-1 packaging sequences can be shortened to contain 4.8% of the wildtype genome rather than 19.6%. This minimizes the number of functional *cis* elements.[96] As internal promoters may still potentially activate neighboring genes, chromatin insulator cassettes can be added to block enhancer function.[97] As integration nearby proto-oncogenes contributes substantially to mutagenesis, efforts have been made to redirect the integration of lentiviral vector to designated regions by replacing the host cell-derived lentiviral integrase cofactor lens epithelium-derived growth factor/p75 (LEDGF/p75) by CBX1. The former binds lentiviral integrase that targets integration to active transcription sites, whereas the latter binds to histone H3 that is di- or trimethylated at K9, which are present in heterochromatin and intergenic regions.[98,99] However, this is of less clinical relevance as the protein needs to be removed from the host system. Lastly, an alternative foamy viral vector that exhibits no preference for integrating at actively transcribed regions, and comes close to random integration could be another delivery system that may be worth pursuing for its biosafety.[100,101]

Nevertheless, no vector system can be defined as absolutely safe with respect to its integration profile, but risks should be kept to a minimum. Therefore, long-term monitoring of potential adverse events using assays with high sensitivity is essential in clinical settings.[81]

3. PERSPECTIVES AND FUTURE DIRECTIONS

Challenges in treating Pompe disease: requirement for high enzyme levels versus biosafety of lentiviral gene therapy

The success of treating lysosomal storage disease depends on sufficient biodistribution of the therapeutic enzyme to the target tissues. In Pompe disease, skeletal muscles, the major affected organs, are difficult to reach via the circulation, presumably owing to the low abundance of the cation-dependent mannose-6 phosphate receptor (CI-MPR) especially in type 2 fibers.[102,103] Furthermore, skeletal muscles comprise a large percentage of the body mass (42% and 36% in male and female adult, respectively),[104] which adds up to the amount of enzyme required. These features partly explain the very high ERT dosages used to treat Pompe patients. Currently, 40 mg/kg weekly and 20 mg/kg bi-weekly infusion of rhGAA are recommended to treat classic infantile patients and adult patients, respectively, which totals 160 and 40 mg/kg enzyme per month. In sharp contrast, the administered dose for all the other LSDs is limited to 2 to 4 mg/kg on a monthly basis.[105] Besides challenges to treat peripheral abnormalities, the glycogen buildup within the central nervous system also appears to be resistant for degradation. At ~6% of WT GAA enzyme activity in gene therapy Pompe mice, there is no reduction of glycogen, whereas 10-11% of WT levels are sufficient to significantly reduce storage product in MLD and MPS IIIA.[106-108] Collectively, the amount of enzyme required in Pompe disease is markedly higher than in other LSDs.

In our lentiviral gene therapy study, the enzyme output correlated with the VCN per cell. However, in our studies, the VCN to achieve normalization of the Pompe muscle phenotype using the GAAco vector was high (>15 VCN/cell), and glycogen in brain was reduced at a maximum of ~38%. So another approach was investigated by enhancing delivery to the skeletal muscle and brain, thereby reducing the required VCN/cell, and consequently improving biosafety (**Chapter 3**). Another process that may be considered is to enhance secretion of the transgene product via other signal peptides.[109] Although a relatively simple vector is probably preferred by the regulatory agencies, we advocate for Pompe disease that additional modifications are vital to balance the therapeutic efficacy and biosafety.

Target patient population

Pompe disease has a wide clinical spectrum, with classical infantile patients on one extreme end and adult patients on the other. At present, we argue that classical infantile patients, especially those who are cross-reactive immunologic material (CRIM)-negative, are the preferred target population for lentiviral gene therapy for the following reasons: (i) In this population, there is still substantial percentage of death (up to 50%) despite the implementation of ERT.[110,111] Thus, a better alternative treatment is required and the benefits may outweigh the risks. (ii) It may be easier to prevent symptoms than to reverse existent pathology. Experiences from the MLD trial showed the best outcomes when gene therapy started pre-symptomatically, or at least at the very early symptomatic stages, prior to the occurrence of any massive damage.[112] Therefore, through newborn screening programs,[113,114] potential patients should be identified and treated in a timely manner. (iii) The clinical symptoms are quite homogenous in classic infantile patients compared to childhood/adult patients, which should make it easier to define a therapeutic endpoint in a clinical trial.

In childhood and adult patients, the disease progression is relatively slow, which may complicate the risk/benefit evaluation. It is also not known to what extent lentiviral gene therapy will be able to reverse the damage. Actually, for adult patients, as the central nervous system appears to be unaffected and they have relatively slow cell proliferation in the liver, liver-delivered AAV gene therapy could be a valid choice for this population given the recently improved efficacy of this therapy.[115]

Conditioning of the patients

One of the decisive factors for successful HSC gene therapy is pre-transplant conditioning, which is mainly based on chemotherapy regimens. In immune deficiencies, such as ADA-SCID and SCID-X1, a nonmyeloablative conditioning is sufficient to create space in the bone marrow, as genetically corrected cells provide selective growth advantages.[116-118] In contrast, a full myeloblative regimen based on busulfan may be required for high levels of engraftment in lysosomal storage disease, especially in Pompe disease, which demands remarkably high amounts of GAA enzyme. In HSC gene therapy for MLD, a median of ~60% engraftment efficiency was achieved.[112] Essentially, in order for HSC gene therapy to work in the brain, sufficient brain conditioning that allows reconstitution of myeloid cells in the brain isindispensable. In this regard, the preferred choice is busulfan, as it promotes myeloid turnover in the brain better than irradiation.[119,120]

As mentioned above, classic infantile patients will be a preferred target population. However, the clinical conditions of these patients are generally poor and feature car-

diorespiratory defects. Therefore, instant implementation of ERT is preferred, not only for survival, but also to improve their overall condition prior to the administration of the gene therapy regimen. In Hurler patients (MPS 1), the use of ERT before hematopoietic stem cell transplantation (without gene modification) improved clinical symptoms, and thereby consequently reduced transplantation-related complications. The reduction of glycosaminoglycans (GAG's) from the bone marrow also seemed to promote engraftment.[121] Unfortunately, we have demonstrated in our *Gaa*$^{-/-}$ mice that ERT prior to gene therapy induces an immune response that eliminates genetically modified hematopoietic cells (**Chapter 6**). Hence, preparation of Pompe patients for gene therapy should be optimized to properly address the pre-existing immunity directed towards the rhGAA. Reagents targeted to eliminate reactive T- , and plasma B cells are of particular interest and should be properly explored in the future. For instance, methotrexate eliminates proliferating T and B cells.[122,123] Rituximab (an anti-CD20 monoclonal antibody) and bortezomib (a proteasome inhibitor) target B cells and long-term antibody-producing plasma cells, respectively.[124] These and many other novel regimens should be tested in combination with busulfan to evaluate whether the pre-existing immunity can be eliminated to ensure a robust engraftment following gene therapy. Optionally, monoclonal antibodies that selectively deplete blood cells will be for the future interest as alternative conditioning regimen, due to their reduced toxicity.[125,126]

Future direction: from gene addition to gene editing via CRISPR/Cas9

Currently, HSC mediated lentiviral gene therapy holds great promise as the next line of care for Pompe disease, especially for classic infantile patients. While the SIN-lentiviral vector demonstrates a relatively safe integration profile, better control of vector integration sites is still desired. Therefore, the use of endonucleases such as zinc-finger nucleases (ZFNs), transcription activator-like effector nucleases (TALENs), and clustered regularly interspaced short palindromic repeats (CRISPR)/Cas9 for targeted transgene integration in a "safe harbor" are promising alternatives to pursue. "Safe harbor" refers to regions in genomic DNA that do not contain oncogenes and that can be disrupted without causing any adverse effect. The adeno-associated virus integration site 1 (*AAVS1*) locus is such safe harbor that is often utilized.[127] Compared to other gene editing tools, CRISPR/Cas9 stands out as the most efficient and easy-to-engineer system.[128] The simplest CRISPR/Cas9 type II system consists of a single guide RNA (gRNA) that binds to the Cas9 nuclease and directs it to a target sequence via complementary baseparing. The targeted region should be attached to a protospacer-adjacent motif (PAM). A double-stranded break is generated upon recognition by the Cas9 protein, and one or multiple correct copies of a gene of interest can be inserted following homology-directed recombination (HDR).[129,130]

In principle, two *ex vivo* strategies can be anticipated for Pompe disease using CRISPR/Cas9-mediated gene editing. A direct modification of hematopoietic stem cells using the CRISPR/Cas9 technology is the most straightforward approach. It can yield up to 20% efficiency repairing with a single-stranded oligodeoxynucleotide (ssODN) in hematopoietic stem cells that still possessed multilineage potential following transplantation into immune deficient mice.[131,132] However, for incorporation of a larger DNA element containing a complete cassette with the *GAA* cDNA, the efficiency is still relatively low. Therefore, selection of cells with correct homologous recombination is required, and that requires longer protocols. This requires improved protocols to maintain stemness during hematopoietic stem cell expansion *in vitro* for extended time periods, which currently remains challenging.[133-135] Another option is to combine genomic editing with induced pluripotent stem cells (iPSCs) followed by reprogramming to hematopoietic stem cells. This strategy offers sufficient time for gene editing, positive selection and cell expansion. While gene editing with CRISPR/Cas9 has been successfully applied to correct numerous mutations in patient-derived iPSCs,[136] the differentiation into sufficient hematopoietic stem cells that can achieve long-term peripheral reconstitution remains unsolved.[137] Currently, the delivery of both endonuclease and repair constructs, the low HDR rates in edited cells, and off-target mutagenesis prevent clinical application.[138] Future investigation into an enhanced delivery system combined with more specific binding properties of the gRNA should help to improve this therapy.

In conclusion, in this thesis we have presented a potentially curative treatment for Pompe disease using a modified lentiviral vector mediated by hematopoietic stem cells. Major issues remain safety of the lentiviral vector expression cassette, and an adequate pre-conditioning regimen. These factors should be carefully addressed during the final stages into a novel therapy for Pompe patients.

REFERENCES

1. Boustany RM. Lysosomal storage diseases--the horizon expands. *Nat Rev Neurol.* 2013;9(10):583-598.
2. Bosch ME, Kielian T. Neuroinflammatory paradigms in lysosomal storage diseases. *Front Neurosci.* 2015;9:417.
3. German DC, Liang CL, Song T, Yazdani U, Xie C, Dietschy JM. Neurodegeneration in the Niemann-Pick C mouse: glial involvement. *Neuroscience.* 2002;109(3):437-450.
4. Farfel-Becker T, Vitner EB, Pressey SN, Eilam R, Cooper JD, Futerman AH. Spatial and temporal correlation between neuron loss and neuroinflammation in a mouse model of neuronopathic Gaucher disease. *Hum Mol Genet.* 2011;20(7):1375-1386.
5. Wilkinson FL, Holley RJ, Langford-Smith KJ, et al. Neuropathology in mouse models of mucopolysaccharidosis type I, IIIA and IIIB. *PLoS One.* 2012;7(4):e35787.
6. Crome L, Cumings JN, Duckett S. Neuropathological and Neurochemical Aspects of Generalized Glycogen Storage Disease. *J Neurol Neurosurg Psychiatry.* 1963;26:422-430.
7. Mancall EL, Aponte GE, Berry RG. Pompe's Disease (Diffuse Glycogenosis) with Neuronal Storage. *J Neuropathol Exp Neurol.* 1965;24:85-96.
8. Martin JJ, de Barsy T, van Hoof F, Palladini G. Pompe's disease: an inborn lysosomal disorder with storage of glycogen. A study of brain and striated muscle. *Acta Neuropathol.* 1973;23(3):229-244.
9. Martini C, Ciana G, Benettoni A, et al. Intractable fever and cortical neuronal glycogen storage in glycogenosis type 2. *Neurology.* 2001;57(5):906-908.
10. Lyman M, Lloyd DG, Ji X, Vizcaychipi MP, Ma D. Neuroinflammation: the role and consequences. *Neurosci Res.* 2014;79:1-12.
11. Walter L, Neumann H. Role of microglia in neuronal degeneration and regeneration. *Semin Immunopathol.* 2009;31(4):513-525.
12. Pais TF, Figueiredo C, Peixoto R, Braz MH, Chatterjee S. Necrotic neurons enhance microglial neurotoxicity through induction of glutaminase by a MyD88-dependent pathway. *J Neuroinflammation.* 2008;5:43.
13. Shoenfeld Y, Gallant LA, Shaklai M, Livni E, Djaldetti M, Pinkhas J. Gaucher's disease: a disease with chronic stimulation of the immune system. *Arch Pathol Lab Med.* 1982;106(8):388-391.
14. Hong YB, Kim EY, Jung SC. Upregulation of proinflammatory cytokines in the fetal brain of the Gaucher mouse. *J Korean Med Sci.* 2006;21(4):733-738.
15. Nixon GF. Sphingolipids in inflammation: pathological implications and potential therapeutic targets. *Br J Pharmacol.* 2009;158(4):982-993.
16. Futerman AH, van Meer G. The cell biology of lysosomal storage disorders. *Nat Rev Mol Cell Biol.* 2004;5(7):554-565.
17. Campos D, Monaga M. Mucopolysaccharidosis type I: current knowledge on its pathophysiological mechanisms. *Metab Brain Dis.* 2012;27(2):121-129.
18. Serrano-Puebla A, Boya P. Lysosomal membrane permeabilization in cell death: new evidence and implications for health and disease. *Ann N Y Acad Sci.* 2016;1371(1):30-44.

19. Ausseil J, Desmaris N, Bigou S, et al. Early neurodegeneration progresses independently of microglial activation by heparan sulfate in the brain of mucopolysaccharidosis IIIB mice. *PLoS One*. 2008;3(5):e2296.

20. Johnson GB, Brunn GJ, Kodaira Y, Platt JL. Receptor-mediated monitoring of tissue well-being via detection of soluble heparan sulfate by Toll-like receptor 4. *J Immunol*. 2002;168(10):5233-5239.

21. Piccinini AM, Midwood KS. DAMPening inflammation by modulating TLR signalling. *Mediators Inflamm*. 2010;2010.

22. Farber K, Kettenmann H. Functional role of calcium signals for microglial function. *Glia*. 2006;54(7):656-665.

23. Hoffmann A, Kann O, Ohlemeyer C, Hanisch UK, Kettenmann H. Elevation of basal intracellular calcium as a central element in the activation of brain macrophages (microglia): suppression of receptor-evoked calcium signaling and control of release function. *J Neurosci*. 2003;23(11):4410-4419.

24. Sama DM, Norris CM. Calcium dysregulation and neuroinflammation: discrete and integrated mechanisms for age-related synaptic dysfunction. *Ageing Res Rev*. 2013;12(4):982-995.

25. Salminen A, Kauppinen A, Suuronen T, Kaarniranta K, Ojala J. ER stress in Alzheimer's disease: a novel neuronal trigger for inflammation and Alzheimer's pathology. *J Neuroinflammation*. 2009;6:41.

26. Zhang K, Kaufman RJ. From endoplasmic-reticulum stress to the inflammatory response. *Nature*. 2008;454(7203):455-462.

27. Calatayud CA, Pasquini LA, Pasquini JM, Soto EF. Involvement of the ubiquitin-mediated proteolytic system in the signaling pathway induced by ceramide in primary astrocyte cultures. *Dev Neurosci*. 2005;27(6):397-407.

28. Oh HL, Seok JY, Kwon CH, Kang SK, Kim YK. Role of MAPK in ceramide-induced cell death in primary cultured astrocytes from mouse embryonic brain. *Neurotoxicology*. 2006;27(1):31-38.

29. Di Malta C, Fryer JD, Settembre C, Ballabio A. Astrocyte dysfunction triggers neurodegeneration in a lysosomal storage disorder. *Proc Natl Acad Sci U S A*. 2012;109(35):E2334-2342.

30. Liu W, Tang Y, Feng J. Cross talk between activation of microglia and astrocytes in pathological conditions in the central nervous system. *Life Sci*. 2011;89(5-6):141-146.

31. Meares GP, Liu Y, Rajbhandari R, et al. PERK-dependent activation of JAK1 and STAT3 contributes to endoplasmic reticulum stress-induced inflammation. *Mol Cell Biol*. 2014;34(20):3911-3925.

32. Boje KM, Arora PK. Microglial-produced nitric oxide and reactive nitrogen oxides mediate neuronal cell death. *Brain Res*. 1992;587(2):250-256.

33. Giri S, Jatana M, Rattan R, Won JS, Singh I, Singh AK. Galactosylsphingosine (psychosine)-induced expression of cytokine-mediated inducible nitric oxide synthases via AP-1 and C/EBP: implications for Krabbe disease. *Faseb J*. 2002;16(7):661-672.

34. Lee SC, Liu W, Dickson DW, Brosnan CF, Berman JW. Cytokine production by human fetal microglia and astrocytes. Differential induction by lipopolysaccharide and IL-1 beta. *J Immunol.* 1993;150(7):2659-2667.

35. Wu YP, Proia RL. Deletion of macrophage-inflammatory protein 1 alpha retards neurodegeneration in Sandhoff disease mice. *Proc Natl Acad Sci U S A.* 2004;101(22):8425-8430.

36. Olson JK, Miller SD. Microglia initiate central nervous system innate and adaptive immune responses through multiple TLRs. *J Immunol.* 2004;173(6):3916-3924.

37. DiRosario J, Divers E, Wang C, et al. Innate and adaptive immune activation in the brain of MPS IIIB mouse model. *J Neurosci Res.* 2009;87(4):978-990.

38. Kawashita E, Tsuji D, Kawashima N, Nakayama K, Matsuno H, Itoh K. Abnormal production of macrophage inflammatory protein-1alpha by microglial cell lines derived from neonatal brains of Sandhoff disease model mice. *J Neurochem.* 2009;109(5):1215-1224.

39. Perry VH, Nicoll JA, Holmes C. Microglia in neurodegenerative disease. *Nat Rev Neurol.* 2010;6(4):193-201.

40. Liu B, Gao HM, Wang JY, Jeohn GH, Cooper CL, Hong JS. Role of nitric oxide in inflammation-mediated neurodegeneration. *Ann N Y Acad Sci.* 2002;962:318-331.

41. Block ML, Zecca L, Hong JS. Microglia-mediated neurotoxicity: uncovering the molecular mechanisms. *Nat Rev Neurosci.* 2007;8(1):57-69.

42. Glass CK, Saijo K, Winner B, Marchetto MC, Gage FH. Mechanisms underlying inflammation in neurodegeneration. *Cell.* 2010;140(6):918-934.

43. Ohgoh M, Shimizu H, Ogura H, Nishizawa Y. Astroglial trophic support and neuronal cell death: influence of cellular energy level on type of cell death induced by mitochondrial toxin in cultured rat cortical neurons. *J Neurochem.* 2000;75(3):925-933.

44. Lee KM, MacLean AG. New advances on glial activation in health and disease. *World J Virol.* 2015;4(2):42-55.

45. Wada R, Tifft CJ, Proia RL. Microglial activation precedes acute neurodegeneration in Sandhoff disease and is suppressed by bone marrow transplantation. *Proc Natl Acad Sci U S A.* 2000;97(20):10954-10959.

46. Baudry M, Yao Y, Simmons D, Liu J, Bi X. Postnatal development of inflammation in a murine model of Niemann-Pick type C disease: immunohistochemical observations of microglia and astroglia. *Exp Neurol.* 2003;184(2):887-903.

47. Pontikis CC, Cella CV, Parihar N, et al. Late onset neurodegeneration in the Cln3-/- mouse model of juvenile neuronal ceroid lipofuscinosis is preceded by low level glial activation. *Brain Res.* 2004;1023(2):231-242.

48. Kay GW, Palmer DN, Rezaie P, Cooper JD. Activation of non-neuronal cells within the prenatal developing brain of sheep with neuronal ceroid lipofuscinosis. *Brain Pathol.* 2006;16(2):110-116.

49. Kielar C, Maddox L, Bible E, et al. Successive neuron loss in the thalamus and cortex in a mouse model of infantile neuronal ceroid lipofuscinosis. *Neurobiol Dis.* 2007;25(1):150-162.

50. Amor S, Peferoen LA, Vogel DY, et al. Inflammation in neurodegenerative diseases--an update. *Immunology.* 2014;142(2):151-166.

51. Archer LD, Langford-Smith KJ, Bigger BW, Fildes JE. Mucopolysaccharide diseases: a complex interplay between neuroinflammation, microglial activation and adaptive immunity. *J Inherit Metab Dis*. 2014;37(1):1-12.
52. Cataldo AM, Broadwell RD. Cytochemical identification of cerebral glycogen and glucose-6-phosphatase activity under normal and experimental conditions. II. Choroid plexus and ependymal epithelia, endothelia and pericytes. *J Neurocytol*. 1986;15(4):511-524.
53. Oe Y, Baba O, Ashida H, Nakamura KC, Hirase H. Glycogen distribution in the microwave-fixed mouse brain reveals heterogeneous astrocytic patterns. *Glia*. 2016;64(9):1532-1545.
54. Brown AM, Tekkok SB, Ransom BR. Glycogen regulation and functional role in mouse white matter. *J Physiol*. 2003;549(Pt 2):501-512.
55. Brown AM, Baltan Tekkok S, Ransom BR. Energy transfer from astrocytes to axons: the role of CNS glycogen. *Neurochem Int*. 2004;45(4):529-536.
56. Brown AM, Ransom BR. Astrocyte glycogen and brain energy metabolism. *Glia*. 2007;55(12):1263-1271.
57. Saez I, Duran J, Sinadinos C, et al. Neurons have an active glycogen metabolism that contributes to tolerance to hypoxia. *J Cereb Blood Flow Metab*. 2014;34(6):945-955.
58. Nave KA. Myelination and the trophic support of long axons. *Nat Rev Neurosci*. 2010;11(4):275-283.
59. Saab AS, Tzvetanova ID, Nave KA. The role of myelin and oligodendrocytes in axonal energy metabolism. *Curr Opin Neurobiol*. 2013;23(6):1065-1072.
60. Funfschilling U, Supplie LM, Mahad D, et al. Glycolytic oligodendrocytes maintain myelin and long-term axonal integrity. *Nature*. 2012;485(7399):517-521.
61. Simons M, Nave KA. Oligodendrocytes: Myelination and Axonal Support. *Cold Spring Harb Perspect Biol*. 2015;8(1):a020479.
62. Nave KA, Werner HB. Myelination of the nervous system: mechanisms and functions. *Annu Rev Cell Dev Biol*. 2014;30:503-533.
63. Hughes EG, Appel B. The cell biology of CNS myelination. *Curr Opin Neurobiol*. 2016;39:93-100.
64. Fields RD. White matter in learning, cognition and psychiatric disorders. *Trends Neurosci*. 2008;31(7):361-370.
65. Nave KA. Myelination and support of axonal integrity by glia. *Nature*. 2010;468(7321):244-252.
66. McKenzie IA, Ohayon D, Li H, et al. Motor skill learning requires active central myelination. *Science*. 2014;346(6207):318-322.
67. Messinger YH, Mendelsohn NJ, Rhead W, et al. Successful immune tolerance induction to enzyme replacement therapy in CRIM-negative infantile Pompe disease. *Genet Med*. 2012;14(1):135-142.
68. Ebbink BJ, Poelman E, Plug I, et al. Cognitive decline in classic infantile Pompe disease: An underacknowledged challenge. *Neurology*. 2016;86(13):1260-1261.

69. Ebbink BJ, Aarsen FK, van Gelder CM, et al. Cognitive outcome of patients with classic infantile Pompe disease receiving enzyme therapy. *Neurology*. 2012;78(19):1512-1518.

70. Spiridigliozzi GA, Keeling LA, Stefanescu M, Li C, Austin S, Kishnani PS. Cognitive and academic outcomes in long-term survivors of infantile-onset Pompe disease: A longitudinal follow-up. *Mol Genet Metab*. 2017.

71. Chiaravalloti ND, DeLuca J. Cognitive impairment in multiple sclerosis. *Lancet Neurol*. 2008;7(12):1139-1151.

72. Gambetti P, DiMauro S, Baker L. Nervous system in Pompe's disease. Ultrastructure and biochemistry. *J Neuropathol Exp Neurol*. 1971;30(3):412-430.

73. Merrill JE, Ignarro LJ, Sherman MP, Melinek J, Lane TE. Microglial cell cytotoxicity of oligodendrocytes is mediated through nitric oxide. *J Immunol*. 1993;151(4):2132-2141.

74. Butovsky O, Landa G, Kunis G, et al. Induction and blockage of oligodendrogenesis by differently activated microglia in an animal model of multiple sclerosis. *J Clin Invest*. 2006;116(4):905-915.

75. Giri S, Khan M, Rattan R, Singh I, Singh AK. Krabbe disease: psychosine-mediated activation of phospholipase A2 in oligodendrocyte cell death. *J Lipid Res*. 2006;47(7):1478-1492.

76. Domingues HS, Portugal CC, Socodato R, Relvas JB. Oligodendrocyte, Astrocyte, and Microglia Crosstalk in Myelin Development, Damage, and Repair. *Front Cell Dev Biol*. 2016;4:71.

77. Ponath G, Ramanan S, Mubarak M, et al. Myelin phagocytosis by astrocytes after myelin damage promotes lesion pathology. *Brain*. 2017;140(Pt 2):399-413.

78. Cheon JE, Kim IO, Hwang YS, et al. Leukodystrophy in children: a pictorial review of MR imaging features. *Radiographics*. 2002;22(3):461-476.

79. Rohrbach M, Klein A, Kohli-Wiesner A, et al. CRIM-negative infantile Pompe disease: 42-month treatment outcome. *J Inherit Metab Dis*. 2010;33(6):751-757.

80. Martin JJ, De Barsy T, De S, Leroy JG, Palladini G. Acid maltase deficiency (type II glycogenosis). Morphological and biochemical study of a childhood phenotype. *J Neurol Sci*. 1976;30(1):155-166.

81. Baum C, Modlich U, Gohring G, Schlegelberger B. Concise review: managing genotoxicity in the therapeutic modification of stem cells. *Stem Cells*. 2011;29(10):1479-1484.

82. Howe SJ, Mansour MR, Schwarzwaelder K, et al. Insertional mutagenesis combined with acquired somatic mutations causes leukemogenesis following gene therapy of SCID-X1 patients. *J Clin Invest*. 2008;118(9):3143-3150.

83. Hacein-Bey-Abina S, Garrigue A, Wang GP, et al. Insertional oncogenesis in 4 patients after retrovirus-mediated gene therapy of SCID-X1. *J Clin Invest*. 2008;118(9):3132-3142.

84. Braun CJ, Boztug K, Paruzynski A, et al. Gene therapy for Wiskott-Aldrich syndrome--long-term efficacy and genotoxicity. *Sci Transl Med*. 2014;6(227):227ra233.

85. Aiuti A, Cattaneo F, Galimberti S, et al. Gene therapy for immunodeficiency due to adenosine deaminase deficiency. *N Engl J Med*. 2009;360(5):447-458.

86. Cicalese MP, Ferrua F, Castagnaro L, et al. Update on the safety and efficacy of retroviral gene therapy for immunodeficiency due to adenosine deaminase deficiency. *Blood*. 2016;128(1):45-54.

87. Aiuti A, Roncarolo MG, Naldini L. Gene therapy for ADA-SCID, the first marketing approval of an ex vivo gene therapy in Europe: paving the road for the next generation of advanced therapy medicinal products. *EMBO Mol Med.* 2017;9(6):737-740.

88. Biffi A, Bartolomae CC, Cesana D, et al. Lentiviral vector common integration sites in preclinical models and a clinical trial reflect a benign integration bias and not oncogenic selection. *Blood.* 2011;117(20):5332-5339.

89. Beard BC, Keyser KA, Trobridge GD, et al. Unique integration profiles in a canine model of long-term repopulating cells transduced with gammaretrovirus, lentivirus, or foamy virus. *Hum Gene Ther.* 2007;18(5):423-434.

90. Cattoglio C, Facchini G, Sartori D, et al. Hot spots of retroviral integration in human CD34+ hematopoietic cells. *Blood.* 2007;110(6):1770-1778.

91. Montini E, Cesana D, Schmidt M, et al. The genotoxic potential of retroviral vectors is strongly modulated by vector design and integration site selection in a mouse model of HSC gene therapy. *J Clin Invest.* 2009;119(4):964-975.

92. Dull T, Zufferey R, Kelly M, et al. A third-generation lentivirus vector with a conditional packaging system. *J Virol.* 1998;72(11):8463-8471.

93. Zufferey R, Dull T, Mandel RJ, et al. Self-inactivating lentivirus vector for safe and efficient in vivo gene delivery. *J Virol.* 1998;72(12):9873-9880.

94. Bukovsky AA, Song JP, Naldini L. Interaction of human immunodeficiency virus-derived vectors with wild-type virus in transduced cells. *J Virol.* 1999;73(8):7087-7092.

95. Cartier N, Hacein-Bey-Abina S, Bartholomae CC, et al. Hematopoietic stem cell gene therapy with a lentiviral vector in X-linked adrenoleukodystrophy. *Science.* 2009;326(5954):818-823.

96. Vink CA, Counsell JR, Perocheau DP, et al. Eliminating HIV-1 Packaging Sequences from Lentiviral Vector Proviruses Enhances Safety and Expedites Gene Transfer for Gene Therapy. *Mol Ther.* 2017.

97. Cesana D, Ranzani M, Volpin M, et al. Uncovering and dissecting the genotoxicity of self-inactivating lentiviral vectors in vivo. *Mol Ther.* 2014;22(4):774-785.

98. Ciuffi A, Llano M, Poeschla E, et al. A role for LEDGF/p75 in targeting HIV DNA integration. *Nat Med.* 2005;11(12):1287-1289.

99. Gijsbers R, Ronen K, Vets S, et al. LEDGF hybrids efficiently retarget lentiviral integration into heterochromatin. *Mol Ther.* 2010;18(3):552-560.

100. Trobridge GD, Miller DG, Jacobs MA, et al. Foamy virus vector integration sites in normal human cells. *Proc Natl Acad Sci U S A.* 2006;103(5):1498-1503.

101. Everson EM, Olzsko ME, Leap DJ, Hocum JD, Trobridge GD. A comparison of foamy and lentiviral vector genotoxicity in SCID-repopulating cells shows foamy vectors are less prone to clonal dominance. *Mol Ther Methods Clin Dev.* 2016;3:16048.

102. Raben N, Danon M, Gilbert AL, et al. Enzyme replacement therapy in the mouse model of Pompe disease. *Mol Genet Metab.* 2003;80(1-2):159-169.

103. Raben N, Fukuda T, Gilbert AL, et al. Replacing acid alpha-glucosidase in Pompe disease: recombinant and transgenic enzymes are equipotent, but neither completely clears glycogen from type II muscle fibers. *Mol Ther.* 2005;11(1):48-56.

104. Marieb EN, and Katja Hoehn. Human Anatomy & Physiology. San Francisco: Benjamin Cummings; 2010.

105. Desnick RJ, Schuchman EH. Enzyme replacement therapy for lysosomal diseases: lessons from 20 years of experience and remaining challenges. *Annu Rev Genomics Hum Genet*. 2012;13:307-335.

106. van Til NP, Stok M, Aerts Kaya FS, et al. Lentiviral gene therapy of murine hematopoietic stem cells ameliorates the Pompe disease phenotype. *Blood*. 2010;115(26):5329-5337.

107. Biffi A, Capotondo A, Fasano S, et al. Gene therapy of metachromatic leukodystrophy reverses neurological damage and deficits in mice. *J Clin Invest*. 2006;116(11):3070-3082.

108. Sergijenko A, Langford-Smith A, Liao AY, et al. Myeloid/Microglial driven autologous hematopoietic stem cell gene therapy corrects a neuronopathic lysosomal disease. *Mol Ther*. 2013;21(10):1938-1949.

109. Sun B, Zhang H, Benjamin DK, Jr., et al. Enhanced efficacy of an AAV vector encoding chimeric, highly secreted acid alpha-glucosidase in glycogen storage disease type II. *Mol Ther*. 2006;14(6):822-830.

110. Chakrapani A, Vellodi A, Robinson P, Jones S, Wraith JE. Treatment of infantile Pompe disease with alglucosidase alpha: the UK experience. *J Inherit Metab Dis*. 2010;33(6):747-750.

111. Hahn A, Praetorius S, Karabul N, et al. Outcome of patients with classical infantile pompe disease receiving enzyme replacement therapy in Germany. *JIMD Rep*. 2015;20:65-75.

112. Sessa M, Lorioli L, Fumagalli F, et al. Lentiviral haemopoietic stem-cell gene therapy in early-onset metachromatic leukodystrophy: an ad-hoc analysis of a non-randomised, open-label, phase 1/2 trial. *Lancet*. 2016;388(10043):476-487.

113. Kemper AR, Hwu WL, Lloyd-Puryear M, Kishnani PS. Newborn screening for Pompe disease: synthesis of the evidence and development of screening recommendations. *Pediatrics*. 2007;120(5):e1327-1334.

114. Chien YH, Chiang SC, Zhang XK, et al. Early detection of Pompe disease by newborn screening is feasible: results from the Taiwan screening program. *Pediatrics*. 2008;122(1):e39-45.

115. Doerfler PA, Todd AG, Clement N, et al. Copackaged AAV9 Vectors Promote Simultaneous Immune Tolerance and Phenotypic Correction of Pompe Disease. *Hum Gene Ther*. 2016;27(1):43-59.

116. Aiuti A, Slavin S, Aker M, et al. Correction of ADA-SCID by stem cell gene therapy combined with nonmyeloablative conditioning. *Science*. 2002;296(5577):2410-2413.

117. Gaspar HB, Bjorkegren E, Parsley K, et al. Successful reconstitution of immunity in ADA-SCID by stem cell gene therapy following cessation of PEG-ADA and use of mild preconditioning. *Mol Ther*. 2006;14(4):505-513.

118. De Ravin SS, Wu X, Moir S, et al. Lentiviral hematopoietic stem cell gene therapy for X-linked severe combined immunodeficiency. *Sci Transl Med*. 2016;8(335):335ra357.

119. Capotondo A, Milazzo R, Politi LS, et al. Brain conditioning is instrumental for successful microglia reconstitution following hematopoietic stem cell transplantation. *Proc Natl Acad Sci U S A*. 2012;109(37):15018-15023.

120. Wilkinson FL, Sergijenko A, Langford-Smith KJ, Malinowska M, Wynn RF, Bigger BW. Busulfan conditioning enhances engraftment of hematopoietic donor-derived cells in the brain compared with irradiation. *Mol Ther.* 2013;21(4):868-876.

121. Cox-Brinkman J, Boelens JJ, Wraith JE, et al. Haematopoietic cell transplantation (HCT) in combination with enzyme replacement therapy (ERT) in patients with Hurler syndrome. *Bone Marrow Transplant.* 2006;38(1):17-21.

122. Joseph A, Munroe K, Housman M, Garman R, Richards S. Immune tolerance induction to enzyme-replacement therapy by co-administration of short-term, low-dose methotrexate in a murine Pompe disease model. *Clin Exp Immunol.* 2008;152(1):138-146.

123. Mendelsohn NJ, Messinger YH, Rosenberg AS, Kishnani PS. Elimination of antibodies to recombinant enzyme in Pompe's disease. *N Engl J Med.* 2009;360(2):194-195.

124. Banugaria SG, Patel TT, Kishnani PS. Immune modulation in Pompe disease treated with enzyme replacement therapy. *Expert Rev Clin Immunol.* 2012;8(6):497-499.

125. Yokoi T, Yokoi K, Akiyama K, et al. Non-myeloablative preconditioning with ACK2 (anti-c-kit antibody) is efficient in bone marrow transplantation for murine models of mucopolysaccharidosis type II. *Mol Genet Metab.* 2016;119(3):232-238.

126. Stahl M, Lu BY, Kim TK, Zeidan AM. Novel Therapies for Acute Myeloid Leukemia: Are We Finally Breaking the Deadlock? *Target Oncol.* 2017.

127. Samulski RJ, Zhu X, Xiao X, et al. Targeted integration of adeno-associated virus (AAV) into human chromosome 19. *Embo J.* 1991;10(12):3941-3950.

128. Mali P, Yang L, Esvelt KM, et al. RNA-guided human genome engineering via Cas9. *Science.* 2013;339(6121):823-826.

129. Cho SW, Kim S, Kim JM, Kim JS. Targeted genome engineering in human cells with the Cas9 RNA-guided endonuclease. *Nat Biotechnol.* 2013;31(3):230-232.

130. Cong L, Ran FA, Cox D, et al. Multiplex genome engineering using CRISPR/Cas systems. *Science.* 2013;339(6121):819-823.

131. Gundry MC, Brunetti L, Lin A, et al. Highly Efficient Genome Editing of Murine and Human Hematopoietic Progenitor Cells by CRISPR/Cas9. *Cell Rep.* 2016;17(5):1453-1461.

132. De Ravin SS, Li L, Wu X, et al. CRISPR-Cas9 gene repair of hematopoietic stem cells from patients with X-linked chronic granulomatous disease. *Sci Transl Med.* 2017;9(372).

133. Schuster JA, Stupnikov MR, Ma G, et al. Expansion of hematopoietic stem cells for transplantation: current perspectives. *Exp Hematol Oncol.* 2012;1(1):12.

134. Nikiforow S, Ritz J. Dramatic Expansion of HSCs: New Possibilities for HSC Transplants? *Cell Stem Cell.* 2016;18(1):10-12.

135. Walasek MA, van Os R, de Haan G. Hematopoietic stem cell expansion: challenges and opportunities. *Ann N Y Acad Sci.* 2012;1266:138-150.

136. Hu X. CRISPR/Cas9 system and its applications in human hematopoietic cells. *Blood Cells Mol Dis.* 2016;62:6-12.

137. Esposito MT. Hematopoietic stem cells meet induced pluripotent stem cells technology. *Haematologica.* 2016;101(9):999-1001.

138. Ott de Bruin LM, Volpi S, Musunuru K. Novel Genome-Editing Tools to Model and Correct Primary Immunodeficiencies. *Front Immunol*. 2015;6:250.

Addendum

LIST OF ABBREVIATIONS

γ-RV	γ-retroviral vector
AAV	Adeno-associated virus
Ab	Antibody
ADA-SCID	Adenosine deaminase-severe combined immunodeficiency
ALD	X-linked adrenoleukodystrophy
AP	Acid phosphatase
ARSA	Arylsulfatase A
BBB	Blood-brain barrier
BM	Bone marrow
CHO	Chinese hamster ovary cells
CI-MPR	Cation-independent mannose 6-phosphate receptor
CISs	Common insertion sites
CNS	Central nervous system
CRIM	Cross-reactive immunologic material
CRISPR	Clustered regularly interspaced short palindromic repeats
CSF	Cerebrospinal fluid
DA	Diaphragm
DAMPs	Danger-associated molecular patterns
DES	Desmin promotor
ELISA	Enzyme-linked immunosorbent assay
ER	Endoplasmic reticulum
ERT	Enzyme replacement therapy
FC	Fold change
GA	Gastrocnemius
GAA	Acid α-glucosidase
GLD	Globoid-cell leukodystrophy
GMA	Glycol methacrylate
GO	Gene ontology
GSDII	Glycogen storage disease type II
GT	Gene therapy
GVHD	Graft versus host disease
Gy	Gray
HDR	Homology-directed recombination
HIV	Human immunodeficiency virus
HS	Heparan sulfate
HSCs	Hematopoietic stem cells
HSCT	Hematopoietic stem cell transplantation

HSPCs	Hematopoietic stem progenitor cells
IGFI	Insulin-like growth factor I
IGFII	Insulin-like growth factor II
IGFIR	Insulin-like growth factor I receptor
IGFIIR	Insulin-like growth factor II receptor
IPA	Ingenuity Pathway Analysis
iPSCs	Induced pluripotent stem cells
IR	Insulin receptor
KO	Knockout
LAMP1	Lysosomal associated membrane protein 1
LSD(s)	Lysosomal storage disease(s)
LTRs	Long terminal repeats
LV	Lentiviral vectors
M6P	Mannose-6-phosphate
M6P/IGFIIR	Mannose-6-phosphate/insulin-like growth factor receptor
MHC	Myosin heavy chain
MLD	Metachromatic leukodystrophy
MND	Myeloproliferative sarcoma virus enhancer, negative control region deleted, dl587rev primer-binding site substituted promoter
MOI	Multiplicity of infection
MPS	Mucopolysaccharidosis
MPSV	Myeloproliferative sarcoma virus
PAS	Periodic acid Schiff staining
PBS	Phosphate-buffered saline
PGK	Phosphoglycerate kinase promoter
PNS	Peripheral nervous system
QF	Quadriceps femoris
qPCR	Quantitative polymerase chain reaction
rhGAA	Recombinant human acid α-glucosidase
SCID-X1	Severe combined immunodeficiency
SF	Spleen focus-forming viral promoter
SFN	Small-fiber neuropathy
SIN	Self-inactivation
TA	Tibialis anterior
TBI	Total body irradiation
VCN	Vector copy number
WAS	Wiskott-Aldrich syndrome
WT	Wildtype

SUMMARY

The work presented in this thesis focuses on the development of *ex vivo* lentiviral gene therapy for Pompe disease. As proof of principle, previous attempts using a third generation of a self-inactivating lentiviral vector carrying a cDNA of the native *GAA* sequence showed sufficient glycogen clearance in heart, and to lesser extent, in the diaphragm. However, the effect in other skeletal muscles, i.e. quadriceps femoris was not significant. Additionally, glycogen was not reduced in brain at all. The major bottleneck could have been insufficient uptake of GAA by the cells of interest due to low abundance of mannose-6-phosphate (M6P) residues on the GAA protein, which are critical for uptake via the cation-independent M6P receptor (CI-MPR) present on the cell surface. Approaches that do not require glycosylation for effective uptake may provide improved uptake and clearance. In addition, more data is pointing out that central nervous system (CNS) pathology may be a major symptom in disease progression in ERT treated patients. It is therefore important to address this in any new therapeutic approach to treat Pompe disease. In **Chapter 2**, we present an overview of the current literature on possible treatment options to address the pathology in the CNS, with a focus on gene therapy.

To further improve the efficacy of lentiviral gene therapy, in **Chapter 3,** we modified the lentiviral vector to contain a codon-optimized (co) *GAA* transgene (hereafter referred as LV-GAAco) that was tagged with a portion of human insulin-like growth factor II (IGFII) (hereafter referred as LV-IGFIIco.GAAco). As the CI-MPR is a bi-functional receptor that binds M6P, and with an even higher affinity IGFII, the fusion of IGFII to the GAA protein mediated at least a 4-fold better uptake in cultured murine *Gaa*$^{-/-}$ muscle cells compared to untagged GAA. In *Gaa*$^{-/-}$ mice, transplantation of hematopoietic stem cells that were transduced *ex vivo* with LV-IGFIIco.GAAco resulted in complete glycogen clearance, not only in heart, but also in skeletal muscles. Histopathology was reversed and motor function was fully restored to wildtype levels. Importantly, this treatment showed exceptional efficiency in alleviating pathology in the brain. Using the LV-IGFIIco.GAAco vector did not only remove glycogen deposits, but also attenuated prominent neuroinflammation. In contrast, gene therapy with LV-GAAco only induced partial glycogen reduction even with a much higher vector copy number.

Furthermore, a thorough analysis to evaluate the therapeutic efficacy in skeletal muscles at the proteomic level was performed using quantitative mass spectrometry in **Chapter 4**. Whereas GAA deficiency caused altered expression of 480 proteins, these were near-completely normalized in LV-IGFIIco.GAAco treated mice. This study, therefore, provided solid evidence of a global reversal of pathology following the

restoration of GAA activity using lentiviral gene therapy, confirming our findings in **Chapter 3**.

Biosafety is another important factor to be considered in lentiviral gene therapy. As the effects were achieved using the strong spleen focus-forming virus (SF) promoter, an alternative promoter that has been used in clinical gene therapy trials is preferred to minimize genotoxic risks. In **Chapter 5**, three promoters that have been clinically applied in lentiviral gene therapy trials were tested. The myeloproliferative sarcoma virus enhancer, negative control region deleted, dl587rev primer-binding site substituted (MND)-derived promoter showed similar efficiency for glycogen reduction compared to that of SF promoter. This work suggested that the previous SF promoter can be substituted by a clinically acceptable promoter without compromising the therapeutic efficacy.

Immune responses to rhGAA are a major side-effect that attribute to reduced efficacy of ERT. In **Chapter 6** we show that *ex vivo* lentiviral gene therapy is able to induce immune tolerance in naïve Pompe mice, not only to the transgene product, but also to ERT with rhGAA. This work implies that established immune tolerance can allow complementary ERT treatment to be effective in the case that the gene therapy would have sub-therapeutic efficacy.

Collectively, the findings in this thesis provided proof of pre-clinical efficacy of lentiviral gene therapy in a mouse model for Pompe disease, and it advocates the future clinical development of this therapy for Pompe patients.

SAMENVATTING

Het werk dat in dit proefschrift wordt gepresenteerd, richt zich op de ontwikkeling van *ex vivo* lentivirale gentherapie voor patiënten met de ziekte van Pompe. Het bewijs dat deze techniek werkt blijkt uit eerdere pogingen met een derde generatie zelf-inactiverende lentivirale vectoren die het cDNA van de naïeve *GAA* sequentie dragen. Deze zorgen voor voldoende klaring van glycogeen in het hart, en in mindere mate, het diafragma. Het effect in andere skeletspieren, b.v. quadriceps femoris was echter niet significant. Daarnaast, was de glycogeen stapeling in de hersenen niet verminderd. Het belangrijkste knelpunt zou onvoldoende opname van GAA door de cellen van belang kunnen zijn doordat er te weinig residuen van mannose-6-fosfaat (M6P) aanwezig zijn op het GAA-eiwit. Deze zijn essentieel voor opname via de kation-onafhankelijke M6P receptor (CI-MPR), welke aanwezig zijn op het celoppervlak. Benaderingen die geen glycosylering vereisen voor effectieve opname kunnen zorgen voor verbeterde opname en klaring. Daarnaast wijzen meer gegevens erop dat pathologie van het centrale zenuwstelsel (CNS) een belangrijk symptoom kan zijn bij de ziekteprogressie bij ERT behandelde patiënten. Het is daarom belangrijk om dit aan te pakken met een nieuwe therapeutische aanpak om patiënten met de ziekte van Pompe te behandelen. In **Hoofdstuk 2** presenteren we een overzicht van de huidige literatuur over mogelijke opties om de pathologie in het CNS behandelen, met een focus op gentherapie.

Om de werkzaamheid van lentivirale gentherapie verder te verbeteren hebben we, in **Hoofdstuk 3**, de lentivirale vector aangepast zodat het een codon-geoptimaliseerd (co) *GAA* transgen bevat (hierna aangeduid als LV-GAAco) die vervolgens werd gelabeld met een deel van het humane insuline-achtige groeifactor II (IGFII) eiwit (hierna aangeduid als LV-IGFIIco.GAAco). Aangezien de CI-MPR een bi-functionele receptor is die M6P bindt, en met een nog hogere affiniteit IGFII, zorgde de fusie van IGFII met het GAA-eiwit voor ten minste een vier keer betere opname in gekweekte spiercellen verkregen uit *Gaa*$^{-/-}$ muizen in vergelijking met niet-labelede GAA. In *Gaa*$^{-/-}$ muizen resulteerde transplantatie van hematopoëtische stamcellen die *ex vivo* werden getransduceerd met LV-IGFIIco.GAAco in volledige glycogeenklaring, niet alleen in het hart, maar ook in skeletspieren. Histopathologie was normaal en de motorfunctie was volledig hersteld naar wild type niveau. Een belangrijke constatering was dat deze behandeling een uitzonderlijke efficiëntie liet zien om bij het verlichten van de pathologie in de hersenen. Het gebruik van de LV-IGFIIco.GAAco vector verwijderde niet alleen glycogeen stapeling, maar verzwakte ook prominente neuro-inflammatie. Dit in tegenstelling tot gentherapie met LV-GAAco, welke alleen een gedeeltelijke glycogeen klaring liet zien, zelfs met een veel hoger vectorkopie nummer.

In **Hoofdstuk 4** werd een grondige analyse uitgevoerd om de therapeutische werkzaamheid in de skeletspieren op het niveau van het proteoom te evalueren met behulp van kwantitatieve massaspectrometrie. Waar de GAA-deficiëntie afwijkende expressie van 480 eiwitten veroorzaakte, werden deze nagenoeg allemaal genormaliseerd in LV-IGFIIco.GAAco-behandelde muizen. Deze studie leverde derhalve solide bewijzen voor een globale omkering van pathologie na herstel van GAA-activiteit met behulp van lentivirale gentherapie, die onze bevindingen in **Hoofdstuk 3** bevestigen.

Bioveiligheid is een andere belangrijke factor om lentivirale gentherapie in aanmerking te laten komen als therapie. Aangezien de effecten werden bereikt met behulp van de sterke miltfocusvormende virus (SF) promotor, heeft een alternatieve promotor die is gebruikt in klinische gentherapieproeven de voorkeur om genotoxische risico's te minimaliseren. In **Hoofdstuk 5** zijn drie promotoren getest die eerder zijn toegepast in klinische trials met lentivirale gentherapie. De myeloproliferatieve sarcoomvirusversterker, met verwijderde negatieve controle-regio, dl587rev primer-bindingsplaats gesubstitueerde (MND) afgeleide promotor vertoonde vergelijkbare efficiëntie in glycogeen klaring in vergelijking met die van de SF promotor. Dit werk suggereerde dat de vorige SF promotor kan worden gesubstitueerd door een klinisch aanvaardbare promotor zonder de therapeutische werkzaamheid in gevaar te brengen.

Immuunreacties tegen rhGAA zijn een belangrijk bijeffect dat bijdraagt aan de verminderde werkzaamheid van ERT. In **Hoofdstuk 6** tonen we aan dat *ex vivo* lentivirale gentherapie immuuntolerantie kan induceren bij naïeve Pompe-muizen, niet alleen voor het transgene product, maar ook voor ERT met rhGAA. Dit werk impliceert dat door de bereikte immuuntolerantie, de complementaire ERT-behandeling effectief kan zijn in het geval dat de gentherapie een subtherapeutische werkzaamheid zou hebben.

Samen leveren de studies in dit proefschrift bewijs van de preklinische werkzaamheid van lentivirale gentherapie in een muizenmodel voor de ziekte van Pompe en pleit het voor de toekomstige klinische ontwikkeling van deze therapie voor Pompe patiënten.

论文概要

本论文研究重点是针对Pompe病进行的体外慢病毒基因治疗。Pompe病是由于编码GAA酶的基因发生突变所导致的全身性糖原积累病，主要表现为全身性的肌无力，病人最终会失去行动能力并需要呼吸支持。目前Pompe病的治疗方法是通过静脉输入外源性的重组人GAA酶（rhGAA），称为酶替代疗法。虽然该疗法一定程度上缓解了病人的症状，但病人需要终生接受治疗。更重要的是，这种酶替代疗法并不能治愈Pompe病，其治疗效果在骨骼肌极为有限。同时，病人体内产生的抗GAA酶抗体会影响酶的活性。因此，我们需要寻求一种新的能够一次性有效治愈Pompe病的方法。使用携带天然GAA序列的第三代自身灭活慢病毒载体的前期实验在小鼠模型中概念性地证明了该治疗方法可以充分地清除组织中积累的糖原，其效果在心肌最为显著，横膈膜次之。然而，该疗法却未能有效地清除累积在其他骨骼肌，即股四头肌中的糖原，尤其对脑部组织几乎无效。其主要的瓶颈在于靶细胞对GAA的摄入不足，这是由GAA蛋白上M6P残基含量不足所导致的。该残基对细胞表面表达的M6P受体（CI-MPR）所引导的吸收至关重要。因此，不依赖糖基化的摄入方式可以更有效地提高对于GAA的吸收和对糖原的清除。需要指出的是，越来越多的临床数据显示，在接受酶替代疗法治疗的患者中，中枢神经系统病变可能是一大尚未解决的难题。这是由于通过静脉输入的酶被血脑屏障阻挡，而不能有效地进入大脑。因此，任何新的治疗Pompe病的方法都必须考虑如何有效地治疗神经系统的异常。在第二章中，我们概述了目前能够治疗中枢神经系统疾病的方法，并着重阐述了基因疗法。

在第三章中，为了进一步提高慢病毒基因治疗的功效，我们改良了慢病毒载体的结构：首先,将原有的天然GAA序列替换成了经过密码子优化的序列（以下简称为LV-GAAco）以提高GAA的表达水平；接着，将含有一部分人胰岛素样生长因子2（IGFII）的序列标记在该载体上（以下称为LV-IGFIIco.GAAco）。前述的CI-MPR是既可以结合M6P，又可以以更高的亲和力结合IGFII的双功能受体。因此，表达了IGFII的GAA蛋白能够以四倍于未融合该标记的酶的效率被培养的来源于Gaa基因敲除小鼠的肌细胞摄取。基于上述发现，我们在体外用改良后的慢病毒载体-LV-IGFIIco.GAAco转染造血干细胞，并将其移植到Gaa基因敲除小鼠。我们发现，该基因疗法能够彻底地将心肌，以及现有酶替代疗法不能有效作用的各种骨骼肌的糖原清除。同时，组织病理也得到了逆转，并且运动功能也完全恢复到了正常小鼠的水平。更重要的是，该疗法在减轻大脑病理方面也表现出了卓越的功效。使用LV-IGFIIco.GAAco载体不仅消除了糖原沉积物，而且减轻了突出的神经炎症。相比之下，即使在更高的病毒载体拷贝数下，使用了LV-GAAco的基因疗法也仅仅能够达到使部分糖原减少的效果。

在第四章中，通过定量质谱法对治疗后的小鼠骨骼肌进行分析，我们更彻底地评估了基因疗法在蛋白组学水平的功效。结果显示，由Gaa缺乏所导致的表达水平改变的480个蛋白，在经过了LV-IGFIIco.GAAco治疗的小鼠中几乎完全恢复了正常的表达水平。因此，本研究提供了确凿的证据证明，通过慢病毒基因治疗恢复GAA活性后，可以整体上逆转Pompe病的各层面的病理。这也在蛋白组学水平佐证了我们在第三章中的发现。

生物安全也是慢病毒基因治疗中需要考虑的一个重要因素。若上述实验使用的较强的SF启动子能够被目前已经处于临床试验阶段的其他启动子替代，那将会大大降低产生基因毒性的风险。在第五章中，我们测试了三种应用于慢病毒基因治疗临床试验阶段的启动子。其中，MND启动子展现了与现有的SF启动子相似的清除糖原的能力。该研究提示，在不影响治疗功效的前提下，之前实验使用的SF启动子完全可以被临床上更能被接受的启动子所代替。

在酶替代疗法中，病人体内针对重组人GAA酶产生的免疫应答是一个主要的副作用。由于抗体中和了输入的GAA酶，从而大大降低了该疗法的效力。在第六章中，我们的研究显示，体外慢病毒基因治疗能够有效地诱导初试Pompe病小鼠不仅对转基因产物，即GAA酶，还对酶替代疗法中使用的重组人GAA酶产生免疫耐受。该结果意味着当基因疗法不能达到治愈效果的情况下，患者可继续接受现有的酶替代疗法作为补充治疗方案。而由基因疗法建立起的免疫耐受可使输入的GAA酶不再被患者免疫系统清除而变得更加有效。

总而言之，本论文的研究结果提供了慢病毒基因治疗在Pompe病小鼠模型中有效性的临床前期证据。同时，该成果也积极地主张在未来针对Pompe病人进一步开展使用该疗法的临床研究。

CURRICULUM VITAE

Personal information

Name: Qiushi Liang
Date of Birth: 24-09-1986
Place of Birth: Chengdu, Sichuan, China
Nationality: Chinese
Tel No.: +8613558665265
Email: liangqiushi@hotmail.com

Education

October 2012 - September 2017: Erasmus University Medical Center, Rotterdam, the Netherlands

- **Ph.D. training** in the Dept. of Hematology, Dept. of Pediatrics and Dept. of Clinical Genetics

September 2010 - September 2012: West China Medical Center, Sichuan University, Chengdu, China

- **Master/Doctoral combined program** of Internal Medicine, specialized in Hematology

September 2005 – June 2010: West China Medical Center, Sichuan University, Chengdu, China

- **M.D.** in Clinical Medicine

March 2007 – January 2009: College of Foreign Languages and Cultures, Sichuan University, Chengdu, China

- **Double degree of B.A.** in English language and literature
  Dissertation entitled *The blogging Phenomenon*, supervised by Prof. Linlan Ma.

Professional experiences

October 2012 - September 2017: Erasmus University Medical Center, Rotterdam, the Netherlands

- **Ph.D. research** in the Dept. of Hematology, Dept. of Pediatrics and Dept. of Clinical Genetics
  Research project: *Hematopoietic stem cell mediated lentiviral gene therapy for Pompe disease.*
  Supervisors*: October 2012 – August 2014, Dept. of Hematology*
  Prof. dr. Gerard Wagemaker; Prof. dr. Arnold G. Vulto; Dr. Niek P. van Til

September 2014 – September 2017, Dept. of Pediatrics and Dept. of Clinical Genetics
Prof. dr. Ans T. van der Ploeg; Prof. dr. Arnold G. Vulto; Dr. W.W.M. Pim Pijnappel; Dr. Niek P. van Til

September 2010 - September 2012: West China Medical Center, Sichuan University, Chengdu, China

- **Postgraduate training** in the Laboratory of Stem Cell Biology, Center for Medical Stem Cell Biology
  Research project: *The biological effect of NIBP in hematopoietic regulation.*
  Supervisors: Prof. dr. Ting Liu; Dr. Yuchun Wang; Dr. Wentong Meng

Medical training

May 2009 – June 2010: West China Medical Center, Sichuan University, Chengdu, China

- **Clinical rotation/Internship** in Depts. of Internal Medicine (Hematology, Endocrinology, Cardiology, Respiration, Neurology), Orthopedics, Gastrointestinal Surgery, Urology, Obstetrics and Gynecology, Pediatrics, Psychiatry and Oncology.

Awards

Best oral presentation: Sophia Research Day (Rotterdam, 2017)
Poster award: Steps Forward in Pompe Disease (Turin, Italy, 2014)
The State Scholarship provided by Chinese Scholarship Council (2012-2016)
First class scholarship of Sichuan University (2005-2011)
Elite students of West China Medical School (2005-2011)

Certificates

Scientific: Article 9 researcher (Dutch laboratory animal law); Animal handling in IVC facilities
Medical: Certificate of Physician Credentials (China); Certificate of Medical Licensure (China)

PHD PORTFOLIO

Name PhD student: Qiushi Liang
PhD period: October 2012 – September 2017
Erasmus MC Department: Pediatrics/Clinical Genetics/Hematology
Research School: Molecular Medicine (Molmed)
Promotors: Prof. dr. Ans T. van der Ploeg; Prof. dr. Arnold G. Vulto
Supervisors: Dr. W.W.M. Pim Pijnappel; Dr. Niek P. van Til

1. PhD training	**Year**	**ECTS**
General courses		
Biomedical Research Techniques XI	2012	1.5
The Basic Introduction Course on SPSS	2013	1
Laboratory animal science	2013	3
Genetics for Dummies: Basic Human Genetics Course	2013	0.5
Photoshop and Illustrator CS6 workshop	2014	0.3
Research management for PhD-students	2014	1
Research Integrity	2017	0.5
Specific courses		
Handling animals housed in IVC's	2013	1
EMC research meetings	2012-2017	5
(Inter)national conferences		
Molecular Medicine Day (2×) (Rotterdam)	2013-2014	1
Nederlandse Vereniging voor Gen en Cel Therapie (NVGCT) Spring Symposium (Lunteren)	2013	1
European Society of Gene and Cell Therapy (ESGCT) (The Hague)	2014	2.5
Steps Forward in Pompe Disease (2×) (Turin, Italy; Amsterdam)	2014, 2016	2
Erfelijke Stofwisselingsziekten Nederland (ESN) meeting (Rotterdam)	2015	0.5
Sophia Research Day (3×) (Rotterdam)	2015-2017	1.5
Muscles2meet, Neuromuscular Young Talent Symposium (Zeist)	2016	1
Presentations		
EMC research meetings (Oral, 13×)	2014-2017	6.5
European Society of Gene and Cell Therapy (ESGCT) (Poster, 1×) (The Hague)	2014	1
Steps Forward in Pompe Disease (Poster, 1×) (Turin, Italy)	2014	1
Erfelijke Stofwisselingsziekten Nederland (ESN) meeting (Oral, 1×) (Rotterdam)	2015	1
Sophia Research Day (Oral, 1×) (Rotterdam)	2017	1
2. Teaching and supervision		
Supervising technician for practical techniques and assays involved in the project	2015. 8. -2017. 8.	4
Total		37.8

ACKNOWLEDGEMENTS / 致谢

Hooray! It is with both joy and sentiment do I start writing this very last chapter of the thesis. Looking back, the journey to get PhD over the past five years has been exceptional and filled with peaks and valleys. As the finishing line is approaching, I want to convey my most sincere gratitude to people whose kindness and support has turned such trip a memorable adventure.

First and foremost, I would like to thank my promoters, Prof. Ans T. van der Ploeg, Prof. Arnold G. Vulto and my co-promoters, Dr. W.W.M Pim Pijnappel and Dr. Niek P. van Til, the four guardian angels to this project and to me. Dear **Ans**, I am really grateful that you have the courage and vision to take over this project and have been supportive ever since. I am in your debt for the opportunity to complete my PhD in the least disturbed manner. I hope I have lived up to your expectations (Judging from that reference letter, I might succeed?) and that the progress we've made so far has proven how wise those decisions were back then. Your enthusiasm and commitment to both clinical practice and scientific research always amazed me and you are definitely the role model for my upcoming career ideally as a physician-scientist. Dear **Arnold**, thank you for standing by my side through my PhD and over the years, I have been enchanted with your great personalities. Your kindness started with our very first correspondence by providing tips to make a comfy stay in Rotterdam which later extended to the croissants and chocolates for literally every meeting we had. Be small gestures as they may, it shows how considerate and caring you are. Personally, I cannot thank you enough for your coordination for relocation and I cherished our quality tea time as a source of personal support. Dear **Pim**, thank you for your rigorous supervision. I have to admit I felt your reservation to this project in the beginning as every good scientist should be: critical. And I was thrilled to see that you were willing to keep an open mind and once you got to know this project, you have been nothing but supportive. You made sure I was able to continue pipetting in the new department without any delay. The weekly discussion showed how meticulous you were with raw data. The brainstorming also impressed me with your broad knowledge in science which I still have a long way to catch up. You are curious, detail-oriented, collaborative, resourceful, a keen observer and a good communicator. I learnt a great deal from you to be a good story teller and your presence in presentations were always reassuring. As a first-time writer, I am also grateful for all your effort to make this thesis a concise piece of work. And I will definitely keep this in mind: *In der Berchränkung zeigt sich erst der Meister*! Dear **Niek**, I cannot thank you enough for your commitment to this project and to me. When I first joined the group, I was lacking any proper lab skills. You were literally the person who trained me from scratch. I remember those days that I was so clumsy in the beginning that I

had broken gels twice in front of you. However, you always treat me with tremendous patience and manage to look for the positive from the most negative situation. Your knowledge, passion and love for this project has continuously inspired me. You were the rock in the group for the first two years and your support continued even after you started a new career in Utrecht. I cannot imagine how overwhelmed it must be to start up a new group, let alone that you have to take care of four children at home! But you make every effort to be in our regular meetings and contribute extensively to my thesis. Your expertise and support meant a lot to me!

Next, I want to thank all the members of my doctoral reading committee, Prof. Peter A.E. Sillevis Smitt, Prof. Rob C. Hoeben and Prof. Brian Bigger for their time and effort to help improve my thesis. Dear **Peter**, thank you for being the secretary of the committee and for working diligently to make sure everything is ready within such tight schedule. Dear **Rob**, it is a great pleasure to collaborate with you on the further clinical development of our therapy and I benefit a lot from your constructive suggestions and comments. Dear **Brian**, I have admired your work in the field and it is such an honor to have you on board. I really appreciate your thoughtful feedback on my thesis. Hope there will be more collaboration to follow.

I would also like to extend my appreciation to the members of the big committee, Prof. Robert M.W. Hofstra, Prof. Edmond H.H.M. Rings and Prof. Pieter A. van Doorn for their commitment to my defense. Dear **Robert**, thank you for accommodating me in the department. I really appreciate your valuable comments during meetings and encouragement after presentations. Dear **Edmond**, although I didn't have the opportunity to know you personally, I have you, together with **Peter** and **Robert**, to thank for the support you've given to the lentiviral gene therapy project. Dear **Pieter**, thank you for taking the time and effort to read my thesis and I look forward to our discussion in my defense.

Next, I want to acknowledge my paranymphs, whom I know from two different periods of my PhD and become my dearest friends ever since. Dear **Yvette**, our relationship started with me shadowing you to bleed mice on the very first day I started my PhD and in the following two years, you were such a great trainer who generously taught me everything about transplantation and animal experiments that is instrumental for this thesis. You are so well-organized and accurate. Peculiarly, you always have this aura around you, signaling, "don't worry, everything is under control" and somehow you manage to make things functional again. Long hours of us working side by side (or the love for sliced pork with garlic sauce?) brought us closer and our friendship has continued even after the separation of our working relationship. I was really honored

to be able to witness your happiness on your wedding day and I truly admire your love and devotion for your family. Looking forward to our trip to Disneyland! Dear **Shami**, strangely enough, I can't picture how we first met. But somehow, we managed to become so close that even Robert called us "twins". Your endearing personality must have brought peace in the chaotic time for me. You helped me find my ways in the lab and walked me through every step from how to prepare paraffin specimen to little tricks for cryo-sections. And as the younger party in this twin relationship, you are actually the one who takes over the caring part. You are outgoing but also disciplined. Thank you for the trust to share all your family stories. For me, I think it is a rare but very noble act to honor your religion and tradition in such a respectful way. I will miss your laughter, your struggling with choices, your dancing eyebrows, your moves in the elevator and those fast food-consuming records we made. Girls, together, you have witnessed my whole PhD with all the joys and pains. I really cherish our friendship and your effort for my defense day. I am sure we will stay in touch and I am looking forward to welcome you in China.

Now, I want to express my heartfelt thanks to my dearest team! Dear **Joon,** thank you for being such an indispensable part of our lentiviral gene therapy project. Your participation starting two years ago has literally rescued me from heavy lab work. I cannot imagine to finish my thesis in time without your help. You are such a reliable people who are always precise and are able to produce beautiful and solid results. As you are getting more experiences in mice experiments, I am sure I will be leaving our fantastic project in good hands and I really hope you will be able to continue and see it through. Do inform me when it makes through clinical trials! Dear **Mike**, I think love-and-hatred is the best description of our relationship. However, I have to admit, apart from all the pranks you pulled on me and that you've been "Susaned" me for years, deep deep deep inside, you are such a wonderful person who iswarm hearted and eager to help. The cover you have designed for this thesis has really startled me which made me feel that all the sufferings I had over the years were almost worth it...almost! I wish you all the best in generating the disease model in rat and implementing the fancy joint transplantation! By the way, maybe a career change after getting your PhD as a designer? Dear **Erik**, thank you for being such a wonderful thesis-writing partners. I think it is over the last year when we were both "struggling" with thesis that we became such close friends. During this period, we have shared our joys, concerns, and mostly, our complains (hope it is not too much!). As you are always one step further than me, you never hesitate to share with me all that I need to do. As a computer geek, you also helped me a lot from graphic software for papers to selection of a proper laptop. I wish you all the best in your thesis defense, and most importantly, your future endeavors in a top-notch scientific lab in Germany! Dear **Monica**, thank

you for the wonderful time we shared in lab and also in Amsterdam and Texel! You are such a caring person and a good cook! Thank you and Angelica for those wonderful hair-cutting dates we've had! Good luck finishing up your thesis! Dear **Douglas**, you are such a genuine person and thoughtful friend. I wish you all the best in the rest of your PhD period. Dear **Pablo** and **Rodrigo**, I have enjoyed our spicy-food hunting journeys and you are such fun people to hang out with. I am also impressed with your critical thinking and passion for science. My best wishes for your PhD and future career! Dear **Merel**, thank you for laying such a solid ground of the project and all your help during the transitional time! I sincerely wish you all the best with your new adventures in Leiden! Dear **Atze** and **Gerben**, being the senior scientists in the group, you have been the wealth of knowledge. I have enjoyed every bit of our discussions. Dear **Tom**, thank you for the generous sharing of your staining expertise and your help with getting those far-fetched items on the shelf! Dear **Stijn**, good luck with all the "8" projects that you are working on and I hope I won't miss your whining too much! Thank you, **Andrea**, **Meneka**, **Suzanne**, **Emma** and **Kasper** for all the encouragement you've given and all the fun time we've shared. I wish you all the best for your future medical and scientific career!

I also want to pay special thanks to group members whom I didn't have the privilege to work with. Dear **Arnold**, you are, with no doubt, one of the most cheerful persons I have ever known and your devotion to science sets great example for me. Dear **Marian** and **Marianne**, thank you for your generous sharing of the legacy of the group and the knowledge of various techniques which has been of great value to my research.

My warmest thanks go to all the colleagues in the department. Dear **Rob**, **Tjakko**, **Vincenzo**, **Renate and Annelies**, thank you for your valuable comments and feedback on my work during the departmental discussions. My lovely roomies in Room 928, I regret to have missed so many dates out with you which made me cherished more of those adventures we've had in scape room. Dear **Katherine**, you are such an adorable person. I really cherish your kind gestures (delicious fried rice, little hugs and kisses) especially in the most stressful period. I also want to thank you for your genius idea of the "mickey ear" for the cover. Dear **Nynke** and **Laura**, you are such bright people and I have really admired all your work! Thank you all for making Room 928 such a "gezellig" place to stay and my best wishes for your PhD studies and future adventures! I also wish to thank **Maria**, **William**, **Isa**, **Adriana**, **Erwin**, **Wim**, **Danny, Fenne**, **Shimriet**, **Rajendra**, **Laura (V)**, **Judith**, **Roy** and **Saif** for all the little chats we have had in the corridor and I wish you all the best with your career. I shall not forget to thank both the technical and administrative support I've got from **Guido**, **Lies-anne**, **Helen**, **Herma**,

Michelle, **Bianca**, **Rachel**, **Jeanette** and **Bep**. Thank you for your effort to make things easy in the lab.

Dear colleagues from the Dept. of Cell and Developmental Biology, thanks for the pleasant working environment. Dear **Joost** and **Willy**, thank you for your kind words every now and then and your constructive comments. Dear **Andrea**, I have really enjoyed our little chats and wish you all the best in finishing your PhD. Dear **Sarra**, it was so cozy to have your company for those crazy sleepless nights. You are such a generous and genuine person and I really admire your passion and dedication for science. By the way, those macarons were délicieux!

Being part of the Center for Lysosomal and Metabolic Disorders, we have extensive connections to clinic. I want to thank all the doctors for the great talks during our meetings which has broadened my understanding of the diseases. I especially value your feedback on my project as it always brings in new ideas that I have overlooked. Dear **Hidde**, I really appreciate your input in our gene therapy meetings and I hope you will stay in this project and help to bring it to clinic! Dear **Hannerieke**, thank you for your critical comments during meetings and dear **Chris** and **Johanneke**, my sincere wishes for your upcoming defense and future career as clinicians. Dear **Nathalie**, **Iris** and **Dorothée**, I can't thank you enough for your crucial administrative support to get to the finish line of my PhD.

Turning back the time machine, I want to acknowledge all the group members back in the Dept. of Hematology. Dear **Gerard**, thank you for accepting me as PhD candidate and bringing me into the group. I sincerely appreciate all your wisdom to the project and I have really enjoyed our conversation full of stories and life experiences. I wish you all the best in life and I hope you enjoy it to the fullest. Dear **Rana**, I will for sure miss our time in KFC! I think it is the mutual support we have given to each other that have helped us go thus far in our PhD. We should both be proud! I am always impressed by the strength in your personality and your courage to stand up for yourself. In life, you are so caring and always treat me like your younger sister and I feel spoiled sometimes by your goodies! It hasn't been easy for you for the past years but please hang in there! Trust me, you are at the stage where you can already see the light at the end of the tunnel! Don't forget you still owe me a trip to Palestine in the olive season! Dear **Leonie**, you are so compassionate and thank you for being such a good listener and advisor! Your pep talk has definitely given me the strength to power through all the difficulties. Although life has not treated you with kindness, I'm relieved to see that it certainly did not take away your love and passion. After rain comes fair sunshine. As now everything is back on track, I am sure you will make amazing achievements in

your new career! This time, amazing does mean AMAZING! Dear **Guus**, thank you for being such wonderful desk mate for two years. I applaud your determination to go back to school and pursue your master studies which have certainly opened up new and better opportunities for you. By the way, now that you have "conquered" south American, maybe it's time to plan a trip to China? Dear **Valentina** and **Pavithra**, thanks for the company and the delicious food. Best of luck to get your PhDs!

I would also like to extend my gratitude to colleagues in the Dept. of Hematology who have been generous and accommodating. Dear **Eric (Braakman)** and **Elwin**, thanks for being so considerate and supportive. Dear **Eric (Bindels)**, I have enjoyed those gezellig moments during Christmas with you and your devotion to research has truly motivated me. Dear **Tom** and **Natalie**, I really appreciate your responsiveness and kind offering. Dear **Onno** and **Paulette**, you have always been the go-to guys in lab and I want to thank you for all the practical help you've given. Dear **Jasper** and **Michael**, changes have brought us together as "hood-mate" in the culture room and unexpectedly, I've had a lot of fun! Dear **Ping** and **Si**, congratulations for that masterpiece you've published after extensive work. Our little chats in Chinese now and then have always been delightful! And I am grateful that our working relationship leads to friendship that has been intensified by our food hunting journeys. Dear **Davine**, **Roberto**, **Keane** and **Patricia**, I have enjoyed every bit of our not-so-long rendez-vous and I wish you all the best in your future career. Dear **Julia**, I worship your bravery to do what your heart desires and I know you will keep rock&roll! Dear **Natasja**, you are so affectionate and my deepest thanks for all your essential support.

I also want to express my sincere thanks to many collaborators and advisors. Dear **Jeroen** and **Erikjan** (Proteomics Center), thank you for producing the proteomic data and assistance in the analysis. Dear **Frank**, **Rob**, **Karin**, **Arjan** and **Robert** (LUMC), thank you for your generosity to share your expertise and your participation and discussion to improve our research. Dear **Wendy** (Pediatrics), thank you for your help on exploring the mechanism of the immune tolerance story and I really appreciate your thorough guidance. My deepest gratitude also goes to **Dimitris** (Biostatistics) for consultant in statistics and to **Gea** and **Ema** (Hospital Pharmacy) for co-ordination of Myozyme delivery.

As the whole thesis is built upon animal experiments, I cannot thank **Jessica**, **Lisette**, **Kim**, **Ineke** and **Jennifer** and other staff of EDC enough for their impeccable work to take care of our mice both in breeding and in experiments. Thank you all being so easy-going, communicative and flexible to changes.

I also want to pay my tribute to Chinese friends in Rotterdam, 老王（汝曦），老刘（静静），若愚，老高（高雅），刘卉，吴斌，鲁涛，长斌，莹莹，展民，黄玲，文浩，瑶瑶，世豪，焦文婷师姐，孙伟师兄，李延伟师兄 and others, thank you all for making the stay in a foreign country so pleasant and thank you for the fantastic dinner and fun night out.

I want to express my gratitude to China Scholarship Council (CSC) and Sichuan University for giving me this opportunity to study abroad and seek personal development. My heartfelt thanks go to 刘霆教授 for his understanding and encouragement he's given me for pursing PhD abroad. I also want to thank 朱焕玲教授 for her kindness and constant support during the process. I am really looking forward to working again with the team with the ultimate goal as an excellent hematologist.

Additionally, I owe deep debts to my best friends back home, 张媛 and 曾陶怡, the photoshop gurus who have helped me with all the nice illustrative figures in the thesis.

Naturally, I have my parents to thank for the love and support they have been giving me over the years. 亲爱的老爸老妈，十分感激你们一直在大洋彼岸对我默默地给予支持。每年准时漂洋过海而来的农历新年贺卡以及源源不断寄来的零食给了我莫大的鼓励和安慰。父母在，不远游，游必有方。虽然在荷兰的生活舒适安逸，但我十分期待今秋的回归，以掀开人生另一篇章。等我回来！